UNIVERSITÀ DEGLI STUDI DI PALERMO

Dottorato di Ricerca in Ingegneria Chimica, Gestionale, Informatica, Meccanica
Indirizzo "Ingegneria Chimica e dei Materiali"
Dipartimento di Ingegneria Chimica, Gestionale, Informatica, Meccanica
Settore Scientifico Disciplinare ING-IND 27

REVERSE ELECTRODIALYSIS PROCESSES FOR THE PRODUCTION OF CHEMICALS AND THE TREATMENT OF CONTAMINATED WASTEWATER

LA DOTTORESSA **Ch.co Adriana D'Angelo**	IL COORDINATORE **Prof. Ing. Salvatore Gaglio**
IL TUTOR **Prof. Ing. Onofrio Scialdone**	IL CO TUTOR **Prof. Ing. Alessandro Galia**

CICLO XXVI
ANNO CONSEGUIMENTO TITOLO 2016

CONTENTS

1. INTRODUCTION

In the last years, research activities increasingly focused on renewable energy sources characterized by no thermal pollution, no emission of environmental unwanted substances and without net emission of greenhouse gases. Different Renewable Energy technologies and resources exist for electricity, heat and biofuel production. Renewable systems acquire natural fuel from ambient environments and numerous mechanisms have been proposed. These technologies are at different stages in their evolution and can be categorized according to their position along the following scheme.
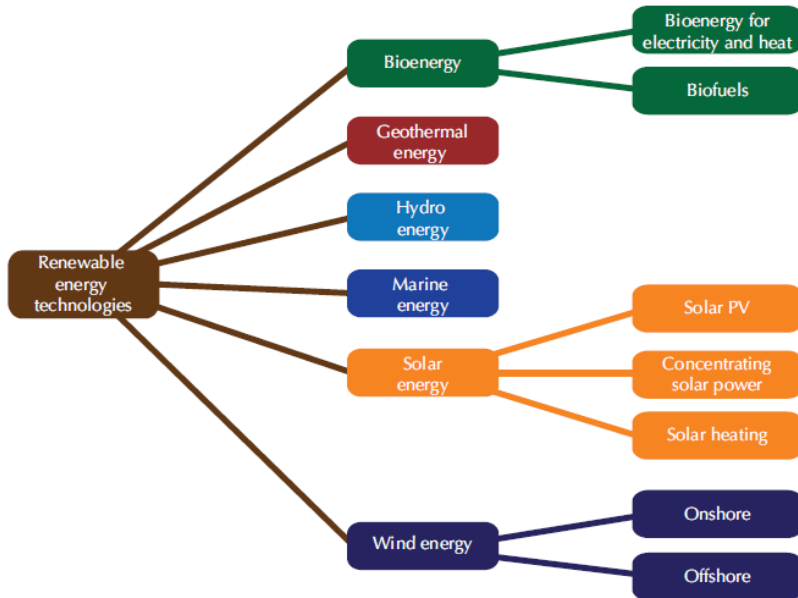
Scheme 1 Selected renewable energy sources and technologies (Renewable Energy: Markets and Prospects by Technology, © OECD/IEA 2011).

New renewable forms of energy are characterized by using the water, but while hydroelectric processes already exploit 800 GW worldwide, marine energy remain an untapped source of energy. Marine Energy can be defined as energy derived from technologies, which utilize seawater as their motive power or harness the chemical

or heat potential of seawater. Five different marine energy technologies under development can be harvested to extract energy from the oceans, each with different origins and requiring different technologies for conversion including:

- ✓ **Tidal power:** the potential energy associated with tides can be harnessed by building a barrage or other forms of construction across an estuary.
- ✓ **Tidal (marine) currents:** the kinetic energy associated with tidal (marine) currents can be harnessed using modular systems.
- ✓ **Wave power:** the kinetic and potential energy associated with ocean waves can be harnessed by a range of technologies under development.
- ✓ **Temperature gradients:** the temperature gradient between the sea surface and deep water can be harnessed using different ocean thermal energy conversion (OTEC) processes.
- ✓ **Salinity gradients:** at the mouth of rivers, where freshwater mixes with saltwater, energy associated with the salinity gradient can be harnessed using the pressure-retarded reverse osmosis process and associated conversion technologies

Table 1 illustrates the estimated global resources of each form. None of these technologies is widely deployed as yet. A significant potential exists for these technologies

Ocean energy resource	How to harness the resource	Theoretical resource
Tidel	Potential energy associated with tides can be harnessed by building barrage or other forms of construction across an estuary.	300+ TWh/years
Waves	Kinetic and potential energy associated with ocean waves can be harnessed using modular technologies	8000 to 80000 TWh/years
Tidal (Marine) Currents	Kinetic energy associated with tidal (marine) currents can be harnessed using modular systems.	800+ TWh/years
Temperature gradients	Thermal energy due to the temperature gradient between the sea surface and deepwater can be harnessed using different Ocean Thermal Energy Conversion processes	10000 TWh/years
Salinity gradients	All the mouth of rivers where fresh water mixes with salt water, energy associated with the salinity gradient can be harnessed using pressure retarded reverse osmosis process and associated conversion technologies	2000 TWh/years

Table 1 Estimated global resources of each form of marine energy resource.

In the framework of a research focused on the study of new renewable sources of energy, salinity gradient power (SGP) could become the source of power in membrane-based systems that capture energy from natural and waste water as a new source of energy. Salinity gradient power (SGP) is the energy generated from the reversible mixing of salt solutions with different concentrations and it is the second largest marine-based energy source, with a global power of 980 GW. Between less popular techniques, reverse electrodialysis (RED) appears as one of the more promising for direct electricity production from salinity gradients, based on the use of many pairs of anion and cation exchange membranes situated between two electrodes. This concept is a very promising process expected to deliver electricity at cost similar to wind power.

The principle of RED technology is well known since 1954, when Pattle for the first time began to speak about SGP potentiality for the RED application.

The research is focused on understanding of RED techniques with the objective of improving the electrode compartments of the system in particular selecting and optimizing materials and components tailored to the requirements of the technology to expand the fields of its application.

Part of the work is carried out in the frame of the EU-funded REAPower program (*Reverse Electrodialysis Alternative Power*), which focuses on RED processes using seawater or brackish water as dilute solution and brine as concentrated one and works intensively on the development of the reverse electrodialysis concept aiming at its commercialization.

For more convenience, it is possible divide the study in different parts to cover the main aspects of the RED process. In the first part, after a long study of the state of art, the behavior of electrode systems was investigated under different operative conditions of interest for RED. The research was first focused on the selection of redox couples and electrode materials with inert anodes and, in particular, on i) reduction/oxidation of iron species, ii) reduction of water and oxidation of chlorides and iii) reduction/oxidation of water. In a second stage, the possible utilization, in

the frame of RED, of a redox process for the wastewater treatment, namely the cathodic reduction of Cr(VI) to Cr(III) or the treatment of wastewater polluted by an azoic dye, the Acid Orange 7 (AO7), was widely studied in order to evaluate the possible utilization of RED for the simultaneous generation of electric energy and the treatment of wastewaters resistant to conventional biological processes, thus enhancing the perspectives of both processes. During this PhD period, an intense experimental campaign carried out on the REAPower demonstration plant (Marsala, Italy) was also performed.

In the second part of the research, another renewable source of energy, Microbial Fuel Cell (MFC) technology has been widely investigated with the aim of generating electricity from biomass using bacteria. This technique exploits the ability of bacterial communities to transfer electrons resulting from the oxidative processes of the organic substance to suitable electrodes. In the past, relatively less effort has been devoted to MFCs than conventional fuel cells (CFCs). While structurally the MFC is very similar to a Conventional Fuel Cell, the two systems have inherent differences that change the reactions, inputs and energy output. Between these differences, we have to include life support requirements of the bio-anode catalyst; variability and adaptation (both desirable and undesirable) of the anode catalyst and organic fuel complexity and flexibility. Despite these differences, in the recent period the versatility of this new system keeps MFCs as a promising fuel source potential. Recently, the utilization of microbial fuel cell for the treatment of wastewater containing organic pollutants has been extensively studied, but in this research the study is also focused on the possibility to expand the role of this process with the aim to increase MFC potentials and power densities and the applications. Part of the laboratory experimental campaign was performed at the research center ITQUIMA, Instituto de Tecnología Química y Medioambiental, in Ciudad Real, Spain.

The possibility to combine a reverse electrodialysis processes with a biotic anode is called Microbial Reverse Electrodialysis cell (MRC), and it was studied in the last section of my work as a new approach to increase the generation of electric energy

by replacing the oxidation process of the water with the process of oxidation of organic compounds to CO_2 using microorganisms. For the first time, the possibility to use this technology for the abatement of pollutant as Cr(VI) was proposed with the aim to achieve a fast abatement of the specie coupled with the utilization of a very small number of membrane pair.

Below it is possible to see a simple scheme, which represents the activities carried out during the thesis.
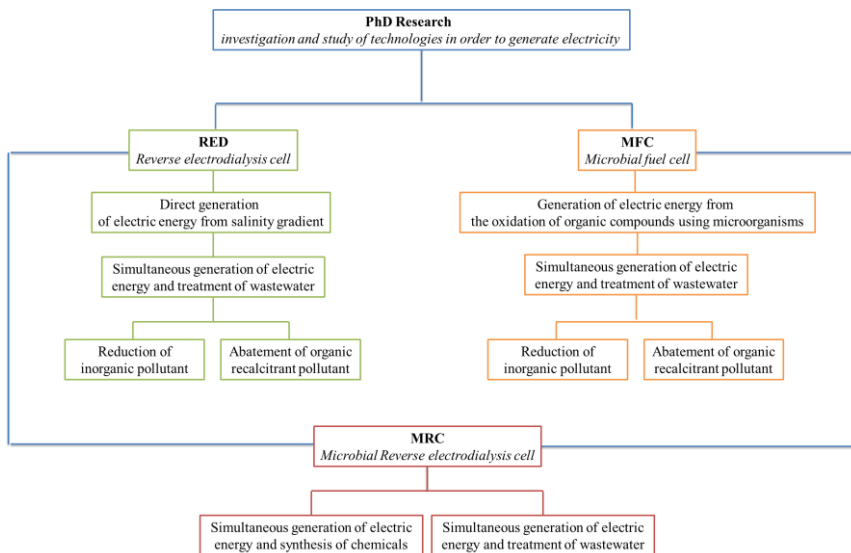
Scheme 2 The present thesis has been organized to cover the main aspects of the RED process and the union of this with other technologies to improve the objectives.

Part I:

1. REVERSE ELECTRODIALYSIS TECHNOLOGY

(History, development up to applications)

1.1   STATE OF ART

1.1.1 Potentiality of Salinity Gradient

In the last decades human activities -particularly burning of fossil fuels- have released huge quantities of carbon dioxide and other greenhouse gases to affect the global climate. The increasing energy demand, the progressive depletion of the conventional fossil resources and an increase of pollution phenomena, have led researchers to drive their work towards the need for renewable, environmental-friendly energy based on renewable resources and huge efforts are being implemented globally to extract energy and/or convert it into useful forms that could be also economically competitive with the resource used up to now. Well-known `green energy` sources including solar, wind, biomass, ocean thermal, wave and tidal have been already taken into account to meet the energy needs.

The energy that can be made available from controlled mixing of two solutions with different salt concentrations takes the name of salinity gradient power (SGP) and this could become the source of power in membrane-based systems that capture energy from natural and waste waters as a new source of energy [1]. The advantages of SGP are: limitless supply (if river and seawater are used), no production of pollutants like NO_x, no CO_2-exhaust, no thermal pollution, no radioactive waste and no daily fluctuations in production due to variations in wind speed or sunshine [2]. Salinity-gradient energy is thermodynamically defined as the free energy change resulting from mixing a concentrated and a diluted salt solution and for ideal dilute solutions (i.e., $\Delta H = 0$), it can be shown that the Gibbs energy of mixing is determined by

$$\Delta_{mix}G = \Delta G_b - (\Delta G_c + \Delta G_d) \qquad\qquad \text{(eq. 1.1)}$$

but

$$\Delta G = \Delta H - T\Delta S = -T\Delta S \qquad\qquad \text{(eq. 1.2)}$$

7
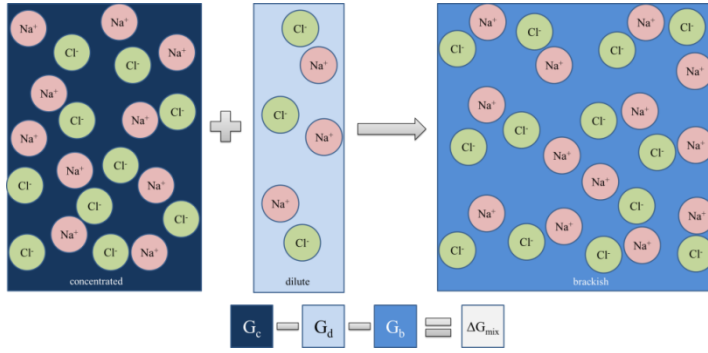
Figure 1.1 Salinity gradient energy. Subscripts indicates *c* concentrated, *d* dilute, *b* brackish solution respectively.

$$\Delta_{mix}G = (n_c - n_d)T\Delta_{mix}s_b - (-n_cT\Delta_{mix}s_c - n_dT\Delta_{mix}s_d) \qquad \text{(eq. 1.3)}$$

where subscripts *c* indicates the concentrated salt solution, *d* the dilute salt solution and *b* the resulting brackish salt solution, *n* is the amount (moles) and *T* the temperature [3].

$\Delta_{mix}s$ represents the contribution of the molar entropy of mixing (J/mol*K) to the total molar entropy of the corresponding electrolyte solution

$$\Delta_{mix}s = -R \sum_i x_i \ln(x_i) \qquad \text{(eq. 1.4)}$$

where *x* is the mole fraction of component "i" (i=Na^+, Cl^-, H_2O).

Thus, equation 1.3 became

$$\Delta G = \sum_i \left(C_{i,c}V_cRT\ln(x_{i,c}) + C_{i,d}V_dRT\ln(x_{i,d}) - C_{i,b}V_bRT\ln(x_{i,b}) \right) \quad \text{(eq. 1.5)}$$

where *C* is concentration (mol/m³), and *V* the volume (m³) of i-specie.

According to the Gibbs free energy of mixing [3] the amount of the energy that theoretically can be generated mixing 1 m³ of river water with the identical sea water volume is 1.7 MJ or even 2.5 MJ when mixed with a large surplus of sea water [4] and it is possible to convert this potential energy into useful electricity with an 85% efficiency [5] (Figure 1.2).
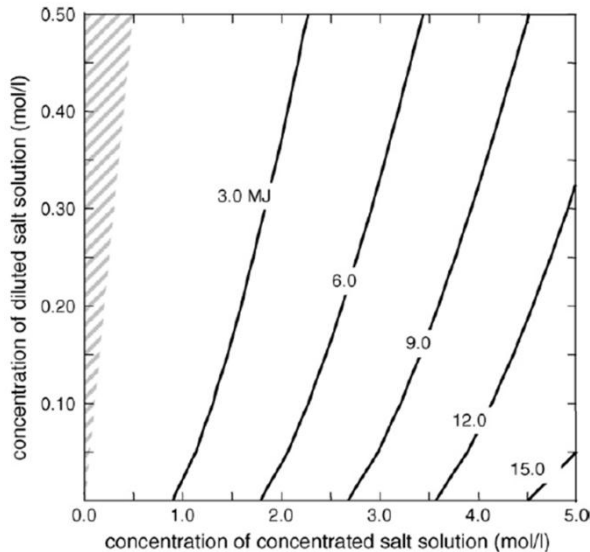
Figure 1.2 Theoretically available amount of energy (MJ) from mixing 1m^3 of a diluted and 1m^3 of a concentrated sodium chloride solution (T = 293 K) [3].

The salinity power available is potentially 2.6 TW [6] from salinity gradient between ocean and annual discharge of river, which should be sufficient to satisfy either the global electricity demand (2 TW) or 16% of the total present energy consumption [7]. Therefore SGP is the energy that use the different in concentration as the driving force that can be generated from reversible mixing of two waters with different salt contents as seawater and freshwater sources [8], from salt ponds and seawater/river water or using thermolytic solutions [9] that can be concentrated with waste heat (> 40 °C) [9-11]. The concept of SGP is already known in the literature and was described for the first time in 1954 by Pattle which postulated: "*When a volume V of a pure solvent mixes irreversibly with a much larger volume of solution, of which the osmotic pressure is P (for seawater ~ 20 atms), the free energy lost is equal to PV. Accordingly, when a river mixes with the sea, the fresh water becomes saline and free energy equal to that obtainable from a 680 foot waterfall is lost*" [12]. His initial work showed the production of energy using an apparatus consisting of 47 cell pairs of membranes across of these fresh and salt water were passed. The maximum electromotive force obtained was 3.1 V and maximum power was 15

9

mW. Very few experiments are found in the literature because until that moment the utilization has been considered to be neither economically feasible nor technically attractive when compared to fossil fuel systems. The main drawback of these membrane-based conversion techniques was the high price of membranes. However, the decreasing prices of membranes for desalination and water reuse applications as well as the increasing prices of fossil fuels make salinity gradient power attractive in near future.

In literature, different technologies have been proposed to convert the salt concentration gradient into energy based on the use of selective membranes which means that the mixing is limited to one of the components, either the solutes or the solvent. Pressure-retarded osmosis (PRO) and reverse electrodialysis (RED) are the most frequently studied membrane-based technologies and two process patents by Loeb describe these apparatuses [13-16]. Of the latest generation, there are the capacitive electrodes that can work synergistically with the ion exchange membranes. Each of these technologies is used in different salinity conditions.

In PRO [3,17] two solutions of different salinity are carried into contact by a semi-permeable membrane (Figure 1.3) which allows the water (solvent) to permeate and retains the dissolvent salts (solute). The osmotic pressure is used to drive water across a suitable membrane and thus generates pressurized water. The chemical potential difference between the solutions causes transport of water from the diluted salt solution to the more concentrated one. The hydraulic pressure of low concentrated water is less than the osmotic pressure of high concentrated water so that water flux through the membrane is against the hydraulic pressure gradient, this fact being the basis for energy production (Figure 1.3) [18].
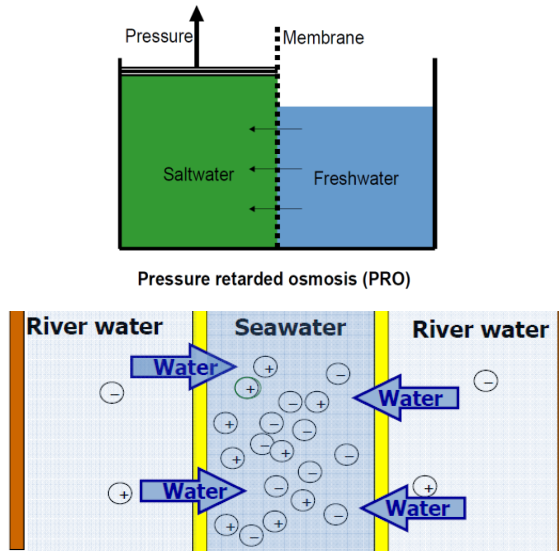
Figure 1.3 PRO use of selective membranes allow the passage of only solvent.

Reverse electrodialysis is a clean, renewable energy with large global potential. It relies on a flow system between electrodes born from the selective transport of aqueous salt ions through an apparatus of perm-selective ion-exchange membranes which separate a concentrated solution from the diluted solution [4,19]. RED process can be seen as the opposite of the Electrodialysis (ED) desalination technology where a voltage is applied at the terminals (electrodes) of the system so as to induce migration movement of all ions driving a salinity gradient between two solutions across the membrane pairs. That means the electric field imposing on the stack represents main driving force of the process. Alternatively, in RED, the ion flow creates an electrical potential capable of generating electricity thank to the formation of appropriate reaction which take place at the electrode-solution interface.

Electrodialysis

Inputs: Energy, Seawater

⬇

Membrane process

⬇

Output: Freshwater

Reverse Electrodialysis

Inputs: Seawater, freshwater

⬇

Membrane process

⬇

Output: Energy
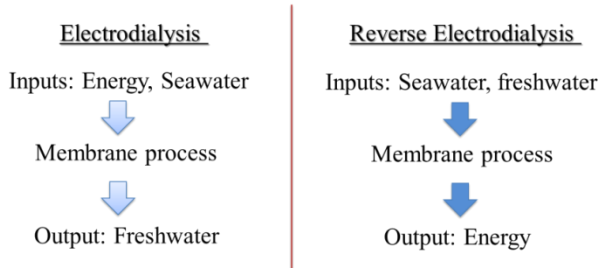
Figure 1.4 Conceptual guide line for ED and RED membranes processes.

A RED stack with n cells is drawn in Figure 1.5.
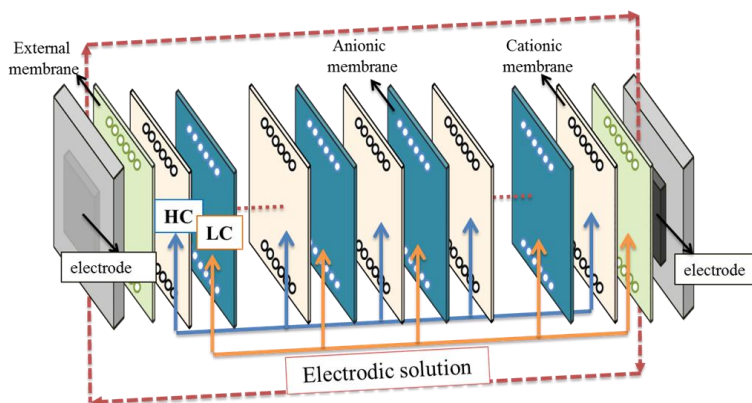
Figure 1.5 Main components of the stack, showing a block of ion exchange membranes situated between the electrodes, the electrodes, flow path of the high and low concentrated solutions (HC and LC respectively) and of electrolyte solution.

Both techniques have demonstrated high power density and energy recovery in their respective environments. Literature suggests that the two techniques have their own field of application: PRO seems to be more attractive for power generation using concentrated saline brines whereas RED shows more affinity using sea and river water. The successful application of PRO and RED are often limited by the cost of membranes. Also, the performance deterioration of membranes is an obstacle for commercialization. For this reason both RED and PRO have experienced an increasing interest among the scientific community during the last decade and the main challenge of both technologies is the development of new membranes with

high performance in terms of high water permeability, low resistance and relatively low cost (especially for RED) and within the context of a new kind of systems.

1.1.2   Principle of a new process (RED)

In RED, each cell contains a cation exchange membrane (CEM), a compartment with a concentrated salt solution (HC), an anion exchange membrane (AEM), and a compartment with a lower salt concentration (LC). The last cell is closed with an extra ion exchange membrane, which can be an anion or cation one depending on the species contained in the electrode compartment [5]. Polymeric net spacers are normally used to maintain the inter-membranes distance [20] adopted as mechanical support for the membranes, giving dimensional stability to the channel, but also to promote fluid mixing thus reducing polarization phenomena. The principle of RED is schematized in Figure 1.6 where the flow of charged ions is converted in a flow of electrons at electrodes by opportune electrodic reactions.
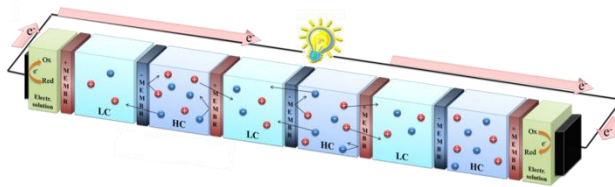
Figure 1.6 RED use of selective membranes allow the passage of only ions. Each cell contains a cation exchange membrane, a compartment with a concentrated salt solution, an anionic exchange membrane and a compartment with a lower salt concentration. in the electrode compartment the ion flow is converted in electron flow by opportune reactions.

After Pattle, other authors collaborated in subsequent years to develop a comprehensive theoretical approach for RED performance and to demonstrate the feasibility of RED power generation technology. In a first moment researchers as Lacey [21], Belfort and Guter [22] presented works on the utilization of ED technology and on performance of modeling ED equations as a function of different factors as membrane potential, diffusion potential, concentration of polarization and internal power less confirming that the largest factor in total cell resistance was the Ohmic scale polarization of membrane surface. Pressure drop and polarization

13

phenomena may reduce significantly the efficiency of membrane processes. In fact, pressure drop is responsible of an energy consumption increase, while polarization phenomena lead to higher power consumption in no spontaneous processes and lower driving force in spontaneous processes because promote membrane fouling and induce internal resistance by obstructing the diffusive membrane layers. In the 1975, Forgacs [23] neglected the effect of concentration polarization and assumed the total permselectivity of membranes to model the performance for generating power of RED system adapting the initial ED theory. Later Weinstein and Leitz [24] published a simplified performance model and wrote that for a RED stack with N membrane pairs the flow of ions, through the IEMs, generates a potential difference that is a function of salinity gradient and depends linearly on the number of exchange ions membranes. The salt concentration difference between both compartments in the cell pair creates a Nernst potential, eq. 1.6,

$$E = 2N\alpha \frac{RT}{zF}\ln\left(\frac{a_c}{a_d}\right) \qquad \text{(eq. 1.6)}$$

across the cell pair which causes an electrical current to flow through the electrical load connected to the electrodes [4], where

R is the universal gas constant (8.314 J/mol·K),

T is the absolute temperature,

α is the average permselectivity of the membrane pair,

F is the Faraday constant (96,485 C/mol),

z is the Electrochemical Valence

a_c and a_d are the activity of species in concentrated and diluted solutions, respectively.

Measuring the potential drop and the current intensity across an external load resistance (R_{ext}), the gross power was obtained as:

$$W = I^2 R_{ext} = \frac{\Delta E^2 \, R_{ext}}{(R_{stack} + R_{ext})^2} \qquad \text{(eq. 1.7)}$$

Weinstein and Leitz concluded that maximal power generation will occur with the least amount of internal stack resistance. Audinos, Kramer and Lacey highlighted economic incentives for RED power generation, but recommended several strategies to minimize the internal resistance of the RED cells and to maximize the net voltage output from the membrane stack.

In order to convert the potential energy in electric energy by RED technique the following components are necessary:

- *ion exchange membranes* (cationic and anionic) [12,24-27] which must be characterized by a low electric energy [28-30] and high permselectivity [30] especially when highly concentrated solution are fed in the system, good mechanical, high chemical [8] and high thermal stability [31] to reduce considerably the overall resistance. All these properties must be accompanied by a significant reduction in IEMs cost to make RED technology economically viable in the near future;

- *gasket integrated with spacers*, which must have a thickness and geometry capable of ensure a reduction in pressure drop leading to increased net power delivered by the system [20,30,32,33];

- *electrode systems,* constituted by the electrodes and the electrode solution which contains a suitable redox couple for electrochemical processes.

For this reason, during the last years, researchers have validated experimental models with much larger RED stacks [2,4] increasing the notoriety of RED capacities. Different authors developed models to quantify internal power losses and optimize membrane stack and spacer design [34,35], compared the performance of several commercial grade membranes [36,37], performed a comprehensive analysis of multiple electrode systems [8] and provided the most comprehensive feasibility analysis to date [38].

In literature, very few experimental data are available on the selection of electrode materials and electrolytes. The behavior of electrode systems was rarely experimentally investigated under operative conditions of interest for RED applications [39].

Novel electrode systems for RED were compared with existing systems for what regard safety, health, environment, technical feasibility, in order to develop the RED process on an applicative scale [8,24,26,40,41] in addition to continuous interest in the development of ion exchange membranes with high performance and low cost [42-45]. As a consequence, recently various authors have carried out a detailed study with the aim of selecting proper redox species and electrodes that have a prior importance for guaranteeing stable performance of the RED process characterized by low potential penalties, low cost, low toxicity, etc. in order to increase the power output generated by RED technology.

1.1.3 Main parameters of a RED process

Below the main parameters that influence the generation of electrical energy are described [3].

The open circuit potential (OCV) is the maximum potential obtainable from the system and considering a stack equipped with N cells is calculated as:

$$OCV = 2N \frac{a_{av}RT}{zF} ln \frac{a_c}{a_d} \qquad \text{(eq. 1.8)}$$

where a_{av} represents the arithmetic mean of the coefficients of the selective permeability of the anionic and cationic membranes, while a_c and a_d are the activities of the concentrated solution and diluted respectively. Activities in the Nernst equation are frequently replaced by concentrations at low solution concentrations.

The measured potential will be actually less of OCV due to the various potential drops within the stack:

$$\Delta V = OCV - IR_{stack} - \Delta E_{redox} \qquad \text{(eq. 1.9)}$$

where the difference of electrode potential ΔE_{redox} depends on thermodynamic potential required to drive the redox reactions (*an* as anode and *cath* as cathode) plus electrode overvpotentials (η) in according to Veermas:

$$\Delta E_{redox} = E_a - E_c + \eta_a - \eta_c \qquad \text{(eq. 1.10)}$$

The Ohmic resistance of the RED stack (R_{stack}) is calculated as a sum of the individual components that are part of the stack (as if their resistances were arranged in series in a hypothetical circuit):

$$R_{stack} = NR_i + R_{el} = \frac{N}{A}\left(R_{AEM} + R_{CEM} + \frac{\delta_c}{k_c} + \frac{\delta_d}{k_d}\right) + R_{el} \qquad \text{(eq. 1.11)}$$

where

N is the number of membrane pairs,

A: Membrane area (m^2),

R_{AEM} and R_{CEM} are respectively the resistance of anionic and cationic membranes per area the membrane (Ω^* m^2),

δ_c (m) and k_c (S/m) are respectively the thickness and the conductivity of the concentrate compartment,

δ_d and k_d are those of the compartment diluted,

R_{el} is the resistance of the electrodes (Ω) and A is the area of the membrane.

The potential and the current density depend on the resistance of the external load; in fact, from the Ohm's law the current density is

$$i = \frac{OCV}{R_i + R_{ext}} \qquad \text{(eq. 1.12)}$$

The gross power density per membrane unit area (W/m^2) can be found from Kirchhoff's law as

$$P_d = \frac{i^2 R_{ext}}{N} = \frac{i\Delta E}{N} = \frac{OCV^2 R_{ext}}{N(R_i + R_{ext})^2} \qquad \text{(eq. 1.13)}$$

when R_{ext} is equal to R_i the maximum gross power density is obtained

$$P_{d,max} = \frac{OCV^2}{(4AR_i)}. \qquad \text{(eq. 1.14)}$$

The power efficiency (η) represents the thermodynamic efficiency of the process and is the fraction of total power extracted by an external load with respect to the total power consumed

$$\eta = \frac{P_d}{P_{tot}} = \frac{i^2 R_{ext} / N}{(i^2 R_{ext} + i^2 R_i) / N} = \frac{R_{ext}}{R_i + R_{ext}}$$ (eq. 1.15)

When the power density is maximum ($R_{ext} = R_i$), the power efficiency is theoretically equal to 50%. A higher efficiency can be achieved at lower power densities ($R_{ext} > R_i$).

Of course, it is important to underline that a consumption of energy is required for pumping the feed solutions through the stack, which can reduce the net power

$$P_{d,net} = P_d - P_{d,pump}$$ (eq. 1.16)

where the $P_{d,pump}$ depends on the pressure drop over the inlet and outlet of the fed solutions (ΔP^c, ΔP^d), their flow rate (v^c and v^d) and the pump efficiency (η_{pump})

$$P_{d,pump} = \frac{\Delta P^c v^c + \Delta P^d v^d}{N A \eta_{pump}}$$ (eq. 1.17)

On the basis of the equations written above it can be stated that energy efficiency and power density are highly dependent on several factors including properties of membranes, spacers, gasket, type of feed, or the redox process selected, operating conditions, electrical load and technical draw of RED system.

1.1.4 Improvements

A mentioned before different research groups have reported effects of some of the controllable parameters on the performance of a RED. To maximize the power density output and thus make the process economically viable it is necessary to minimize *Ohmic* and *non-Ohmic resistances*. The first resistance is due to the various contributions of membranes (AEMs and CEMs), diluted channels, concentrated channels and electrodic compartments. The Ohmic resistances are also

influenced by the presence of a spacer. Non-Ohmic resistances are given by two contributions caused by the ions transport from the concentrated channel to the diluted channel. One depend to the variation of salinity gradient along the fluid flow direction and the other is related to the concentration polarization phenomena in the diffusion boundary layers at the membrane-solution interfaces. In this regard, below the main factors required to reduce the resistance of the stack are listed.

The Resistance of diluted compartment can be decreased by using a concentrated salt solution such as sea water in the diluted compartment, in order to increase the conductivity, and a water solution with a very high amount of salt in the concentrate compartment. The mass transfer rate of the ions from one channel to other is strongly affected by the thickness of the channel created for the flow of the salt solutions. The resistance of the solution in the channel is directly related to the thickness of the channel and it can be very high for a highly dilute solution [40]. Veermas [32] analysing the influence of different types of spacers with a thickness between 485 μm and 60 μm on power output concluded that less is the thickness of spacers higher is the power density extracted by the system in perfect agreement with the results of other researches. In general the use of thinner spacers reduce the electrical resistance of the compartment increasing the power output as shown in the Table below.

Author	Power Density (W/m²)	Membrane Thickness (μm)
Pattle [12]	0.05	700
Jagur-Grodzinski et al. [26]	0.41	550
Weinstein et al. [24]	0.17	1000
Audinos [46]	0.40	3000
Turek [27]	0.46	190
Veerman et al. [34]	0.95	200

Table 1.1 Power densities obtained as function of membranes thickness. The power density obtained by Audinos was connected to a concentrated solution equal to 295 g/L.

Then, Długołecki et al. [47] showed that the use of ion-conductive materials allow to halve the resistance when river water and seawater are used as feed. Starting from these results, further efforts have been focused on the construction of profiled membranes in order to substitute the spacers.

Concentration polarization phenomena are affected by the mixing within the channel between the fluid bulk and the membrane-solution interface (Figure 1.7).
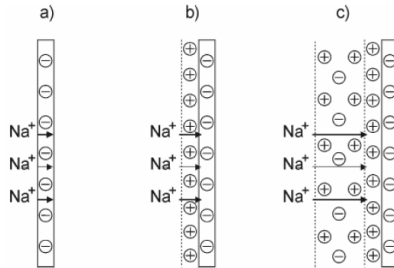
Figure 1.7 A) In a cation exchange-membrane the counter-ions concentration is much higher than the co-ions concentration and generates B) at the membrane-solution interface an electric double layer, a very thin layer (nm scale) of positive charges [48-50] and C) diffusion boundery layer, a region of negative charge.

Because the concentration field in the channel depends on channel geometry, flow rate and solution properties, the effect can be minimized by improving the hydrodynamics of the stack. As reported by Veerman, high flow rates maintain high concentration differences across the membranes and reduce concentration polarization. On the other hand, high flow rates cause higher pressure losses and lower the net power output. Thus, there is flow regime where net power output has a maximum (Figure 1.8).
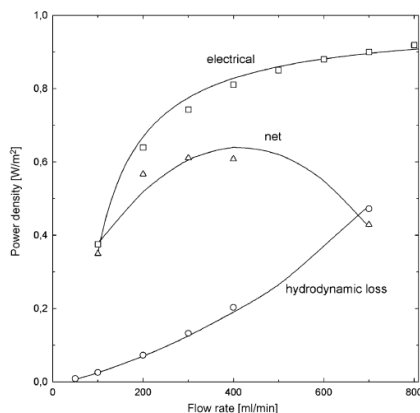
Figure 1.8 Generated electrical power, hydrodynamic loss and the supplied net power in a 50 cell stack.

Another contribution of the resistance of stack is the *membranes resistance.* There are several different ion-exchange membranes available for electrodialysis applications. Dlugolecki et al. [42] made a comparison of some of the important properties of various ion- exchange membranes such as perm-selectivity, resistance, thickness, ion-exchange capacity. Experimental estimation of the performance of different membranes was carried out by Veerman et al. [36]. Using membranes characterized by a thin layer of material is necessary to have a low resistance, a limited range of the pore size, high selectivity, and a large porous surface to facilitate the permeability.

The selection of membrane is important also to limited the formation of eddy currents which cause, besides, a decrease of efficiency of the stack and the power obtained. Their formation depends from two distinct situations, from the transport of unwanted co-ions and from the presence of preferential paths of the ionic current due to the transport of ions through the in and out feed channels.

1.1.5   System design

As previously mentioned the first RED stack design derives by commercial electrodialysis units. There are three different kind of flow configuration utilized in transfer process to feed solutions with different salt concentrations: co-current, counter-current and cross-flow operation modes (Figure 1.9). In these cases, the electrode compartment is composed of one single electrode for compartment, but additionally, a RED system can be operated with electrode composed by multiple segments (Figure 1.9d).
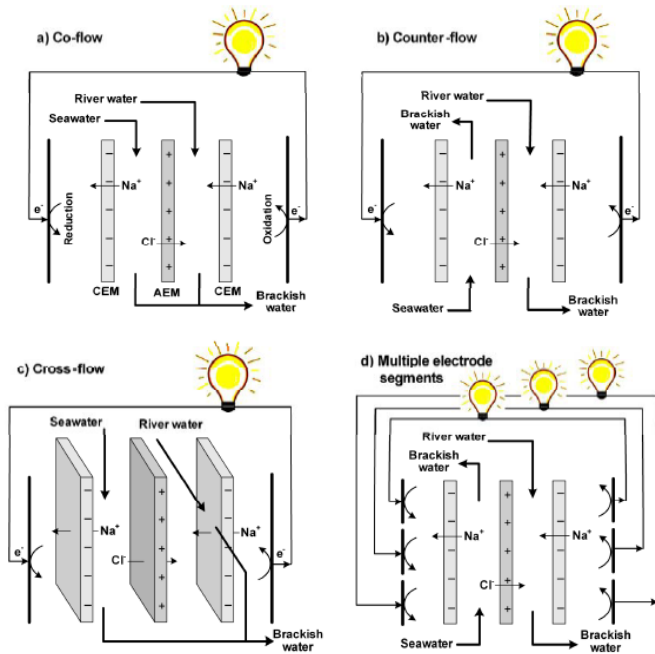
Figure 1.9 Principle of RED using a) co-flow, b) counter-flow, c) cross-flow and d) counter-Flow with segmented electrodes. For simplicity, each setup is presented with one RED cell.

The difference between the various stack designs lies only in the direction of flow path. In co-current mode (Figure 1.10), saline and fresh solutions enter flow compartments in the same parallel direction, and thus mix in the same direction.
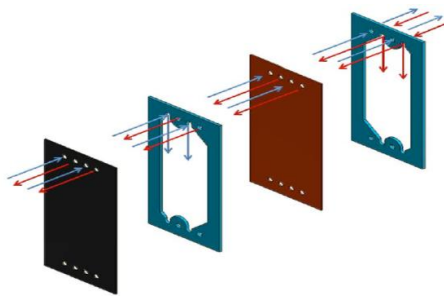
Figure 1.10 Co-current flow scheme for a one cell pair in a RED system. red and blue arrows refer to the concentrated and dilute solutions, respectively.

Co-current flow configuration is generally preferable in order to avoid losses due to local pressure difference across membranes unlike of counter-current mode where

solutions flow counter to each other, and thus mix in opposite directions (Figure 1.11).
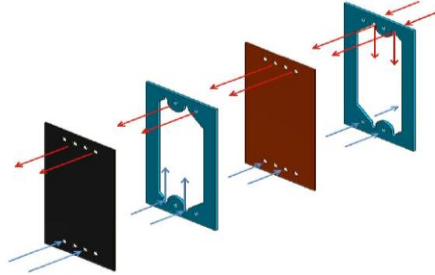
Figure 1.11 Counter-current flow scheme for a one cell pair in a RED system. Red and blue arrows refer to the concentrated and dilute solutions, respectively.

Veerman demonstrated that, if on the one hand, RED processes characterized by counter-current flow mode improved the overall performance [35], on the other hand increased the risk of internal leakages [19]. Recently a new stack design was proposed where the flow direction of one solution is substantially perpendicular to the flow direction of the other fluid and this configuration takes the name of cross-flow arrangement (Figure 1.11) [51].
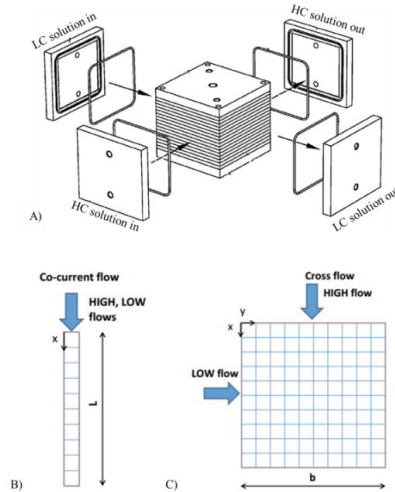
Figure 1.11 A) Cross flow scheme for a RED system. In B) and C) is possible to compare co-current flow and the new flow configuration.

Using a cross-flow configuration stack one tries to ensure a more homogeneous flow distribution within compartments, in order to reduce the concentrated pressure drops at inlet/outlet that is the internal resistance of the stack [52].

1.1.6   The REAPower Project

The basic idea of the EU-funded REAPower project (Reverse Electrodialysis Alternative Power), relies on the reverse electrodialysis technology where there is an extraction of the "osmotic energy" from two salt solutions showing a large difference in salt concentration.

Up to recently, research focused mainly on the combination of fresh water as the low concentration solution (LC) and seawater as the high concentration solution (HC). However this approach has an important limitation: the electrical resistance within the LC compartment filled with the fresh water (typical conductivity < 0.05 S/m) is very high when compared to the HC compartment filled with seawater (typical conductivity of 4.8 S/m). As a result the LOW compartment with the fresh water completely dictates the overall resistance of the cell pair. The LOW compartment resistance cannot be minimized by reducing its width, because of practical restrictions. This high resistance limits the power that can be extracted by the reverse electrodialysis method. REAPower is overcoming this limitation by using seawater (or brackish water) as dilute and brine as concentrate allows to reduce significantly the internal electrical resistance, keeping an high salinity gradient as driving force for the RED process for generating electricity and offering an incredible potential for the improvement of the electrical performance. If on the one hand the presence of highly concentrated solutions inside the system is required to prevent the increase of the resistance of the diluted compartment when dilute aqueous solutions are used, on the other hand the concentrated fluid strongly affects the membranes properties, such as permselectivity and electric resistance.

The aim of the REAPower project was to explore how this new approach could be implemented in practice for enabling the SGP-RE technology to play an important

role in the energy mix of the next decades. The following specific scientific and technological objectives were set at the beginning of the project:

✓ Choosing, optimize, and if necessary create the components of the system that are suitable for solutions with high concentrations of salts (such as spacers, membranes, stack technical draw);

✓ Develop a model that simulates the system effectively and then optimize the design of the stack using a computer modelling tool;

✓ Verify the model, and assess the developed system through experimental investigation on laboratory stacks;

✓ Make a prototype powered with real sea water and brackish water to assess and improve system performance;

✓ Analyse the economic aspects on the basis of the previous tests and estimate the prospects of the technology;

✓ Finally, define the future activities for a possible commercialization of this technology.

For achieving these objectives, a multidisciplinary consortium consisting of key players from the industry and academia were brought together to work across traditional boundaries, contributing to the establishment of a strong scientific and technical base for European science and technology in this emerging area of energy research. The department of chemical engineering of University of Palermo was one of the partners of the project and it played an important role working in three different field of actions:

1) Selection and optimization of different components of electrode system in order to obtain the best performance with regard to the transfer of the electrons of appropriate electrodes (research presented in this thesis);

2) Development of a multi-scale model and process simulation (Fluid dynamics and transport phenomena by means of CFD);

3) Development, validation of a process simulator for a RED stack and simulation of the pilot plant in Marsala.

The promising results collected in lab and the ability to overcome practical challenges in scaling up the stacks has allowed us to take the big step and test the technology in a real environment. Different natural fonts of water of high salt concentration can be used as fluid to feed in the RED stack as natural brine from solar ponds in sea salt production facilities, salt mines, or very salty lakes or brine from industrial processes like oil drilling, textile industry or some food industries. The first REAPower pilot plant to generate electricity from brine was installed in Ettore-Infersa saltworks in Marsala (Trapani, Sicily), which provides access to natural streams of both solutions required for power production: sea or brackish water as dilute solution and brine from the saltworks as concentrated solution (Figure 1.12).

Figure 1.12 Location of the first prototype of RED plant to generate electric current using natural brine solution of salt work of Marsala.

1.2 THE RED TECHNOLOGY TO GENERATE ELECTRIC ENERGY

(Conventional redox processes for RED and study on selection and optimization of electrode materials)

1.2.1 Introduction

The selection of suitable conditions for the electrode system is of a prior importance for guaranteeing stable performance of the RED process. Up to few years ago, less attention has been given to the selection of the electrodic material redox couple system; only few research groups [11,12,25,26,46,53] started to addressed the attention on the choice of adequate electrodes and electrode rinse system. It is necessary to attend Veerman et al. [8] to have an extensive study of many different electrode systems where factors such as electrode over-potential, evolution of gases and mechanical stability of the electrodes were investigated in order to improve the performance of the RED technique. Different kinds of electrode systems for RED were compared with the main aim to ensure the safety, health, environment, technical feasibility and economics.

The electrode system consisted of end-plates, where are placed anode and cathode, which constrained the membrane stack and provided flow chambers for different salt concentration solution and a specific electrode rinse fluid. The last one component of the electrode system is the outer exchange membrane that gives a strong contribution at the stability of the total systems. The exchange membrane has the role to control mass transfer of species from and to electrode compartments avoiding a variation of the chemical stability of the electrode rinse solution, the contamination of concentrated and diluted solutions and to consent only the transport of the ions necessary to sustain the electric current drained from the stack. Only the flow of positive and negative ions is allowed (toward cathode and anode respectively) to sustain the electric current drained from the stack. Of course, this aspect depend on the composition of the electrode compartment solutions but also on the nature of the outer membranes that confine the electrode solution with the side one.

The characteristics relating electrode rinse solution necessary to develop RED plant in applicative field are [2,8,24,42]:

✓ *Chemical and electrochemical stability of redox species* as a function of various parameters in order to ensure on the one hand no formation of hazardous or toxic products of decomposition of redox species that can negatively affect the process also in low concentrations and, on the other hand, greater stability for long time of the redox species minimizing their consumption [8].

✓ *Good solubility of redox species* to grant an appreciable current density sustained by the redox processes with lower possibility of involvement of the solvent in electrodic processes. If the solubility of the redox couple is high, the concentration of the species in the bulk of the solution will be too high and therefore there will be high speed in the mass transport[1] and high current density[2]. Furthermore, because the concentration of bulk is tied to the current limit[3], then the higher the solubility the greater will be the value of the current limit.

✓ *Low toxicity of redox species*. Most of the redox couples cited in the literature and used for other purposes (transition metals as Cr, Ce, Co or V) have to be discarded because give toxic substances that could potentially pollute the effluent streams, thus reducing the choice to a limited number of possibilities. Important in this way is the behavior of outer exchange membrane and if it is necessary is possible to change the structure of stack inserting a chamber of security between the electrode and the adjacent compartment.

✓ *Low cost* of redox species and easy availability.

Electrode materials also must present the following properties [2,8,24,42]:

---

[1] Flick low: $J = -D(\partial C / \partial x|_{x\,=\,0})$

[2] $|i| = nFJ = nFD(\partial c / \partial x|_{x\,=\,0})$

[3] $i_L = \dfrac{nFDC_b}{\delta}$

✓ *Physical and chemical stability* to grant stable electro-catalytic properties and to avoid contamination of electrolyte solution.

✓ *Low cost.*

✓ *Low potential drops* at electrode-solution interphase. Zero equilibrium voltage is immediately obtained using same redox couple at both electrodes. In this way the overall cell potential generated in a stack is greater respect terminal potential drops [4,8].

According to Veerman [8], electrode system can be grouped in two categories (see Figure 1.13): without opposite electrode reactions (where the electrodes alternatively grow and dissolve thus being dimensionally not stable that is a major drawback for the electrochemical engineering of the stack [12,26,46]) or with opposite electrode reactions (e.g., the direct and the reversed reaction take place at the anode and the cathode, respectively).

The most adopted electrode systems without opposite electrode reactions are often based on gas-evolving redox processes, such as in the case of electrode systems containing NaCl [8,42,46,54] and Na_2SO_4 [8,27,55] water solutions

The disadvantage of these systems is the higher potential required for the production of gas. If a NaCl solution is used in the electrode compartments, hydrogen and oxygen evolutions are expected at cathode and anode, respectively:

Catodo) $2H_2O + 2e^- \rightarrow H_2(g) + 2OH^-$ (react. 1.1)
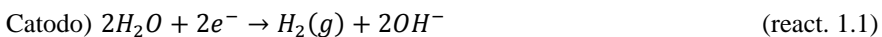
E^0= -0,83 V (SHE- standard hydrogen electrode)

Anodo) $2Cl^- \rightarrow Cl_2 + 2e^-$ (react. 1.2)

E^0= +1,36 V (SHE)

e/o

$H_2O \rightarrow 1/2\, O_2 + 2H^+ + 2e^-$ (react. 1.3)

E^0= +1,23 V (SHE)

Depending of the electrode material, the pH, the concentration of NaCl, and the current density, the one or the other anodic process will take place. All the

electrochemical processes involved are well known and we have a lot of information about these. There isn't the need to provide additional reagents for redox processes to benefit of this system and the production of chlorine, being a strong oxidant, could be used in order to disinfect the solutions at the input. Instead disadvantages of this type of system are: need to work at high potential, the development of gas (Cl_2 and H_2) that cause high resistances to electrodes and possible succeeding reaction with the formation of products such as hypochlorous acid and/or hypochlorite, depending on pH, and ClO [15,24, 54,56-58]. The pH must be maintained low (around 2-3) to facilitate the discharge of Cl^- and avoid the formation of hypochlorite and chlorate and a circulating system with resistant CEM is necessary. In this case, ClO^- and Cl_2 species are confined in the electrode rinse solution and can not discharge on the compartment adjacent. In addition, it is necessary to purify the solution to protect the membranes and the electrodes from fouling and poisoning.

Turek et al. [27,55] avoided the formation of chlorine by using an electrode rinse solution with Na_2SO_4. In this case the reactions at the electrodes will be:

Catodo) $2H_2O + 2e^- \rightarrow H_2 + OH^-$ (react. 1.4)

Anodo) $H_2O \rightarrow 1/2\ O_2 + 2H^+ + 2e^-$ (react. 1.5)

The main advantages of this system are: the wide knowledge on redox processes and electrodes; the process is clean from the environmental point of view because pollutants are not produced. On the other hand, the generation of oxygen at the anode is characterized by high potential losses (1,8 V). Other drawbacks are the necessity to stock electrogenerated gases preventing their hazardous mixing and the necessity to use the supporting electrolyte to ensure the conductivity (then adding another reagent).

A variant of the latter system is to send oxygen to the cathode. In this case, the reactions are:

Catodo) $1/2\,O_2 + 2H^- + e^- \rightarrow H_2O$ (react. 1.6)

$E^0 = +0,816$ V (SHE)

Anodo) $H_2O \rightarrow 1/2O_2 + 2H^+ + 2e^-$ (react. 1.7)

$E^0 = +1,23$ V (SHE)

in this way the reduction of oxygen requires low potential and there is no formation of pollutants.

In all cases a significant number of cells are required to overcome the cell equilibrium potential before electricity production is possible and further gas formation (Cl_2 and O_2 at the anode and H_2 at the cathode) can cause problems at the electrodes (electrical obstruction) and Cl_2 is highly corrosive. A comparison between some of the more promising redox processes for RED applications was carried out during my PhD research.

In order to limit gas production, an alternative are the electrode systems characterized by opposite reactions. When opposite reactions is adopted the system have zero equilibrium voltage, the electrodic thermodynamic potential is null and energetic losses at electrode surface are due to overpotentials, which are strictly related to the choice of the electrode and to the concentration polarization. If electrode rinse solution is recirculated no net modification of the chemical composition occurs and it is possible to assemble a RED stack with a very few cell pairs because there is not a significant energy consumption. First experiments with Cu–CuSO$_4$ [11,12,53], Ag–AgCl [25,46], Zn–ZnSO$_4$ [26] electrode systems have used reactive electrodes which played an important role in the redox process. The electrodes alternatively grow and dissolve and the service life of electrodes is reduced drastically due to the inversion of electrode reactions.

In order to avoid problems in the variation of composition of electrodic systems (electrode and solution) the utilization of homogeneous redox couples Fe^{3+}/Fe^{2+} with inert electrodes is suggested in 2010 by Veerman. The electrode proposed as anode as well as cathode were DSA (dimensionally stable anode) that is titanium mesh

31

electrodes, coated with Ru-Ir mixed metal oxides. The reactions for $FeCl_3/FeCl_2$ electrode system are:

Catodo) $Fe^{3+} + e^- \rightarrow Fe^{2+}$ (react. 1.8)

Anodo) $Fe^{2+} \rightarrow Fe^{3+} + e^-$ (react. 1.9)
$\qquad$ E^0=0,77 V (SHE)

The redox couple Fe^{2+}/Fe^{3+} is stable at a pH below 2-3 and in the presence of an inert gas, such as nitrogen. The disadvantages of this system are: the presence of O_2 that oxidizes Fe^{2+} to Fe^{3+} and the diffusion of H^+ ions through the end-membranes that induces an increase of the pH causing a continuous supply of HCl to correct the pH. Because the addition of HCl cause an unacceptable flow of H^+ towards the near effluent from an environmental point of view, the utilization of a RED system with bipolar membrane was proposed [59] to send the generate NaOH to the output stream and HCl to the electrolyte maintaining a pH neutral.

Another kind of electrode rinse solution was proposed always with the couple Fe^{2+}/Fe^{3+}:

$[Fe(CN)_6]^{3+} + e^- \rightleftarrows [Fe(CN)_6]^{4+}$ (react. 1.10)
$E^0 = 0.356$ V (SHE)

and using same inert electrodes.

Following Figure (Figure 1.13) summarizes the main RED electrode systems studied until this moment. The red dashed line underlines the electrode systems suggested by Veerman.

Electrodic Systems

With opposite electrode reactions

Without opposite electrode reactions

Inert electrodes

Active electrodes

DSA (Ru/Ir)

- Fe^{2+}/Fe^{3+} [8]

Cath: $Fe^{3+}+e^- \rightarrow Fe^{2+}$
Anode: $Fe^{2+} \rightarrow Fe^{3+}+e^-$
tot: // //

- $Fe(CN)_6^{3-}/Fe(CN)_6^{4-}$ [8]

Cath: $Fe(CN)_6^{3-}+e^- \rightarrow Fe(CN)_6^{4-}$
Anode: $Fe(CN)_6^{4-} \rightarrow Fe(CN)_6^{3-}+e^-$
tot: // //

Carbon electrodes

- Fe^{2+}/Fe^{3+} [8]

Cath: $Fe^{3+}+e^- \rightarrow Fe^{2+}$
Anode: $Fe^{2+} \rightarrow Fe^{3+}+e^-$
tot: // //

- $Fe(CN)_6^{3-}/Fe(CN)_6^{4-}$ [8]

Cath: $Fe(CN)_6^{3-}+e^- \rightarrow Fe(CN)_6^{4-}$
Anode: $Fe(CN)_6^{4-} \rightarrow Fe(CN)_6^{3-}+e^-$
tot: // //

- $Cu-CuSO_4$ [11,12,53]

Cath: $Cu^{2+}+2e^- \rightarrow Cu$
Anode: $Cu \rightarrow Cu^{2+}+2e^-$
tot: // //

- $Zn-ZnSO_4$ [26]

Cath: $Zn^{2+}+2e^- \rightarrow Zn$
Anode: $Zn \rightarrow Zn^{2+}+2e^-$
tot: // //

- $Ag-AgCl$ [25,46]

Cath: $AgCl+e^- \rightarrow Ag+Cl^-$
Anode: $Ag+Cl^- \rightarrow AgCl+e^-$
tot: // //

- Metal-SEAwater [24]

Cath: $2H_2O+2e^- \rightarrow H_2+2OH^-$
Anode: $2Cl^- \rightarrow Cl_2+2e^-$
tot: $2H_2O+2Cl^- \rightarrow H_2+2OH^-+Cl_2$

- C/Pt-NaCl [26]

Cath: $\frac{1}{2}O_2+2H^++2e^- \rightarrow H_2O$
Anode: $H_2O \rightarrow \frac{1}{2}O_2+2H^++2e^-$
$2Cl^- \rightarrow Cl_2+2e^-$

- $Ti/Pt-Na_2SO_4$ [27,55]

Cath: $2H_2O+2e^- \rightarrow H_2+2OH^-$
Anode: $H_2O \rightarrow O_2+2H^++2e^-$
tot: $H_2O \rightarrow H_2+\frac{1}{2}O_2$

- $DSA-NaCl/NaCl+Fe(CN)_6^{4-}$ [8]

Cath: $2H_2O+2e^- \rightarrow H_2+2OH^-$
Anode: $2Cl^- \rightarrow Cl_2+2e^-$
tot: $2H_2O+2Cl^- \rightarrow H_2+2OH^-+Cl_2+2e^-$

- C-SEAwater [8,54]

Cath: $2H_2O+2e^- \rightarrow H_2+2OH^-$
Anode: $2Cl^- \rightarrow Cl_2+2e^-$
tot: $2H_2O+2Cl^- \rightarrow H_2+2OH^-+Cl_2$

Figure 1.13 Redox processes studied in the frame of electrodic system. The red dashed line underlines the electronic systems suggested by Veerman.

In this thesis, the possible utilization of three iron redox couples ($FeCl_3/FeCl_2$, hexacyanoferrate(III)/hexacyanoferrate(II), and Fe(III)-EDTA/Fe(II)-EDTA) for RED in the presence of inert electrode, such as titanium mesh electrode or carbon materials, was investigated in detail by electroanalytical investigations and experiments performed in a lab RED stack to obtain better energy efficiency of the device as a function of different parameters, more easy design of the stack and lower cost of electrodes.

1.3 ELECTROCHEMICAL PROCESS FOR THE TREATMENT OF WATER CONTAMINATED BY INORGANIC OR ORGANIC POLLUTANTS.

(Main processes to remove dye and heavy metal)

1.3.1 Introduction

The increasing amount and variability of toxic pollutants such as pesticides, herbicides, chemicals and pharmaceuticals, dye stuff and food packing units is causing a continuous change of the environment. Effluents of a large variety of industries usually contain important amounts of pollutant. The discharge of these organic and inorganic compounds in the environment causes considerable non-aesthetic pollution and serious health-risk factors. In addition, toxic pollutants not only contaminate surface water sources, but also underground water in trace amounts by leaching from the soil after rain and snow.

Dyes represent one of the problematic pollutant groups; they are emitted into wastewater from various industrial branches, mainly from the dye manufacturing and textile finishing and also from food coloring, cosmetics, paper and carpet industries. Very large amounts of synthetic dyes are discharged in the environment from industrial effluents and most of these compounds are not degradable in conventional wastewater treatment plants. Dye are characterized by a typical chromophore group which gives a distinctive coloring solution. One of the richest classes of dyes is formed by azo-derivates (N=N) (Figure 1.14), although there are sulphur and phtalocyanine derivatives that are frequently utilized.
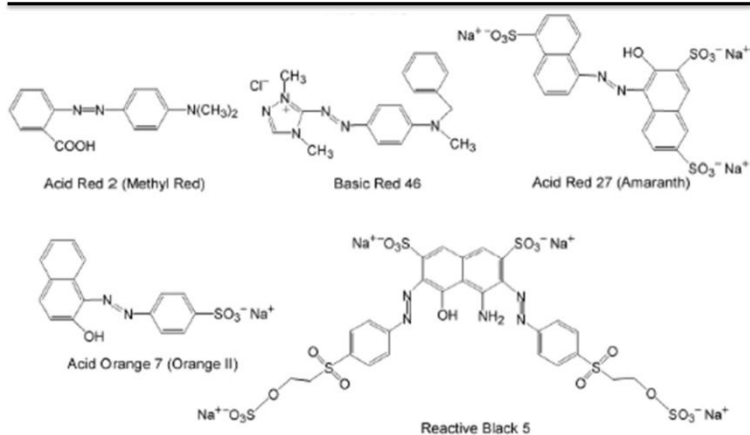
Figure 1.14 Chemical structure of typical synthetic organic azo-dyes.

Most dyes used in textile industries are stable to light and are not biologically degradable. The environmental impact and toxicity of these compounds have been studied in literature.

Unlike organic contaminants, a category of inorganic compounds, the heavy metals, are not biodegradable and tend to accumulate in living organisms and many heavy metal ions are known to be toxic or carcinogenic. Toxicity of heavy metals has triggered a number of studies aimed at removal of the metal ions from aqueous solutions. Among the most dangerous heavy metals are listed zinc, copper, nickel, mercury, cadmium, lead and hexavalent chromium. The last one is of particular concern because it is carcinogenic and mutagenic, diffuses quickly in soil and aquatic environment, is a strong oxidizing agent, and irritates plant and animal tissues in small quantities.

Heavy metal	Toxicities
Cr(VI)	Headache, nausea, diarrhea, vomiting, carcinogenic to human
Cr(III)	
Zn(II)	Depression, lethargy, neurologic signs such as seizures and ataxia, and increased thirst
Cu(II)	Liver damage, Wilson disease, insomnia
Cd(II)	Kidney damage, renal disorder, Itai-Itai, probable human carcinogen
Ni(II)	Dermatitis, nausea, chronic asthma, coughing, human carcinogen

Table 1.2 Heavy metals more hazardous and their toxicities.

Up to a few decades ago, physical-chemical treatment, advanced oxidation processes and biological treatment (Table 1.3) are the techniques [60-63] used in the treatment plants intended for the purification of any industrial wastewater.

INDUSTRIAL WASTEWATER TREATMENT		
PHYS-CHEM/CHEMICAL TREATMENT	ADVANCED OXIDATION PROCESSES	BIOLOGICAL TREATMENT

Main physico-chemical processes:
• Coagulation
• Ion-exchange
• Carbon adsorption
• Reverse osmosis
• Electrodialysis
• Chemical oxidation
• Ozonation
• Enzimatic decomposition
	Chemical, photochemical and photocatalytical production of a strong oxidizing agent:
	hydroxil radical
	
	$H_2O_2 \rightarrow \cdot OH + \cdot OH$
	$H_2O \rightarrow \cdot H + \cdot OH$
	
	• Fenton process
		• Activated sludge process
		• Mixed cultures:
		  - Aerobic processes
		  Mineralization in the presence
		  of O_2 in CO_2
		
		  - Anaerobic processes
		  Acidification in absence of O_2
		  in carbonic acid, CH_4 and H_2
		• Pure cultures

Table 1.3 Techniques used for industrial wastewater treatment.

In the last years, it has been shown that electrochemical tools are particularly useful for the treatment of waste water containing organic pollutants resistant to conventional biological processes or toxic for microorganisms [64-66] and a large number of inorganic ones and for disinfection purposes [67]. These methods offer numerous advantages as the utilization of a green reagent such as the electron, limited costs and the possibility to treat a very large number of different organic compounds without the need to transport or stock of chemicals oxidants and reductants. Electrochemical treatment techniques are becoming an alternative wastewater treatment method and represents an interesting option as many electrochemical and chemical reactions occur simultaneously when they are applied.

These techniques have attracted a great deal of attention because of their versatility and environmental compatibility which makes possible the treatments of wastewater. The main electrochemical procedures are electrocoagulation (EC), direct electrochemical oxidation (EO) with different anodes, cathodic reduction, indirect electro-oxidation with active chlorine (IOAC), electro-Fenton (EF) [65-72] and photoassisted systems like photoelectro-Fenton (PEF) and photoelectrocatalysis (see Figure 1.15). These techniques present high efficiency, easy operation and compact facilities.
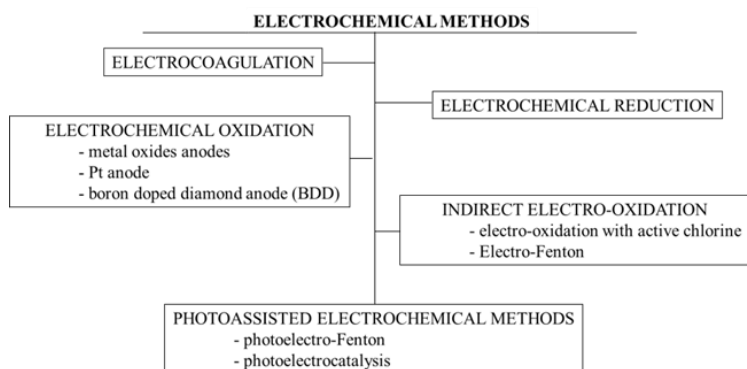
Figure 1.15 Electrochemical methods.

The electrochemical processes offer several characteristics as versatility, energy efficiency favourite by small power losses due to poor current distribution, potential drops and side reactions, environmental compatibility and inexpensive costs.

Electrocoagulation

The electrocoagulation process may be a better alternative than the conventional coagulation and produce just a small amount of sludge. This technique generates in situ the coagulant by a sacrificial anode, aluminium or iron electrodes which are dissolved electrically (see Table below). EC has proven very effective in the removal of contaminants from water and have been in existence for many years using a variety of electrode geometries. The reactor is made up of an electrolytic cell with a pairs of conductive metal plates in parallel (Figure 1.16).

37
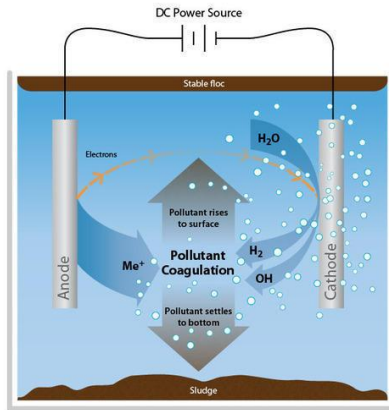
Figure 1.16 Electrocoagulation reactor

How is possible to see in the following Table that reports the main reactions, the metal ions generation takes place at the anode while hydrogen gas is released from the cathode and help particles to float to the top of reactor. The metal hydroxides formed destabilize the contaminants, promotes the aggregation of the suspended particles and remove dissolved and suspended pollutants.

$$\text{ELECTROCOAGULATION}$$

With Iron anode:

$$Fe \rightarrow Fe^{2+} + 2e^- \qquad\qquad (E^0 = -0.44 \text{ V vs. SHE})$$

In presence of oxigen

$$Fe^{2+} + 10\,H_2O + O_2 \rightarrow 4Fe(OH)_3 + 8H^+$$

$$8H^+ + 8e^- \rightarrow 4H_2\uparrow \text{ (cathode)}$$

$$\text{Dye-H} + (HO)OFe_s \rightarrow \text{Dye-OFe}_s + H_2O$$

With Steel anode:

$$Al \rightarrow Al^{3+} + 3e^- \qquad\qquad (E^0 = 1.66 \text{ V vs. SHE})$$

$$3H_2O + 3e^- \rightarrow OH^- + 3/2H_2\uparrow \text{ (cathode)}$$

$$Al + 3H_2O \rightarrow Al(OH)_3 + 3/2H_2\uparrow$$

$$\text{Dye-H} + (HO)OAl_s \rightarrow \text{Dye-OAl}_s + H_2O$$

Table 1.4 Electrocoagulation reactions to remove organic compounds.

Two possible processes can verified:

* the dye can act as a ligand to bind a hydrous iron moiety of the floc yielding a surface complex,

* or Fe(OH)$_3$ flocs, having large surface complexes, contain areas of apparent positive or negative charge that can attract the opposite regions of the dyes.

The particles floated to the top of the reactor can be remove by filtration. Various works reported in literature shown that with increasing concentration higher removal rate are obtained. Good results are carried out using aluminum electrode to remove heavy metal such as Zn^{2+}, Cu^{2+}, $Cr_2O_7^{2-}$, Ag^+ and Ni^+. Other advantages of this process are low operative cost, the effective removal of organic matter and inorganic species using a minimal chemical addition and producing a small amount of sludge products. Between disadvantages, there are the necessity to regularly replace the sacrificial electrodes and the possible loss of efficiency due to formation of an impermeable oxide film on the cathode.

Electrochemical reduction

To maximize the removal of heavy metal from contaminated wastewater, electrical potential has been utilized to modify the conventional chemical precipitation. Various works carried out to treat water contaminated by Cr(VI) using direct electrochemical reduction on carbon electrodes (such as carbon felt or reticulated vitreous carbon) [72] or on steel rods [73] allowed to achieve an almost total conversion of Cr(VI) in Cr(III) under proper operative conditions. The electrochemical reduction occurs through the transfer of electrons from the cathode to the pollutant such as in the case of Cr(VI) ad detailed below:

(steel-anode)

$$6Fe^0 \rightarrow 6Fe^{2+} + 12e^-$$ (react. 1.11)

$$2Fe^{2+} \rightarrow 2Fe^{3+} + 2e^-$$ (react. 1.12)

(cathode)

$$4Cr_2O_7^{2-} + 14H_2O + 14e^- \rightarrow 4Cr_2O_4^{2-} + 26OH^- + H_2$$ (react. 1.13)

(Net reaction)

$$6Fe^0 + 4Cr_2O_7^{2-} + 14H_2O \rightarrow 4FeCr_2O_4 + Fe(OH)_3 + 20OH^- + H_2 \quad \text{(react. 1.14)}$$
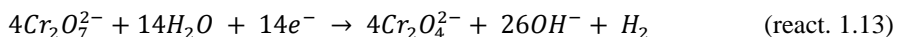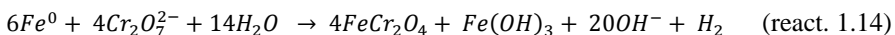
P. Lakshmipathiraj et al. [73] show that Cr (VI) was reduced to trivalent chromium below its detection limit using NaCl as electrolyte. The reduction become very low with NaNO$_3$ and negligible with Na$_2$SO$_4$ as supporting electrolyte. Electrochemical processes can work in acid or basic condition and good results are collected for the treatment of inorganic pollutants with an initial concentration increased to 2000 mg/L [74,75]. Grebenyuk et al. [76,77] reported that heavy metal removal can be carried out through electrochemical oxidation/reduction processes in an electrochemical cell without a continuous feeding of redox chemicals, thus avoiding a costly space, time and energy consumption.

Few materials have been proposed in literature to use the direct electroreduction of dyes in aqueous solution [78,79]. This conventional method offers poor decontamination of wastewaters in comparison to more potent direct and indirect electro-oxidation methods.

Electrochemical oxidation

Electrochemical oxidation offers an attractive procedure for the treatment of aqueous streams containing small-to-medium concentrations of soluble organic compounds [65,69,70,80]. Aim of this mechanism is the mineralization of the contaminants to carbon dioxide, water and inorganics or their transformation into harmless products. Electrochemical oxidation can be subdivided in two important categories:

∗ Direct anodic oxidation
∗ Indirect oxidation using appropriate oxidants.

Two approaches of electro-oxidation process in wastewater treatment have been proposed by Comninellis [81]: the direct anodic oxidation where the organics are transformed into biodegradable compounds and the mineralization of the organic

pollutants [81]. The generation of adsorbed hydroxyl radical, the process competition of oxygen evolution and the kind of electrode material affect the feasibility of this process. The anode material plays an important role in this process and as shown in Figure 1.17 the direct electrochemical oxidation may take place on active (Ti/Pt-Ir [82,83], Ti/RuO$_2$, glassy carbon [84], carbon fibers [85], carbon felt [86], vitreous carbon [87,88], MnO$_2$ [89,90], Pt-carbon black [91,92], steel [93]) and no-active anode (BDD film electrodes is the best kind of anode and shows excellent electrochemical stability)
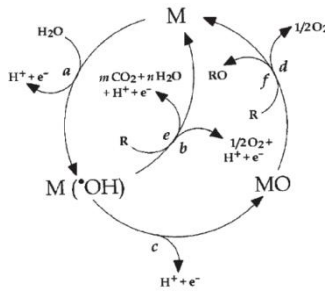
Figure 1.17 Direct anodic oxidation.

Table 1.5 Direct anodic oxidation processes in the presence of active and non active anode material.

$$BDD + H_2O \rightarrow BDD(\cdot OH) + H^+ + e^- \qquad\qquad (react.\ 1.15)$$
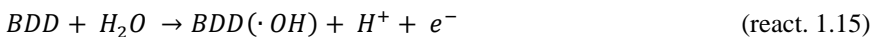
Despite its high cost, the anode BDD has a high overvpotential for oxygen evolution, high stability even in the presence of strong acids and a wide range of potential in which it is possible to discharge the water.

Besides direct oxidation, organic pollutants can also be treated by an indirect electrolyses. The indirect electrochemical oxidation processes can use two different main kind of oxidants to treat wastewater contaminated by organic pollutant: *active chlorine* (in the form of chlorine, hypochlorous acid and hypochlorite) electrogenerated in effluent containing chloride ions, and *electro-Fenton's reagents* (see Table 1.6).

ELECTROCHEMICAL OXIDATION

Indirect Anodic Oxidation

Electro-Fenton	Electrogeneration of Active Chlorine
$O_2 + 2H^+ + 2e^- \rightarrow H_2O_2$	$2\,Cl^- = Cl_2 + 2e^-$
$H_2O_2 + Fe^{2+} \rightarrow Fe^{3+} + \cdot OH + OH^-$	$Cl_2 + H_2O = HOCl + H^+ + Cl^-$

Table 1.6 Main indirect anodic oxidation.

When in the system are present chloride ions, hypochlorous acid may be produced on the anode during electrolysis and will react with organic matters [72]

$$Dye - ClO^- \;\rightarrow\; CO_2 + H_2O + Cl^- \qquad\qquad \text{(react. 1.16)}$$

Various anodic reactions may limit the concentration of the hypochlorite ions:

$$ClO^- + H_2O \rightarrow ClO_2^- + 2H^+ + 2e^- \qquad\qquad \text{(react. 1.17)}$$
$$ClO_2^- + H_2O \rightarrow ClO_3^- + 2H^+ + 2e^- \qquad\qquad \text{(react. 1.18)}$$
$$ClO_3^- + H_2O \rightarrow ClO_4^- + 2H^+ + 2e^- \qquad\qquad \text{(react. 1.19)}$$

Another kind of process that reduce the concentration of the reagent can take place at the cathode with the reduction of hypochlorite ion to chlorine ion.

All these electrode processes are a function of applied current density, agitation, temperature, concentration of chlorides and especially the activity of the electrocatalytic electrode material. However, the possible formation of chlorinated organic compounds as intermediates of reaction has prevented the application to a large scale of this type of processes. In addition, if the effluent is free of chloride ions it is necessary to add them with a consequent consumption of large amounts of salt in order to improve the efficiency of the process

During electro-Fenton process (Figure 1.18), the oxygen present in the air is reduced to hydrogen peroxide at a suitable cathode surface. The hydrogen peroxide is a substance which has water and oxygen as products. It is not a strong oxygen transfer agent but it is converted in hydroxide radical in the presence of a catalytic amount of iron two at very acid pH becoming ineffective under moderate or strongly alkaline operative condition. In optimal process conditions (pH=3) the predominant species of Fe(III) is $Fe(OH)^{2+}$, and then the reaction that occur is:

$$Fe^{2+} + H_2O_2 \rightarrow Fe(OH)^{2+} + \cdot OH \qquad\qquad \text{(react. 1.20)}$$

This reaction occurs continuously regenerating Fe^{2+} ions at the cathode according to the reaction:

$$Fe(OH)^{2+} + e^- = Fe^{2+} + OH^- \qquad\qquad \text{(react. 1.21)}$$
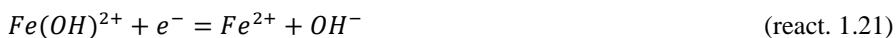
A big advantage of this process is sure the on-site production of H_2O_2 that oxides the organic matter [65,67,72,94,95]. The O_2 is efficiently reduced at various electrode materials such as reticulated carbon vitreous [96], carbon felt [97-102] ACF [103,104], three-dimensional graphite [105], graphite cloth [106], graphite–polytetrafluoroethylene (PTFE) [107,108], Pt–carbon [109] and carbon–PTFE O_2-diffusion [110].
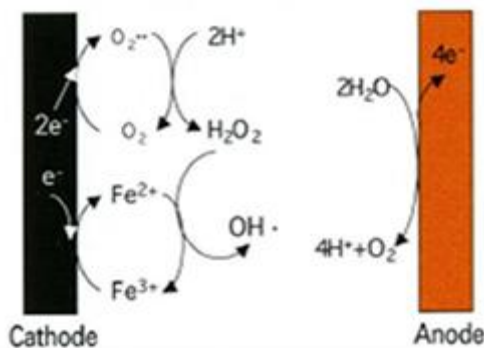
Figure 1.18 Mechanism of ElectroFenton process

Also in this case, Fenton's reagent is relatively non expensive and the process is easy to operate and maintain. By contrast, ferrous ions may be deactivated due to formation of complex with some iron complexing reagent such as phosphate anions and intermediate oxidation products.

If we compare the oxidizing power of two oxidant reagents, hydroxyl radical is the strongest oxidant (E^0 = 2.80 V vs. SHE), but, having much shorter lifetime than HClO (E^0 = 1.49 V vs. SHE). Therefore, for decontamination of the dye wastewater, which commonly contains amounts of inorganic salts, especially chloride, indirect oxidation by electrogenerated active chlorine is more cost-efficient and practical.

Photoassisted electrochemical methods

Another efficient methods for destroying synthetic organic compounds from wastewater are based on the photochemical or photocatalytic reaction between UV irradiation (UVA 315–400 nm, UVB 285–315 nm and UVC < 285 nm) and the pollutants. The rate of degradation of organic pollutant with electro–Fenton like reagents is strongly accelerated by irradiation with UV-VIS light [111,112]. Where the solution is treated under EF conditions and simultaneously irradiated with either artificial UVA light of λmax = 360 nm[106,107,110] or sunlight [70,115-117] (Figure1.19).
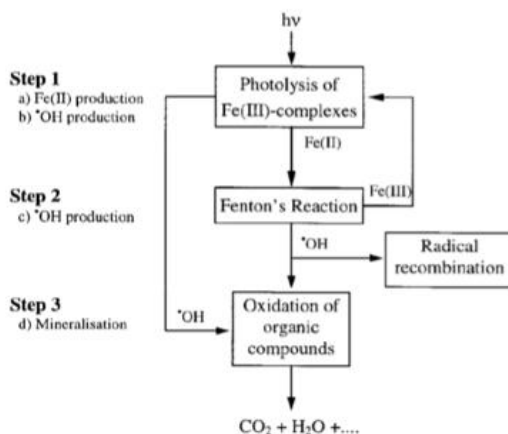
Figure 1.19 Reaction pathways of the Photo-Fenton-Process.

In these conditions, the photolysis of $Fe(OH)^{2+}$, the predominant species of Fe^{3+} in the pH range 2.5−4.0 allows Fe^{2+} regeneration, to catalyze Fenton's reaction, and ·OH radical production

$$Fe(OH)^{2+} \xrightarrow{h\nu} \cdot OH \qquad \text{(react. 1.22)}$$

In addition the degradation action of UVA irradiation favors the photolysis of Fe(III)−carboxylate complexes, as reaction 1.23 depicts for Fe(III)−oxalate complexes, with organic compounds

$$2Fe(C_2O_4)_n^{(3-2n)} \xrightarrow{h\nu} 2Fe^{2+} + (2n-1)C_2O_4^{2-} + CO_2 \qquad \text{(react. 1.23)}$$
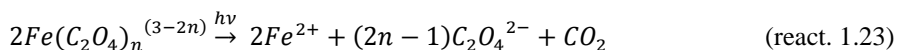
Direct photochemical degradation of organic pollutant can occur when more energetic UV irradiation are used (UVC). In this case, the rate of photolysis of H_2O_2 to ·OH is much faster.

Among photoassisted electrochemical technologies good results are obtained using the *photoelectrocatalytic method* that use a semiconductor metal oxide as catalyst and of oxygen as oxidizing agent. Between all catalysts tested, only TiO_2 in the anatase form seems to have the most interesting attributes such as high stability,

good performance and low cost. Electron excitation and positively charges holes (oxidant reagents) are produced in a TiO_2-based thin film anode irradiated with an UV light.

$$TiO_2 \overset{h\nu}{\to} e^- + h \qquad \text{(react. 1.24)}$$

in which e^- is the electron transfer and h the hole.

In this way on the hand the electrons formed can reduce some metals and dissolve O_2 with the formation of $\cdot O^{2-}$ radical, on the other hand remaining holes are capable to react of oxidize species adsorbed (H_2O and OH^-) give $\cdot OH$ radical

$$TiO_2(h^+) + H_2O_{ad} \to TiO_2 + \cdot OH_{ad} + H^+ \qquad \text{(react. 1.25)}$$

$$TiO_2(h^+) + HO_{ad}^- \to TiO_2 + \cdot OH_{ad} \qquad \text{(react. 1.26)}$$
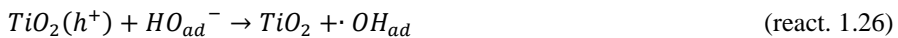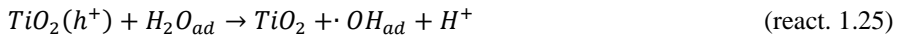
It is possible that some adsorbed substrate can directly react with electron transfer. Among photoassisted electrochemical technologies, no indications have been found in the literature on their application on industrial scale due to slower degradation of compounds and high energy consumption.

Same literature works reported the possibility to use combined processes where there is the combination of different abatement techniques with the aim of improving the performance of the degradation of organic pollutants (Figure 1.20).
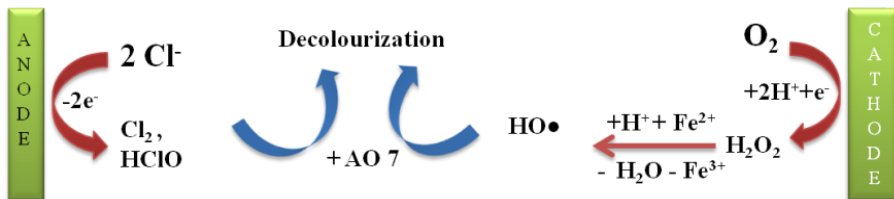
Figure 1.20 Example of combined process: Electro-Fenton at cathode and oxidation by electrogenerated active chlorine at DSA anode.

1.3.2 Improvements

The application of electrochemical methods to treat water contaminated by organic and inorganic pollutant is limited by various factors including the cost of electrode materials such as the diamond or gas diffusion electrode, the cost of electric energy and the necessity to add to the system a supporting electrolyte when the wastewater does not present an adequate conductivity. In order to minimize these problems, various attempts were performed in particular in order to avoid the significant economic penalty for the process due to energy necessary to drive the redox processes coupled with the cost of electrodes and electrolytes. Part of my PhD thesis was dedicated to select the redox processes to enhance the value of the overall process, and in this frame, the RED may be considered as a new approach for the simultaneous generation of electric energy and the treatment of wastewaters contaminated by recalcitrant pollutants.

1.4   REFERENCES

[1] B.E. Logan, M. Elimelech, Membrane-based processes for sustainable power generation using water, Nature. 488 (2012) 313–319.

[2] J Veerman, J., et al., *Reverse electrodialysis: A validated process model for design and optimization.* Chemical Engineering Journal, 166 (2011) 256-268.

[3] J.W. Post, J. Veerman, H.V.M. Hamelers, G.J.W. Euverink, S.J. Metz, K. Nymeijer, et al., Salinity-gradient power: Evaluation of pressure-retarded osmosis and reverse electrodialysis, J. Memb. Sci. 288 (2007) 218–230.

[4] J. Veerman, M. Saakes, S. J. Metz and G. J. Harmsen, "Reverse electrodialysis: Performance of a stack with 50 cells on the mixing of sea and river water," *J Membrane Sci* 327 (2009) 136-144.

[5] J. W. Post, H. V. M. Hamelers and C. J. N. Buisman, "Energy recovery from controlled mixing salt and fresh water with a reverse electrodialysis system," *Environ Sci Technol* 42 (2008) 5785-5790.

[6] G.L. Wick, W.R. Schmitt Prospects for renewable energy from sea. Mar. Technol. Soc. J. 11 (1997) 16-21.

[7] Energy information administration; www.eia.doe.gov

[8] J. Veerman, M. Saakes, S. J. Metz and G. J. Harmsen, "Reverse electrodialysis: evaluation of suitable electrode systems," *J Appl Electrochem* 40 (2010) 1461-1474.

[9] R.D. Cusick, Y. Kim, B.E. Logan, Energy Capture from Thermolytic Solutions in Microbial Reverse-Electrodialysis Cells, Science, 335 (2012) 1474-1477.

[10] E. Brauns, Towards a worldwide sustainable and simultaneous large-scale production of renewable energy and potable water through salinity gradient power by combining reversed electrodialysis and solar power?, Desalination. 219 (2008) 312–323.

[11] R.E. Pattle, Electricity from Fresh and Salt Water – without Fuel, Chem. Proc. Eng., 35 (1955) 351-354.

[12] R.E. Pattle, "Production of Electric Power by Mixing Fresh and Salt Water in the Hydroelectric Pile", Nature, 174 (1954) 660-661.

[13] S. Loeb, Energy production at the Dead Sea by pressure-retarded osmosis: challenge or chimera, Desalination, 120 (1998) 247–262.

[14] S. Loeb, Large-scale power production by pressure retarded osmosis, using river water and sea water passing through spiral modules, Desalination, 143 (2002) 115–122.

[15] S. Loeb, Method and apparatus for generating power utilizing reverse electrodialysis, (1979), US 4,171,409

[16] S. Loeb, Method and apparatus for generating power utilizing pressure-retarded osmosis, (1980), US 4,193,267

[17] A. Achilli, A.E. Childress, Pressure retarded osmosis: From the vision of Sidney Loeb to the first prototype installation — Review, Desalination. 261 (2010) 205–211.

[18] S. Loeb, Production of Energy from Concentrated Brines by Pressure-retarded Osmosis. 1. Preliminary Technical and Economic Correlations, J. Membr. Sci., 1 (1976) 49-63.

[19] J. Veerman, M. Saakes, S. J. Metz and G. J. Harmasen, Reverse Electrodialysis: A Validated Process Model for Design and Optimization, J. Chem. Eng., 166 (2011) 256-268.

[20] L. Gurreri, A. Tamburini, A. Cipollina, G. Micale, M. Ciofalo, CFD prediction of concentration polarization phenomena in spacer-filled channels for reverse electrodialysis, J. Memb. Sci. 468 (2014) 133–148.

[21] Lacey office of saline water research and development report 135, (1965) U.S. Government Printing Office, Washington, D.C.

[22] G. Belfort, G.A. Guter, An electrical analogue for electrodialysis. Desalination, 5 (1968), 267-291

[23] C. Forgacs, Generation of Electricity by Reverse Electrdialysis (RED), (1975) Ben-Gurion University of the Neger, Israel.

[24] Weinstein, J.N. and F.B. Leitz, Electric power from differences in salinity: the dialytic battery. Science, 191 (1976) 557-559.

[25] R. Audinos, Electrodialyse inverse. Etude de l'energie electrique obtenue a partir de deux solutions de salinites differentes J. Power Sources. 10 (1983) 203–217.

[26] J. Jagur-Grodzinski, R. Kramer, Novel process for direct conversion of free energy of mixing into electric power. Ind. Eng. Chem. Process Des. Dev. 25 (1986) 443–449.

[27] M. Turek, B. Bandura, Renewable energy by reverse electrodialysis. Desalination 205 (2007) 67–74.

[28] M. Tedesco, A. Cipollina, A. Tamburini, W. van Baak, G. Micale, Modelling the Reverse ElectroDialysis process with seawater and concentrated brines, Desalin. Water Treat. 49 (2012) 404–424.

[29] P. Długołecki, B. Anet, S.J. Metz, K. Nijmeijer, M. Wessling, Transport limitations in ion exchange membranes at low salt concentrations, J. Memb. Sci. 346 (2010) 163–171.

[30]A.H. Galama, D.A. Vermaas, J. Veerman, M. Saakes, H.H.M. Rijnaarts, J.W. Post, et al., Membrane resistance: The effect of salinity gradients over a cation exchange membrane, J. Memb. Sci. 467 (2014) 279–291.

[31] A. Daniilidis, D.A.A. Vermaas, R. Herber, K. Nijmeijer, Experimentally obtainable energy from mixing river water, seawater or brines with reverse electrodialysis, Renew. Energy. 64 (2014) 123–131.

[32] D.A.A. Vermaas, M. Saakes, K. Nijmeijer, Doubled Power Density from Salinity Gradients at Reduced Intermembrane Distance, Environ. Sci. Technol. 45 (2011) 7089–7095.

[33] S. Pawlowski, J. Crespo, S. Velizarov, Pressure drop in reverse electrodialysis: Experimental and modeling studies for stacks with variable number of cell pairs, J. Memb. Sci. 462 (2014) 96–111.

[34] J. Veerman, J.W. Post, M. Saakes, S.J. Metz, G.J. Harmsen, Reducing power losses caused by ionic shortcut currents in reverse electrodialysis stacks by a validated model, J. Memb. Sci. 310 (2008) 418–430.

[35] J. Veerman, M. Saakes, S.J. Metz, G.J. Harmsen, Electrical power from sea and river water by reverse electrodialysis: A first step from the laboratory to a real power plant, Environ. Sci. Technol. 44 (2010) 9207–9212.

[36] J. Veerman, R. M. de Jong, M. Saakes, S. J. Metz and G. J. Harmsen, Reverse electrodialysis: Comparison of six commercial membrane pairs on the thermodynamic efficiency and power density. J. Membr. Sci. 343 (2009) 7-15.

[37] J.W. Post, H.V.M. Hamelers, C.J.N. Buisman, Influence of multivalent ions on power production from mixing salt and fresh water with a reverse electrodialysis system, J. Memb. Sci. 330 (2009) 65–72.

[38] J. W. Post, C. H. Goeting, J. Valk, S. Goinga, J. Veerman, H. V. M. Hamelers and P. J. F. M. Hack, Towards implementation of reverse electrodialysis for power generation from salinity gradients. Desalination and Water Treatment, 16 (2010) 182-193.

[39] J. W. Post, H. V. M. Hamelers and C. J. N. Buisman, Energy recovery from controlled mixing salt and fresh water with a reverse electrodialysis system, Environ. Sci. Technol. 42 (2008) 5785-5790.

[40] P. Dlugolecki, A. Gambier, K. Nijmeijer and M. Wessling, Practical Potential of Reverse Electrodialysis As Process for Sustainable Energy Generation, *Environ. Sci. Technol.* 43 (2009) 6888-6894.

[41] J.X. Qu, S.M. Liu, Electrode for electrodialysis. Desalination 46 (1983) 233-242.

[42] P. Długołęcki, K. Nijmeijer, S. Metz and M. Wessling, Current status of ion exchange membranes for power generation from salinity gradients, J. Membr. Sci. 319 (2008) 214-222.

[43] A. Daniilidis, R. Herber and D. A. Vermaas, Upscale potential and financial feasibility of a reverse electrodialysis power plant, Applied Energy 119 (2014) 257-265.

[44] J.G. Hong, B. Zhang, S. Glabman, N. Uzal, X. Dou, H. Zhang, X. Wei, Y. Chen, Potential ion exchange membranes and system performance in reverse electrodialysis for power generation: A review, J. Membr. Sci. 486 (2015) 71–88.

[45] S. Pawlowski, P. Sistat, J.G. Crespo, S. Velizarov, Mass transfer in reverse electrodialysis: Flow entrance effects and diffusion boundary layer thickness, J. Membr. Sci. 471 (2014) 72–83.

[46] R. Audinos, Electric power produced from two solutions of unequal salinity by reverse electrodialysis, Indian Journal of Chemistry 31A (1992) 348-354.

[47] P. Długołecki, J. Dabrowska, K. Nijmeijer, M. Wessling, Ion conductive spacers for increased power generation in reverse electrodialysis, J. Memb. Sci. 347 (2010) 101–107.

[48] H. Strathmann, Membrane Science and Technology Ion-Exchange Membrane Separation Processes, 9, 1st Edition, Elsevier, 2004.

[49] I. Rubinstein, SIAM, Electro-Diffusion of Ions, Edition, Philadelphia, 1990.

[50] A. J. Bard, L. R. Faulkner, Electrochemical Methods, Edition, Wiley, New York, 1980.

[51] C.H. Goeting, J. Valk, Membrane stack for a membrane based process and method for producing a membrane therefor, 2011.

[52] L. Gurreri, A. Tamburini, A. Cipollina, G. Micale, CFD analysis of the fluid flow behavior in a reverse electrodialysis stack, Desalin. Water Treat. 48 (2012) 390–403.

[53] R.E. Pattle, Improvements to electric batteries. Patent GB 731.729 (1955).

[54] F. Suda, T. Matsuo, D. Ushioda, Transient changes in the power output from the concentration difference cell (dialytic battery) between seawater and river water. Energy 32 (2007) 165–173.

[55] M. Turek, B. Bandura, P. Dydo, Power production from coal-mine brine utilizing reversed electrodialysis. Desalination 221 (2008) 462–466.

[56] G.L. Wick, *Power from salinity gradients.* Energy 3 (1987) 95-100.

[57] G.D. Metha, Performance of present-day ion-exchange membranes for power generation using a saturated solar pond. J. Membr. Sci. 11 (1982) 107-120.

[58] L.R. Czarnetzki, L.J.J. Janssen, Formation of hypochlorite, chlorate and oxygen during NaCl electrolysis from alkaline solutions at an RuO$_2$/TiO$_2$ anode. J. Appl. Electrochem. 22 (1992) 315-324.

[59] H.V.M. Hamelers, J.W. Post, S.J. Metz, Device and method for performing a reversed electrodialysis process. Patent WO 2007/094659 A1 (2007).

[60] D.G. Hoover, G.E. Borogonovi, S.H. Jones and M. Alexander, Anomalies in mineralization of low concentrations of organic compounds in lake water and sewage, App Environ Microbiol, 51 (1986) 226-320.

[61] OJ. Murphy, GD: Hitchens, L. Kaba, CE. Verotsko, Direct electrochemical oxidation of organics for wastewater treatment, Wat Res, 26 (1992) 443

[62] J. O'M. Bockris (Ed.), 'Electrochemistry of Cleaner Environments' (Plenum, New York, 1975).

[63] J.D. Genders and N. Weinberg (Eds), 'Electrochemistry for a Cleaner Environment', Electrosynthesis Co., East Amherst, New York (1992).

[64] C. Comninellis, A. Cieciwa, G. Foti, in Electrochemistry for the Enviroment, C. Comninellis, G. Chen Eds. (Springer, New York, 2010) chap. 1.

[65] C. A. Martínez-Huitle, S. Ferro, Electrochemical Oxidation of Organic Pollutants for the Wastewater Treatment: Direct and Indirect Processes, Chem. Soc. Rev. 35 (2006) 1324-1340.

[66] E. Brillas, I. Sirés, M. A. Oturan, Electro-Fenton Process and Related Electrochemical Technologies Based on Fenton's Reaction Chemistry, Chem. Rev. 109 (2009) 6570-6631.

[67] C. A. Martínez-Huitle, E. Brillas, Electrochemical Alternatives for Drinking Water Disinfection, Angew. Chem. Int. Edit. 47 (2008) 1998-2005.

[68] C.A. Martınez-Huitle, E. Brillas, Decontamination of wastewaters containing synthetic organic dyes by electrochemical methods: A general review, Appl. Catal. B: Environ. 87 (2009) 105–145.

[69] K. Rajeshwar, J.G. Ibanez, Environmental Electrochemistry, Capther 5, Academic Press, San Diego, CA, (1997)

[70] E. Brillas, P.L. Cabot, J. Casado, in: M. Tarr (Ed.), *Chemical Degradation Methods for Wastes and Pollutants Environmental and Industrial Applications*, Marcel Dekker, New York (2003) 235–304.

[71] G. Chen, G. Chen, Electrochemical technologies in wastewater treatment, Sep. Purif. Technol. 38 (2004) 11–41.

[72] O. Scialdone, A. Galia, S. Sabatino, Abatement of Acid Orange 7 in macro and micro reactors. Effect of the electrocatalytic route, Appl. Catal. B: Environ. 148–149 (2014) 473-483.

[72] C.E. Barrera-Díaza, V. Lugo-Lugo, B. Bilyeu, A review of chemical, electrochem-ical and biological methods for aqueous Cr(VI) reduction J, Hazard. Mater.223–224 (2012) 1.

[73] P. Lakshmipathiraj, G. Bhaskar Raju, M. Raviatul Basariya, S. Parvathy and S. Prabhakar, [Removal of Cr (VI) by electrochemical reduction](), Separation and Purification Technology 60 (2008) 96–102.

[74] N. Kongsricharoern, C. Polprasert, Chromium removal by a bipolar electrochemical precipitation process, Water Sci. Technol. 34 (9) (1996) 109–116.

[75] T. Subbaiah, S.C. Mallick, K.G. Mishra, K. Sanjay, R.P. Das, Electrochemical precipitation of nickel hydroxide, J. Power Sources 112 (2002) 562–569

[76] V.D. Grebenyuk, T.T. Sobolevskaya, A.G. Machino, Prospective of development of electroplating production effluent purification method, Chem. Technol. Water 11 (5) (1989) 407–411.

[77] V.D. Grebenyuk, G.V. Sorokin, S.V. Verbich, L.H. Zhiginas, V.M. Linkov, N.A. Linkov, J.J. Smit, Combined sorption technology of heavy metal regeneration from electroplating rinse waters, Water SA 22 (4) (1996) 381–384.

[78] L. Fan, Y. Zhou, W. Yang, G. Chen, F. Yang, Electrochemical Degradation of Amaranth Azo Dye in Water on ACF, J. Hazard. Mater. B137 (2006) 1182‑1188.

[79] R. Jain, M. Bhargava, N. Sharma, Electrochemical Studies on a Pharmaceutical Azo Dye: Tartrazine, Ind. Eng. Chem. Res. 42 (2003) 243‑247.

[80] D. Pletcher, F.C. Walsh, Industrial Electrochemistry, 2nd ed., Blackie Academic & Professional, London, 1993

[81] Ch. Comninellis, Electrochim. Electrocatalysis in the electrochemical conversion/combustion of organic pollutants for waste treatment, Acta 39 (1994) 1857‑1862.

[82] J. Naumczyk, L. Szpyrkowicz and F. Z. Grandi, Electrochemical treatment of textile wastewater, Water Sci. Technol. 34 (1996) 17–24.

[83] O. J. Murphy, G. D. Hitchens, L. Kaba and C. E. Verostko, Direct electrochemical oxidation of organics for wastewater treatment, Water Res. 26 (1992) 443–451.

[84] M. Grattell, D. W. Kirk, Can. J. Eng. 68 (1990) 997–1003.

[85] L. Szpyrkowicz, J. Naumczyk and F. Z. Grandi, Application of electrochemical processes for tannery wastewater treatment, Toxicol. Environ. Chem. 44 (1994) 189–202.

[86] A. M. Polcaro and S. Palmas, Electrochemical Oxidation of Chlorophenols, Ind. Eng. Chem. Res. 36 (1997) 1791–1798.

[87] J. Manriquez, J. L. Bravo, S. Gutierrez-Granados, S. S. Succar, C. Bied-Charreton, A. A. Ordaz and F. Bedioui, Electrocatalysis of the oxidation of alcohol and phenol derivative pollutants at vitreous carbon electrode coated by nickel macrocyclic complex-based film, Anal. Chim. Acta 378 (1999) 159–168.

[88] C.S. Hofseth and T.W. Chapman, Electrochemical destruction of dilute cyanide by copper-catalyzed oxidation in a flowthrough porous electrode, J. Electrochem. Soc., 146 (1999) 199–207.

[89] G. Rajalo and T. Petrovskaya, Selective electrochemical oxidation of sulphides in tannery waste- water, Environ. Technol. 17 (1996) 605–612.

[90] N. N. Rao, K. M. Somasekhar, S. N. Kaul and L. Szpyrkowicz, Electrochemical oxidation of tannery wastewater, J. Chem. Technol. Biotechnol. 76 (2001) 1124–1131.

[91] J. L. Boudenne, O. Cerclier, J. Galea and E. V. Vlist, Electrochemical oxidation of aqueous phenol at a carbon black slurry electrode, Appl. Catal., A 143 (1996) 185–202.

[92] J. L. Boudenne and O. Cerclier, Performance **of** carbon black-slurry electrodes for 4-chlorophenol oxidation, Water Res. 33 (1999) 494–504.

[93] G.V. Sleptsov, A.I. Gladikii, E.Y. Sokol, S.P. Novikova, Elektron. Obrab. Mater. 6 (1987) 69–72.

[94] M.A. Oturan, J.J. Aaron, N. Oturan, J. Pinson, Degradation of chlorophenoxyacid herbicides in aqueous media, using a novel electrochemical method, Pestic. Sci. 55 (1999) 558–562.

[95] S. Hammami, N. Bellakhal, N. Oturan, M.A. Oturan, M. Dachraoui, Degradation of Acid Orange 7 by electrochemically generated• OH radicals in acidic aqueous medium using a boron-doped diamond or platinum anode: A mechanistic study, Chemosphere 73 (2008) 678-684.

[96] A. Alvarez Gallegos, Y. Vergara Garcıa, A. Zamudio, Solar hydrogen peroxide, Sol. Energy Mater. Sol. Cells 88 (2005) 157–167.

[97] E. Kusvuran, O. Gulnaz, S. Irmak, O.M. Atanur, H.I. Yavuz, O. Erbatur, Comparison of several advanced oxidation processes for the decolorization of Reactive Red 120 azo dye in aqueous solution, J. Hazard. Mater. B109 (2004) 85–93.

[98] E. Kusvuran, S. Irmak, H.I. Yavuz, A. Samil, O. Erbatur, Comparison of the treatment methods efficiency for decolorization and mineralization of Reactive Black 5 azo dye, J. Hazard. Mater. B119 (2005) 109–116.

[99] A. Lahkimi, M.A. Oturan, N. Oturan, M. Chaouch, Removal of textile dyes from water by the electro-Fenton process, Environ. Chem. Lett. 5 (2007) 35–39.

[100] S. Hammami, N. Oturan, N. Bellakhal, M. Dachraoui, M.A. Oturan, Oxidative degradation of direct orange 61 by electro-Fenton process using a carbon felt electrode: application of the experimental design methodology, J. Electroanal. Chem. 610 (2007) 75–84.

[101] M.A. Oturan, E. Guivarch, N. Oturan, I. Sires, Oxidation pathways of malachite green by Fe 3+-catalyzed electro-Fenton process, Appl. Catal. B: Environ. 82 (2008) 244–254.

[102] N. Daneshvar, S. Aber, V. Vatanpour, M.H. Rasoulifard, Electro-Fenton treatment of dye solution containing Orange II: Influence of operational parameters, J. Electroanal. Chem. 615 (2008) 165–175.

[103] A. Wang, J. Qu, J. Ru, H. Liu, J. Ge, Mineralization of an azo dye Acid Red 14 by electro-Fenton's reagent using an activated carbon fiber cathode, Dyes Pigments 65 (2005) 227–233.

[104] L. Xu, H. Zhao, S. Shi, G. Zhang, J. Ni, Electrolytic treatment of CI Acid Orange 7 in aqueous solution using a three-dimensional electrode reactor, Dyes Pigments 77 (2008) 158–164.

[105] C.-T. Wang, J.-L. Hu, W.-L. Chou, Y.-M. Kuo, Removal of color from real dyeing wastewater by Electro-Fenton technology using a three-dimensional graphite cathode, J. Hazard. Mater. 152 (2008) 601–606.

[106] J.M. Peralta-Hernandez, Y. Meas-Vong, F.J. Rodrıguez, T.W. Chapman, M.I. Maldonado, L.A. Godınez, Comparison of hydrogen peroxide-based processes for treating dye-containing wastewater: decolorization and destruction of Orange II azo dye in dilute solution, Dyes Pigments 76 (2008) 656–662.

[107] M. Zhou, Q. Yu, L. Lei, G. Barton, Electro-Fenton method for the removal of methyl red in an efficient electrochemical system, Sep. Purif. Technol. 57 (2007) 380–387.

[108] M. Zhou, Q. Yu, L. Lei, The preparation and characterization of a graphite–PTFE cathode system for the decolorization of CI Acid Red 2, Dyes Pigments 77 (2008) 129–136.

[109] Z. Shen, J. Yang, X. Hu, Y. Lei, X. Ji, J. Jia, W. Wang, Dual electrodes oxidation of dye wastewater with gas diffusion cathode, Environ. Sci. Technol. 39 (2005) 1819–1826.

[110] C. Flox, S. Ammar, C. Arias, E. Brillas, A.V. Vargas-Zavala, R. Abdelhedi, Electro-Fenton and photoelectro-Fenton degradation of indigo carmine in acidic aqueous medium, Appl. Catal. B: Environ. 67 (2006) 93–104.

[111] J. Kiwi, C. Pulgarin, P. Peringer, M. Gratzel, Beneficial effect of homogeneous photo-Fenton pretreatment upon the biodegradation of anthraquinone sulfonate in wastewater treatment, Appl. Catal. B: Environ. 3 (1993) 85-89.

[112] C. Pulgarin, J. Kiwi, Overview on photocatalytic and electrocatalytic pretreatment of industrial non-biodegradable pollutants and pesticides, Chimia 50 (1996) 50-55.

[113] Y. Zuo, J. Hoigné, Formation of hydrogen peroxide and depletion of oxalic acid in atmospheric water by photolysis of iron(III)- oxalato complexes. Environ. Sci. Technol., 26(5) (1992) 1014-1022.

[114] I. Sirés, F. Centellas, J.A. Garrido, R.M. Rodríguez, C. Arias, P.L. Cabot and E. Brillas, Mineralization of clofibric acid by electrochemical advanced oxidation processes using a boron-doped diamond anode and Fe^{2+} and UVA light as catalysts. Appl. Catal. B-Environ., 72(3-4) (2007) 373-381.

[115] W. Gernjak, M. Fuerhacker, P. Fernandez-Ibanez, J. Blanco, S. Malato, Solar photo-Fenton treatment—process parameters and process control, Appl. Catal. B: Environ. 64 (2006) 121–130.

[116] A. Duran, J.M. Monteagudo, E. Amores, Solar photo-Fenton degradation of Reactive Blue 4 in a CPC reactor, Appl. Catal. B: Environ. 80 (2008) 42–50

[117] M. Skoumal, R.M. Rodríguez, P.L. Cabot, F. Centellas, J.A. Garrido, C. Arias, E. Brillas, Electro-Fenton, UVA photoelectro-Fenton and solar photoelectro-Fenton degradation of the drug ibuprofen in acid aqueous medium using platinum and boron-doped diamond anodes, Electrochimica Acta, 54 (7) (2009) 2077-2085.

2. EXPERIMENTAL SET-UP

At first the research was focused on the electrode compartment of reverse electrodialysis system, selecting and optimizing materials and components tailored to the requirements of the RED technology to generate electric energy. Hence, the initial objectives of this study are:

- to study conventional redox process with low energetic losses and cost;

- to investigate electrode materials, electrolyte and outer membranes;

- to study different configurations for the electrode circuit.

The utilization of one or more electrochemical processes aimed to the treatment of wastewaters with the purpose of developing a process for the simultaneous generation of electric energy and the abatement of organic and inorganic pollutants driven by salinity gradients is the fulcrum of the second section of the Part 1 of this thesis.

In order to pursue the first objectives listed before and to select the electrochemical process more promising to treat organic and inorganic pollutant in wastewater, preliminary investigation was carried out using electrolyses system.

Only later, on the basis of the results obtained an extensive experimental campaign was carried out using RED stack.

2.1 EXPERIMENTAL APPARATUS

2.1.1 Electrolyses system

Electrolyses were performed both in a bench-scale batch undivided cell (50 mL) and in two or three compartments cells divided by ion-exchange membranes.

The following Figure shows the photo of the undivided cell used. It is a cell with a glass "body" with an outer jacket. The "head" is characterized by five holes where it was possible to insert: cathode, anode, reference and if is necessary an airlock.

Anode and cathode are connected with a galvanostatic potentiostat (Amel 2055 potentiostat) and SCE was used as reference electrode and all potentials reported in this study are referred to it.
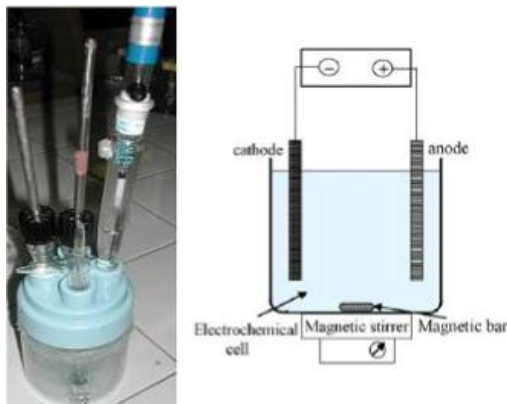
Figure 2.1 Photo of undivided electrolysis cell adopted and simple draw of the system.

This kind of electrolysis cell was used to:
- evaluate the stability of the redox couple used in the time
- monitor the removal of inorganic pollutant or abatement of the dye.

When the divided assay was employed, the anodic and cathodic compartments were divided by an ion-exchange membrane (see Figure 2.2).
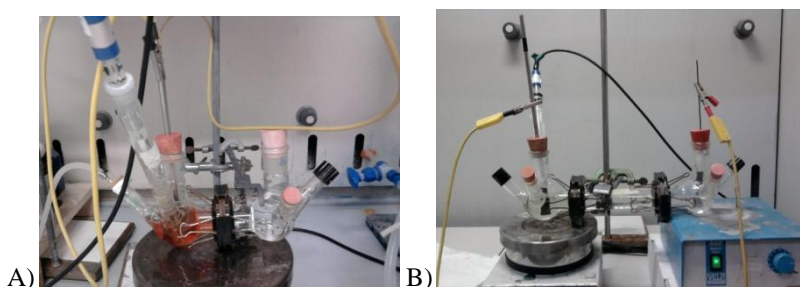
Figure 2.2. Photos of two (A) and three (B) compartments electrochemical cells.

Cationic (CEM) and anionic (AEM) membranes, thickness 120 μm, adopted to perform the experiments are reported in Table 2.1.

56

Name	Code	Company	Type
Fumasep	FKS	Fumatech (Germany)	CEM
	FAD	Fumatech (Germany)	AEM
Selemion	CMV	Asahi glass	CEM
	AMV	Asahi glass	AEM
Fuji	C	FujiFilm	CEM
	A	FujiFilm	AEM
Nafion	324	Du pont	CEM

[a] Polymer matrix: PET, PA, PEEK for Fumasep, Poly(styrene-co-divinybenzene) for Selemion and Perfluorinated bilayer membranes for Nafion membranes.

Table 2.1 Ion exchange membranes tested during the lab experiments.

The volume of each compartment was generally 70 mL for both part. When three compartment cell was used, different water solution with several concentrations of electrolyte were filled in the central compartment.

Bi-compart and three-compart electrochemical cell were used:

- to maintain separate anode and cathode compartments to have two separate processes,
- to evaluate the possible passage of the dye or its by-products formed during the electrolysis,
- to monitor the performance of process.

All cells are kept under vigorous stirring by a magnetic stirrer.

Electrodes used to study the electrode system for the generation of electric energy were: compact graphite tipo E (Carbon Lorraine), $Ti/IrO_2–Ta_2O_5$ (De Nora SpA) or in few cases boron doped diamonds (BDD) (Condias) and titanium mesh coated with platinum (De Nora SpA). Wet surface area in most cases was 6–7 cm^2.

Electrode used to treat wastewater containing organic pollutant were the following. Titanium meshes of $RuO_2–IrO_2$ (Magneto), $IrO_2–Ta_2O_5$ (De Nora) and Boron doped diamond (BDD) plates (Condias) were used as anodes while Ni (Carlo Erba) plates and carbon felt (The Electosynthesis Co.) as cathodes. The electrodic compartment was equipped with a cathode and an anode with a geometric surface of 5 cm^2.

To treat Cr(VI) aqueous solution, the following electrode are used: Carbon felt (The Electosynthesis Co), compact graphite (Carbone Lorraine) or reticulated vitreous carbon (80ppi, Electrosynthesis Co) were used as cathode (geometric exposed area

5.5 cm^2) and a Saturated Calomel Electrode (SCE) as the reference electrode. Titanium meshes of IrO$_2$-Ta$_2$O$_5$ (Magneto) were used as anode.

2.1.2 RED stack system

The lab scale stack, assembled between the anode and cathode chambers (10 cm x 10 cm x 2 mm), consisted of internal ion-exchange membranes (FujiFilm), gaskets integrated with spacers (Deukum, 0.28 mm thickness), two outer anionic or cationic membranes to separate electrodic compartments and side ones (Selemion AEM or NAfion CM), creating more pairs of alternating high concentrated (HC) and low concentrated (LC) chambers.
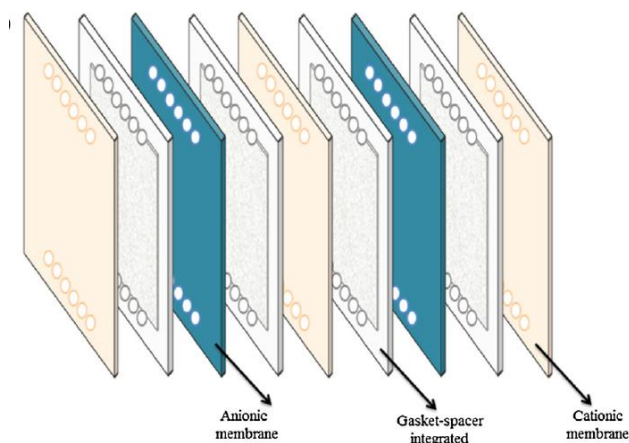
Figure 2.3 Reports the main components of the cell pairs**.**

Two peristaltic pumps (from General Control SpA) continuously fed the HC and LC solutions at a flow rate of 190 mL/min. Two or one hydraulic circuits were used for electrodic solution/s. When two separated recirculation systems were used, the two electrodic solutions were continuously recirculated to the electrode compartments and to two different reservoirs, by two peristaltic pumps (General Control SpA) with a flow rate of 75 mL/min (Figure 2.4a). When one single hydraulic circuit was used involving both cathode and anode compartments, the electrodic solution was continuously recirculated between the two electrodic compartments by one

58

peristaltic pump (General Control SpA) with a flow rate of 75 mL/min using just one reservoir (Figure 2.4b)
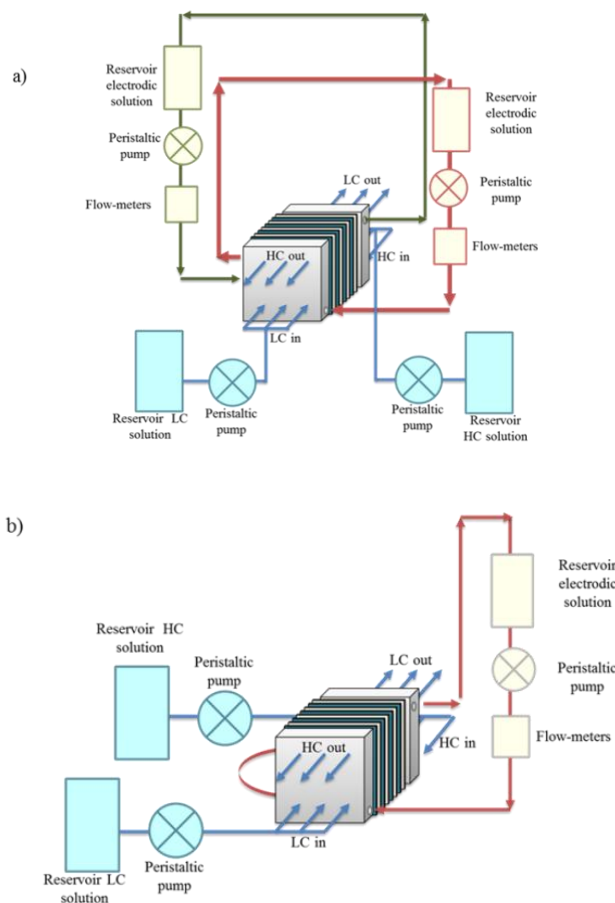
Figure 2.4 Scheme of the device (a) with four different circulating solution: HC, LC anodic and cathodic solution and (b) with three different hydraulic circuit for HC, LC and only one electrodic solution.

For water/Na_2SO_4 system, two different electrodic patterns were first used for anode and cathode compartments in order to avoid the possible formation of hazardous gaseous mixtures of hydrogen and oxygen, thus leading to a very fast increase of pH in the cathodic compartment and to a corresponding decrease in the anodic one as an

effect of water reduction and oxidation reactions, respectively. Then, some experiments were performed with the water/Na_2SO_4 system with only one electrodic system, in order to avoid strong variations of pH, equipped with two reservoirs where oxygen and hydrogen gas were removed by nitrogen flux (Figure 2.5).
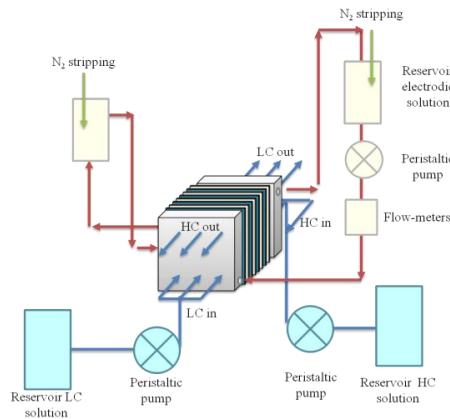
Figure 2.5 Simple scheme of system assembled when water/Na_2SO_4 is used in the electrode compartments.

The Figure below shows a photo of the main components used to assemble a stack to reverse electrodialysis
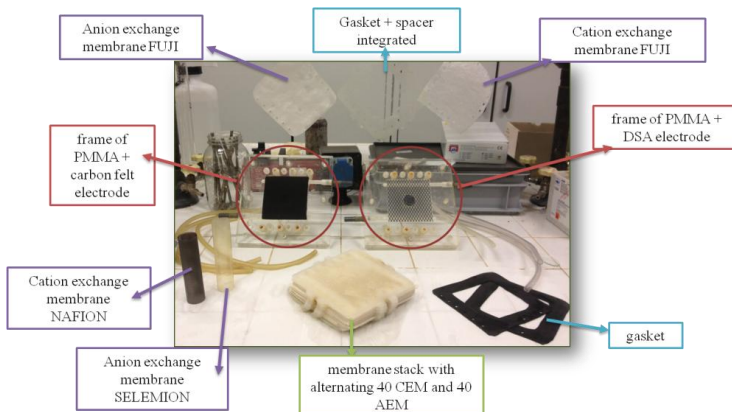
Figure 2.6 Photo that reports the main components of a RED stack assembled with 40 membrane pairs.

2.2 CHEMICALS

2.2.1 Electrolyses experiments

Generate electric energy

The solutions used in anode and cathode compartments were prepared using distilled water, 0.035 M Na_2SO_4 (Sigma Aldrich) or NaCl (Sigma Aldrich) adjusting the pH value to the target one by adding proper amounts of H_2SO_4 (Sigma Aldrich), HCl (Sigma Aldrich) or NaOH (Applichem). The central compartment solution in the three compartment cell was constituted by an aqueous solution of NaCl.

$FeCl_2$ and $FeCl_3$ from Sigma Aldrich, $K_3[Fe(CN)_6]$ and $K_4[Fe(CN)_6]$ from Labochem and Fe(III)-EDTA sodium salt from Sigma Aldrich were used as received. Fe(II)-EDTA was prepared according to reference [1] with Na_2EDTA (Carlo Erba) and $FeSO_4*7H_2O$ (Carlo Erba). The supporting electrolyte was composed by 0.035 mol/L Na_2SO_4 (Sigma Aldrich) and H_2SO_4 (Sigma Aldrich) or NaOH (Applichem) or by NaCl (Sigma–Aldrich). All these chemicals were analytical grade.

Abatement of recalcitrant organic pollutant

The aqueous solution used in the electrode compartment was prepared using deionized water, 150 mg/L of Acid Orange 7 (AO7) (Sigma Aldrich), 0.035 M Na_2SO_4 (Sigma Aldrich) or 1 g/L NaCl (Sigma Aldrich) as supporting electrolyte adjusting the pH to the proper value by adding proper amounts of H_2SO_4 or HCl (Sigma Aldrich).

For electro-Fenton processes (EF), $FeSO_4$ (0.5 mM) was added to the solution and compressed air was fed (0.35 L/min) to the electrodic solution by a diffuser.

Abatement of recalcitrant inorganic pollutant

To monitored the removal of Cr(VI) only experiments in divided cell were carried out. The anodic compartment was filled by 70 mL of water solution with 0.1 M of

Na$_2$SO$_4$ as supporting electrolyte, 0.5 mg/L of Cr(VI) in the form of Cr$_2$O$_7^{2-}$ adding H$_2$SO$_4$ to correct the pH. The water solution used in the catodic compartment was prepared using always 0.1 M of Na$_2$SO$_4$ as supporting electrolyte and H$_2$SO$_4$ to adjust the pH.

2.2.2 RED experiments

In all experiments, NaCl solutions of different molarities were annotated as "river", "sea" and "brine". They correspond to following sodium chloride concentrations: river 0.01 mol/L, sea 0.5 mol/L, and brine 5.0 mol/L.

Generate electric energy

Electrodic solution used in the stack for the generation of electric energy was prepared by dissolving into deionized water:

- Na$_2$SO$_4$ (0.04 M) (Sigma Aldrich) for water/Na$_2$SO$_4$ system;
- NaCl or KCl (0.01-01-0.5 M) (Sigma Aldrich) for water/NaCl system;
- FeCl$_2$ and FeCl$_3$ or [Fe(CN)$_6$]$^{4-}$/[Fe(CN)$_6$]$^{3-}$ (0.3 M) from Sigma Aldrich or (0.3 M) from Labochem for iron redox couple systems.

All these chemicals were analytical grade. pH was adjusted to the target initial (pH = 2) value by adding proper amounts of H$_2$SO$_4$ (Sigma Aldrich) or HCl (Sigma Aldrich).

Various cathode and anodes were used: carbon felt (Carbone Lorraine) or titanium meshes coated with Pt (Magneto) cathode and titanium meshes coated with IrO$_2$–Ta$_2$O$_5$ or RuO$_2$–IrO$_2$ (Magneto) anode (geometric surface area 100 cm^2).

Abatement of recalcitrant pollutants

For experiments carried out in order to evaluate the abatement of recalcitrant pollutants, Acid Orange 7 and Cr(VI) were selected as model pollutants.

For the abatement of AO7 the two electrodic chambers contained a carbon felt cathode (Carbone Lorraine) and a titanium meshes coated with Ru-Ir anode (Magneto). The following solutions were used for electrode compartments:

• for experiments performed with two separated solutions flowing in the electrodic compartments, anodic solution contained 150 mg/L of Acid Orange 7 (AO7), NaCl or KCl (0.085 M) and HCl (pH = 2) and cathodic solution AO7 (150 mg/L), Na_2SO_4 (0.085 M), 0.5 mM $FeSO_4*7H_2O$ and H_2SO_4 (pH = 2);

• for experiments performed with one hydraulic circuit connecting both cathodic and anodic compartments, the electrolytic solution contained 150 mg/L of Acid Orange 7 (AO7), NaCl or KCl (0.085 M) and 0.5 mM $FeSO_4*7H_2O$ adjusting the pH value to 2 (by addition of H_2SO_4).

For experiments carried out in order to evaluate the reduction of Cr(VI), the two electrode chambers contained a carbon felt cathode (Carbone Lorraine) chosen according to the pertaining literature [2-4] and a titanium meshes coated with Ti/IrO_2-Ta_2O_5 anode (Magneto). Experiments were performed with two separated solutions flowing in the electrodic compartments:

• anodic solution contained 0.1 M Na_2SO_4 (Sigma-Aldrich) and H_2SO_4 (pH = 2)

• cathodic solution contained Cr(VI) (Sigma-Aldrich) with an initial concentration of 2, 25 and 50 mg/L, 0.1 M Na_2SO_4 (Sigma-Aldrich) as supporting electrolyte at a pH = 2 (H_2SO_4).

2.3   ANALYSIS EQUIPMENTS

pH

The pH measurements were carried out with a HI 8314 membrane pH-meter, calibrated with three buffers of pH 4, 7 and 10 purchased from Hanna for the anodic oxidation experiments.

Spectrophotometric UV analysis

The concentration of the partners of the redox couples (Fe(II)/Fe(III)), AO7, Cr(VI) were estimated by photometric UV analyses.

- The concentration of Fe(II) was evaluated for experiments performed with $FeCl_2/FeCl_3$ after treatment with phenatroline. Ions Fe^{2+} form a red colour complex with 1,10-phenantrolin with λmax = 510 nm. The analyses were effectuated by measuring the absorbance for each sample using Agilent Cary 60 UV Spectrophotometer.

In order to detect the concentration of iron (II) ions by spectrophotometric analyses, samples were prepared putting 1 mL of phenantrolin + 1 mL of a buffer solution constituted of sodium acetate/ acetic acid + xx mL of H_2O if is necessary to dilute + (4- xx mL) of the sample taken from the electrochemical cell during the experiments or prepared for the calibration curve.

In order to estimate the concentration of total iron (i.e. iron (II) and iron (III)), is necessary to add some ascorbic acid, which by its high reducing power, reduce Fe^{3+} ions to Fe^{2+} and make the ionic form of iron (II) stable. After 30 minutes is possible to analyse these samples.

- The concentration of ferrocyanide and ferricyanide were evaluated at 320 and 420 nm by using Agilent Cary 60 UV Spectrophotometer.
- In the case of active chlorine a Merck Chlorine test containing dipropyl, p-phenylenediamine (DPD) was used.
- The removal of color was monitored from the decay of the absorbance (A) at λ = 482 nm for AO7 [5].
- The removal of Cr(VI) was monitored by using Agilent Cary 60 UV Spectrophotometer. Cr(VI) was detected at λ = 540 nm, after treatment with 1,4-diphenylcarbazide and its concentration was determined after proper calibration using the Lambert Beer law. The lower detection limit for Cr(VI) was 0.01 mg/L.

COD (Chemical Oxygen Demand)

The trend of some of the oxidative processes was also monitored by measuring the COD. This parameter represents the measurement of the oxygen equivalent to the organic matter contained in a sample that is susceptible to be oxidized by a strong chemical oxidant. The COD value is given in concentration of oxygen (mg/L O_2) COD has been determined by the potassium dichromate method according to the following reaction:

$$C_xH_yO_z + m\ Cr_2O_7^{2-} + 8m\ H^+ \rightarrow x\ CO_2 + (y+8m)/2\ H_2O + 2m\ Cr^{3+} \qquad \text{(react. 2.1)}$$
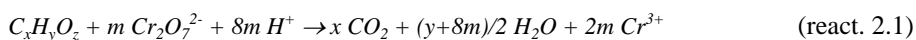
where m = (2x/3) + y/6 − z/3.

The oxidation takes place by adding 2 or 3 mL of solution (depending on the range of the concentration of COD) to a Merck vial containing both silver compound as catalyst to oxidize resistant organics and mercuric sulphate to reduce interference from the oxidation of chloride ions by dichromate in sulphuric acid. After reaction of the mixture for 2 h at 148 °C in a thermoreactor (Merck, Spectroquant Thermoreactors TR320) and cooling at room temperature, the COD value was obtained from the spectrophotometric absorbance of Cr^{3+} formed, by an Agilent Cary 60 UV Spectrophotometer.

TOC (total organic carbon)

Total Organic Carbon (TOC) analysis of a solution is based on the complete conversion of all carbon atoms present in the sample up to CO_2 and constitutes another global parameter that serves to evaluate the degree of mineralization of a pollutant during its destruction. This technique allows evaluating the degree of mineralization of the starting pollutant during the electrochemical processes. This parameter was analyzed by a TOC analyzer Shimadzu VCSN ASI TOC-5000 A. The TOC value is given in milligrams of carbon per liter (mg/L), performing the average of three consecutive measurements with a precision of about 2%. The calibration of the equipment was made using potassium hydrogen phtalate standards in the range between 20 and 400 mg/L.

Cyclic Voltammetry (CV) is performed by cycling the potential of a working electrode, and measuring the resulting current. Cyclic voltammetry was performed at compact graphite and Ti/IrO_2–Ta_2O_5 electrodes using an Autolab PGSTAT12 potentiostat to study the behavior of redox coupled.

HPLC

Degradation products of AO7 were identified by HPLC analyses using an Agilent HP 1100 HPLC equipped with UV–Vis detector (adopted λ = 210 nm) and comparison with pure standards [6]. The presence of carboxylic acids (oxalic, maleic, malonic and lattic acids from Sigma–Aldrich) were identified by Prevail Organic 5µ column. The mobile phase was a buffer solution containing KH_2PO_4 (Sigma Aldrich +99%) and H_3PO_4 at a pH of 2.5, prepared with water Sigma Aldrich G-chromasolv for gradient elution. The eventual presence of chloro-organic compounds was evaluated by HPLC-MS Thermo TSQ Quantum Access. The HPLC column was ZIC-HILIC 150 mm x 2.1 mm, 5 µm. The mobile phase was CH_3CN–CH_3COONH_4 10 mM (90:10 v/v).

2.4   ELECTROCHEMICAL PARAMETERS

In RED experiments, power production was studied by measuring both the potential drop across a fixed external resistance (range 4.6 Ω) and the current intensity by a multimeter Simpson. The overall external resistance was given by the contribution of an external resistance (range 1–160 Ω, selected value 1 Ω) and that of cables and an amperometer (with an estimated resistance of about 3.6 Ω). Power was calculated by multiplying the electrical current and the total cell potential. Reported power densities were based on the cathode geometric area (100 cm^2). Power production during batch recycle experiments was measured in the same way across a fixed external resistance (about 4.6 Ω). Power density can be computed by the ratio between the power and the total area of all membranes or the total area of cationic

membranes (Pmem) or the geometric area of cathode (P). In Figure 2.7 it is possible see a simple scheme of electric circuit containing a load (resistor), an amperometer and a voltmeter.
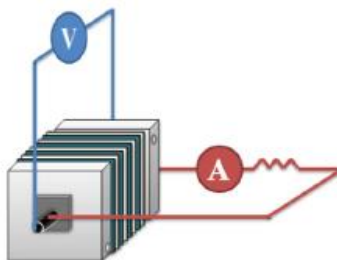
Figure 2.7 Scheme of electric circuit connected to the stack.

2.5   REFERENCES

[1] J.G. Ibanez, C.S. Choi, R.S. Becker, Aqueous redox transition metal complexes for electrochemical applications as a function of pH, J. Electrochem. Soc. 134 (1987) 3083-3089.

[2] M. Abda, Z. Gavra, Y. Oren, Removal of chromium from aqueous solutions by treatment with fibrous carbon electrodes: column effects, J. Appl. Electrochem.19 (1991) 734-739.

[3] E.P.L. Roberts, H. Yu, Chromium removal using a porous carbon felt cathode, J.Appl. Electrochem. 32 (2002) 1091-1099.

[4] I. Frenzel, H. Holdik, V. Barmashenko, D.F. Stamatialis, M. Wessling, Electrochemical reduction of dilute chromate solutions on carbon felt electrodes, J.Appl. Electrochem. 36 (2006) 323-332.

[5] S. Garcia-Segura, F. Centellas, C. Arias, J.A. Garrido, R.M. Rodriguez, P.L. Cabot, E. Brillas, Comparative decolorization of monoazo, diazo and triazo dyes by electro-Fenton process, Electrochim. Acta 58 (2011) 303-311.

[6] O. Scialdone, A. Galia, S. Sabatino, Abatement of Acid Orange 7 in macro and micro reactors. Effect of the electrocatalytic route, Appl. Catal. B: Environ. 148–149 (2014) 473-483.

3.   RESULTS AND DISCUSSION

The performances of reverse electrodialysis (RED) processes depend on several factors, including the nature of the electrode material and of the redox couple adopted to make possible the conversion between electric power and chemical potential. A preliminary experimental campaign was conducted via electrolysis to understand which are the best operating conditions to obtain optimal results.

3.1   SELECTION OF REDOX PROCESS AND OPTIMIZATION OF ELECTRODE MATERIALS

A large number of studies was devoted to the behavior of redox couples for numerous applications. In particular, redox systems containing iron species are regarded as very promising for their low toxicity, high stability and coupled with high presence in nature.

Redox processes (V vs. SHE)	ΔV (V)	Stability of redox species and electrodes	Toxicity	Examples of applications
$H_2O \rightarrow 2H^+ + 0.5\,O_2 + 2e^-$ (0.99 V at pH 2) $H_2O + e^- \rightarrow OH^- + 0.5\,H_2$ (0.83 V at pH = 14)	2.4–2.5[a]	Very high	No with suitable supporting electrolytes	Electrolytic splitting of water for hydrogen generation [1] electrodialysis (ED) Investigations for SGPRE [2-4].
$Cl^- \rightarrow 0.5\,Cl_2 + e^-$ (1.36 V) $H_2O + e^- \rightarrow 0.5\,H_2 + OH^-$ (0.83 V at pH = 14)	2.25–2.35[a]	Very high	Possible concerns for chlorine, active chlorine, chlorate and perchlorate potential formation.	Production of chlorine and soda [14] ED investigations for SGP-RE [2,5,7]
$Fe^{3+} + e^- \rightarrow Fe^{2+}$ (E = 0.77 V)	0.4–0.6[b]	Very high for pH < 3–4 and in absence of air [this study]	Very low in water solutions	Widely adopted in fenton and electro- fenton applications Investigations for SGP-RE [2,this study]
$[Fe(CN)_6]^{3-} + e^- \rightarrow [Fe(CN)_6]^{4-}$ (E = 0.356 V)	0.2–0.4[b]	Very high in absence of air and light [this study]	Very low toxicity release of toxic gas after reaction with strong acids. Possible release of HCN under no proper operative conditions [this study]	Widely adopted for studies on electrodes characterization. Investigations for SGP-RE [2,this study]
Fe(III)-EDTA + e^- → Fe(II)-EDTA (E = -0.13 V)	(-0.08)–(-0.2)[c]	Stable in the absence of light [8-10] for pH between 5.5–7[c] and 3–7[d,e]	EDTA widely used in foods and medicine (to remove excess iron from the body). Iron EDTA is recognized as safe for the food uses [11].	Foods and medicine

Table 3.1 main characteristics of investigated redox processes. [a] Computed by the sum of anode voltage on Ru at pH of 2, cathode voltage at Pt at pH 14 and Ohmic drops in the anode and cathode compartments at 1 mA/cm^2 estimated on the basis of literature [14]. [b] Computed on the basis of electrolyses in undivided cells at 1 mA/cm^2 at graphite electrode for Fe(III)/Fe(II) and at Iridium based electrodes for $[Fe(CN)_6]^{3-}$/$[Fe(CN)_6]^{4-}$. [c] The CV of a test sample was stable for at least 20 weeks at these pH. [d] Stability tested by a serie of CV. [e] Below a pH of 3, the complex appeared to decompose whereas at higher pH than 7, the solution became turbid.

On the basis of these considerations in this work I selected the following redox coupled iron-based: $FeCl_3/FeCl_2$, $[Fe(CN)_6]^{3-}/[Fe(CN)_6]^{4-}$ and Fe(III)-EDTA/Fe(II)-EDTA, chosen according by the literature data because they have a good potential for RED application. The results obtained operating with these redox couples were compared with the data collected using the classical system water/Na_2SO_4.

$FeCl_3/FeCl_2$

In order to test the stability of iron redox couple $FeCl_3/FeCl_2$, a cyclic voltammetric investigation was performed. Because in the presence of oxygen the iron rapidly passes from Fe^{3+} to Fe^{2+}, measures have been taken to prevent this transformation. A series of cyclic voltammetries was carried out to study the electroanalytical behavior of 20 mM of the iron couple in water solutions of Na_2SO_4 0.035 M at graphite electrodes at various scan rates (0.01 – 1 V/s) in the range 0-1 V vs SCE under nitrogen atmosphere. Fe(III)/Fe(II) couple is usually used at pH < 3 to prevent the precipitation of ferric oxyhydroxides; thus experiments were conducted at pH = 2. The E_p was about 190 mV at 10 mV/s, $i_{p,a}/i_{p,c}$ was close to 1 for all the tested scan rates where $i_{p,a}$ and $i_{p,c}$ are anodic and cathodic peak current densities, respectively. As shown in the Figure below, i_p changed linearly with the square root of the scan rate (Figure 3.1).
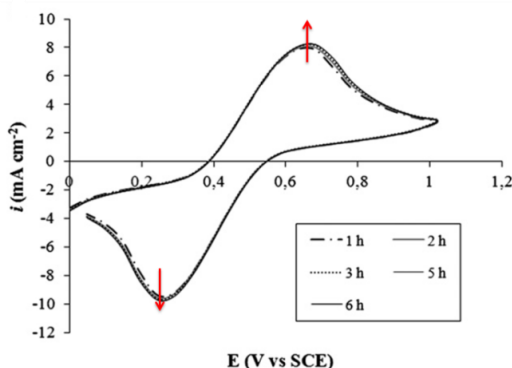
Figure 3.1 Cyclic voltammogram snapshots of $FeCl_3/FeCl_2$ performed at graphite in a water solution of Na_2SO_4 taken at 1 h intervals during potential cycling with a scan rate of 0.1 V/s at a pH of 2 under nitrogen atmosphere. T = 25 °C. V = 50 mL. Concentration of the couple 20 mM.

As shown in Figure 3.1, a slight increase of the current of the peaks associated to the Fe(II)/Fe(III) couple was observed increasing the working time (from 1 hour to 6 hours). This behavior cam be associated to an improvement and activation of the electrode area. Similar results were recorded using a pH solution of 3 but changes occurred working at pH 5 (Figure 3.2). Indeed, in the last case, if on one hand the shape of the cycles has not undergone great changes from the other side a slow but continuous decrease of both anodic and cathodic peaks was observed due to not stability of couple at pH > 3 (the solution became slightly turbid).
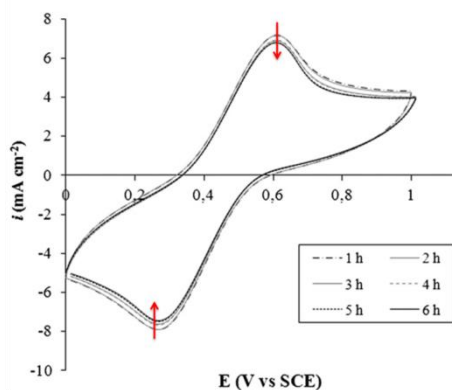
Figure 3.2 Cyclic voltammogram snapshots of $FeCl_3$/$FeCl_2$ performed at graphite in a water solution of Na_2SO_4 taken at 1 h intervals during potential cycling with a scan rate of 0.1 V/s at a pH of 5 under nitrogen atmosphere. T = 25 °C. V = 50 mL. Concentration of the couple 20 mM.

To test the stability of the redox couple in long time several electrolysis, experiments were carried out in undivided cell under nitrogen atmosphere, at an initial pH of 2, with a concentration of both iron species of 0.3 M and NaCl 0.5 M as supporting electrolyte. Electrolyses were conducted under amperostatic mode (10 mA/cm^2). In some experiments compact graphite was used as electrode materials (both as anode and as cathode), in other ones Pt was chosen as cathode electrode. As reported in Figure 3.3, working with compact graphite, good results were obtained along the entire duration of the experiment both as regards the stability of the concentration of the irons (5 days) that the pH of the solution.
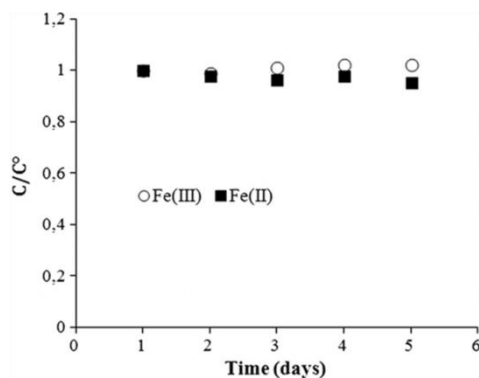
Figure 3.3 Concentration profiles of Fe(II) (■) and Fe(III) (○) with the time passed for long-time electrolysis perfomed with an initial concentrations of the couple FeCl$_3$/FeCl$_2$ of about 300 mM (each) and an initial pH of 2 at compact graphite electrodes in undivided cell with water solution of NaCl 0.5 M under amperostatic alimentation with a current density of 10 mA/cm^2 under nitrogen atmosphere.

The cell potential (0.4 - 0.5 V) and the electrode potentials did not show relevant changes both for duration of 5 days and for longer times (10). When compact graphite was changed with Pt a different behavior was recorded. Although the cell potential was reduced to about 0.15 V obtaining in this way minor overvpotentials and consequently minor cell potential, the system showed a change of the color due to the deposition of metallic iron after 3 hours of experiment.

Some amperostatic electrolyses were repeated in a three compartment cell equipped with anionic membranes to estimate the mass transfer across the membranes of iron ions from electrode compartments to the central compartment containing water solution with different concentration of NaCl. Figure 3.4 reports the results obtained testing different kind of anionic exchange membranes: Nafion, Selemion, Fumasep and Fuji. In the end compartments, the anode and the cathode processes occurred in the presence of an initial concentration of Fe(II) and Fe(III) both 0.3 M, in an aqueous solution with HCl (pH = 2). The central compartment was filled with a 0.5 M NaCl solution. As shown in Figure 3.4, a very slow decrease of the pH was observed in the central compartment while no appreciable drift of the pH was observed in the anode and cathode compartments after 3 h.
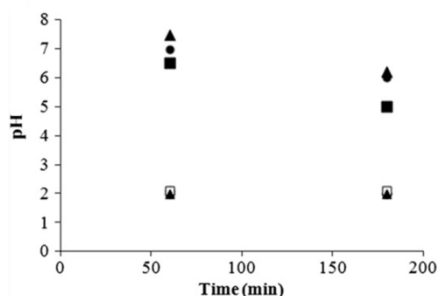
Figure 3.4 Reports the plot pH vs. time passed in the lateral and central compartments during electrolyses performed with DSA electrodes with the redox couple $FeCl_3/FeCl_2$ in a three compartment cell in the presence of Fumasep (triangle), Selemion (circle), Fuji (square) anionic membranes. Passage of cathode compartment: ▲●■. Passage of anode compartment: Δ○□. Passage of central compartment: ▲●■.

Instead, the passage in the central compartment of the redox couple and of the active chlorine depended drastically on the nature of the adopted anionic membrane. No significant passage of both species was observed with Selemion membranes (Figure 3.5).
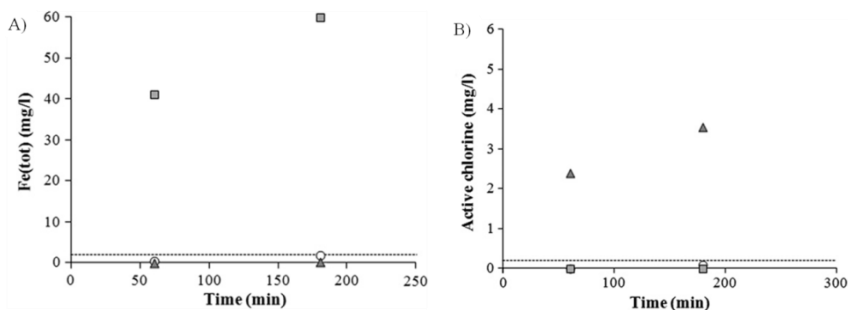
Figure 3.5 Reports the concentrations of Fe(tot) (A) and active chlorine (B) detected in the central compartment during electrolyses performed with DSA electrodes with the redox couple $FeCl_3/FeCl_2$ in a three compartment cell in the presence of Fumasep (triangle), Selemion (circle), Fuji (square) anionic membranes. Dashed line represents the Italian law limit for iron and active chlorine.

Some experiments were carried out in a two compartment cell (one compartment equipped with cathode, anode and reference and a water solution of NaCl 0.1 M, $FeCl_2/FeCl_3$ 0.3 M at a pH of 2; other compartment with a water solution of NaCl

73

0.1 M) separated by a Selemion membrane with a current density of 10 mA/cm^2 for 10 days, to evaluate the pH behavior of the electrode compartment. The electrode potentials and the concentrations of iron species did not change appreciably during the experiments while the pH of the electrode compartment did not show an appreciable increase during the whole experiments. On the basis of these experiment is possible to consider that because, in RED system the electrode rinse solution is continuously recirculated, the slow passage of protons to the central compartments will led inevitably to a continuous increase of the pH. Thus, a periodic acidification of the electrolytic solution could be required to avoid the precipitation of iron oxyhydroxides.
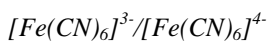
$[Fe(CN)_6]^{3-}/[Fe(CN)_6]^{4-}$

Also in this case, the electroanalytical behavior of the couple $[Fe(CN)_6]^{3-}$ /$[Fe(CN)_6]^{4-}$ was studied by cyclic voltammetry. A water solutions of Na_2SO_4 0.035 M containing various iron couple concentrations from 2 to 30 mM using DSA and graphite electrodes were studied at various scan rates (0.01 – 1 V/s). As reported in Figure 3.6, the cyclic voltammograms showed a symmetric wave for all the tested concentrations with $i_{p,a}$ and $i_{p,c}$ that increased linearly with the concentration.
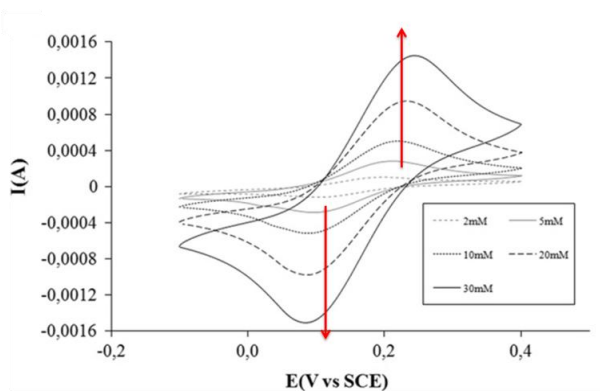
Figure 3.6 Reports the cyclic voltammograms with potential limits: -0.1 to 0.4 V/SCE at various concentrations: 2, 5, 10, 20, 30 mM or iron couple with scan rate of 0.1 V/s.

The ΔE_p was about 80 mV for compensated scans and $i_{p,a}/i_{p,c}$ was close to 1.

Extending the anodic potential limit to 1.1 V, the presence of an anodic peak at about 0.9 V and of two cathodic waves at about 0.75 e 0.5 V was observed. According to the literature [12] the anodic peak at 0.9 V can be attribute to the formation of a redox couple Prussian Blue/Berlin Green on the surface
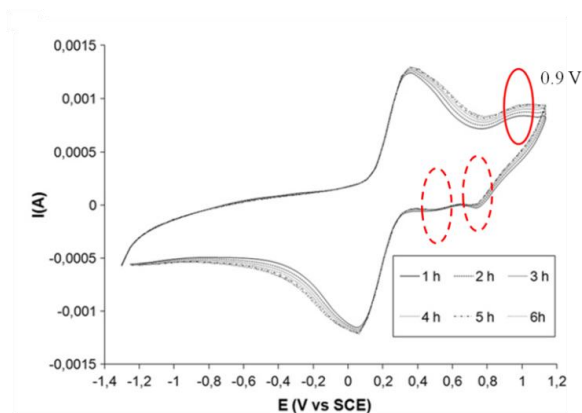
Figure 3.7 Reports the cyclic voltammograms with potential limits: -1.3 to 1.1 V/SCE at concentration of 10 mM of iron couple with scan rate of 0.1 V/s.

After six hours of experiment, the peak currents did not decrease. Thus, the formation of hydrogen cyanide can be excluded (typically the peak appears between -0.33 and 1.4 V [13]).

No presence of anodic and cathodic peak was recorded in the range -1.3 to 1.1 V/SCE when DSA (Ti/IrO$_2$–RuO$_2$) was used as electrodes. In this case a higher dimensional stability was obtained. When the potential of the DSA electrodes was cycled for six hours in the presence of ferro/ferricyanide couple, the anodic peak did not change appreciably while a very slight decrease of the cathodic one was observed. The cyclic voltammetric study was also perfomed in the presence of NaCl (4M). A drastic increase of the anodic current at potentials close to 1.2 V and 1.05 V for graphite and DSA electrodes, respectively, and the appearance of a cathodic peak at about 0.8–1 V were observed as a result of conversion of Cl$^-$ to active chlorine.

Several experiments were carried out using an undivided electrochemical cell to test the stability of redox couple in the time. Some precautions were necessary to avoid the oxidation of Fe(II) into Fe(III) and the formation of HCN in the presence of light

$$4[Fe(CN)_6]^{3-} + 12H_2O \rightarrow 4Fe(OH)_3 + 12HCN + 12CN^- \qquad \text{(react. 3.1)}$$
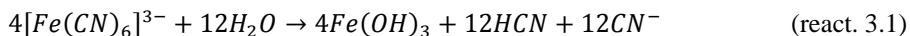
Thus experiments under dark and nitrogen atmosphere were carried out. Electrolyses were performed at DSA electrodes under amperostatic alimentation with a current density of 9 mA/cm^2. As shown in Figure 3.8, no appreciable variation of the concentration of the couple was observed for all the duration of the electrolysis.
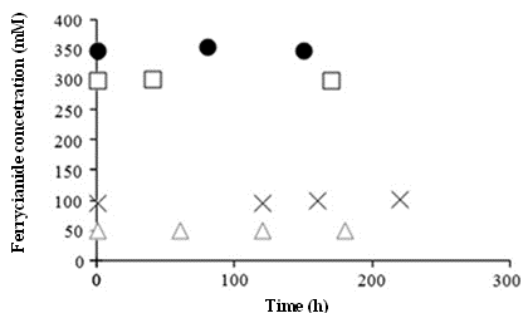
Figure 3.8 Concentration profiles of [Fe(CN)$_6$]$^{3-}$ with the charge passed for long-time electrolyses performed with different initial concentrations of the couple (50 (Δ) 100 (x), 300 (□), 360 (●) mM) at DSA electrodes in undivided cell with water solution of Na$_2$SO$_4$ 0.1 M under amperostatic alimentation with a current density of 9 mA/cm^2 under dark and nitrogen atmosphere.

The current density applied corresponded to a high anodic potential of about 1.4 V vs. SCE that caused the reaction between ferrocyanide with free ion Fe(III) and ferricyanide with Fe(II). Indeed, during the experiment a change of color was recorded and at the end the electrode which presented a blue deposition (HCN compounds) on its surface. At these potentials, the anodic oxidation of water is likely to occur with the formation of protons and a strong local acidification of the solution in the porous structure of the anode, thus allowing the acid promoted decomposition of ferricyanide to free Fe(III) by the reaction

$$[Fe(CN)_6]^{3-} \rightarrow Fe^{3+} + 6CN^- \qquad \text{(react. 3.2)}$$

that is expected to take place at very acidic pH. To limit the formation of these compounds it is necessary to work with a limiting current (eq. 3.1) for the oxidation of ferrocyanide strongly higher than the applied current and as a consequence with higher concentration of ferrocyanide or lower current densities

$$i_{lim} = \frac{F\mathcal{D}[Ferrocyanide]}{\delta} \qquad\qquad \text{(eq. 3.1)}$$

where F is the Faraday constant, $\mathcal{D}$ the diffusion coefficient, *[Ferrocyanide]* the bulk concentration of ferrocyanide, and δ the thickness of the stagnant layer.

To confirm the effect of the current density, some electrolyses were carried out using 9.5 and 39 mA/cm^2. As expected, working at 9.5 mA/cm^2 the anode potential increased up to 1.4 V, the color of the solution changed and after 6 days the anode presented a marked blue color. Several experiments were reproduced using different concentration of species (0.05-0.36 M). Decreasing the concentration of iron ferrocyanide, anode collapsed and showed a blue coloration, the presence of iron(III) was detected and the anode potential increased during the experiment up to about 1.3 V vs. SCE after few hours.

Some experiment were repeated using compact graphite as electrodes because less expensive than DSA electrodes. Also in this case no appreciable modification was observed under optimal operative conditions.

As in the case of $FeCl_2$/$FeCl_3$, also with ferrocyanide/ferricyanide couple the passage of ion across the ion exchange membranes was evaluated. Three compartment cells were used putting in the central zone various concentrations of NaCl (0, 0.5, 5 M) and Fumasep, Nafion and Fuji cationic membranes were selected. In the presence of Fumasep membrane no presence of ferrocyanide and ferricyanide in the central compartment was observed in all the experiments. When the concentration of NaCl was increased to 5 M, a concentration of active chlorine of about 3 mg/L was detected that is higher than the Italian limit value of 0.2 mg/L (of course is necessary to consider that 1 hour a contact time drastically higher with respect to that expected in a stack for RED, in which the solutions are recirculated).

Fe(III)-EDTA/Fe(II)-EDTA

Same experiments were carried out using Fe(III)-EDTA/Fe(II)-EDTA as iron couple. In literature, the chemical stability of Fe(III)-EDTA was shown to be dependent on pH, exposure to light and temperature [8] while Fe(II)-EDTA is easily oxidized to Fe(III)-EDTA in the presence of air [9]. The electroanalytical behavior of the couple Fe(III)-EDTA/Fe(II)-EDTA was here studied in water solutions of Na_2SO_4 0.035 M at DSA and graphite electrodes at various scan rates (0.01 − 0.1 V/s) at a pH of 7 in the range -0.5 + 0.2 V vs. SCE. The cyclic voltammogram on a graphite electrode showed a symmetric wave for all the tested scan rates. The ΔE_p was about 120 mV and $i_{p,a}/i_{p,c}$ was about 0.95 at 10 mV/s. As shown in Figure 3.9 experiments were repeated for long time.
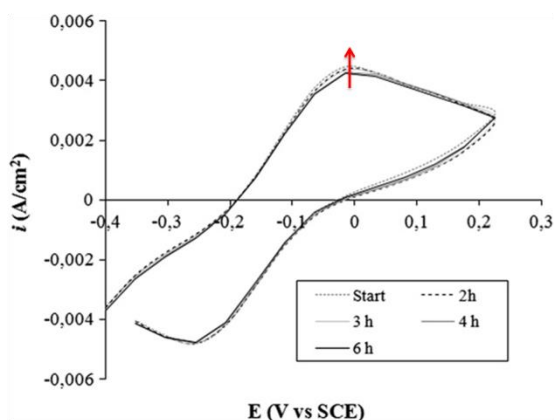
Figure 3.9 Cyclic voltammograms of Fe(III)-EDTA/Fe(II)-EDTA performed at graphite in a water solution 0.035 mM Na_2SO_4 under dark in nitrogen purged solution. Cyclic voltammogram snapshots taken at 1 h intervals during potential cycling in 10 mM Fe(III)-EDTA/Fe(II)-EDTA solution with a scan rate of 0.1 V/s. T = 25 °C. V = 50 mL.

After 6 hours the cathodic peak current did not change while a very slight decrease of the anodic one was observed, thus suggesting a very slow degradation of Fe(II)-EDTA. When the electrodes were changed (utilization of DSA) a lower ratio of $i_{p,a}/i_{p,c}$ of about 0.82 was measured.

Electrolyses performed in undivided cell under amperostatic alimentation with a current density of 2 mA/cm^2 recorded a continuous decrease of the concentration of Fe(II)-EDTA while the total concentration of soluble iron did not change appreciably. The anodic potential increased from 0.12 to 1.4 V and the solution changed its yellow color to a red and contained some precipitates. This suggests that iron(III) was formed by decomposition of Fe(II)-EDTA, and that the precipitates were Fe(OH)$_3$. When experiments were repeated observing the cathode potential the decomposition process did not involve significantly the Fe(III)-EDTA and there was no change in the system. To have more information on the process, few experiments were repeated with a very high oxygen overpotential anode such as Boron doped diamond (BDD). In the case of BDD the anode potential reached values of about 1.4 V, too low for the oxygen evolution reaction on BDD, thus suggesting that the decomposition of Fe(EDTA) takes place.

Water/Na$_2$SO$_4$ system

Before carrying out RED experiments, another electrode system has been studied. This system showed no iron ions but only an aqueous solution containing Na$_2$SO$_4$ as supporting electrolyte. Electrolysis experiments were carried out using a three compartment cell, where in anode and cathode compartments were occurred the oxidation and reduction of water, to evaluate the passage of species between electrode and lateral compartments. Amperostatic electrolyses were performed in cells equipped with cationic membranes to avoid the passage of chloride ions to the anode compartment and that of hydroxyl ions from the cathode to the confining one. The electrode used were: Ti/IrO$_2$Ta$_2$O$_5$ and Ni as anode and cathode, respectively. A decrease of the pH was observed in the anode compartment as a result of the anodic process of water coupled with the formation of active chlorine (Figure 3.10A). About this, the formation of active chlorine in the anode compartment was dependent on the nature of the membrane. As reported in Figure 3.10B when nafion membranes were used a limitation of migration of Cl$^-$ was recorded. The passage of protons from the anodic compartment to the central one caused a slow decrease of the pH also in the central compartment (Figure 3.10A).
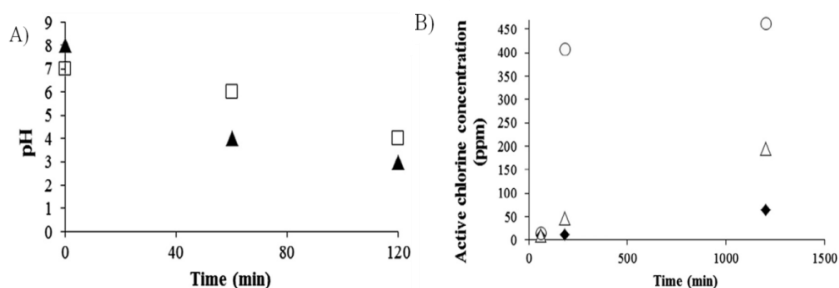
Figure 3.10 Electrolyses performed with Ti/IrO$_2$–Ta$_2$O$_5$ anode and Nickel cathode in the presence of Nafion (♦), Selemion (Δ), and Fuji (○) cationic membranes in a three-compartment cell. Lateral compartments contain water solution of Na$_2$SO$_4$ (20 mM), central compartment water solution of 0.5 M NaCl. (A) reports the plot pH vs. time passed in anodic and central compartments with Nafion membrane while (B) reports the concentrations of active chlorine detected in the anode compartment.

With all the tested membranes and with 0.5M of NaCl, the concentration of active chlorine was negligible in the central compartment also after many hours with respect to the law limits for discharged waters. Only when the concentration of NaCl was increased in central compartment a low concentration of active chlorine was detected. No formation of chlorite, chlorate and toxic perchlorate was detected both in the anode and central compartments.

3.2   GENERATION OF ELECTRIC CURRENT

In this section of the thesis the possible utilization of various redox processes (reduction/oxidation of iron species, oxidation and reduction of water, oxidation of chlorine and reduction of water) was studied in a stack equipped with 10–50 cell pairs. The effect of selected redox processes on power density output and eventual contamination of saline solutions flowing in the stack was evaluated in detail. The effect of the number of cell pairs and of the concentration of saline solutions was also investigated.

Effect of the redox processes

Different redox systems were studied in a stack equipped with 40 cells pair to evaluate the effect of redox processes on the performances of reverse electrodialysis. Experiments were carried out with different redox systems:

- water/Na_2SO_4 (0,04 M) (Cationic Nafion external membranes),
- water/KCl (0,085 M) (Cationic Nafion external membranes),
- $FeCl_2$/$FeCl_3$ (0.3 M) (Anionic Selemion external membranes),
- $[Fe(CN)_6]^{4-}$/$[Fe(CN)_6]^{3-}$ (0.3 M) (Cationic Nafion external membranes)

with an external resistance varied between 1 and 160 Ohm.

When water/Na_2SO_4 was used as electrodic solution it was necessary to use a system with two separated hydraulic circuit for anodic and cathodic solutions in order to avoid the possible formation of hazardous gaseous mixture of hydrogen and oxygen. As shown in the following Figure 3.11 the power output P was strongly dependent on the selected redox processes and increased with the following order:

P(water/Na_2SO_4) < P(water/KCl)<< ($FeCl_2$/$FeCl_3$) < P($[Fe(CN)_6]^{4-}$/$[Fe(CN)_6]^{3-}$)

which is consistent at least from a qualitative point of view with the trend of potentials required to drive the corresponding redox processes (see Table 3.2).
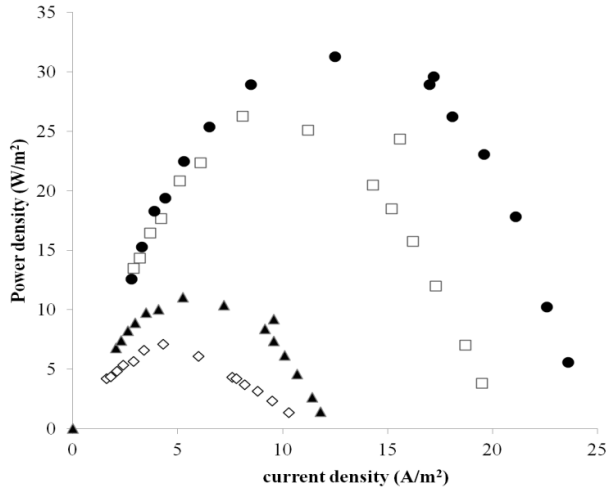
Figure 3.11 Plot of power density (computed as the ratio between the power and the geometric area of electrode) vs. current density recorded in a stack of 40 cells pairs with different redox systems: ($\Diamond$) water/Na_2SO_4 (0,04 M) at Pt cathode and Ti/ $IrO_2Ta_2O_5$ anode (Nafion CEM), ($\blacktriangle$) water/KCl (0,085 M) at Pt cathode and Ti/RuO_2-IrO_2 anode (Nafion CEM), ($\square$) $FeCl_2$/$FeCl_3$ (0.3 M) at Carbon Felt electrodes (Selemion AEM), ($\bullet$) $[Fe(CN)_6]^{4-}$/$[Fe(CN)_6]^{3-}$ (0.3 M) at Carbon Felt cathode and Ti/IrO_2Ta_2-O_5 anode (Nafion CEM) with an external resistance varied between 1 and 160 Ohm with fixed HC (NaCl 0.5 M) and LC (NaCl 0.01 M) compositions.

Of course, in agreement with eqs

$$\Delta E = OCV - IR_{stack} - \Delta E_{redox} \qquad \text{(eq. 3.2)}$$

$$\Delta E_{redox} = E_{an} - E_{cat} + \eta_{an} - \eta_{cat} \qquad \text{(eq. 3.3)}$$

where E_{an} and E_{cat} are the potential of process in anode and cathode respectively while η_{an} and η_{cat} represent the energetic losses near the electrodes, the best results are obtained working with iron couples because the thermodynamic potential required to drive the redox reactions is null (since opposite anodic and cathodic reactions are involved) and the electrode potentials are only given by overpotentials that, according with the data collected during experiments of electrolysis, at adopted electrodes are lower for $[Fe(CN)_6]^{4-}$/$[Fe(CN)_6]^{3-}$ couple.

The main data recorded during the experimental campaign are summarized in Table 3.2.

Redox proc and electrodes	Max power (W)	Max Power density respect to geometric area of chatode (P)	Max power respect to total area of cationic membranes (W/m²)	ΔV	Current Density (A/m²)
$H_2O \rightarrow 2H^+ + 0.5\ O_2 + 2e^-$ $H_2O + e^- \rightarrow OH^- + 0.5\ H_2$	0,07	7,1	0,18	1,8	4,1
$Cl^- \rightarrow 0.5\ Cl_2 + e^-$ $H_2O + e^- \rightarrow 0.5\ H_2 + OH^-$	0,11	11,03	0,27	2,4	5,3
$Fe^{3+} + e^- = Fe^{2+}$	0,26	26,2	0,66	3,24	8,1
$[Fe(CN)_6]^{3-} + e^- = [Fe(CN)_6]^{4-}$	0,31	31,25	0,78	2,5	12,5

Table 3.2 Maximum power output for adopted redox system

Regarding the system water/Na_2SO_4 two different configuration of stack were used. In a first moment, as mentioned before, a stack assembled with two hydraulic circuits was used to limit the possibility to create a mixture explosive due to the formation of H_2 and O_2. Using this experimental set up a very highly instability of electrode system was recorded. Indeed, the half processes are characterized by a very fast increase of pH in the cathodic compartment and to a corresponding decrease in the anodic one as an effect of water reduction and oxidation reactions, respectively. In order to limit the passage of ion from electrode compartment to the side one cation exchange membrane Nafion was used according with the results showed in paragraph 3.1. If in one hand this membrane limits the passage of chlorine and OH^- on the other hand allows the transfer of H^+ in the saline compartments leading the pH to a value of 3. In order to limit the drastic change of pH a series of experiment was carried out using a stack with only one electrode system in which the solution was recirculated between anode and cathode compartments stripping with N_2 the gases formed. As shown in Table 3.2, the power output with water/Na_2SO_4 is much lower than that obtained with the other systems because, in this case, the redox reactions require relevant thermodynamic potentials coupled with high overpotentials. Results slightly better were obtained using KCl as electrolyte.

Several experiment were carried out using KCl both as supporting electrolyte and as redox species.
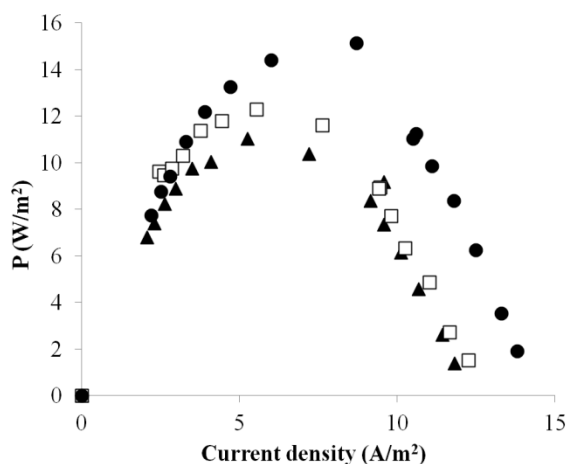
Figure 3.12 Plot of power density (computed as the ratio between the power and the geometric area of electrode) vs. current density recorded in a stack of 40 cells pairs with KCl at Pt cathode and Ti/RuO$_2$–IrO$_2$ anode. Concentration of KCl: 0.085($\blacktriangle$), 0.1 ($\square$) and 0.5 M ($\bullet$). Anionic Selemion external membranes. External resi stance varied between 1 and 160 Ohm with fixed HC (NaCl 0.5 M) and LC (NaCl 0.01 M) compositions.

As shown in Figure 3.12, an increase of KCl concentration gave rise to higher power output. This is probably due to two concomitant effects: (i) higher concentrations of KCl enhance the conductivity of the electrode compartment lowering the resistance of the stack and (ii) higher concentrations of KCl avoid energetic penalties due to concentration polarization by chlorides in the anodic diffusion layer.

Among the redox couple studied, the couple FeCl$_2$/FeCl$_3$ can be considered one of the best candidates for reverse electrodialysis applications for different reasons: high stability under proper operative conditions in terms of high concentrations of species, low pH and absence of air; very low toxicity; very low energetic penalty and low cost of the redox components and electrodes.

Effect of the number of cells pair

The measurements were repeated using FeCl$_2$/FeCl$_3$ as redox species with a stack equipped with a different number of cells pair: 10, 40 and 50. Experiments were carried out using carbon felt as electrodes and fed concentrated (0.5 M) and dilute solutions (0.01 M) of NaCl. As shown in Table 3.3 and Figure 3.13, when the

84

number of membrane pairs was increased from 10 to 50, a drastic increase of power density output occurred at higher values of current density and cell potential. Working with 10 cell pairs, the power density respect to the geometric area of the electrode was 3.9 W/m^2, corresponding a total cell potential of 1 V and current density of 4.5 A/m^2 (Figure 3.13).

Number of cell	Max power (W)	Max Power density respect to geometric area of chatode (P)	Max power respect to total area of cationic membranes (W/m²)	ΔV	Current density (A/m²)
10	0,039	3,9	0,39	0,97	4,4
40	0,25	25,1	0,625	2,44	11,2
50	0,36	36,4	0,73	2,45	13,5

Table 3.3 Effect of number of membrane pairs.

When the number of membrane pairs was increased to 40 and 50, a drastic increase of power density output occurred at higher values of current density and cell potential.
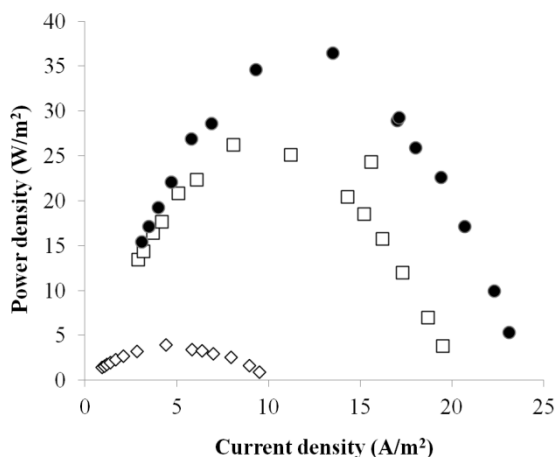
Figure 3.13 Plot of power densities (computed as the ratio between the power and the geometric area of electrode) vs. current density recorded in a stack equipped with 10 (◊), 40 (□) and 50 (●) membrane pairs for $FeCl_2/FeCl_3$ with carbon felt electrodes with an external resistance varied between 1 and 160 Ohm with fixed HC (NaCl 0.5 M) and LC (NaCl 0.01 M) compositions. The electrodic solution contained $FeCl_2/FeCl_3$ (0.3 M), NaCl (0.1 M) as supporting electrolyte and HCl (pH = 2) and was under nitrogen atmosphere. Flow rate of HC and LC solutions: 190 mL/min. Flow rate of electrodic solution: 75 mL/min. Outer membranes: Anionic-exchange Selemion. Inner membranes: Fuji AEM and CEM.

The enhancement of power density was a result of the lower impact of the energetic loss due to the redox processes compared with the overall power generation. According to electrolyses experiments, the power loss due to the redox processes at a current density of about 10 A/m² can be roughly estimate to be close to 0.03 – 0.035W (3 – 3.5 W/m² with respect to the cathode surface) which represents an high value for the experiments carried out with 10 cell pairs (maximum power output 0.039 W) but quite small if compared with the maximum power output observed for experiments performed with 50 cell pairs (0.36 W).

Effect of salinity gradient

In order to evaluate the effect of the salt concentration of HC and LC compartments, it is useful to remember that the electromotive force for a stack assembly of N membrane pairs fed with water solutions of NaCl is expected to depend on the concentration gradient between HC and LC compartments according to equation:

$$E = 2N\alpha \frac{RT}{zF} \ln\left(\frac{a_c}{a_d}\right) \qquad \text{(eq. 3.4)}$$

Sea (NaCl=0.5 M) and river waters (NaCl=0.01 M) are characterized by an high ratio between the concentration of NaCl in HC e LC solutions $[NaCl]_{HC}/[NaCL]_{LC} \sim$ 50 and by a correspondent ratio $a_c/a_d \sim 37$ but also by a very low conductivity in the LC compartment (~500 μS/cm) which leads to high values of Ri (stack internal resistance). Another interesting feedstock can be composed by brine (NaCl=5M) and seawater (NaCl=0.5M) which presents a lower ratio $[NaCl]_{HC}/[NaCL]_{LC} \sim 10$ but quite high conductivity in both HC (~250000 μS/cm) and LC (~25000 μS/cm) solutions.

As shown in Figure 3.14, it possible to observe that the utilization of NaCl concentrations similar to that of brine/seawater solutions allows to achieve a drastic increase of the power output in spite of the lower $[NaCl]_{HC}/[NaCL]_{LC}$ ratio as a result of the higher conductivity of LC solution.
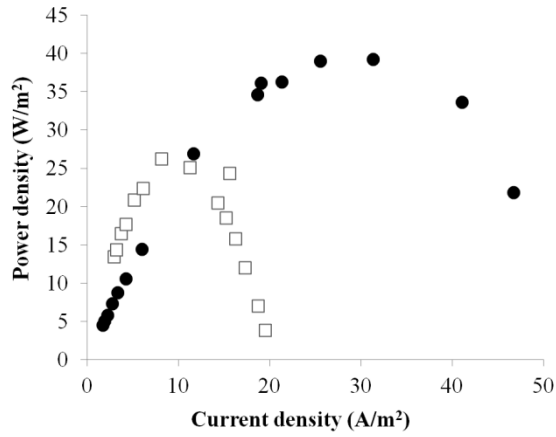
Figure 3.14 Plot of power densities vs. current density recorded in a stack equipped with 40 membrane pairs for $FeCl_2/FeCl_3$ (0.3 M) with an external resistance variable, with two different HC and LC compositions: HC (0.5M) and LC (0.01M) (□), HC (5M) and LC (0.5M) (●).

During the experiment it was observed that the concentration of ions of dilute solutions increases during the passage in the stack but anyway a quite low overall conductivity is expected as an effect of the low residence time of the dilute solution inside the stack (lower than 1 min).

3.3   ABATEMENT OF ACID ORANGE 7

The simultaneous generation of electric energy and the treatment of wastewaters contaminated by an organic pollutant resistant to conventional biological processes was achieved for the first time using proper redox processes by reverse electrodialysis using salinity gradients (Figure 3.15).
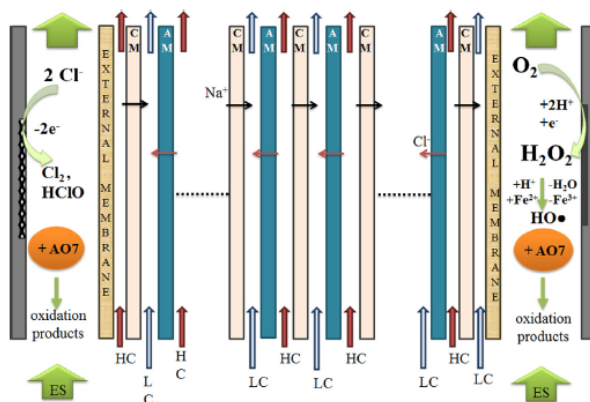
Figure 3.15 Scheme of RED stack showing all components of the system, the ion flow trough the IEMs and the reactions to minerilize the colorant.

During this experimental phase, I examined the decoloration of an aqueous solution contaminated by a model organic recalcitrant compound, the Acid Orange 7 (AO7) (Figure 3.16), largely used as a model substrate for the aromatic azo dyes.
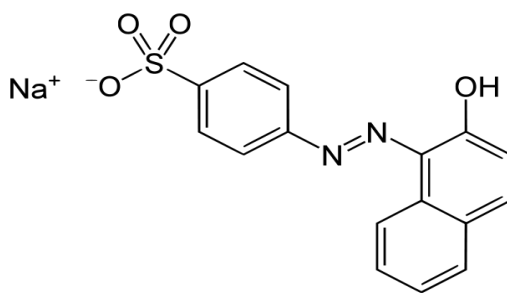
Figure 3.16 Molecule of Acid Orange 7.

AO7 resists to biological processes, light irradiation and chemical oxidation. Its degradation has been studied by several research groups; Kiwi et al. [14] reported a catalytic photo-assisted system, Fe^{3+}/nafion/glass fibers, Bandara et al. [15] used

photo-Fenton reactions in the presence of natural sunlight, Daneshvar et al. [16] employed electrocoagulation, Ramirez et al. [17] investigated optimum conditions for Fenton's oxidation, Ray et al. [18] performed photocatalytic oxidation in the presence of TiO_2 and Inoue et al. [19] used ultrasound waves.

3.3.1   Electrolyses

Electrolyses were performed to study the degradation of AO7 in a bench-scale batch undivided cell (50 mL) and in a two compartments cell divided by ion-exchange membrane (see chapter 2 to know the components of system). Several anionic and cationic membrane were tested to research the membrane capable of preventing any passage of pollutants from the electrolytic solutions to the side compartments. IEMs tested were: Selemion (poly(styrene-co-divinybenzene)), Nafion membranes (perfluorinated layer) and Fuji (with a polymer matrix of hydrocarbons). All results are reported in Table 3.4 in which is possible to see that the choice of the ion exchange membrane to use is driven mainly by the passage of iron ions.

Type	Name	Passage of AO7 (mgL^{-1})	Passage of iron (mgL^{-1})
AM	AMV Selemion (Asahi Glass)	<0.1	<1
AM	Fuji (FujiFilm)	<0.1	~4
CM	324 Nafion (Du Pont)	<0.1	>15
CM	Fuji (FujiFilm)	n.d.	n.d.

Table 3.4 Ability of the membranes to block the passage of AO7 and iron ions.

Electrolyses experiments were leaded to select the redox processes more suitable to treat aqueous solutions of AO7 by RED. On the basis of literature data, electro-Fenton (EF), indirect oxidation with electrogenerated active chlorine at DSA anodes (IOAC) and direct oxidation on Boron doped Diamond (BDD) were tested.

The main results are collected in the Table below in which are reported the cell potential, the removal of color and of all organic matter expressed as chemical oxygen demand (COD) as a function of treatment time (Table 3.5).

Electrochemical Process	Electrodes	Cell voltage (V)	Abatement of color (%) and time (h)	Abatement of COD (%) and time (h)
Direct anodic oxidation	BDD anode Ni cathode	~4.8	~96 (2 h) >99 (4 h)	>95 (4 h)
Electro-Fenton	Ti/IrO$_2$Ta$_2$O$_5$ anode Carbon felt cathode	~3.3	~97 (<1 h) ~97 (4h)	~50 (4 h)
Oxidation by electrogenerated active chlorine	−Ti/RuO$_2$–IrO$_2$ anode −Ti/IrO$_2$–Ta$_2$O$_5$ anode Ni cathode	~3.5	>99 (<0.5 h) >99 (0.5 h)	~60 (4 h) ~37 (4 h)

Table 3.5 Electrolyses of water solution of AO7 by different electrocatalytic methods. Aqueous solution of AO7 (150 mg/L) and Na$_2$SO$_4$ (0.035 M) or NaCl (1 g/L) (for oxidation by electrogenerated active chlorine) performed in an undivided cell under amperostatic mode (current density: 10 mA/cm^2). For electro-Fenton FeSO$_4$ (0.5 mM) was added to the system. Surface of electrodes 5 cm2. Room temperature. pH = 2.

According to the literature, all these electrochemical methods allowed to achieve a very fast removal of the dye from the solution. Between all methods, processes based on the utilization of direct oxidation at boron doped diamond (BDD) gave the faster abatement of COD (95% then 4 hours of treatment). Nevertheless, BDD process was penalized by larger anodic potentials, a slower removal of azo-dye and, in addition, the electrode is very expensive (about one order of magnitude higher than that of quite cheap carbon felt and Ir or Ru based adopted electrodes). Thus, RuO$_2$–IrO$_2$ based materials were chosen as anodes for the electrochemical oxidation of AO7 by electrogenerated active chlorine under operative conditions suggested by Scialdone et al. [20] in order to limit the formation of toxic compounds containing chlorine. ElectroFenton process gave a fast removal of color but a slower decrease of COD. Despite that, it is considered very promising process due to the low cell potential and the low cost of the electrode (carbon felt).

Among, the main electrochemical procedures used for the degradation of azo-dye, EF, indirect oxidation with electrogenerated active chlorine at DSA anodes (IOAC) and the combination of both processes were chosen to test the capacity of RED system to treat wastewater contaminated. When EF and oxidation by electrogenerated active chlorine were combined, chlorides oxidation to active chlorine and oxygen reduction to hydrogen peroxide took place as anodic and

cathodic processes, respectively. Main reactions occurring in electrode compartments are detailed in the following:

- Anode compartment

$$2\,Cl^- \rightarrow Cl_2 + 2e^- \qquad\qquad \text{(react. 3.3)}$$

$$Cl_2 + H_2O = HOCl + H^+ + Cl^- \qquad\qquad \text{(react. 3.4)}$$

$$HOCl + AO7 \rightarrow oxidation\ products \qquad\qquad \text{(react. 3.5)}$$

- Cathode compartment

$$O_2 + 2H^+ + 2e^- \rightarrow H_2O_2 \qquad\qquad \text{(react. 3.6)}$$

$$H_2O_2 + Fe^{2+} + H^+ \rightarrow Fe^{3+} + OH\cdot + H_2O \qquad\qquad \text{(react. 3.7)}$$

$$Fe^{3+} + e\text{-} \rightarrow Fe^{2+} \qquad\qquad \text{(react. 3.8)}$$

$$OH\cdot\ + AO7 \rightarrow oxidation\ products \qquad\qquad \text{(react. 3.9)}$$
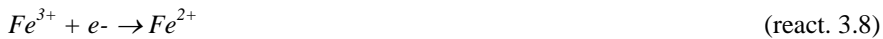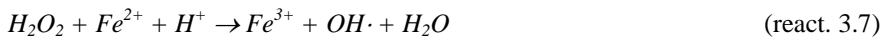
In this way is possible to treat a water solution containing the organic pollutant in both electrode compartments.

3.3.2   RED system

The generation of electric energy by RED was studied both in the absence and in the presence of AO7, in a stack equipped with 40 cells pair fed with concentrated (5 M, brine) and diluted (0.5 M, seawater) solutions of NaCl working with two different hydraulic circuits for the electrodic solution in order to monitor the process in each compartment. Polarization curves, reported in Figure below, were generated changing the external resistance between 160 and 1 Ohm. In the absence of AO7, the maximum power (normalized to cathode area of 10 cm x 10 cm x 2 mm) was 11.1W/m^2. The cell obtained peak power at a total cell voltage of 2.1 V and current density of 5.3 A/m^2. The addition of AO7 (150 mg/l) increased slightly the power. Peak power of about 12.9 W/m^2 was achieved at a cell voltage of 1.6 V and current density of about 8 A/m^2.
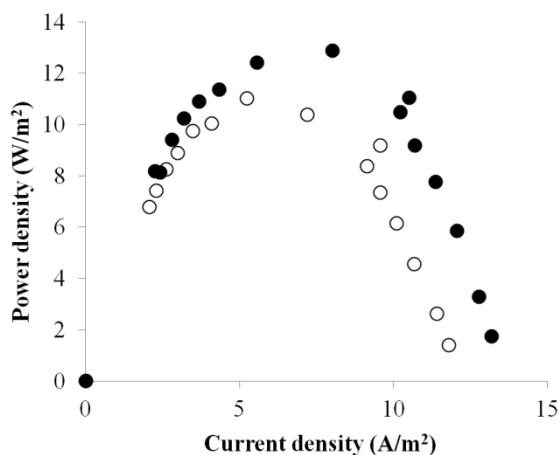
Figure 3.17 Experiments performed in a stack equipped with 40 cell pairs fed with HC (5 M NaCl) and LC solutions (0.5 M NaCl). Two separated cathodic (0.085 M Na_2SO_4 and 0.5 mM $FeSO_4$ at a pH of 2 (H_2SO_4)) and anodic solution (0.085 M NaCl at a pH of 2 (HCl)) were fed to the stack. In graph is reported power densities (normalized to the cathode geometric area of 100 cm^2) as a function of current densities recording changing the external resistance between 160 and 1 Ohm in the absence (○) and after addition of AO7 (150 mg/L) (●) to the electrodic solution.

This improved performance could be due to a shift of the equilibrium of electrode reactions towards the products (hydrogen peroxide and active chlorine) driven by their reaction with AO7. Then, I examined the abatement of AO7 with a low external resistance (4.6 Ohm) to work with higher current density. For adopted system, the oxidation of AO7 was achieved in the anodic compartment by electrogenerated active chlorine (react. 3.5) while at cathodic one by electrogenerated hydroxyl radicals (react. 3.9). A very fast removal of azo-dye was achieved in both compartments coupled with a progressive reduction of COD (Figure 3.18) and with the generation of electric energy. In particular, the current density presented initial and final values of about 13 and 9 A/m^2, respectively, and power densities of about 5 W/m^2 were recorded.
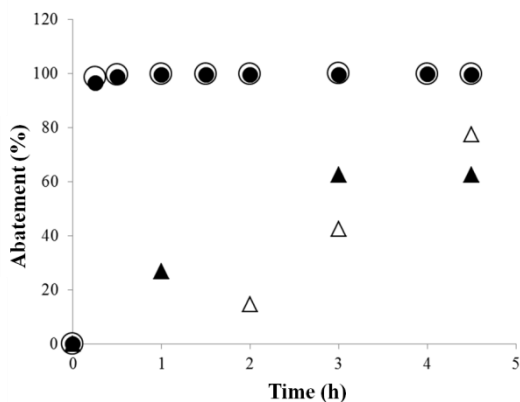
Figure 3.18 Reports the abatement of (circles) color and (triangles) COD in both compartment; white symbol referred to anodic mineralization, black symbol to Electro-Fenton process.

The total removal of dye was coupled with a progressive reduction of COD (60% and 76% in cathode and anode compartment respectively).

Some experiments were repeated with the same electrodes by using only one circuit involving both cathodic and anodic compartments. Despite the discoloration remained very fast (Figures 3.19, 3.20) slower abatements of TOC (38%) occurred as a result of the fact that H_2O_2 can react with HClO

$$H_2O_2 + HClO \rightarrow O_2 + H_2O + H^+ + Cl^- \qquad \text{(react. 3.10)}$$

leading to lower concentrations of the two oxidants (Figure 3.20).
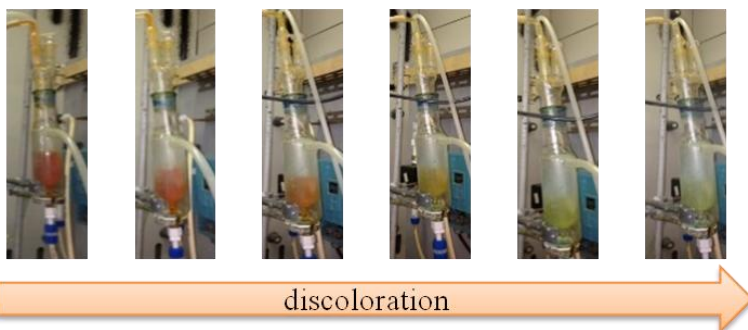
Figure 3.19 Sequence of photos that showed the dye removal.
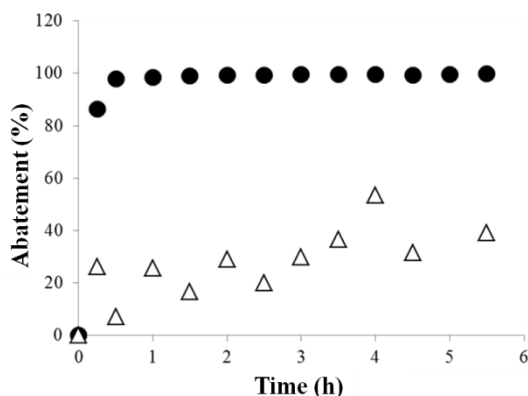
Figure 3.20 Plot of abatement % of AO7 (•) and COD (Δ) vs time. Electrode solution contained 150 mg/L AO7, 0.085 M NaCl, 0.5 mM $Fe_2SO_4*7H_2O$ and H_2SO_4 to obtain a pH = 2. Electrode used: Ti/RuO_2-IrO_2 and Carbon felt as anode and cathode respectively. Stack was equipped with 40 cell pairs and was fed with HC (5M NaCl) and LC (0.5 MNaCl) solutions.

Using this second RED system (with one hydraulic circuit), I studied the effect of salinity gradient and the effect of number of membrane on the performance of reverse electrodialysis technology to treat wastewater.

Effect of salinity gradient

How shown in Figure 3.21, it was possible to evaluate the effect of the salinity gradient on the process both in terms of abatement of TOC and of discoloration for a stack equipped with 40 cell pairs. The water solutions used during these experiments were: 5 M and 0.01 M (HC and LC respectively) in the system A; and 0.5 M and 0.01 M (HC and LC respectively) in the system B. The higher salinity gradient gave rise to a drastic increase of both current density and cell potential. As a result, the initial power density increased from about 13 to 48 W/m^2, for the experiments carried out with the lower (system A) and higher (system B) salinity gradient. All data are listed in the Table below.

Entry	Concentration of HC (and LC) solution (M)	Time of treatment	Abatement of color (and TOC) (%)	Cell voltage (V)	Current density (A/m²)	Power density (W/m²)
System A	0.5 (0.01)	4	>99 (55)	0.7 (initial) 0.2 (final)	20 (initial) 4.3 (final)	13.3 (initial) 0.9 (final)
System B	5 (0.01)	4	100 (58)	1.6 (initial) 1.0 (final)	30 (initial) 22 (final)	48 (initial) 22 (final)

Table 3.6 Effect of the salinity gradient on the removal of AO7 and the generation of electric energy
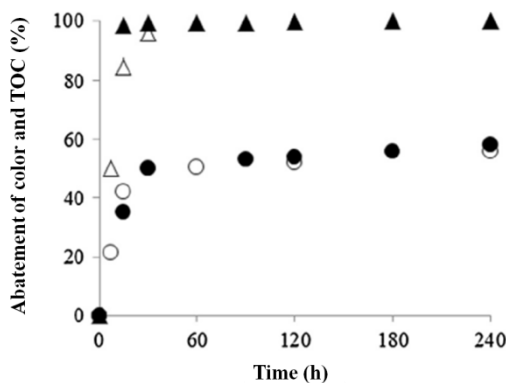
Figure 3.21 Abatement of color (triangles) and TOC (circles) vs. time achieved in a stack equipped with 40 cell pairs fed with a concentration of NaCl in HC of 5 (closed symbol) or 0.5 M (open symbols) and a concentration of NaCl in LC solution of 0.01 M.

However, only slightly higher abatements of TOC were achieved using system A as water solutions.

In order to analyze the effect of the number of membrane, water solutions containing NaCl 5 M and 0.01 M were used to exploit the benefits of a large salinity gradient. Because the electromotive force for a stack increases linearly with the number N of membrane pairs (Nernst equation, eq. 3.4), an increase of power density output is expected to take place coupled with higher values of current density as a result of the lower impact of the energetic loss due to the redox processes compared with the overall power generation according to the equations

$$P = I^2 R_e = \frac{\Delta V^2 R_e}{(R_e + R_i)^2} = \frac{\Delta V^2 R_e}{(R_e + R_{el} + R_{cells})^2}$$ (eq. 3.5)

where R_e, R_{el}, R_{cells} represent external resistance, and resistances of electrode compartments and of the cell pairs, respectively. However, for a very large number of cells the voltage penalty of redox processes will become negligible with respect to the overall cell voltage and the current density is likely not to depend more on N. To evaluate the effect of the number of cell pairs, some experiments were performed with a stack equipped with 60 cell pairs and a single circuit for the electrode compartments with high salinity gradient. The increase of membrane gave rise to a drastic increase of both cell potential and current density that increased from about 48 to 61 W/m^2 (see Table 3.7).

Number of cell pairs	Time of treatment	Abatement of color (and TOC) (%)	Cell voltage (V)	Current density (A/m^2)	Power density (W/m^2)
40	4	100 (58)	1.6 (initial) 1.0 (final)	30 (initial) 22 (final)	48 (initial) 22 (final)
60	2	>99 (63)	1.6 (initial) 1.2 (final)	37.5 (initial) 27 (final)	61 (initial) 45 (final)

Table 3.7 Effect of the number of membranes on the removal of AO7 and the generation of electric energy.

In both experiments a complete removal of the color was achieved after few minutes. During experiment using 60 membrane pairs, a different abatement of TOC was observed during first 60 minutes (more fast) but the final abatement was only slightly higher than that achieved with 40 membrane pairs. To better understand the abatement of organic material, main by-products were here identified by HPLC analyses.

The oxidative degradation of AO7 starts with the breaking of the azo bond, the most active group in the structure [15].

Figure 3.21 General reaction sequence proposed for the mineralization of AO7 in aqueous acid medium by hydroxyl radicals following electro-Fenton process.

During the degradation process, several intermediates were achieved. Polyhydroxylated and quinoid structures are unstable and lead to the formation of short-chain carboxylic acids by oxidative ring opening reactions. In order to evaluate these by-products, HPLC analyses were carried out. Among the possible biodegradable carboxylic acids, AO7 was mainly converted to hydroquinone, oxalic, malonic, formic and lactic acids. The abatement of organic pollutant was monitored by TOC analyses. From the data collected, the abatement of TOC was faster at the beginning but became quite slow with increasing treatment time because carboxylic acids can form during the process Fe(III)-carboxylic acids complexes very resistant to the mineralization [21], thus explaining the slow final oxidation stage of the last by-products to CO_2. When two hydraulic circuits were used, the formation of oxalic acid and hydroquinone was detected in both electrode solutions while formic and malonic acids were found only in the anodic and in the cathodic compartment, respectively. The presence of lactic acid was detected in both compartments but with a substantial higher concentration in the case of the anodic process.

3.4   TREATMENT OF Cr(VI)

The simultaneous generation of electric energy and the treatment of waters contaminated by inorganic pollutant was carried out during my thesis with the aim to expanding the field of application of RED technology. Chromium has been chosen as model of inorganic pollutant.

Chromium is widely used in industrial field due to its several properties, such as hardness, resistance to corrosion and oxidation and coloration of its compounds. The main sources of contamination are:

- ✓ refractory production (materials resistant to high temperatures, suitable and indispensable for the construction furnaces) where the chromite is used ($FeO*Cr_2O_3$);
- ✓ chromium plating processes. The chromium in this case constitutes a screen to the atmospheric agents. The solutions used in industrial have concentrations ranging between 200 and 400 g/L of chromium added as $K_2Cr_2O_7$;

- ✓ paint industry,
- ✓ textile industry, the chromium in the form of $Cr_2(SO_4)_3$ is used as a mordant because for hydrolysis form Cr $(OH)_3$, which subsequently fixing the dye;
- ✓ production of materials based hard alloys
- ✓ disposing of sewage sludge and compost;
- ✓ leather tanning.

Trivalent chromium is relatively harmless, whereas hexavalent chromium is about 100–1000 times more toxic [22]. It is a strong oxidizing agent that is carcinogenic and mutagenic and diffuses quickly through soil and aquatic environments. Indeed, the concentration of Cr(VI) is limited in groundwater by a World Health Organization provisional guideline value of 0.05 mg/L [23]. Cr(VI) does not form insoluble compounds in aqueous solutions, so separation by precipitation is not feasible. Chemical and electrochemical reduction of toxic Cr(VI) into the less toxic Cr(III) (which forms insoluble precipitates) is an effective approach widely studied in literature [24-29]; recently also the application of MFC appears interesting for the cathodic reduction of Cr(VI) [30].

In this frame my research is collocated proposing for the first time the utilization of salinity gradient to generate electric energy and simultaneously treat Cr(VI) compounds present in water. A first series of electrolyses was carried out to select the cathode materials and ion exchange membranes capable of preventing the transfer of ions. Then, working with RED system, the effect on the process of many operating parameters was investigated. Parameters characteristic of the electrode compartments are: initial concentration of Cr(VI), the flow rates of electrode solutions and the concentration of the supporting electrolyte; also parameters characteristic of the rest of stack were investigated: the extent of the salinity gradient, the number of membrane pairs and the flow rates of the solutions fed HC and LC compartments.

3.4.1 Electrolyses

First experiments were carried out in a two compartment divided cell equipped with graphite, carbon felt or reticulated vitreous carbon cathode under a potentiostatic mode (near the reduction peak of Cr). A working potential of -1.2 V vs. SCE was initially used according with the potential evaluated by focused cyclic voltammetric experiments and by previous studies [28]. A diluted water solution of Cr(VI) (2 mg/L) loaded with Na_2SO_4 (0.1 M) as supporting electrolyte was used with low pH that gave higher rates for the removal of Cr(VI) probably due to the formation of a passivation layer of $Cr(OH)_3$ for pH higher than 2 [30-32]. Cr(VI) was added as $K_2Cr_2O_7$ so the reaction that takes place at the cathode is

$$Cr_2O_7^{2-} + 14H^+ + 6e^- \rightarrow Cr^{3+} + 7H_2O \qquad \text{(react. 3.11)}$$
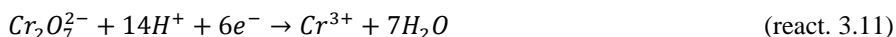
As shown in Figure 3.22, according to literature, the utilization of a carbon felt cathode gave faster abatements and higher current with respect to that achieved at compact graphite cathode because of the higher active surface.
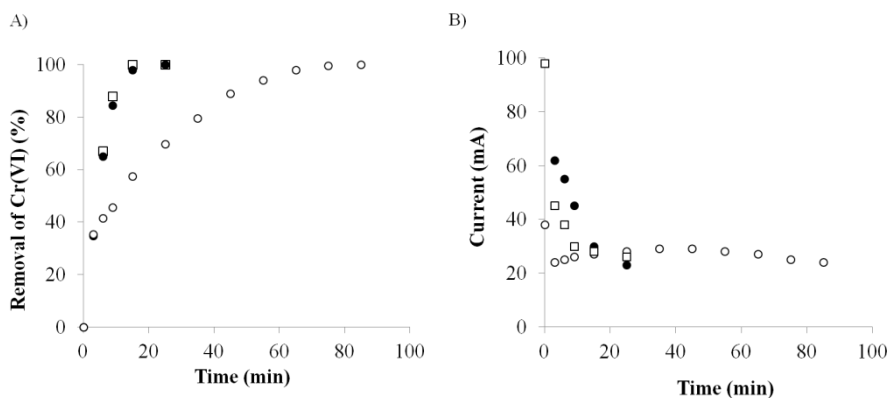
Figure 3.22 Electrolyses performed in a two-compartments divided cell. Figure A reports the effect of the nature of the cathode material on the removal of Cr (VI) for potentiostatic experiments (-1.2 V vs. SCE) performed with carbon felt (•), reticulated vitreous carbon (□) and compact graphite (○). Figure B reports the current densities vs. time.

Indeed, carbon felt presents a three dimensional structure with dramatically higher surface with respect to the geometric one. Just slightly slower abatements of Cr(VI) were achieved when the carbon felt was replaced with reticulated vitreous carbon.

Other electrolyses were performed in a divided cell to evaluate the possible passage of Cr(VI) to the side compartment. The cathodic compartment, containing a diluted water solution of Cr(VI) was separated by the anodic one by a cationic exchange membrane. Two different cationic membranes, characterized respectively by perfluorinated (Nafion) and hydrocarbon (Fuji) macromolecular structure, were used to prevent the passage of chromate species. All membranes tested showed excellent performance but I decided to use Nafion membrane for its well known high physical and chemical stability also in contact with acidic solutions.

At the end, to evaluate the effect of working potential and current density on the process some experiments were carried out at carbon felt cathode under both potentiostatic (working potential: 0.5, 0.7, 1.2 and 1.5 V vs. SCE) and amperostatic mode (current density: 8, 20, 54 and 108 A/m^2). Increased values of the working potential from 0.5 to 1.2 V vs. SCE gave higher current densities and faster conversions of Cr(VI) as shown in the following Figure.
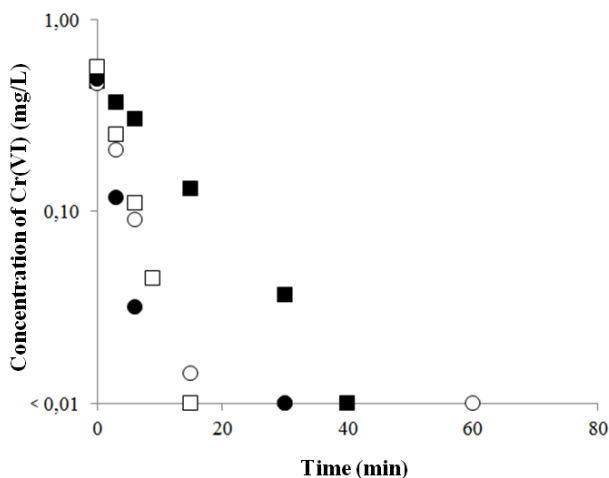
Figure 3.23 Reports the effect of the working potential (0.5 (■), 0.7 (o), 1.2 (●) and 1.5 V (□) vs. SCE) for potentiostatic electrolyses performed with carbon felt cathode on the removal of Cr(VI).

Between -1.5 V and -1.2 V working potential a slight lower abatement of Cr(VI) was achieved in the first case. At this high value of the working potential, it is possible that the cathodic reduction of water takes place, consuming part of the charge passed as shown by focused cyclic voltammetric experiments performed with a carbon felt cathode. the removal of Cr(VI) is hampered by the basification of the water present inside the inner structure of the carbon felt due to water reduction.

When experiments were carried out under amperostatic mode (Figure 3.24), higher abatements were achieved upon increasing the current density from 8 to 54 but no to 108 A/m^2. Under the last condition, the pH of the bulk of the solution changed significantly during the electrolysis reaching basic values in the last part of the experiments as a result of the massive water reduction on the cathode. In this way a drastic slower abatement of Chromium(VI) was achieved.
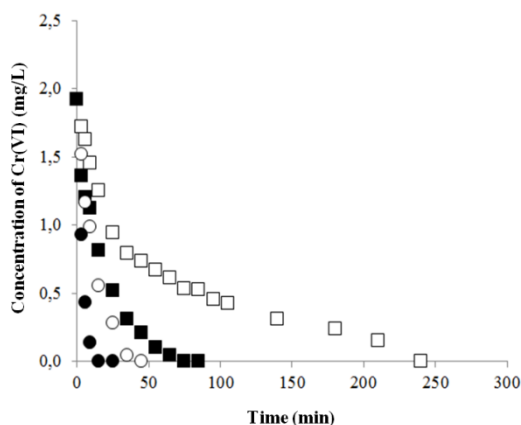
Figure 3.24 Reports the effect of the current density (8 (■), 20 (o), 54 (•) and 108 A/m^2 (□)) for amperostatic electrolyses with carbon felt cathode.

3.4.2 RED system

Effect of the chromium(VI) and supporting electrolyte concentrations

First RED experiments were carried out in a stack equipped with a carbon felt cathode and DSA-O_2 anode (geometric area of 100 cm^2) and 10 membrane pairs feeding to the cathodic compartment a water solution with different initial concentrations of Cr(VI) (2, 25 and 55 mg/L). A large salinity gradient was used: the concentration of NaCl was 5 M and 0.01 M in the HC and LC compartments, respectively.

Main reactions occurring in electrode compartments are:

Cathode:

$$Cr(VI) + 3e^- \rightarrow Cr(III) \qquad\qquad (react. 3.12)$$

$$2H_2O + 2e^- = H_2 + 2OH^- \qquad\qquad (react. 3.13)$$

Anode:

$$H_2O = \tfrac{1}{2}O_2 + 2H^+ + 2e^- \qquad\qquad (react. 3.14)$$

The effect of the concentration of Cr(VI) on its removal rate was studied in detail by carrying out some experiments with a fixed external loading and different initial Cr(VI) concentrations. As reported in the Table below, the current density and the cell potential increased with the Cr(VI) concentration thus leading to an enhancement of the power densities.

Concentration of NaCl in HC and LC (M)	Initial Cr(VI) concetration (ppm)	Number of membrane pairs	Time[a] (min)	Cell potential (V)		Current density (A/m^2)		Power density (W/m^2)	
				Initial value	Final value	Initial value	Final value	Initial value	Final value
5 – 0.01	2	10	6	0.84	0.16	8.5	3.3	7.1	0.5
5 – 0.01	25	10	20	0.90	0.09	10	2.8	9.0	0.3
5 – 0.01	55	10	25	1.14	0.35	12.2	2.9	13.9	1.0

Table 3.8 Effect of initial concentration of Cr(VI). [a] Time necessary to achieve a concentration of Cr(VI) lower than 0.01 mg/L.

Thus, as shown in Figure 3.25, for high enough Cr(VI) concentration, the reduction of Cr(VI) to Cr(III) occurred at a rate fast enough to convert the ionic flux in a significant current output at low cathode potential thus offering to the external load higher potential and current output.
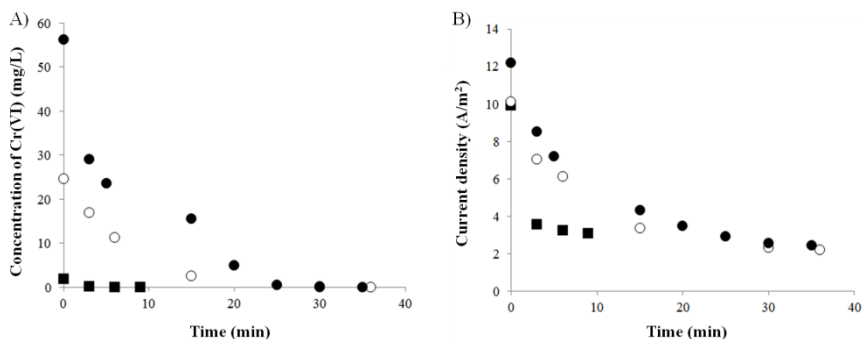
Figure 3.25 Effect of Cr(VI) concentration on reverse electrodialysis process in experiments performed with 10 cell pairs. Figure A reports the concentration of Cr(VI) vs. time achieved in the cathodic compartment in the experiments performed with an initial concentration of Cr of 2 (■), 25 (o) and 55 mg/L (●) and an external resistance of 1 Ohm. Figure B reports the current density profile vs. time for experiments reported in Figure A.

In order to evaluate the effect of the chromium concentration for the same system, the dependence of the power output on the external resistance was also measured. As shown in Figure 3.26, the addition of 25 mg/L of Cr(VI) resulted in an increase of both the current density and the power output as an effect of the lower potential penalty given by the cathodic reduction of Cr(VI) with respect to the cathodic reduction of water. Indeed, from ($P = I^2 R_e = R_e \Delta V^2/(R_e + R_i)^2$) the power output should present a maximum if $R_e = R_i$ and it should increase up on lowering the internal resistance R_i or reducing the potential drops required for electronic processes (as in the case of reduction of water and Cr(VI)).

104
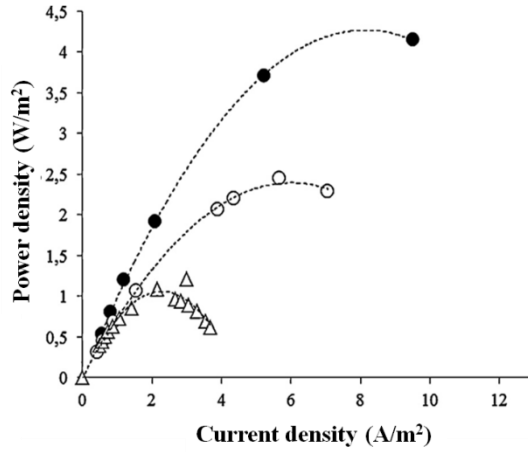
Figure 3.26 Power densities (normalized to the cathode geometric area of 100 cm^2) vs.current densities recorded changing the external resistance in the absence (Δ) and in the presence of 25 (o) and 50 ($\bullet$) mg/L of Cr(VI) in the cathodic solutions.

A supplementary addition of Cr(VI) to have a concentration of 50 mg/L gave an increase of the power output. These data suggest that the Cr(VI) reduction is limited by the kinetics of the mass transfer of Chromium to the electrocatalytic sites [33].

Another parameter of electrode solution that can be changed to study its effect on the performance of the system is the concentration of supporting electrolyte. In order to evaluate in a more clear way the effect of the resistance of electrode compartments on the overall power density, some experiments were carried out with a concentration of 0.1 and 0.5 M of Na_2SO_4 as supporting electrolyte in the electrode compartments in the presence of Cr(VI) (25 mg/L) in the cathodic one using 10 cell pairs. As reported in Figure below, increasing Na_2SO_4 concentration an higher power output and a faster removal of Cr(VI) were obtained.
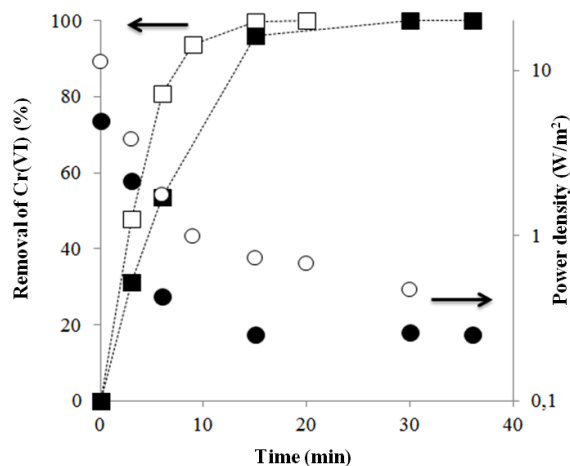
Figure 3.27 Effect of the concentration of the supporting electrolyte on the removal of Cr(VI). Abatement of Cr(VI) (square symbols) and the power density (circle symbols) achieved in a stack equipped with 10 cell pairs equipped with carbon felt cathode with a concentration of Na_2SO_4 of 0.1 (black symbols) or 0.5 M (white symbols) as supporting electrolyte in both electrode compartments.

Thus, the higher was the concentration of the supporting electrolyte the bigger was the conductivity of the electrode compartments lowering the overall resistance of the stack and increasing the potential and the current density outputs.

Effect of the salinity gradient

As already seen in the case of AO7 abatement, the electromotive force of the stack depends also on solute activities in concentrated and diluted solutions. So, several experiments were performed with an initial concentration of Cr(VI) of 25 mg/L, a fixed external load of 4.6 Ohm, with 50 membrane pairs, to evaluate the effect of the salinity gradient on the removal of Cr(VI). As reported in Figure 3.28, a higher salinity gradient (NaCl 5 M and 0.01 M in HC and LC, respectively) gave higher current densities ($\sim$25-30 A/m^2).
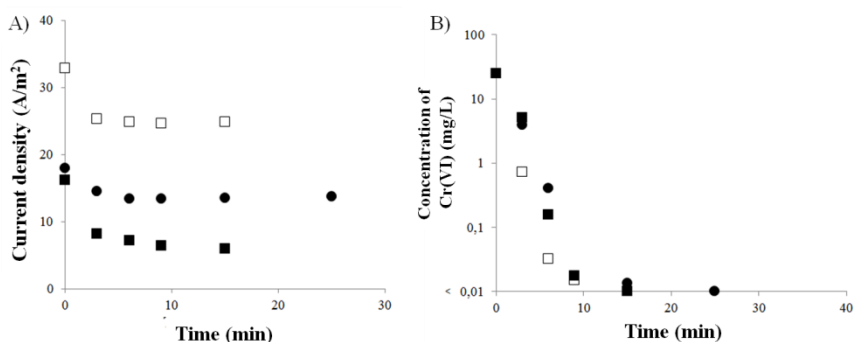
Figure 3.28 Current density (A) and concentration of Cr(VI) (B) vs treatment time achieved during experiments performed in a stack equipped with 50 cell pairs with carbon felt as cathode (100 cm^2) and Ti/IrO$_2$-Ta$_2$O$_5$ as anode. Feeds: NaCl 5 and 0.01 M in HC and LC, respectively ($\square$); NaCl 0.5 and 0.01 M in HC and LC ($\bullet$); NaCl 5 and 0.5 M in HC and LC ($\blacksquare$).

In Table 3.9 are reported the main results recordered during these experiments. With the other two salinity gradients (SR=50, and SR=10), current densities assumed lower values but sufficiently high to give always a fast removal of Cr(VI).

Concentration of NaCl in HC and LC (M)	Initial Cr(VI) concetration (ppm)	Number of membrane pairs	Time[a] (min)	Cell potential (V)		Current density (A/m^2)		Power density (W/m^2)	
				Initial value	Final value	Initial value	Final value	Initial value	Final value
5 – 0.01	25	50	15	0.76	0.27	18	6.1	13.7	1.6
5 – 0.5	25	50	15	1.8	1.39	33	25	59.4	34.7
0.5 – 0.01	25	50	15	1.32	0.75	18	13.5	23.8	10.1

Table 3.9 Effect of salinity gradient using a RED stack assembled with 50 cell pairs. [a] Time necessary to achieve a concentration of Cr(VI) lower than 0.01 mg/L.

Similar experiments were repeated using a RED stack assembled with 10 cell pairs to obtain a slower removal of Cr(VI) in order to evaluate better the effect of salinity ratio. Results are reported in Figure 3.29 and principal data are collected in Table 3.10

A)

B)
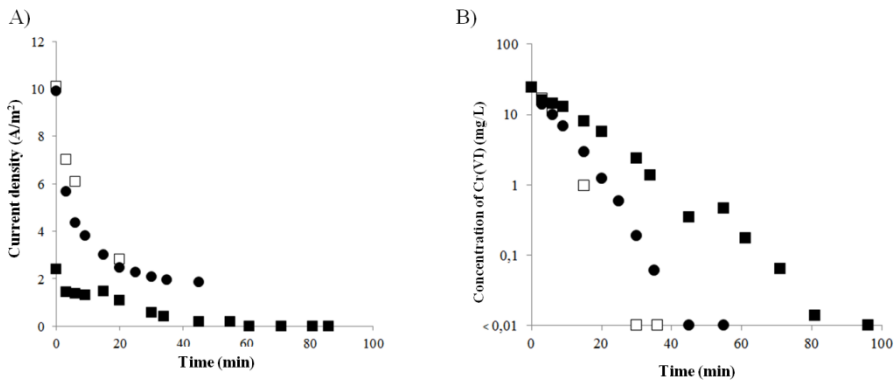
Figure 3.29 Current density (A) and concentration of Cr(VI) (B) vs treatment time achieved during experiments performed in a stack equipped with 10 cell pairs with carbon felt as cathode (100 cm^2) and Ti/IrO$_2$-Ta$_2$O$_5$ as anode. Feeds: NaCl 5 and 0.01 M in HC and LC, respectively (□); NaCl 0.5 and 0.01 M in HC and LC (•); NaCl 5 and 0.5 M in HC and LC (■).

Concentration of NaCl in HC and LC (M)	Initial Cr(VI) concetration (ppm)	Number of membrane pairs	Time[a] (min)	Cell potential (V)		Current density (A/m^2)		Power density (W/m^2)	
				Initial value	Final value	Initial value	Final value	Initial value	Final value
5 – 0.01	25	10	20	0.90	0.09	10	2.8	9.0	0.3
5 – 0.5	25	10	89	0.49	0.004	2.4	0.002	1.2	8E-6
0.5 – 0.01	25	10	45	0.68	0.14	9.9	1.86	6.7	0.3

Table 3.10 Effect of salinity gradient using a RED stack assembled with 10 cell pairs. [a] Time necessary to achieve a concentration of Cr(VI) lower than 0.01 mg/L.

As shown in Table 3.10, faster Cr(VI) removal and higher current densities were obtained by increasing the salinity gradients. Instead, drastically low current densities and the slowest removal of Cr(VI) were achieved by using NaCl concentrations similar to that of salt pond/seawater solutions (5 and 0.5M in HC and LC), in spite of the high conductivity achieved in all compartments. It seems reasonable to assume that the anodic oxidation and the cathodic reduction of water, that takes place when low concentrations of Cr(VI) are reached, present quite high potential penalties close to the electromotive force generated by 10 membrane pairs with this low salinity gradient. This is confirmed in Figure 3.29B in which the

reduction of Cr(VI) concentration vs. time (when in the system are fed solution with a SR of 10) is more less than when I used a salinity ratio equal to 500 and 50.

Effect of the number of membrane pairs and of flow rate of HC, LC and electrode solutions

To evaluate the effect of the number of membrane pairs on the removal of Cr(VI) (25 mg/L), some experiments were carried out with 10, 40 and 50 membrane pairs, using an external fixed load resistance. These experiments were performed using a concentration of NaCl of 5 and 0.5 M in the HC and in the LC compartments, respectively. As reported in Table 3.11, an increase of the current density and of the power output was achieved increasing the number of membrane pairs.

Concentration of NaCl in HC and LC (M)	Initial Cr(VI) concetration (ppm)	Number of membrane pairs	Time[a] (min)	Cell potential (V)		Current density (A/m²)		Power density (W/m²)	
				Initial value	Final value	Initial value	Final value	Initial value	Final value
5 – 0.5	25	10	86	0.49	0.004	2.4	0.002	1.2	8E⁻⁶
5 – 0.5	25	40	15	0.90	0.18	13.5	3.4	12.1	0.6
5 – 0.5	25	50	15	0.76	0.27	18	6.1	13.7	1.6

Table 3.11 Effect of number of cell pairs. [a] Time necessary to achieve a concentration of Cr(VI) lower than 0.01 mg/L.

Furthermore, the higher current density achieved with an higher number of membrane pairs allowed to accelerate the Cr(VI) removal (Figure 3.30).
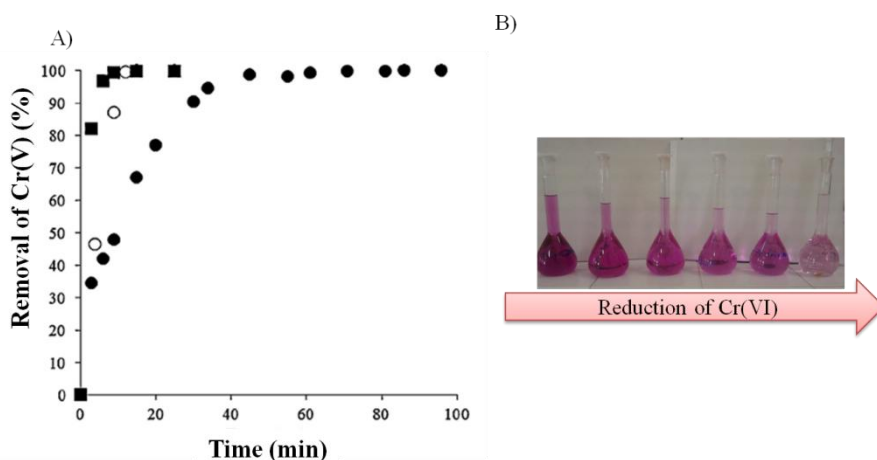
Figure 3.30 A) Effect of the number of membrane pairs. reports the removal 25 mg/L of Cr(VI) achieved in the cathodic compartment of a stack equipped with 10 (●), 40 (○) and 50 (■) membrane pairs fed with HC and LC solutions (5 M and 0.5 M NaCl, respectively). Figure B) shows a series of photo made during a treatment process.

Indeed, by working with10 membrane pairs about 1 h was necessary for the removal of 99% of initial Cr(VI) while with 50 membrane pairs about 9 min were sufficient to achieve the same results.

The dependence of the power output on the external resistance was measured with a stack equipped with 10 or 50 membrane pairs. The solutions fed to the stack presented a concentration of NaCl of 5M (HC) and 0.01M (LC). As shown in Figure 3.31A, a drastic increase of the power density was achieved upon increasing the number of membrane pairs from 10 to 50 because of the higher cell potentials and current intensities (Figure 3.31B). A maximum power density slightly lower than 3.7 and higher than 55 W/m^2 was obtained with 10 and 50 cell pairs, respectively, with an initial concentration of Cr(VI) of 50 mg/L.
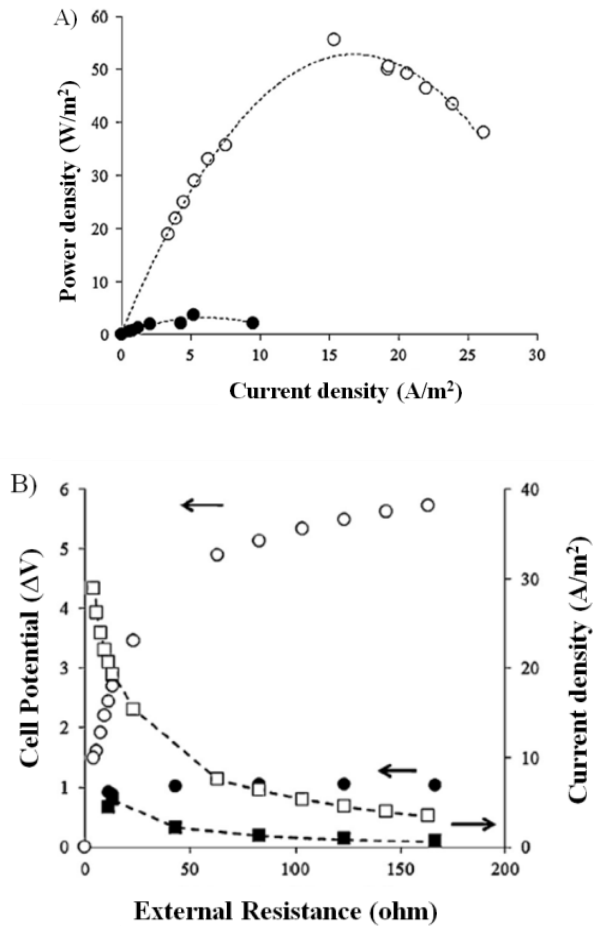
Figure 3.31 Effect of the number of membrane pairs. A) reports the profile of power densities (normalized to the cathode geometric area of 100 cm^2) vs. current densities recorded changing the external resistance in a stack equipped with 10 (●) or 50 membrane pairs (○) fed with a SR of 500 and with an initial concentration of 50 mg/L of Cr(VI). B) reports the profiles of cell potential (○ for 50 and ● for 10 membrane pairs) and current density (□ for 50 and ■ for 10 membrane pairs) (normalized to the cathode geometric area of 100 cm^2) vs. external resistance under the same conditions of Figure A.

A series of experiments was carried out in a stack equipped with 10 membrane pairs to evaluate the effect of the flow rates of HC, LC (and also electrode solutions) on the process. The effect of the flow rates of HC and LC solutions on RED processes was previously investigated by various authors [34-36]. Fluid dynamics was found to influence polarization phenomena for channel filled with net spacers. This is due

111

mainly to the presence of relevant velocity components perpendicular to the membranes [36]. All the factors promoting fluid mixing within the channel such as increased flow rates are expected to improve the ratio between the ions concentrations in the bulk and in the membrane-solution interface, thus leading to higher power outputs. As reported in Figure 3.32, higher flow rates (400 mL/min) allowed to obtain higher current densities and, as a consequence, faster removal of Cr(VI).
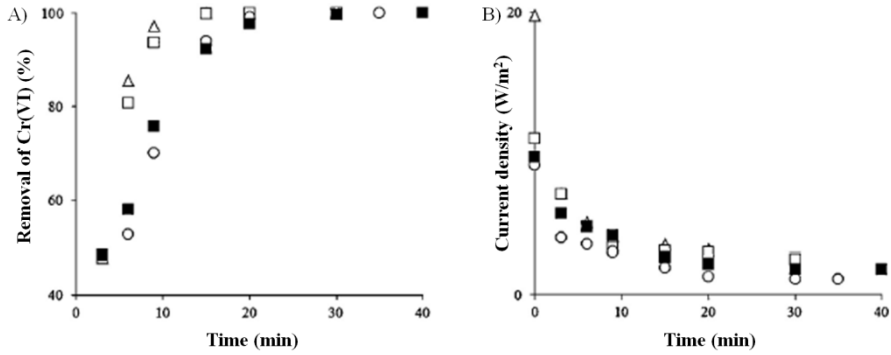
Figure 3.32 Effect of the flow rate of HC, LC and electrode compartments on the removal of Cr(VI) (A) and the current density (B) vs. time. Flow rate of electrodic solutions:75 mL/min (open symbols) or 35 mL/min (■); flow rate of HC and LC solutions: 90 (o), 190 (□,■) and 400 (Δ) mL/min. Experiments performed in a stack equipped with 10 membrane pairs.

In this condition the fluid velocity was 2.5 cm/s. The fluid velocity (v) is defined as the mean feed flow velocity inside a single spacer-filled channel. It can be estimated as:

$$v = \frac{Q}{N\delta b\epsilon_{sp}}$$
(eq. 3.6)

where Q is the total volumetric flow rate (L/h), N is the number of cell pairs, δ is the spacer thickness, b is the compartment width and ε_{sp} is the spacer porosity. Fluid velocity was varied from 0.5 to 4 cm/s in both dilute and concentrate compartments (Figure 3.33).
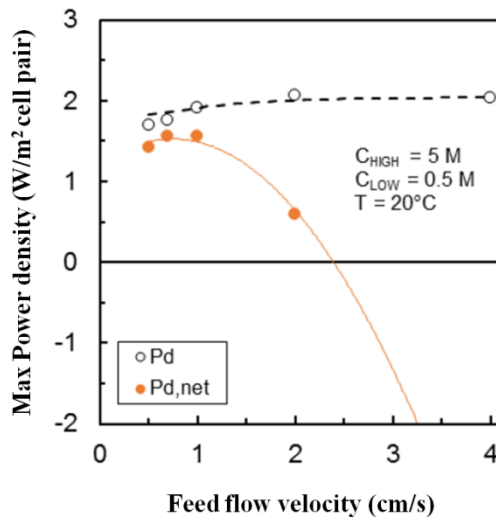
Figure 3.33 Effect of feed flow velocity on the measured gross and net power density. Experimental data for a 50 cell pairs stack equipped with Fujifilm (120 μm) membranes, 270 μm woven spacers. HC = 5 M; LC= 0.5 M; T = 20°C. The net power density at 4 cm/s (-4.4 W/m^2) is not shown in the graph.

Tedesco et al. [37] studied that the increase in fluid velocity (from 0.5 to 4 cm/s in both dilute and concentrate compartments) slightly enhances the gross power density achieved in the stack. This is mainly due to the reduction in residence time and the improvement of mixing phenomena inside compartments, although the latter play a minor role when seawater and brine are used. The most important influence is registered on the net power density, which dramatically falls for flow velocities above 1 cm/s due to the significant increase in hydraulic losses. In fact, the net power density becomes negative (i.e. the pumping power exceeding the gross power produced by the RED unit) for flow velocities between 2 - 3 cm/s. In this context the fluid velocity obtained (2.5 cm/s) was outside the range suggested by Tedesco et al. [37] which must be between 0.5 and 1cm/s to obtain an optimal net power output.

In the same graph (Figure 3.32), the effect of flow rate (75 mL/min and 35 mL/min) of electrode solutions was reported. The experiments carried out with a higher flow rate gave slightly higher current density and removal of Cr(VI) for the same amount of time passed. According to the literature [33], this result indicates that, under adopted operative conditions, the reduction of Cr(VI) is limited by the kinetic of

mass transport from the bulk of the solution to the cathode surface which is accelerated by higher flow rates.

Performance of the process for a longer time

In order to evaluate the performances of the process for a longer treatment time, several additions of Cr(VI) to the system were carried out at fixed intervals of times. The addition of Cr(VI) to the cathodic solution gave rise to an enhancement of the power density that decrease with the removal of Cr(VI) as reported. More relevant, quite similar curves power density vs. time and concentration of Cr(VI) vs. time were recorded when the concentration of Cr(VI) was restored to the initial values.
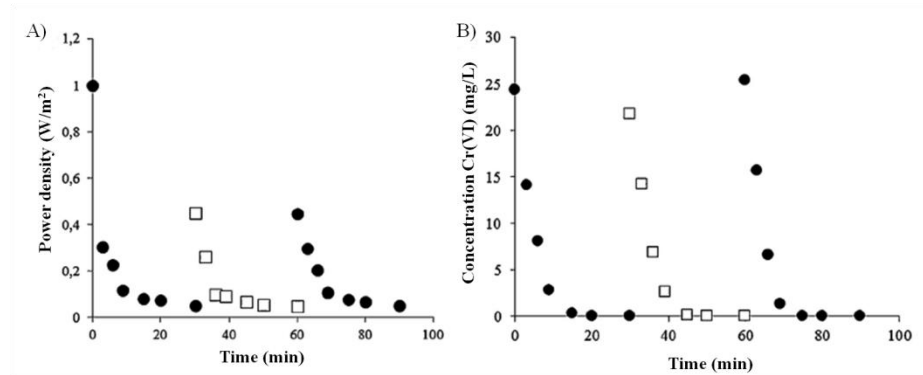
Figure 3.34 Effect of the addition of Cr(VI) to the cathodic compartment. Plot of power density (A) and concentration of Cr(VI) (B) vs. time achieved in a stack equipped with 10 membrane pairs.

These results confirm the stability of the system, show the good reproducibility and prove the positive effect of the presence of Cr(VI) on the generation of electric energy.

New technical draw of RED stack

At the end, some RED experiments were carried out in the two stacks equipped with 10 membrane pairs, 2 mg/L of Cr(VI) and a carbon felt cathode with different geometric area of 28 and 100 cm^2 for the small and the larger stack, respectively.

114

The utilization of a stack of smaller dimensions (see Figure 3.35) has the advantage of reducing the volumes of all solutions fed and in particular, the volume of the cathodic solution that containing chromium. In the case in which there is a malfunction of the instrument (i.e losses or bypass of a solution containing Cr(VI) from the cathode compartment to the side compartments) the use of a small stack can facilitate the management of waste solutions.

Figure 3.35 Photo of stack assembled with 10 cell pairs and characterized by electrodes with a geometric area of 28 cm^2.

A scheme of the new stack is reported below with the photo of electrodes are reported in Figures 3.36 and 3.37.
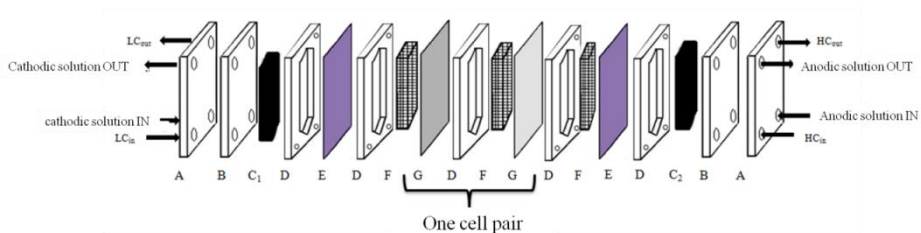
Figure 3.36 Diagram of the components of the stack. A: steel plates, B: sheets of Teflon, C1: cathode, C2: anode, D: gasket, E: ion exchange membranes external, F: spacers, G: ion exchange membranes internal.
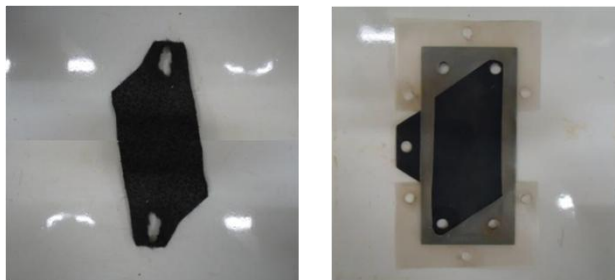
Figure 3.37 Electrodes: carbon felt (left) and DSA-O_2 with gasket (right).

Quite small current and power densities were achieved in both stacks. The removal of Cr(VI) was successfully achieved in both stacks coupled with the generation of electric current. The larger stack gave as expected faster removal of Cr(VI) as a result of the higher surface of electrodes and membranes. Cr(VI) reached a value lower than the detection limit (0.01 mg/L) after about 6 and 30 min for small and big stack, respectively.

The new stack designs presents for each solution (HC, LC, anodic, cathodic) a single feeding channel and a discharge one unlike the previous stack in which there are three supply channels for each salt solutions, arranged in alternate manner, and one for each electrode solutions. In this way, it was possible to reduce the flow rates of the solutions: 8 mL/min for the electrode compartments and 11 mL/min for the HC and LC solutions and, at the same time, it was possible to obtain satisfactory results both as production of electric current that as abatement of the pollutant inorganic.

3.5   REFERENCES

[1] Ullmann's Encyclopedia of Industrial Chemistry, seventh ed.Chapters on Electrochemistry and on Chlorine, Wiley VCH, 2006.

[2] J. Veerman, M. Saakes, S.J. Metz, G.J. Harmsen, Reverse electrodialysis: evaluation of suitable electrode systems, J. Appl. Electrochem. 40 (2010) 1461-1471.

[3] M. Turek, B. Bandura, Renewable energy by reverse electrodialysis, Desalination 205 (2007) 67-74.

[4] M. Turek, B. Bandura, P. Dydo, Power production from coal-mine brine utilizing reversed electrodialysis, Desalination 221 (2008) 462-466.

[5] R. Audinos, Electric power produced from two solutions of unequal salinity by reverse electrodialysis, Indian Journal of Chemistry 31A (1992) 348-354.

[6] J. Jagur-Grodzinski, R. Kramer, Novel process for direct conversion of free energy of mixing into electric power, Ind. Eng. Chem. Process Des. Dev. 25 (1986) 443-449.

[8] W. Sunda, S. Huntsman, Effect of pH, light, and temperature on Fe–EDTA chelation and Fe hydrolysis in seawater, Mar. Chem. 84 (2003) 35-47.

[9] S. Sebig, R. van Eldik, Kinetics of [FeII (EDTA)] oxidation by molecular oxygen revisited. New evidence for a multistep mechanism, Inorg. Chem. 36 (1997) 4115-4120.

[10] E. Juzeliunas, K. Juttner, EQCM study of iron deposition from Fe II/Fe III (EDTA) solutions, Electrochim. Acta 43 (1998) 1691-1696.

[11] J. Heimach, S. Rieth, F. Mohamedshah, R. Slesinski, P. Samuel-Fernando, T.Sheehan, R. Dickmann, J. Borzellca, Safety assessment of iron EDTA [sodium iron (Fe^{3+}) ethylenediaminetetraacetic acid]: summary of toxicological, fortification and exposure data, Food Chem. Toxic. 38 (2000) 99-111.

[12] H. Gomathi, G. Prabhakara Rao, Simple electrochemical immobilization of the ferro/ferricyanide redox couple on carbon electrodes, J. Appl. Electrochem. 20 (1990) 454-456.

[13] C.M. Pharr, P. Griffiths, Infrared spectroelectrochemical analysis of adsorbed hexacyanoferrate species formed during potential cycling in the ferrocyanide/ferricyanide redox couple, Anal. Chem. 69 (1997) 4673-4679.

[14] J. Kiwi, M.R. Dhananjeyan, J. Albers, O. Enea, Photo-assisted immobilized Fenton degradation up to pH 8 of azo dye orange II mediated by Fe^{3+}/nafion/glass fibers, Helv. Chim. Acta 84 (11) (2001) 3433–3445.

[15] J. Bandara, C. Morrison, J. Kiwi, C. Pulgarin, P. Peringer, Degradation/decoloration of concentrated solutions of orange II. Kinetics and quantum yield for sunlight induced reactions via Fenton type reagents, J. Photochem. Photobiol. A: Chem. 99 (1) (1996) 57–66.

[16] N. Daneshvar, H. Ashassi-Sorkhabi, A. Tizpar, Decolorization of orange II by electrocoagulation method, Sep. Purif. Technol. 31 (2) (2003) 153–162.

[17] J.H. Ramirez, C.A. Costa, L.M. Madeira, Experimental design to optimize the degradation of the synthetic dye Orange II using Fenton's reagent, Catal. Today 107/108 (2005) 68–76.

[18] M.B. Ray, A. Bhattacharya, S. Kawi, Photocatalytic degradation of orange II by TiO2 catalysts supported on adsorbents, Catal. Today 98 (3) (2004) 431–439

[19] M. Inoue, F. Okada, A. Sakurai, M. Sakakibara, A new development of dyestuffs degradation system using ultrasound, Ultrason. Sonochem. 13 (4) (2006) 313–320

[20] O. Scialdone, A. Galia, S. Sabatino, Abatement of Acid Orange 7 in macro and micro reactors. Effect of the electrocatalytic route, Appl. Catal. B: Environ. 148–149 (2014) 473-483.

[21] I. Sirés, J.A. Garrido, R.M. Rodríguez, E. Brillas, N. Oturan, M.A. Oturan, Catalytic behavior of the Fe^{3+}/Fe^{2+} system in the electro-Fenton degradation of the antimicrobial chlorophene, Appl.Catal. B: Environ. 72 (2007) 382-394.

[22] R.M. Cespon-Romero, M.C. Yebra-Biurrun, M.P. Bermejo-Barrera, Preconcentration and speciation of chromium by the determination of total chromium and chromium(III) in natural waters by flame atomic absorption spectrometry with a chelating ion-exchange flow injection system, Anal. Chim. Acta 327 (1996) 37–45.

[23] Guidance for Drinking Water Quality, second edition, vol. 1. Recommendations, Geneva, WHO, 45 (1993).

[24] C.E. Barrera-Díaza, V. Lugo-Lugo, B. Bilyeu, A review of chemical, electrochem-ical and biological methods for aqueous Cr(VI) reduction J, Hazard. Mater.223–224 (2012) 1-12.

[25] P. Lakshmipathiraj, G. Bhaskar Raju, M.R. Basariya, S. Parvathy, S. Prabhakar, Removal of Cr (VI) by electrochemical reduction, Sep. Purif. Technol. 60 (2008) 96-102.

[26] C.M. Welch, O. Nekrassova, R.G. Compton, Reduction of hexavalent chromium at solid electrodes in acidic media: reaction mechanism and analytical applications, Talanta 65 (2005) 74-80.

[27] D. Golub, Y. Oren, Removal of chromium from aqueous solutions by treat-ment with porous carbon electrodes: Electrochemical principles, J. Appl.Electrochem. 19 (1989) 311-316.

[28] A.J. Chaudary, N.C. Goswanmi, S.M. Grimes, Electrolytic removal of hexavalentchromium from aqueous solutions, J. Chem. Tech. Biotech. 78 (2003) 877-883.

[29] F. Rodriguez-Valadez, C. Ortiz-Éxiga, J.G. Ibanez, A.A. Ordaz, S. Gutierrez-Granados, Electroreduction of Cr(VI) to Cr(III) on reticulated vitreous carbonelectrodes in a parallel-plate reactor with recirculation, Environ. Sci. Technol.39 (2005) 1875-1879.

[30] G. Wang, L. Huang, Y. Zhang, Cathodic reduction of hexavalent chromium[Cr(VI)] coupled with electricity generation in microbial fuel cells, Biotechnol. Lett. 30 (2008) 1959-1966.

[31] I. Frenzel, H. Holdik, B. Barmashenko, D.F. Stamatialis, M. Wessling, Electrochemical reduction of dilute chromate solutions on carbon felt electrodes, J. Appl. Electrochem. 36 (2006) 323-332.

[32] C.M. Welch, O. Nekrassova, R.G. Compton, Reduction of hexavalent chromium at solid electrodes in acidic media: reaction mechanism and analytical applications, Talanta 65 (2005) 74-80.

[33] E.O. Vilar, E.B., Cavalcanti, H.R., Carvalho, F.B., Sousa, Cr (VI) electrochemical reduction using RVG 4OOO graphite felt as the electrode, Braz. J. Chem. Engin.20 (2003) 291.

[34] R E. Lacey, Ocean Eng. 7 (1980) 1-47.

[35] M. Tedesco, A., Cipollina, A., Tamburini, W. van Baak, and G. Micale, Modelling the Reverse ElectroDialysis process with seawater and concentrated brines, Desalin. Water Treat. 49 (2012) 404-424.

[36] L. Gurreri, A. Tamburini, A. Cipollina, G. Micale, M. Ciofalo, CFD simulation of mass transfer phenomena in spacer filled channels for reverse electrodialysis applications, Chem. Eng. Trans. 32 (2013) 1879-1884.

[37] M. Tedesco, A., Cipollina, A., Tamburini, G., Micale, J. Helsen, and M. Papapetrou, REAPower - Use of Desalination Brine for Power Production through Reverse Electrodialysis, Desalin. Water Treat. 53 (2014) 3161-3169.

4.   APPLICATION OF RED PROCESS IN A PILOT PLANT

4.1   INTRODUCTION

Up to now, reverse electrodialysis technology has been largely studied through laboratory experiments, leading to significant improvements in the process performance. Most of the works presented in literature are limited to the utilization of artificial water solutions (to simulate river and seawater) to feed in the system [1-5]. Just very few examples are reported in the literature on the performance of RED process using natural solutions. Among these, the experimental campaign performed in Harlingen (Netherlands) [6,7] showed interesting data on the use of real fresh water and seawater on laboratory-scale RED stack without give information about the scale-up. In these works, Veerman et al. reported some drawbacks that may occur by working with real solutions, one among all the fouling phenomena. In fact, using real solutions, a 40% reduction of the power output was observed during the first day of operation due to the presence of colloidal and organic fouling, fatal for AEMs. Because natural solutions contain many salts in addition to NaCl, the effect of bivalent ions on RED performance has been recently investigated by Vermaas [8] which confirms that bivalent ions such as Mg^{2+}, SO_4^{2-}, having lower mobility inside IEMs, increase the membranes resistance causing a power reduction. The use of highly concentrated solutions has been recently proposed to enhance the performance of RED technology and has been proven the positive effect of these solutions on power density [9-11].

In order to test the RED process on real environment, a further scale-up was required. Therefore, important activities were carried out using the first RED pilot plant fed with real brackish water and saltworks brine. The plant, in question, is located in a saltworks area in Marsala, situated on the west coast of Sicily (Trapani, Italy). The Ettore-Infersa saltworks is an ideal location for demonstrating the application of RED process in real environment, providing seawater, brackish water and concentrated brines as possible feed streams. As we know, in a saltworks seawater is collected in several large basins in which, thanks to the evaporation process (caused by sun energy and wind), increases its salt concentration rising from

one tank to another achieving in the last basins the saturation for NaCl only obtainable using a careful flow regulation to ensure the precipitation of salts as calcium sulphates and carbonates. The Ettore-Infersa saltworks in Marsala has been selected as installation site of the REAPower pilot plant (Figure 4.1) for the presence of brackish water, good to optimise the salinity gradient for power production and because this natural solution is generally rather clean and practically free of suspended solids (Table 4.1), thus requiring minor pre-treatments, especially compared to what normally required by seawater.

Figure 4.1 Satellite image of the REAPower plant installation site (*Ettore-Infersa* saltworks, Marsala, Italy). Three different solutions are available for power production by RED: saturated brine from ponds, seawater from an open channel and brackish water.

Solution	Conductivity (mS/cm)	Molarity (mol/L)	Suspended solids concentrations (mg/L)
Breackish water	3.4	0.03	-
Seawater	49	0.5	74-200
Brine	220	5	20

Table 4.1 Composition of natural solutions at pilot plant in Marsala; the molarity is calculated from measured conductivity assuming that only NaCl is present.

The pilot plant involved three intake lines: two intake centrifugal pumps (Schmitt MPN 130, Kreiselpumpen GmbH & Co.KG, Germany) for seawater and for brine have been installed, while a direct connection from the well is used for brackish water (Figure 4.2) (operating with immersed centrifugal pump with open impeller).

121

Regarding the dilute solution, this is firstly sent to a filtration zone (where membrane pumps Shurflo SH-4111-03 are used) and then to two storage vessels (4 m^3 of total capacity) that ensure a proper availability of diluted solution (these reservoirs are installed within the salt warehouse). The brine filtration zone, instead, is installed directly into the main building, where the RED prototypes are installed. Just before the main feed pumps of the saline solutions at the inlet of the RED unit, two small buffer tanks (125 L capacity) for diluted and concentrated solutions are positioned.

Figure 4.2 Process flow diagram of the REAPower pilot plant. Installed by Scalici Claudio.

In 2010, Post et al. [12] published some information on the use of the Blue Energy pilot plant (located on Afsluitdijk, a 32 km-long dyke that separates the Ijssel Lake from the Wadden Sea). The information reported by Post are the only on the activity leaded with a pilot plan and describe the capacity of the Blue Energy plant when this is fed with seawater and fresh water at 220 m^3/h flow rate, with an expected power target capacity of 50 kW (which requires the installation of 100,000 m^2 of membranes).

This chapter describes the activities carried out using the REAPower pilot plant (Figure 4.3). The results below are related to the study on:

- ✓ effect of the variation of flow rate of fresh and exhausted electrode solution of $FeCl_2/FeCl_3$ and without the ion redox couple;
- ✓ effect of the variation of flow rates of saline solutions;
- ✓ removal of azo-dye (AO7) from electrode compartment.

4.2   REVERSE ELECTRODIALYSIS STACK

The device used was characterized by 500 cell pairs with 44x44 cm^2 membrane active area and cross-flow arrangement. The prototype (Figure 4.3B) is equipped with following Fuji ion exchange membranes:

- Anionic Exchange membranes, AEM 80045-01characterized by thickness 120 µm, permselectivity (0.5 M - 4 M) 0.65, electrical resistance 1.55 Ωcm^2, hydraulic permeability 4.96 mL/bar h m^2;
- Cationic exchange membranes CEM 80050-04 characterized by thickness 120 µm, permselectivity (0.5 M - 4 M) 0.90, electrical resistance 2.96 Ωcm^2, hydraulic permeability 4.72 mL/bar h m^2.

Each membrane is separated from the adjacent one by a gasket integrated with a spacer (Deukum GmbH, Germany) of thickness 270 µm. Electrodes are placed at the ends of the package of membrane electrodes. 4 electrodes (10 cm x 10 cm) are used as anodes and other four as cathodes. The electrode material employed was mixed oxides of tantalum and iridium.

About the electric analyses (Figure 4.3C), the measuring instrumentation is constituted by temperature/conductivity sensors/transmitters (Jumo CTI-500) and pressure transducers (Jumo Midas SW) for both inlet/outlet solutions. The inlet flow rate of both concentrate and dilute were measured by magnetic flowmeters (Khrone IFC 100 C). The properties of electrode rinse solution were also monitored in terms of conductivity, temperature, flow rate and pH by the same type of instrument. The stack potential was acquired by a data logger, while the external current was measured by an external amperometer.
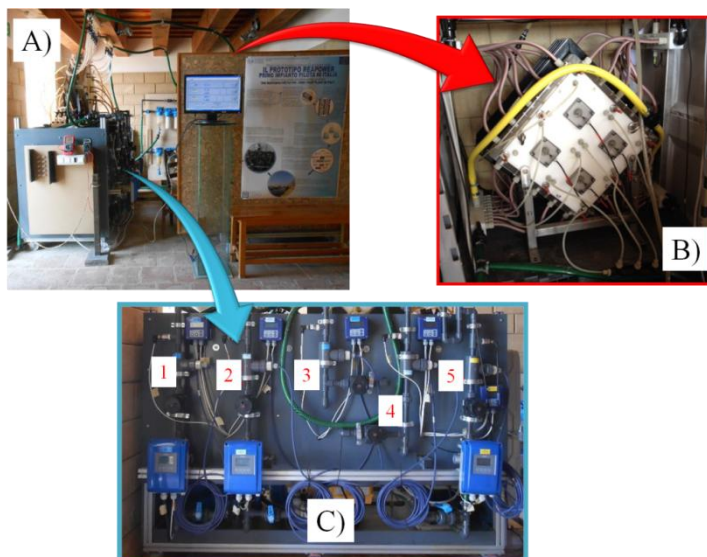
Figure 4.3 A) Final view of the REAPower demonstration plant. B) front-end panel of the supporting tray. Numbers indicate the five pipelines used: HIGH inlet (1), LOW inlet (2), HIGH outlet (3), LOW outlet (4), Electrode Rinse Solution (5). C) Large prototypes (44 x 44 cm^2, 500 cell pairs) installed.

A scheme of electric circuit is reported in Figure 4.4. The system performance in terms of power generation was investigated connecting the RED unit with an external load. As variable-resistance load ten halogen lamps (100 W each) installed in parallel/series were used (Figure 4.4B).
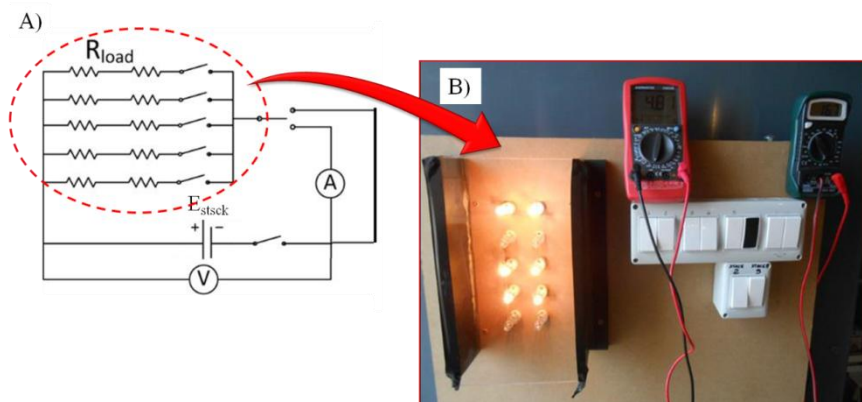
Figure 4.4 A) Electric circuit of RED system. B) Halogen lamp used as external load.

The stack potential and all the properties of solutions (conductivity, temperature, inlet flow rates, and pressure drop) were collected by the acquisition system (LabVIEWTM, National Instruments, USA) at a frequency of 1 Hz.

4.3   GENERATION OF ELECTRIC ENERGY

Effect of the redox processes

Several experiments were carried out working with two different electrode rinse solution: with or without an iron redox couple. In one case a solution containing 0.3 M $FeCl_2$, 0.3 M $FeCl_3$, 2.5 M Na_2SO_4 as supporting electrolyte at pH 2 was fed, in the second case a solution containing only 2.5 M NaCl was used (called white solution). As reported in Figure 4.5, according with the data recorded during lab-scale experiments, the power output from the system depends on the redox processes selected. Indeed, when Fe(II)/Fe(III) couple was used the power output increased which is consistent with the trend of potential required to drive the corresponding redox processes. Indeed, trends reported in Figure 4.5 are justified considering that for water/NaCl systems, redox reactions require relevant thermodynamic potentials coupled with high overvoltages while when iron redox couple was used the thermodynamic potential required to drive the redox reactions is null (since opposite anodic and cathodic reactions are involved) and the electrode potentials are only given by cathode and anode overpotentials (see paragraph 3.2). When water solution contained only NaCl was used in the electrode compartment, the possible formation of chlorine was monitored. In this case a concentration of about 5 mg/L was recorded.
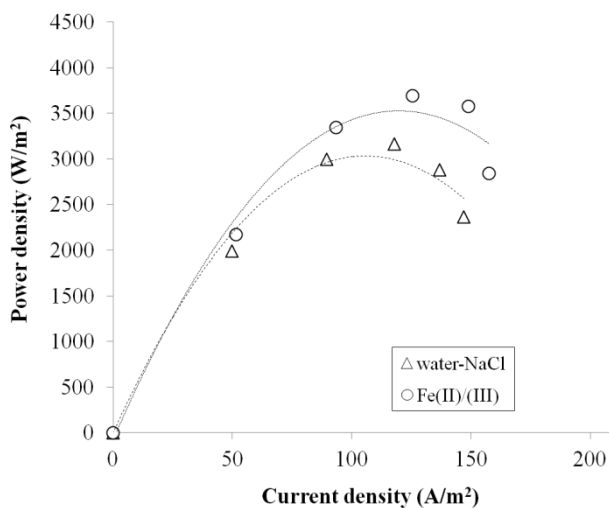
Figure 4.5 Plot of power density (computed as the ratio between the power and the geometric area of electrode) vs. current density recorded in a stack of 500 cells pairs with different redox systems. Electrode rinse solution flow rate 2 L/min, HC and LC flow rate 23 L/min.

Effect of feed flow rate of electrode rinse solution

A series of test was performed to investigate the effect of electrode rinse solution flow rate. For these experiments three kind of electrode solutions were used:

- (SOLUTION 1) a fresh water solution of $FeCl_2/FeCl_3$ 0.3 M with Na_2SO_4 2.5 M as supporting electrolyte and HCl to work at pH of 2;
- (SOLUTION 2) an exhausted electrode solution (that is a solution that has been used for a long time);
- (SOLUTION 3) a fresh water solution without iron redox couple (using NaCl 2.5 M as supporting electrolyte).

In all cases brine and fresh water solution were fed in HC and LC compartments.

Figure 4.6 reports the effect of increasing flow rates on power density working with SOLUTION 1. The flow rates used were: 2, 3 and 4 L/min. An increase of the flow rate corresponds to a higher power density output from the system (calculated

126

respect to the electrode surface). Indeed, using a flow rate of 4 L/min a power output of about 171 W was obtained, slightly higher than that obtained working with the lower flow rate (155 W). We can record that the power output was calculated using the Ohm's law ($P = E_{stack} * I$) where stack voltage and current were recorded varying the external load (by turning on / off the lights).
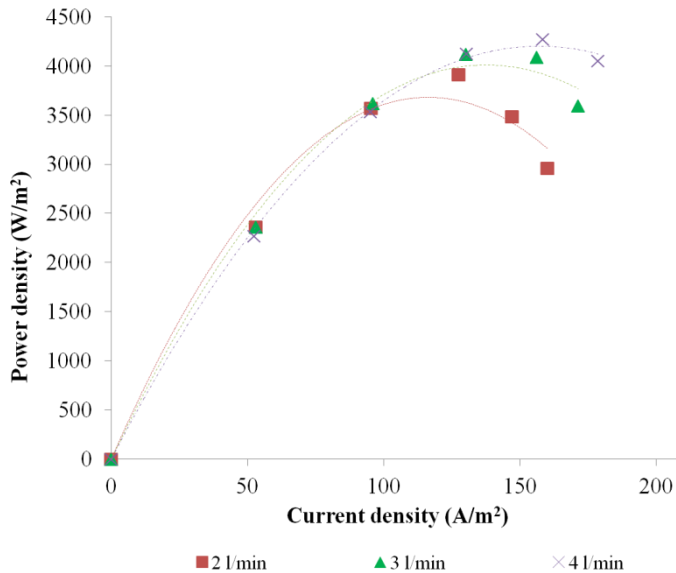
Figure 4.6 Power density as function of current density varying the electrode rinse solution flow rate.

Although an increase in the power output has been observed using an electrode solution flow rate of 4 L/min, a higher flow rate in the electrode compartments is not recommended due to the high local pressure drops. Indeed increasing the flow rate from 2 to 4 L/min, pressure drop increased from 0.4 up to 0.7 bar becoming comparable with the pressure drop in the diluted compartments. The change of flow rate on the electrode solution causes an alteration also in the polarization curve (Figure 4.7). In the high current range, there is a clear deviation of the polarization curve from the linear behavior. From the slopes of the curves we can obtain the internal resistance of electrode compartment and the change in this resistance may be caused to mass transport phenomena of electrode rinse solution.
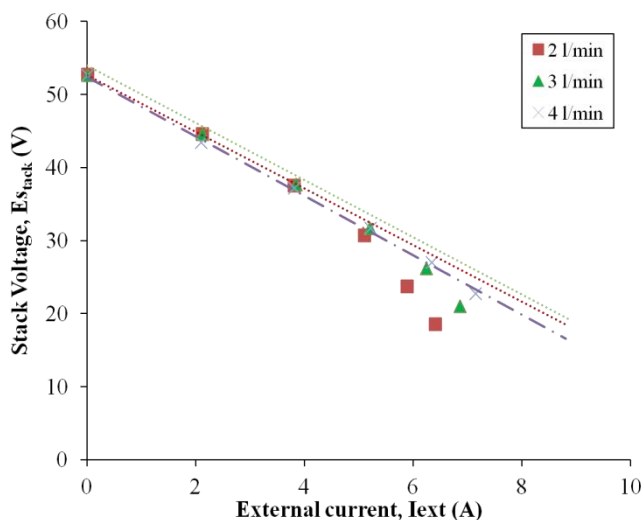
Figure 4.7 Polarization curve. Influence of feed electrode rinse solution flow rates on process performance.

To monitor the possible transition of iron ions in the salt compartment adjacent to the electrode compartments spectrophotometric measurements (UV-vis) were performed on aliquots of the sample taken from the electrode compartment at the end of each test. The concentration of iron (II) / (III) ions stays consistent during each test but, as you can see from the Figure below, varying the flow rate of electrode solution, the concentration of iron ions changes (trend marked by the arrows). Lesser is the flow, greater is the loss of concentration of iron. Indeed, because the solution is stagnant for a longer time interval in the electrode compartment the ions pass through the membrane into the adjacent compartment. To underline the concept another test was carried out fed electrode solution with a flow rate of 1.4 L/min. Results circled in green confirm what has been said above.
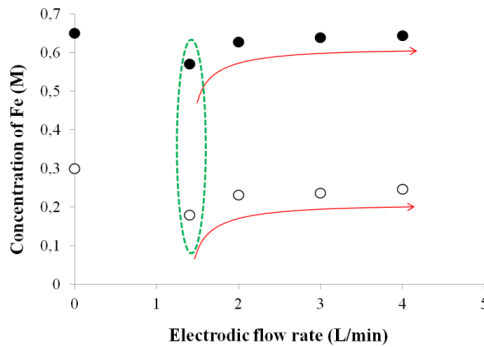
Figure 4.8 Influence of flow rate on the passage of iron ions across the ion exchange membrane that separates electrode compartment with saline one. Results circled in green were recorded by working with a flow rate of 1.4 L/min. Arrows outline the variation of ions concentration ions with variable flow rate. White symbols indicate that the experiment has been conducted using a fresh iron electrode solution, black symbols are referred to exhausted iron solution.

Equal experiment were repeated changing electrode solutions. Figure 4.9 compares between the curves of power density as a function of current density obtained by working with fresh iron (white symbols) and exhausted iron solution (filled symbols). The set of data represented by circles are related to the test with a flow rate of the solution electrode equal to 4 L/min, while the results represented with squares have been obtained by working with the lower flow rate (2 L/min).
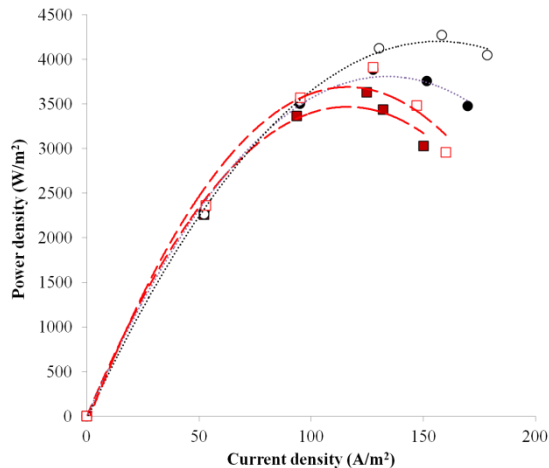
Figure 4.9 Comparison between curve of power density as function of current density obtained working with fresh (circle symbol) and exhausted iron ion solution (square symbol) at different flow rate: 2 (closed symbol) and 4 L/min (open symbol).

129

When a fresh electrode solution is used system performances are better than when a exhausted solution is fed. This can be explained assuming an aging of the solution. In fact the solutions used for several months showed the presence of a precipitate on the bottom of the electrode reservoirs probably caused to condition changes (i.e. pH changes).

When the concentration of $FeCl_2/FeCl_3$ was increased no significant changes were observed.

Same tests ware repeated using "white solution" (without iron redox couple). Also in this case increasing the electrode solution flow rate, a variation of the power outputs was recorded. The power delivered by the system increases, but in a less significant way with respect to that observed in the presence of iron ions.
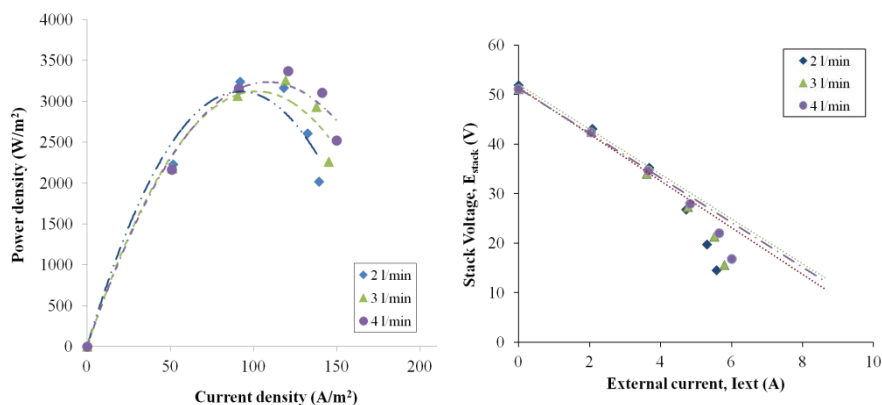
Figure 4.10 Effect of the variation electrode solution flow rate using a water solution containing NaCl 2.5M in the electrode compartment. A) power density vs. current density; B) polarization curves.

In these cases, increasing concentrations of Cl_2 were recorded rising with the flow rate (from 5 mg/L to 11 mg/L).

Effect of HC and LC solution flow rate on power output

Also the flow conditions for the diluted and concentrated water solutions can affect the power output from the system. Such phenomenon was experimentally observed varying the flow rate for HC and LC in the following manner:

- ✓ HC and LC 16 L/min;
- ✓ HC and LC 23 L/min;
- ✓ HC 32 L/min and LC 23 L/min.
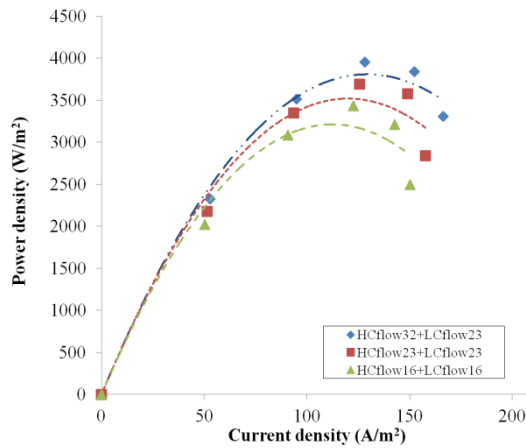
Figure 4.11 Plot of power density vs current density in a stack equipped with 500 membrane pairs for $FeCl_2/FeCl_3$ electrode solution with a flow rate of 2 L/min and varying HC and LC flow rates.

A power output of 158 W was reached using feed flow rates of 32 L/min (HC) and 23 L/min (LC). Lower values were recorded by decreasing the flow rate of both salt solutions: 148 W for HC and LC flow rates equal to 23 L/min and 136 W for HC and LC flow rates equal to 16 L/min.

The effect of increasing power is also due to the lower residence time of solutions inside stack, leading to a higher OCV (Figure 4.12).
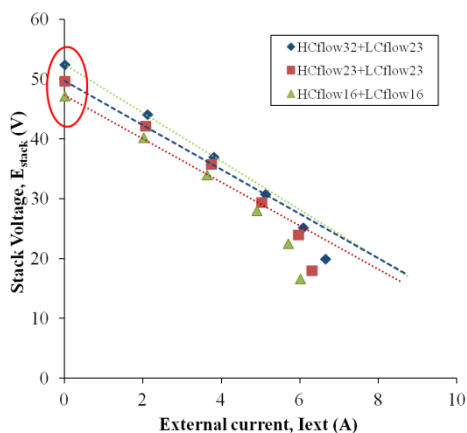
Figure 4.12 Plot of polarization curves for a stack equipped with 500 membrane pairs for $FeCl_2/FeCl_3$ electrode solution with a flow rate of 2 L/min and varying HC and LC flow rates.

The concentration of iron ions in the electrode compartment remained indifferent changing the flow rate of saline solutions. No passage of ions was recorded in each case of study.

The influence of HC and LC flow rates was monitored when a water solution containing NaCl was fed in electrode compartment. As reported in Figure 4.13 there aren't significant variations on power output.
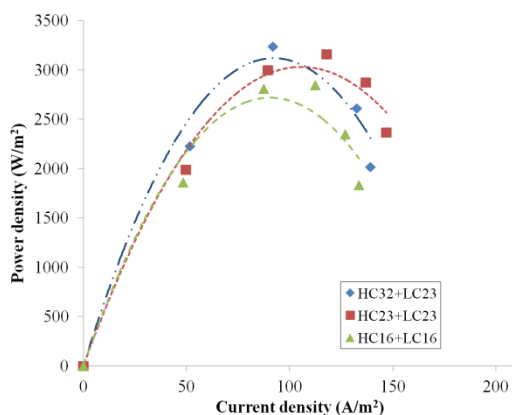
Figure 4.13 Plot of power densities (computed as the ratio between the power and the geometric area of electrode) vs. current density recorded in a stack under the influence of different HC and LC flow rates using water/NaCl electrode solutions.

132

During the experimental campaign carried out with the prototype several tests were performed in order to study the stability of electrode system in the time. Experiments carried out during several months using the same solution electrode showed a good stability of the redox couple.

4.4 REMOVAL OF POLLUTANT PRESENT IN THE ELECTRODE SOLUTION

Eventually, the possibility to remove an organic pollutant from the electrode solution has been tested. Also in this case, the same azo-dye used in lab experiments was selected as model organic pollutant: Acid Orange 7, AO7. Experiments were performed by feeding in the electrode compartment (only one hydraulic circuit) an aqueous solution containing AO7 (150 mg/L), Na_2SO_4 (0.085 M), 0.5 mM $FeSO_4$ * $7H_2O$ and H_2SO_4 (pH = 2). As shown in the following Figure the total removal of dye was obtained. Only 15 minutes were necessary to obtain a removal of the color higher than > 98%.
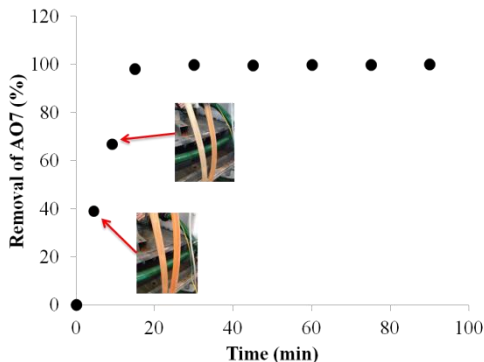
Figure 4.14 Abatement of color vs. time achieved with a stack equipped with 500 cell pairs and fed brine and fresh artificial solutions. The left tube is full of solution outbound from the stack, the right tube is full of solution in entry in the stack.

NPOC measurements were carried out to monitor the pollution abatement. After 80 minutes of treatment a reduction of only 30% was recorded. This is justified considering the big volumes used during the test (25 liters in RED pilot plant vs 250 mL in lab scal experiment).

133

As reported in Figure 4.15, during the test of abatement the power output by the system decreased with the reduction of the dye concentration reaching a final constant value of about 60 W.
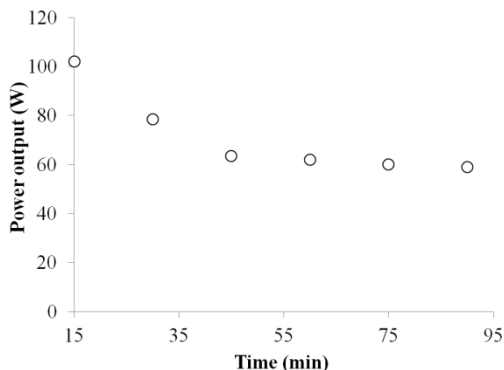
Figure 4.15 Power vs. Time recorded using the lower R (10 lamps on) using a stack equipped with 500 cell pairs and fed brine and fresh artificial solutions.

In the last graph (Figure 4.16), the curves of power density as a function of the current density at the beginning and end of the test abatement are reported.
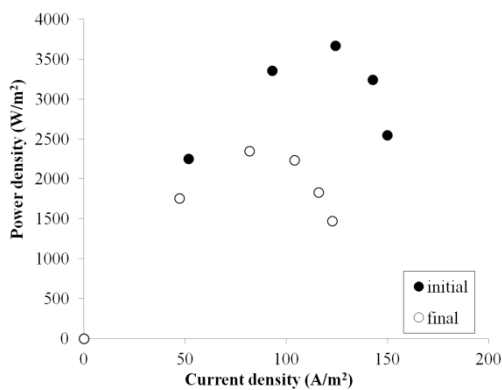
Figure 4.16 Power density vs. current density recorded using the lower R (10 lamps on) using a stack equipped with 500 cell pairs and fed brine and fresh artificial solutions. Data are registered at the start and the end of the experiment.

4.5   REFERENCES

[1] R.E. Pattle, Production of Electric Power by mixing Fresh and Salt Water in the Hydroelectric Pile, Nature. 174 (1954) 660.

[2] R. Audinos, Inverse Electrodialysis. Study of Electric Energy Obtained Starting with Two Solutions of Different Salinity, J. Power Sources. 10 (1983) 203–217.

[3] J.N. Weinstein, F.B. Leitz, Electric power from differences in salinity: the dialytic battery, Sci. (New York, NY). 191 (1976) 557.

[4] J. Jagur-Grodzinski, R. Kramer, Novel process for direct conversion of free energy of mixing into electric power, Ind. Eng. Chem. Process Des. Dev. 25 (1986) 443–449.

[5] J. Veerman, M. Saakes, S.J. Metz, G.J. Harmsen, Reverse electrodialysis: Performance of a stack with 50 cells on the mixing of sea and river water, J. Memb. Sci. 327 (2009) 136–144.

[6] D.A.A. Vermaas, D. Kunteng, J. Veerman, M. Saakes, K. Nijmeijer, Periodic feedwater reversal and air sparging as antifouling strategies in reverse electrodialysis, Environ. Sci. Technol. 48 (2014) 3065–3073.

[7] D.A.A. Vermaas, D. Kunteng, M. Saakes, K. Nijmeijer, Fouling in reverse electrodialysis under natural conditions, Water Res. 47 (2013) 1289–1298.

[8] D.A. Vermaas, J. Veerman, M. Saakes, K. Nijmeijer, Influence of multivalent ions on renewable energy generation in reverse electrodialysis, Energy Environ. Sci. 7 (2014) 1434–1445.

[9] A. Daniilidis, D.A.A. Vermaas, R. Herber, K. Nijmeijer, Experimentally obtainable energy from mixing river water, seawater or brines with reverse electrodialysis, Renew. Energy. 64 (2014) 123–131.

[10] R.E. Lacey, Energy by reverse electrodialysis, Ocean Eng. 7 (1980) 1–47.

[11] M. Tedesco, P. Mazzola, A. Tamburini, G. Micale, I. D. L. Bogle, M. Papapetrou, A. Cipollina (2014): Analysis and simulation of scaleup potentials in reverse electrodialysis, Desalination and Water Treatment, DOI: 10.1080/19443994.2014.947781

[12] J.W. Post, C.H. Goeting, J. Valk, S. Goinga, J. Veerman, H.V.M. Hamelers, et al., Towards implementation of reverse electrodialysis for power generation from salinity gradients, Desalin. Water Treat. 16 (2010) 182–193.

Part II:

5.   MICROBIAL FUEL CELL: MFC

(Another kind of system for the production of electricity)

5.1 STATE OF ART

For many years, experts are gone in search of interesting environmentally-compatible energy resources as alternative of the fossil fuel forthcoming depletion. Among these options, fuel cells appear as a good choice. Fuel cells are divided into two chambers, each containing an anode and a cathode respectively. The anode side is characterized by the presence of hydrogen or methanol used as electron donors (Figure 5.1). This specie is oxidized on the anode surface, leading to the formation of electrons and cations:

- the electrons generated create current in an external circuit going through a load,
- the cations through a cation exchange membrane pass to the cathode side of the fuel cell, in order to equalize the charge transferred by the electrons.

Simultaneously in the cathode takes place an oxidation reaction. The driving force of the reaction is the potential difference across the circuit.
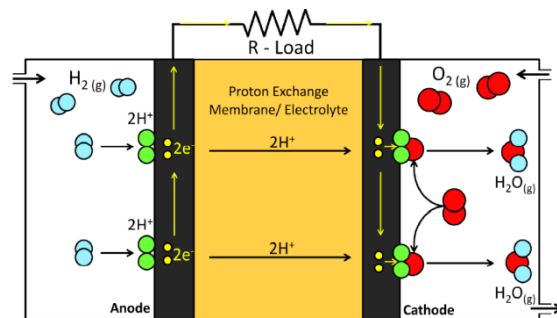
Figure 5.1 Representation of a fuel cell which uses hydrogen as fuel in the anodic compartment.

In spite of the interesting idea, fuel cell technology show several drawbacks such as hard operative conditions, limited resources, utilization of expensive catalytic material and poisoned of electrode by CO which can be formed if the used fuel gas is not pure. In order to exceed these disadvantages, bioelectrochemical system have been proposed as innovative technique to generate energy from organic medium

working under mild reaction conditions (ambient temperature, normal pressure, and neutral pH) and using as catalyst either a microorganism or an enzyme.

The concept of utilizing microorganisms to generate electricity was first recognized in the 18th century. Potter was the first person to demonstrate a half cell using microorganisms (Escherichia coli) to generate electricity in 1911 [1]. The results of these experiments were not reported for almost 20 years. Some studies on microbial and bio-fuel cells were reported between the 1950s and the 1980s, though little attention was paid to this technology until recently [2-4] when the potentiality of these biological fuel cell for clean, sustainable and renewable energy production becomes more clear.

The bioelectrochemical systems can classified in different categories depending on the process of generation and storage of electricity. In some cases, the generation of current by a conventional fuel cell is preceded by a conversion of an organic waste into hydrogen or ethanol, in other cases there is a combination between photochemically active and biological systems.

A promising technology that does not require of supply electric energy is Microbial fuel cell which uses an anode-bacteria where active microorganisms (living catalysts) are capable to convert bio-waste to electrons, oxidizing organic matter (present naturally in the environmental or in waste) to generate electrons, protons, and other metabolic products. The cathode can use a variety of electron acceptors; however the most widely used are ferricyanide and oxygen [5,6]. Although ferricyanide is often used in MFC research when cathode effects are not of interest to the researcher, since it has a very high potential and makes for an excellent cathode reagent, with little or no limitation to the system, on other hand it is a toxic compound, and if it pass through the membrane can have a negative impact on the anodic cultures.

Although the power generation from MFCs has improved considerably in recent years, it is still a big challenge [7-10] but can be safely inserted in the energy market. The components of a MFC are: *anode compartment* where fuel is oxidized

by bacteria; a *membrane* that separates anode and cathode; an *external circuit* to transfer electrons from anode to cathode (Figure 5.2).
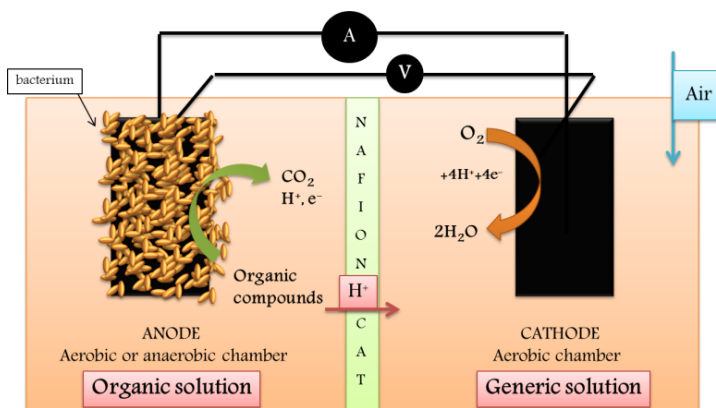
Figure 5.2. Scheme of a generic microbial fuel cell.

Suspended microorganisms and/or bound microorganisms to a support material, forming a biofilm, in the anodic chamber oxidizes organic matter and produce electrons, protons and other metabolic products. Once electrons and protons are in the cathode, they react with oxygen from the air and produce water and electrical current.

5.2   MICROORGANISMS AND BIOFILM FORMATION

The bacteria that are capable of exocellular electron transfer are namely *Exoelectrogens*. First studies have assumed that the active bacteria in MFCs were mainly the iron reducing bacteria, such as Shewanella and Geobacter species, but searches have revealed much greater variety of bacteria. Among the active bacteria various categories can listed such as Gram-positive bacteria, Gram-negative bacteria, yeast, cyanobacteria, algae, and even fungi. The ability of these microorganisms to maximize the energetic gain during the conversion of the substrate determines their capacity of survival and growth. The mechanism of biofilm formation is highly complex and it is derived by various elements:

- substrates,

- bacteria,

- electrode materials,

- operating conditions.

Depending of type of substrate change the morphology of biofilm because microorganisms have different mode (proteins, genes) to degrade the organic medium. Thus, the selection of suitable Colonia and adequate substrate are fundamental to determine the output of MFC.

A series of sequential processes are necessary to obtain the anode-bacteria, including transport of microorganisms from bulk solution to an electrode surface, initial attachment to the surface of electrode, formation of microcolonies and biofilm maturation. Different types of adhesion of bacteria on the surface are possible (Figure 5.3)
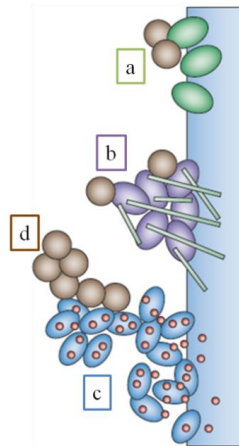
Figure 5.3 Different types of possible interactions between the microorganisms and the electrode surface.

In the Figure the bacteria corresponding to [11]:

- a (green) are exoelectrogens that transfer electrons by direct contact mediated by redox-active proteins such as cytochromes present on the outer surface of the bacterial cell membrane,

- b (purple) are microorganisms that produce nanowires,
- c (blue) are bacteria that uses endogenous (and therefore self-produced) mediators,
- d (brown) represent other non-exoelectrogenic bacteria that live off the products produced by other bacteria or possibly use mediators or nanowires produced by other microorganisms can also be present.

At the beginning, artificial shuttle were used to make possible the adhesion of microorganisms to surface such as neutral red and methyl viologen; then it was shown that different mechanisms of electron transfer from inside the bacterial cell to the electrodes by the secretion of soluble shuttle such as flavin [12], ribloflavin [13] or pyocyanin [14] species can occur.
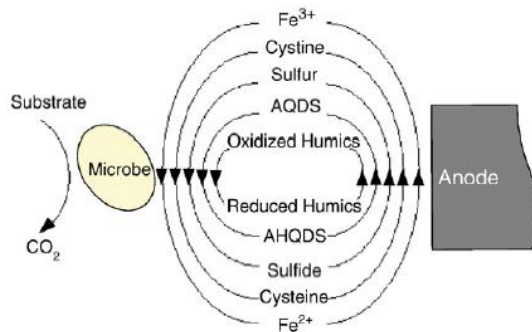
Figure 5.4 Simple scheme of various compounds using as electron shuttles between active microorganism and the anode.

'Mediator way' is the most common electron transfer mode used in MFCs and can be classified into two sub-types: indirect transfer systems that involve freely diffusing mediator molecules (i.e., diffusive MET) and indirect transfer systems in which the mediator is integrated into the electrode or the cell membrane (i.e., non-diffusive MET).

The biofilm formed can be mono-layer or multi-layer. In this second case, between microorganisms and electrode, there are a dense network of nanowire with metallic

141

conductivity responsible for the conductive biofilms of high current production. Shewanella [15,16] and Geobacter [17-19] species mediate the long-range electron transfer in this way.

Biofilms can be formed by a single bacterial species (pure-culture biofilm) or by multiple bacterial species (mixed-culture biofilm) such as a waste water or sludge. MFCs that make use of mixed bacterial cultures have some important advantages over MFCs driven by axenic cultures: higher resistance against process disturbances, higher substrate consumption rates, smaller substrate specificity and higher power output [20,21]. Mostly, the electrochemically active mixed cultures are enriched either from sediment (both marine and lake sediment) [22,23] or activated sludge from wastewater treatment plants [20,22,23-26].

5.3   TYPOLOGIES OF BACTERIA

The most common microorganisms are part of Pseudomonas and Geobacteraceae families. Both are used as pure cultures, namely cultures in which there is only one microbial species.

Shewanella

Among the Pseudomonas a kind of bacteria most used is the *Shewanella putrefaciens*, a particular biotype that is isolated from the marine waters. *Shewanella putrefaciens* was first shown to produce electricity in the absence of exogenous mediators in 1999 [27]

Shewanella are characterized by cytochromes [28] in the outer membrane that allow a direct electron transfer by contact, but they can also extrude electrically conductive nanowires (Figure 5.5).
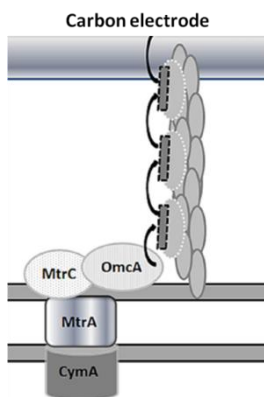
Figure 5.5 Shows a schematic microbe–electrode interactions for Shewanella species.

Electrons pass along the pilus by "hopping" from heme to heme in a mechanism which is basically a series of quantum mechanical tunneling through the protein matrix between hemes.

Many studies have been conducted using *Shewanella oneidensis* as bacteria; these have the particular advantage of carrying out the normal metabolic processes of oxidation of the organic substrate even in the presence of oxygen, extremely interesting property, which opens frontiers innovative regarding the construction of modern microbial fuel cells. S. oneidensis produce flavins that can function as electron shuttles [29]. This bacterium has a big variety of multiple methods that can be used for exocellular electron transfer, but the possible interaction of electron-transferring molecules (cytochromes, flavins or those in nanowires) with the carbon electrode causes a decrease of the power produced by them of 56% than an acclimated wastewater inoculum in an air cathode MFC due to the presence of metal oxide.

Geobacter

One of the most extensively studied microorganisms capable of high current densities in a MFC is G. sulfurreducens, microorganism rod-shaped, obligate anaerobic and non-fermentative. Oxygen is toxic to G. sulfurreducens in large quantities, greater than 10% in the gas phase, and can severely limit growth even in

143

small quantities. However it was shown that it is aerotolerant under specific working conditions using cysteine and 0.5% yeast extract in order to eliminate residual oxygen and promote growth after the exposition [30]. Pure cultures of *G. sulfurreducens* have been found to produce near or greater than maximum power of mixed species biofilms [31,32] belongs to class of microbes referred to as electricigens, a term used to describe microbes that conserve energy to support growth by completely oxidizing organic compounds to carbon dioxide with direct electron transfer to the anode of the MFC [33]. These microorganisms present various advantages such as: high coulombic efficiency due to the complete oxidation of the organic substrate with transfer of electrons to the electrode; long time stability associated with the conservation of energy for maintenance and growth from the electron transfer to the anodes and direct electron transfer to the anode by the bacteria negating the need for the addition of any exogenous or production of electron mediators. *G.* sulfurreducens has also shown a very high propensity to form thick biofilms (greater than 50 μm thick) in which electrons are transferred via membrane bound cytochromes from bacteria situated near the electrode and by the formation of conductive nanowires from cells furthest from the electrode (Figure 5.6). Electron conducting nanowire proposed for Geobacter consisting of a pilus devoid of cytochromes. Electrons pass along the pilus displacement of delocalized electrons contained in overlapping π–π orbitals of the rings from aromatic amino acids. Thus, this mechanism is analogous to electron conduction by a metallic wire.
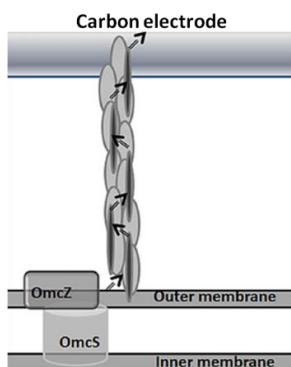
Figure 5.6 Shows a schematic microbe–electrode interactions for Geobacter species.

This bacterium is typically fed with acetate as a substrate. However it has been known to consume lactate, hydrogen and pyruvate as well [34-36].

Mixed culture

It was observed that the interaction of several microbial species leads to a clear improvement of the performance of MFC. This is due to the fact that the various bacterial species working in parallel can better adjust to operational changes [37].

Based on experiments conducted in the laboratory, researchers have observed that the use of activated sludge is optimal for the MFC and can be effectively utilized as a sustainable source of fuel to generate electricity using low cost MFC. Active sludge contains appropriate concentrations of nitrogen and phosphorus to ensure the effective development of biomass. Because the ratio C:N:P is higher than that required by normal cellular metabolism of 100:5:1 a number of different bacterial strains are formed, including many species of electrogens, often capable to form a bio anode or a bio-cathode. In 2007 Murano and Scott [38] have used sludge manure as fuel at low cost to produce electricity using MFC, without addition of mediators. In 2013, Vologni and others have used sludge from the primary and secondary clarification of some plants, once again getting satisfactory results in the production of energy [39]. Vologni has discovered that the addition of a phosphate buffer solution does increase the generation of current of 0.8 A/m^2, as well as increase the power density of 0.18 W/m^2.

Currently many aspects of the MFC activated sludge are being studied with the aim of increasing the energy efficiency of the process.

5.4   MICROBIAL METABOLISM

As previously mentioned, the bacteria in microbial fuel cells act as catalysts for anode reduction by some bacterial substrate. In MFC, heterotrophic bacteria, which include all pathogens, obtain energy from oxidation of organic substrates containing often carbohydrates, lipids, and proteins that serve as electron donors for redox reactions at the anode. In general, in the MFC most used bacteria gain energy by

transferring electrons from a reduced substrate at a low potential, such as glucose or acetate, to an electron acceptor with a high potential, such as oxygen.

The main reactions inside the MFC are the following ones when acetate is used:

Anodic oxidation reaction:

$$CH_3COO^- + 4H_2O \rightarrow 2HCO_3^- + 9H^+ + 8e^- \qquad \text{(react. 5.1)}$$

$$CH_3COO^- + 3H_2O \rightarrow HCO_3^- + CO_2 + 8H^+ + 8e^- \qquad \text{(react. 5.2)}$$

Cathodic reduction reaction:

$$O_2 + 4H^+ + 4e^- \rightarrow 2H_2O. \qquad \text{(react. 5.3)}$$

Typical electrode reactions (shown below) occur using glucose as an example substrate:

Anode reactions

$$C_6H_{12}O_6 + H_2O \rightarrow 4H_2 + CO_2 + C_2H_4O_2 \text{ or} \qquad \text{(react. 5.4)}$$

$$C_6H_{12}O_6 \rightarrow 2H_2 + CO_2 + 2C_4H_8O_2 \qquad \text{(react. 5.5)}$$

Cathodic reduction reaction:

$$O_2 + 4H^+ + 4e^- \rightarrow 2H_2O. \qquad \text{(react. 5.3)}$$
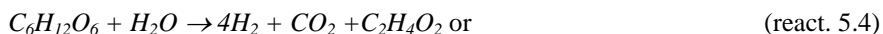
Oxidative mechanisms are driven by the potential of the anode that plays an indispensable role to determine the power output of the fuel cell because the electron transfer performance across the microbial membrane depends on the electrode potential (anode or cathode). Typical electron transporters are the nicotinamide adenine dinucleotide dehydrogenase (NADH), and flavin adenosine dinucleotide hydrogenase ($FADH_2$) obtained by reduction of NAD^+ and FAD^+. These redox molecules carrier and transfer electrons to electron transport chain (ETC) that are composed by ubiquinone, coenzyme Q or cytochrome and NADH dehydrogenase. Standard redox potentials of redox molecules are given in the following Table.

Redox reaction	E_0' (V)
Ferredoxin (Fe^{3+}) + e^- Ferredoxin (Fe^{2+})	−0.42
$NAD^+ + H^+ + 2e^-$ NADH	−0.32
$Pyruvate^{2-} + 2H^+ + 2e^-$ Lactate^{2-}	−0.18
$FAD + 2H^+ + 2e^-$ FADH$_2$	−0.18
$2H^+ + 2e^-$ H$_2$	−0.42
$S + 2H^+ + 2e^-$ H$_2$S	−0.27
Cytochrome c (Fe^{3+}) + e^- cytochrome c (Fe^{2+})	+0.25
Cytochrome b (Fe^{3+}) + e^- cytochrome b (Fe^{2+})	+0.07
Ubiquinone + $2H^+ + 2e^-$ ubiquinoneH$_2$	+0.10
Fumarate$^{2-} + 2H^+ + 2e^-$ succinate^{2-}	+0.03
$O_2 + 4H^+ + 4e^-$ 2H$_2$O	+0.84
$Fe^{3+} + e^-$ Fe^{2+}	+0.77

Table 5.1 Bacterial potential for electricity generation.

At high anodic potentials, bacteria can use the respiratory chain in an oxidative metabolism and their growth rate can be most fast. If the anode potential decreases there are two possible pathways:

- in the presence of alternative electron acceptors such as sulphate, electrons are deposited onto these components;

- in the absence of electron acceptors (such as sulphate, nitrate or other) fermentation will be the main process when the anode potential remains low.

How confirmed by literature (see Table review reported below [40]), in the initial years, simple substrates like acetate and glucose were commonly used, but in recent years researchers are using more unconventional substrates with an aim of utilizing waste biomass or treating wastewater on one hand and improving MFC output on the other.

Type of substrate	Concentration	Source inoculum	Type of MFC (with electrode surface area and/or cell volume)	Current density (mA/cm^2) at maximum power
Acetate	1 g/L	Pre-acclimated bacteria from MFC	Cube shaped one-chamber MFC with graphite fiber brush anode ($7170\ m^2/m^3$ brush volume)	0.8
Arabitol	1220 mg/L	Pre-acclimated bacteria from MFC	One-chamber air-cathode MFC (12 mL) with non-wet proofed carbon cloth as anode ($2\ cm^2$) and wet proofed carbon cloth as cathode ($7\ cm^2$)	0.68
Azo dye with glucose	300 mg/L	Mixture of aerobic and anaerobic sludge	One-chamber air-cathode MFC with carbon paper anode ($36\ cm^2$)	0.09
Carboxymethyl cellulose (CMC)	1 g/L	Co-culture of *Clostridium cellulolyticum* and *G. sulfurreducens*	Two-chambered MFC with graphite plates as electrodes ($16\ cm^2$) and ferricyanide catholyte	0.05
Cellulose particles	4 g/L	Pure culture of *Enterobacter cloacae*	U-tube MFC with carbon cloth anode ($1.13\ cm^2$) and carbon fibers as cathode	0.02
Corn stover biomass	1 g/L COD	Domestic wastewater	One-chamber membrane-less air-cathode MFC with carbon paper anode ($7.1\ cm^2$) and carbon cloth cathode	0.15
Cysteine	385 mg/L	Sediment sample from 30 cm depth	Two-chambered MFC with carbon paper as electrodes ($11.25\ cm^2$)	0.0186
1,2-Dichloroethane	99 mg/L	Microbial consortia from acetate enriched MFC	Two-chambered MFC with graphite plate anode ($20\ cm^2$) and graphite granules cathode	0.008
Ethanol	10 mM	Anaerobic sludge from wastewater plant	Two-chambered aqueous cathode MFC with carbon paper electrodes ($22.5\ cm^2$)	0.025
Farm manure	3 kg in water (20% w/v)	Self build up of anaerobic environment	One reactor vessel of manure with anode at the bottom and cathode above the manure; carbon cloth electrodes ($256\ cm^2$)	0.004
Furfural	6.8 mM	Pre-acclimated bacteria from anode of a ferricyanide-cathode MFC	One-chamber air-cathode MFC with carbon paper anode and cathode ($7\ cm^2$)	0.17
Galactitol	1220 mg/L	Pre-acclimated bacteria from MFC	One-chamber air-cathode MFC (12 mL) with non-wet proofed carbon cloth as anode ($2\ cm^2$) and wet proofed carbon cloth as cathode ($7\ cm^2$)	0.78
Glucose	6.7 mM	Mixed bacterial culture maintained on sodium acetate for 1 year (*Rhodococcus* and *Paracoccus*)	One-chamber air-cathode MFC (12 mL) with non-wet proofed carbon cloth as anode ($2\ cm^2$) and wet proofed carbon cloth as cathode ($7\ cm^2$)	0.70
Glucuronic acid	6.7 mM	Mixed bacterial culture	One-chamber air-cathode MFC (12 mL) with non-wet proofed carbon cloth as anode ($2\ cm^2$) and wet proofed carbon cloth as cathode ($7\ cm^2$)	1.18
Lactate	18 mM	Pure culture of *S. oneidensis* MR-1	Two-chambered MFC with graphite felt electrode ($20\ cm^2$)	0.005
Landfill leachate	6000 mg/L	Leachate and sludge	Two-chambered MFC with carbon veil electrode ($30\ cm^2$)	0.0004
Macroalgae, *Ulva lactuca*	2500 mg/L COD	Primary clarifier overflow of wastewater plant	One-chamber air-cathode MFC (25 mL) with graphite brush anodes and platinized cathode	0.25
Malt extract, yeast extract and glucose	1%	Pure culture of *E. cloacae*	Two-chambered salt bridge MFC with mediators and graphite plate as electrode ($15\ cm^2$)	0.067
Mannitol	1220 mg/L	Pre-acclimated bacteria from MFC	One-chamber air-cathode MFC (12 mL) with non-wet proofed carbon cloth as anode ($2\ cm^2$) and wet proofed carbon cloth as cathode ($7\ cm^2$)	0.58
Microalgae, *Chlorella vulgaris*	2500 mg/L COD	Primary clarifier overflow of wastewater plant	One-chamber air-cathode MFC (25 mL) with graphite brush anodes and platinized cathode	0.20
Microcrystalline cellulose	7.5 g/L	Rumen microorganism from rumen of a cow	Two-chambered MFC with graphite plates as electrodes ($84\ cm^2$)	0.02
Nitrilotriacetic acid (NTA)	48.5 mg/L	Oligotrophic consortium enriched with river water	Two-chambered MFC with graphite felt as electrodes ($24\ cm^2$)	0.0005
Phenol	400 mg/L	Mixed aerobic activated sludge and anaerobic sludge (1:1, v/v)	Two-chambered MFC with aqueous air cathode, carbon paper electrode ($25\ cm^2$)	0.1
Propionate	0.53 mM	Anaerobic sludge	Two-chambered MFC with carbon paper as electrodes ($22.5\ cm^2$)	0.035
Ribitol	1220 mg/L	Pre-acclimated bacteria from MFC	One-chamber air-cathode MFC (12 mL) with non-wet proofed carbon cloth as anode ($2\ cm^2$) and wet proofed carbon cloth as cathode ($7\ cm^2$)	0.73
Sodium formate	20 mM	Anaerobic digested fluid from a sewage treatment plant	Two-chambered MFC with graphite felt as electrodes ($4.5\ cm^2$)	0.22

Table 5.2 List of substrates that have been used in MFC studies.

5.5   ELECTRICITY GENERATION

The preferred substrate for many organisms is acetate and this is therefore used as an example in this section. The half cell reactions for a bacteria respiring with acetate as the electron donor and an air cathode system are reported before (eq. 5.1-5.3). The reactions can be evaluate in terms of Gibbs free energy calculated as

$$\Delta G_r = \Delta G_r^0 + RT ln \left(\frac{a_{products}}{a_{reagents}} \right) \qquad \text{(eq. 5.1)}$$

where ΔG_r^0 0 (J) is the Gibbs free energy under standard conditions usually defined as 298.15 K, 1 bar pressure, and 1 M concentration for all species, R (8.31447 J/molK) is the universal gas constant, T (K) is the absolute temperature, $a_{products}$ is the activities of the products and $a_{reagents}$ is the activities of the reactants. The free energy can be written as:

$$\Delta G = -n \times F \times \Delta E \qquad \text{(eq. 5.2)}$$

Where n is the number of electrons exchanged, F the Faraday's constant (96485 Coulomb/mol) and ΔE the potential difference between electron donor and acceptor, known as the electromotive force which is equal to

$$\Delta E_{emf} = E_{cat} - E_{an} \qquad \text{(eq. 5.3)}$$

Where

$$E_{an} = E_{an}^0 - \frac{RT}{8F} ln \left(\frac{[CH_3COO^-]}{[HCO_3^-]^2 [H^+]^9} \right) \qquad \text{(eq. 5.4)}$$

$$E_{cat} = E_{cat}^0 - \frac{RT}{4F} ln \left(\frac{1}{pO_2 [H^+]^4} \right) \qquad \text{(eq. 5.5)}$$

Using Nernst equation, the theoretical maximum potential that can be extracted by a MFC during the oxidation of acetate with a ΔG_{cell}= -842.2 kJ/mol is calculate as

$$\Delta E_{emf} = \frac{-\Delta G}{nF} \qquad\qquad\qquad\text{(eq. 5.6)}$$

and it is equal to 1.09 V, much higher than practical value which is approximately in the range of 0.6 V to 0.8 V for an open circuit. This discrepancy is due to losses during metabolism and energy taken up by the bacteria, which cannot be avoided if the bacteria are to derive any gain from respiring on the anode

$$\Delta E_{cell} = \Delta E_{emf} - (\sum \eta_a + |\sum \eta_c| + IR_\Omega) \qquad\qquad\text{(eq. 5.7)}$$

where $\sum \eta_a$ and $|\sum \eta_c|$ are the overpotentials losses at the electrodes and IR_Ω is the loss due to electrolyte resistance. In general the cell voltage varies linearly with the current

$$\Delta E_{cell} = OCV - IR_{int} \qquad\qquad\qquad\text{(eq. 5.8)}$$

where IR_{int} consider all internal resistance of the cell. The maximal open circuit potentials (OCV) observed are about 750 – 800 mV but when one closes the circuit the value decrease due to overpotentials losses [41]. There are three main kinds of overpotentials (Figure 5.7):

- activation overpotentials, occur during the transfer of electrons from or to a compound owing to energy needed for redox reactions (losses 3 and 5),
- Ohmic losses, which include both the resistance to the flow of ions through the CEM and the resistance to the flow of electrons through the solution, electrodes and interconnections (loss 4),
- concentration polarization (6).
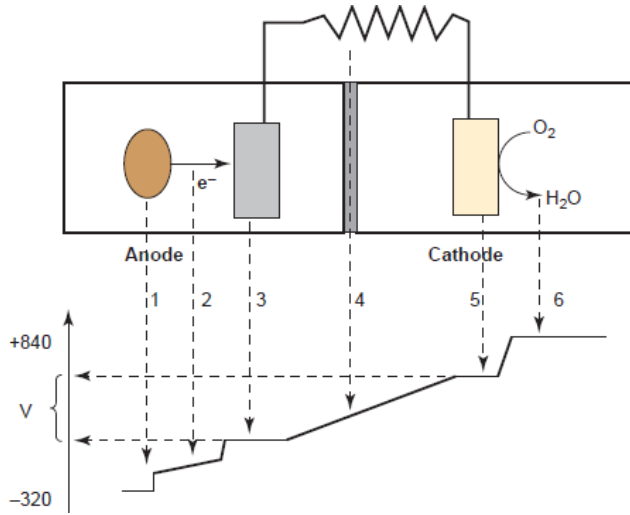
Figure 5.7 Potential losses during electron transfer in a MFC. The loss indicates with the number 1 is referred to bacterial electron transfer, loss 2 is referred to electrolyte resistance, losses 3 and 5 are due to electrodes, loss 4 signals the membrane resistance and the number 6 indicates the losses owing to electron acceptor reduction.

In the Figure there is another loss (1) which is referred to bacteria metabolic losses. As mentioned before microorganisms transport electrons from a substrate at a low potential (anode) to an acceptor of electron characterized by an higher potential (cathode). Thus to optimize the potential of the system the anode potential should be sufficiently low without obstructing the fermentation substrate.

There are other many operating variables, which influence the cell potential and thus the performances of a MFC. In order to get the minimal electricity losses in the system, these variables must be optimized. The performance of a MFC is optimal when the pH is constant in the anode chamber without using any buffer solution [42] and a pH in the range of 6.5 - 8.5 stimulate the growth of electrogenic microorganisms [42,43]. MFC is also strongly affected by temperature, either due to the kinetics and mass transfer (activation energy, membrane conductivity and coefficient of mass transfer), the thermodynamics (free energy and potential electrodes) and the nature and distribution of microbial communities [44]. According to Larrosa-Guerrero [45], regardless of cell size best yields are achieved

151

at higher temperatures indeed operating at a temperature of 35º C the MFC eliminates the 95% of COD and achieves the maximum power.

Regarding to the concentration of organic matter, it is observed that the higher concentration, the higher is the electrical current. It can be due to an increase of the growth of microorganism capable of adapting to the environment developing a biofilm [46] or to the formation of electron transfer mediators in wastewater [47]. Another variable that affects the potential is the feed rate: an increase of this parameter enhances the output potential [48] but if the feed rate is too high, the power density worsens [49]. High feed rates involve low residence time so a part of organic matter passes through the cell without being oxidised [50]. In the case of external resistance, the electrical current increases and the response time to get the steady state decreases with low external resistances [51].

Another essential parameter in the design of biological processes is the sludge age or solid retention time because indicates the time spent by microorganisms in the reactor and needed to its reproduction. Microorganisms unable to adapt to the medium, and its conditions, in a set of time are washed. However, microorganisms capable of regeneration keep in the system. Despite the numerous studies of variables, studies regarding the influence of sludge age in the performance of a MFC have not been found. For these reasons, the objective of this research was to evaluate the performance of microbial fuel cells, both the electrochemical behavior and depuration capacity, varying the sludge age.

5.6   DESIGN OF MFC

There are a number of different designs for microbial fuel cells. The simplest form of MFC is the sediment MFC (Figure 5.8), where an anode is buried sufficiently deep in sediments in order to be sure of oxygen absence, as it is consumed by aerobes or facultative anaerobes in the sediment above the anode [52]. The cathode is suspended in the oxygenated water above the anode [52].
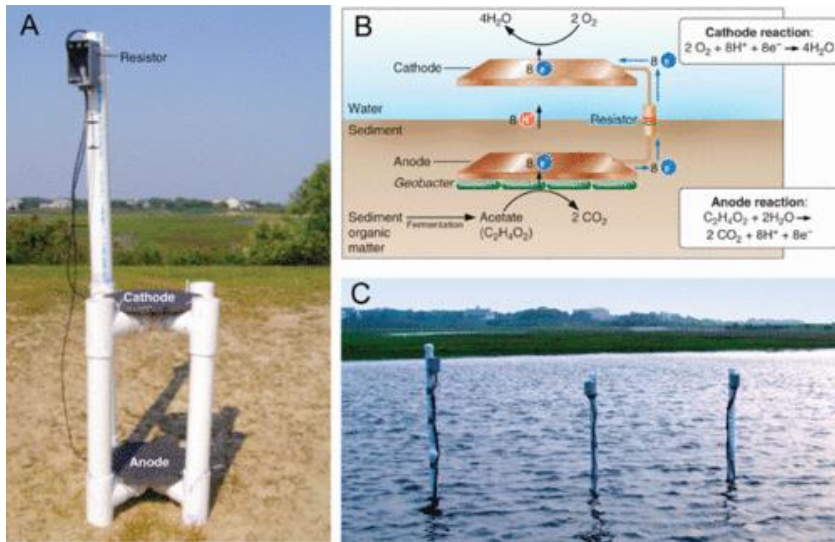
Figure 5.8 A) and C) Examples of sediment MFC. In this the anode is collocated inside the sediment present in the sea, the cathode can be situated or exposed on the air on in water. Figure B) shows a typical process that occur.

These MFCs generally provide very little power; however they are very inexpensive and usually cathode catalysts aren't used and the presence of CEM isn't necessary because the ions seep through pores in the sediment. Often sediment MFCs are used to study marine sediment rich in organic matter.

The most famous kind of MFC is an H-type cell. This kind of system is ease of construction and to sterilize. It is classified as a classical MFC in so far as the fuel and comburent are never in direct contact between them. This cell consists of two glass bottles that have been attached at the bottom through two tube. These two tubes are clamped together with a separator, an ion exchange membrane, between them to connect the internal circuit of the cell. Sometimes, it is possible to have a salt bridge to link two chambers. CEM or salt bridge mainly functions as medium for transfer of proton to close the circuit. The salt bridge MFC produces little power due the high internal resistance obtained and for this H-type MFC is preferred.
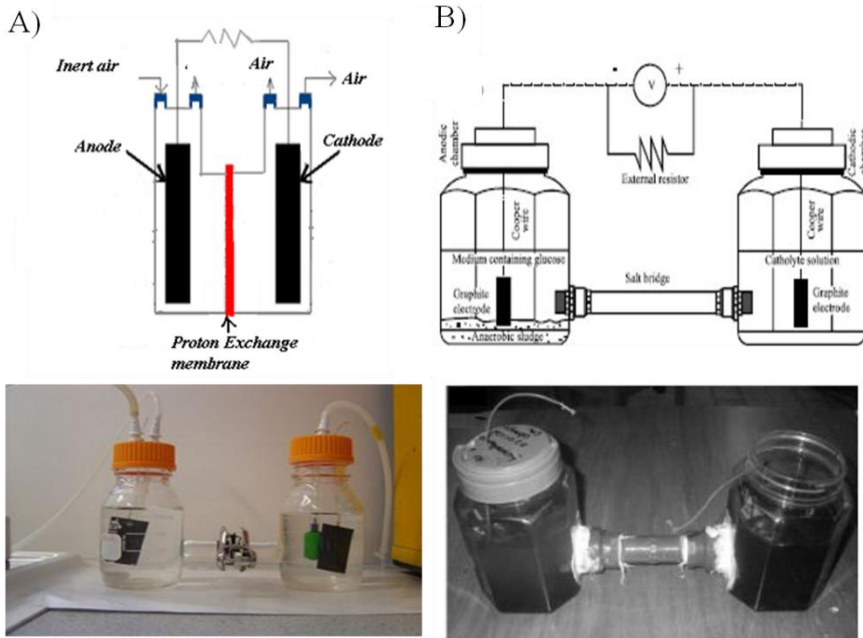
Figure 5.9 Simple designs and photos of double chambered Microbial Fuel Cell, A) H-type cell, B) salt bridge cell.

In both cases electrodes are inserted through holes drilled in the lids of these bottles. In the cathodic compartment oxygen or air is insufflated, or the chamber is filled with a ferricyanide solution [53,54]. The disadvantage is a very low area for ion transfer between the anode and cathode, as well as the need to force oxygen into the cathode chamber in most cases.

Among different kind of double chamber of MFC there is a system characterized by the absence of a tube that connect the two compartment. In this case anodic and cathodic environmental are maintained separated by a CEM and the system is maintained united pressing up onto either side of the membrane and clamped together at the ends.

Another typology of MCF is the Single Chambered Fuel cell (see Figure 5.10). It is constituted by only one chamber which is collocated between the electrodes. This system can or may not contain the proton exchange membrane. In many cases, the

cathode is placed at the interface with the external environment in such a way to be able to use the oxygen present in the air.
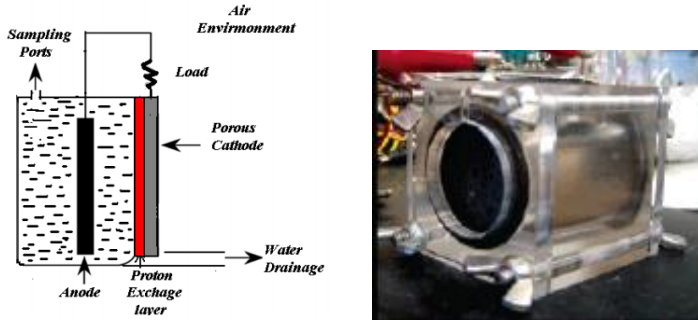
Figure 5.10 Scheme a single chamber MFC characterized by air cathode.

These kinds of MFC are simpler to realize than the double chambered fuel cells and thus have found extensive utilization and research interests lately. Very often, carbon electrodes are used as anodes while the cathodes are either porous carbon electrodes or PEM pasted with flexible carbon cloth electrodes. When working with these systems, it is necessary to moisturize the cathode with opportune solutions of electrolytes in order to prevent the drying of cathode and also of membrane.

In order to increase the area for ion transfer a different typology of single compartment MFC was created. It has a tubular anode with a cathode wrapped around it (Figure 5.11) [55]. The solution is collocated between the two electrodes. In this way if an appropriate cathode is used it is possible to prevent leakage and the ion exchange membrane can be removed.
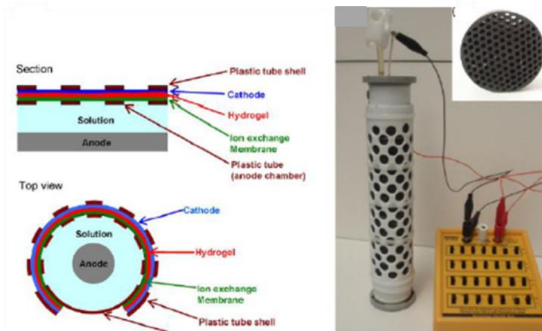
Figure 5.11 Tubular up flow air cathode MFC. On the left are shown section and top views. On the right system view. Top right it is possible to see a porous monolithic carbon anode.

155

The last famous type of MFC is that in which fuel cells are stacked to form battery of fuel cell (see Figure 5.12).
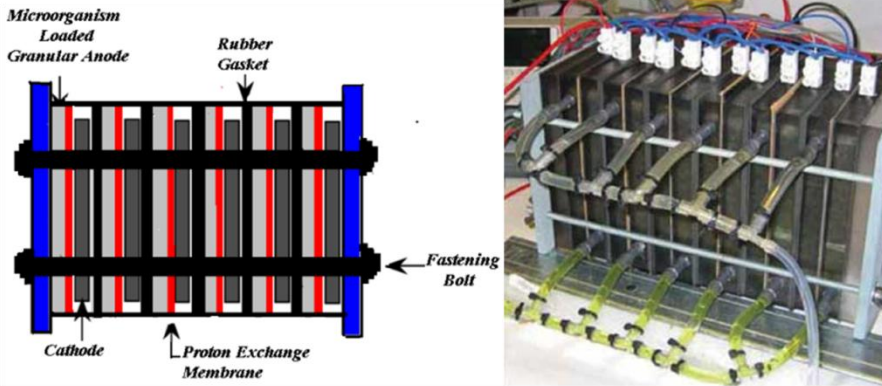
Figure 5.12 Schematic design and picture of Stacked type Microbial Fuel Cell.

How is possible to see in the Figure there aren't tubes that connect the various cells. This type of construction leads to an increase of the potential produced by the whole system [56]. The MFCs can be stacked in parallel or in serie.

5.7   ELECTRODE MATERIALS

It is necessary to spend few words regarding electrode materials used in the MFC. A variety of different materials have been used for MFC anodes. The anode is the most delicate component within an MFC as it is located in direct contact with the organic matter. Therefore it is of fundamental importance that the material forming the electrode is chemically stable and biocompatible, as well as, of course, a good electrical conductor. If in principle the copper seemed to be a good candidate, the studies have shown that traces of copper ions released from the electrode may be toxic to the bacteria used. Among the most promising materials there are graphite electrode, as well as a polished gold electrode and stainless steel plate electrode [22] and between these, graphite electrode is the most used because it is inexpensive, it is easy to manage and leads to good results promoting the biofilm formation. In order to increase the power density and the capacity of bacteria to create a biofilm, a more

rough or porous electrodes are investigated [57,58]. The most commons are reported in the following Figure (Figure 5.13).
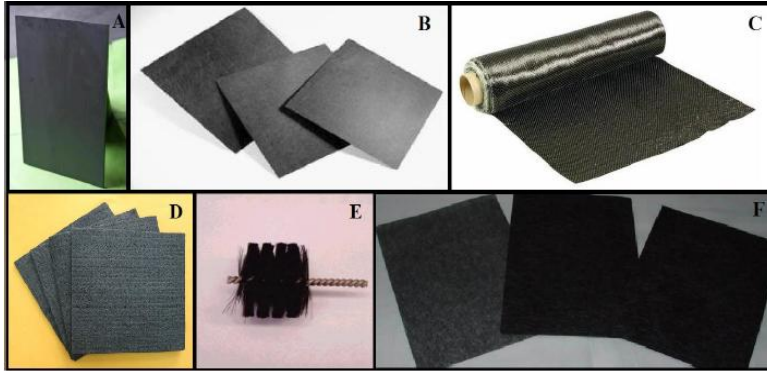
Figure 5.13 Various possible materials for MFC anodes with a carbonaceous nature.

The cathode is the element that allows the passage of electrons coming from the oxidation of organic matter to the acceptor final. In most cases air cathode is used as cathode (for a hydrogen fuel cell). Air cathode MFCs produce from 0.5 to 1 W/m^2 (normalized by the projected surface area of the cathode) for more common conditions, and 2–2.4 W/m^2 under optimal conditions [59]. To favour the oxygen reaction, the cathode needs the presence of a catalyst; typical catalysts are platinum or platinum and ruthenium that have considerable costs.

5.8   ADVANTAGES AND DISADVANTAGES

The main advantages of MFCs include:
-        Direct generation of electricity; no additional conversion step is required;
-        MFCs are considered an energy-saving technology due to their pointless of aeration or temperature maintenance (indeed MFCs can be operated at temperatures below 20 ºC), their low sludge generation compared to the conventional activated sludge process and are efficient at low substrate concentration levels, in terms of both electricity generation and organic removal.

Technology	Power	COD
MFC	0.024 kW	0.076 kWh/kg
Activated sludge-based aerobic process	0.3 kW	0.6 kWh/kg

Table 5.3 Power and COD average estimated to be consumed in MFC [60] and in an activated sludge based process [61].

- Our previous studies and others' have found that MFCs can improve biodegradation of organics, even some refractory compounds;

- MFCs can be diversified with new functions such as hydrogen production, desalination, and heavy metal removal.

MFCs are still in the development stage, yet the technology has advanced significantly in the past decade. In order to make the MFC technology attractive in real world applications, low power generation (i.e. low solution conductivity, low pH buffering capability, irregular substrate distribution and hydraulic pressure distribution), high capital cost (i.e. expensive anode material, expensive current collector for cathode, expensive diffusion layer materials and binders for cathode, expensive catalysts for cathode, low power harvesting efficiency (i.e. great power loss due to electrode Ohmic resistance) and poor long-term system stability (decline of electrochemical activity of anodic biofilm, deterioration of cathode performance, clogging of the system) must change.

5.9   FUTURE PERSPECTIVES

Even more potential MFC applications have been established until now. MFC technology appears a promising candidate for realizing sustainable wastewater treatment.
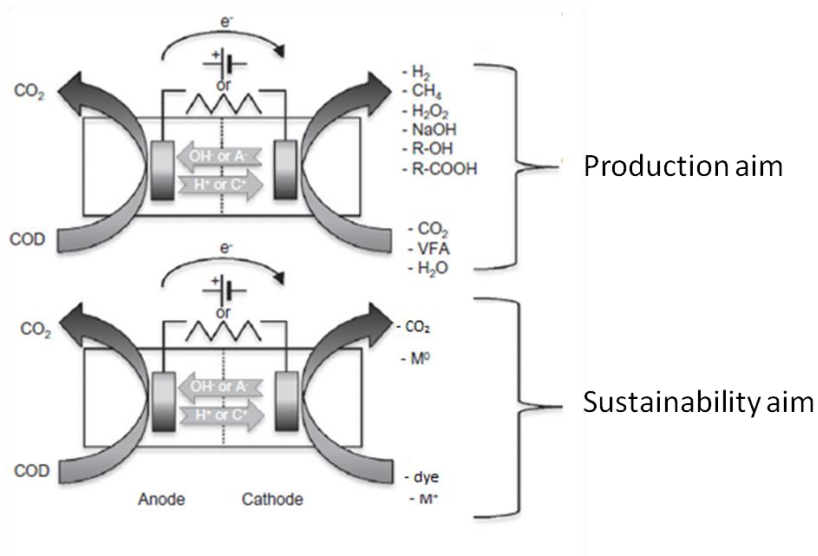
Figure5.14 schematic representation of an utilization of a MFC to add value to the overall process of the system.

The utilization of microbial fuel cell for the treatment of wastewater containing organic pollutants has been extensively studied in the last period to add value to the overall process of MFC achieving A good effluent quality with COD < 20 mg/L [62]. MFCs were considered to be used for treating waste water early in 1991 [63] and in literature there are very interesting reviews on the utilization of microbial fuel cell for the azo dyes [64-67] or inorganic pollutants [68] treatment and the electricity generation. MFCs are also capable of efficiently removing a large variety of nutrients [69], recalcitrant cellulose [70,71] leachates [72], volatile fatty acids [73] and nitrate and sulfur compounds [74,75]

5.9   REFERENCES

[1] Potter, M.C. (1911) Electrical effects accompanying the decomposition of organic compounds. *Proc R Soc Lond B Biol Sci* 84: 260–276.

[2] Allen, R. M., & Bennetto, H. P. (1993). Microbial fuel-cells: electricity production from carbohydrates. Applied Biochemistry & Biotechnology, 39 , 27-40.

[3] Bennetto, H. P., Stirling, J. L., Tanaka, K., & Vega, C. A. (1983). Anodic reactions in microbial fuel cells. Biotechnology and Bioengineering, 25 (2), 559-568.

[4] Bullen, R. A., Arnot, T. C., Lakeman, J. B., & C., W. F. (2006). Biofuel cells and their development. Biosensors and Bioelectronics, 21 , 2015-2045.

[5] Z. Du, H. Li, and T. Gu, "A state of the art review on microbial fuel cells: A promising technology for wastewater treatment and bioenergy.," *Biotechnology advances*, vol. 25, May. 2007, 464-482.

[6] B.E. Logan, Microbial fuel cell, Published by John Wiley & Sons, Inc., Hoboken, New Jersey.

[7] R. Audinos, Electrodialyse inverse. Etude de l'energie electrique obtenue a partir de deux solutions de salinites differentes, J. Power Sources. 10 (1983) 203–217.

[8] J. Jagur-Grodzinski, R. Kramer, Novel process for direct conversion of free energy of mixing into electric power, Ind. Eng. Chem. Process Des. Dev. 25 (1986) 443–449.

[9] M. Turek, B. Bandura, Renewable energy by reverse electrodialysis, Desalination. 205 (2007) 67–74.

[10] K. Y. Cheng, G. Ho, R. Cord-Ruwisch, Energy-efficient treatment of organic wastewater streams using a rotatable bioelectrochemical contactor (RBEC), Bioresource Technology, 126 (2012) 431–436.

[11] B.E. Logan, Exoelectrogenic bacteria that power microbial fuel cells, Nature Reviews/Microbiology, 7 (2009) 375-381

[12] H . Von Canstein, J . Ogawa, S . Shimizu, JR. Lloyd, Secretion of flavins by Shewanella species and their role in extracellular electron transfer, Appl. Environ. Microb. 74 (2008) 615–623.

[13] M.G. Mehta-Kolte, D.R. Bond, Geothrix fermentans secretes two different redox-active compounds to utilize electron acceptors across a wide range of redox potentials. Appl. Environ. Microb. 78 (2012) 6987–6995.

[14] D.B. Baron, E . La Belle, D. Coursolle, J.A. Gralnick, D.R. Bond, Electrochemical measurements of electron transfer kinetics by Shewanella oneidensis MR-1, J. Biolog. Chem. 284 (2009) 28865–28873.

[15] Y.A. Gorby, et al, Electrically conductive bacterial nanowires produced by Shewanella oneidensis strain MR-1 and other exoelectrogens. Proc. Natl. Acad. Sci. U.S.A. 103 (2006) 11358–11363.

[16] K.M. Leung, G. Wanger, M.Y. El-Naggar, Y. Gorby, G. Southam, W.M. Lau, J. Yang, Shewanella oneidensis MR-1 bacterial nanowires exhibit p-type, tunable electronic behaviour. Nano Letters 13 (2013) 2407–2411.

[17] S. Bonanni, D. Massazza, J.P. Busalmen, Stepping stones in the electron transport from cells to electrodes in Geobacter sulfurreducens biofilms, Phys. Chem. Chem. Phys. 15 (2013) 10300–10306.

[18] R.M. Snider, S.M. Strycharz-Glaven, S.D. Tsoi, J.S. Erickson, L.M. Tender, Long-range electron transport in Geobacter sulfurreducens biofilms is redox gradient-driven. Proc. Natl. Acad. Sci. U.S.A. 109 (2012) 15467–15472.

[19] N.S. Malvankar, M.T. Tuominen, D.R. Lovley, Lack of cytochrome involvement in long-range electron transport through conductive biofilms and nanowires of Geobacter sulfurreducens, Energy Environ. Sci. 5 (2012) 8651–8659.

[20] K. Rabaey, N. Boon, S. D. Siciliano, M. Verhaege, W. Verstraete, Biofuel cells select for microbial consortia that self-mediate electron transfer. Appl. Environ. Microbiol. 70(9) (2004) 5373-5382.

[21] K. Rabaey, W. Ossieur, M. Verhaege, W. Verstraete, Continuous microbial fuel cells convert carbohydrates to electricity (2004)

[22] Bond D.R., Lovley D.R. Electricity production by Geobacter sulfurreducens attached to electrodes. Appl. Environ. Microbiol. 69 (2003) 1548-1555.

[23] L.M. Tender, C.E. Reimers, H.A. Stecher III, D.E. Holmes, D.R. Bond, D.A. Lowy, K. Pilobello, S.J. Fertig, D.R. Lovley, Harnessing microbially generated power on the seafloor. Nat. Biotechnol. 20 (8) (2002) 821–825.

[24] B. H. Kim, H. S. Park, H. J. Kim, G. T. Kim, I. S. Chang, J. Lee, N. T. Phung, Enrichment of microbial community generating electricity using a fuel-cell-type electrochemical cell, Appl. Microbiol. Biotechnol. 63 (2004) 672-681.

[25] W. Lee, S. Kang, H. Shin, Sludge characteristics and their contribution to microfiltration in submerged membrane bioreactors, J. Membr. Sci. 216 (2003) 217-227.

[26] Park, Biological nitrogen removal with enhanced phosphate uptake in a sequencing batch reactor using single sludge system, Wat. Res. 35 (2001) 3968–3976.

[27] B. H. Kim, H.J. Kim, M.S. Hyun, D.H. Park, Direct electrode reaction of Fe(III)-reducing bacterium, Shewanella putrefaciens. J. Microbiol. Biotechnol. 9 (1999) 127–131.

[28] C.R. Myers, J. M. Myers, Localization of cytochromes to the outer membrane of anaerobically grown Shewanella putrefaciens MR-1. J. Bacteriol. 174 (1992) 3429–3438.

[29] H. Von Canstein, J. Ogawa, S. Shimizu, J. R. Lloyd, Secretion of flavins by Shewanella species and their role in extracellular electron transfer. Appl. Environ. Microbiol. 74 (2008) 615–623.

[30] W. Lin, M. Coppi, and D. Lovley, Geobacter sulfurreducens can grow with oxygen as a terminal electron acceptor, Appl. Environ. Microbiol. 70 (2004) 2525-2528.

[31] K.P. Nevin, H. Richter, S.F. Covalla, J.P. Johnson, T.L. Woodard, A.L. Orloff, H. Jia, M. Zhang, D.R. Lovley, Environ. Microbiol. 10 (2008) 2505–2514.

[32] S. Ishii, K. Watanabe, S. Yabuki, B.E. Logan, Y. Sekiguchi, Comparison of electrode reduction activities of Geobacter sulfurreducens and an enriched consortium in an air-cathode microbial fuel cell, Appl. Environ. Microbiol. 74 (2008) 7348–7355.

[33] D.R. Lovley, Bug juice: harvesting electricity with microorganisms, Nature Rev. Microbiol. 4 (2006) 497–508.

[34] A.M. Speers and G. Reguera, Electron donors supporting the growth and electroactivity of Geobacter sulfurreducens anode biofilms., Appl. Environ. Microbiol. 78 (2012) 437-444.

[35] Z.M. Summers, T. Ueki, W. Ismail, S. a Haveman, and D.R. Lovley, Laboratory evolution of Geobacter sulfurreducens for enhanced growth on lactate via a single-base-pair substitution in a transcriptional regulator. The ISME journal, (2011) 1-9.

[36] T.H. Yang, M.V. Coppi, D.R. Lovley, and J. Sun, Metabolic response of Geobacter sulfurreducens towards electron donor/acceptor variation. Microb. cell fact. 9 (2010) 90-105.

[37] Sharma, Vinay , Kundu. Biocatalysts in microbial fuel cell. Enzyme Microb. Technol. 47 (2010) 179-188

[38] K. Scott, C. Murano, A study of a microbial fuel cell battery using manure sludge waste. J. Chem. Technol. Biotechnol. 82 (2007) 809–817.

[39] V. Vologni, R. Kakarla, I. Angelidaki, B. Min,Increased power generation from primary sludge by a submersible microbial fuel cell and optimum operational conditions. Bioprocess Biosyst. Eng. 36 (2013) 635–642.

[40] D. Pant et al., A review of the substrates used in microbial fuel cells (MFCs) for sustainable energy production, Bioresource Technology 101 (2010) 1533–1543.

[41] K. Rabaey. W. Verstraete, Microbial fuel cells: novel biotechnology for energy generation, TRENDS in Biotechnology 23 (2005) 291-298

[42] V.B. Oliveira, M. Simões, L.F. Melo, A. Pinto, Overview on the developments of microbial fuel cells, Biochem. Eng. J. 73 (2013) 53–64.

[43] B.H. Sorensen, N. Nyholm, A. Baun Algal toxicity tests with volatile and hazardous compounds in air-tight test flasks with CO_2 enriched headspace. Chemosphere 32 (1996) 1513–1616.

[44] E. Martin, O. Savadogo, S.R. Guiot, B. Tartakovsky, The influence of operational conditions on the performance of a microbial fuel cell seeded with mesophilic anaerobic sludge, Biochem. Eng. J. 51 (2010) 132–139.

[45] A. Larrosa-Guerrero, K. Scott, I.M. Head, ffect of temperature on the performance of microbial fuel cells. Fuel, 89(12) (2010) 3985-3994.

[46] A. González del Campo, P. Cañizares, M.A. Rodrigo, F.J. Fernández, J. Lobaton, Microbial fuel cell with an algae-assisted cathode: a preliminary assessment, J. Power Sources 242 (2013) 638-645

[47] M.A. Rodrigo, P. Cañizares, J. Lobato, R. Paz, C. Sáez, J.J. Linares, Production of electricity from the treatment of urban waste water using a microbial fuel cell. J. Power Sources 169 (2007) 198–204.

[48] J.R. Kim, J. Rodríguez, F.R. Hawkes,R.M. Dinsdale, A.J. Guwy, G.C. Premier,Increasing power recovery and organic removal efficiency using extended longitudinal tubular microbial fuel cell (MFC) reactors, Energy Environ. Sci. 4 (2011) 459-465.

[49] I. Ieropoulos, J. Greenman, C. Melhuish, Improved energy output levels from small-scale microbial fuel cells, Bioelectrochem. 78 (2010) 44–50.

[50] M. Di Lorenzo, K. Scott, T.P. Curtis, I.M. Head, Effect of increasing anode surface area on the performance of a single chamber microbial fuel cell, Chem. Eng. J. 156 (2010) 40–48.

[51] M. Di Lorenzo, T.P. Curtis, I.M. Head, K. Scott, A single-chamber microbial fuel cell as a biosensor for wastewaters, Water Res. 43 (2009) 3145–3154.

[52] Z. He, H. Shao, and L.T. Angenent, Increased power production from a sediment microbial fuel cell with a rotating cathode, Biosens. Bioelectron. 22 (2007) 3252-3255.

[53] S.E. Oh, B.E. Logan, Proton exchange membrane and electrode surface areas as factors that affect power generation in microbial fuel cells, Appl. Microbiol. Biotechnol. 70 (2006) 162-169.

[54] Z. Liu and H. Li, Effects of bio- and abio-factors on electricity production in a mediatorless microbial fuel cell, Biochem. Eng. J., 36 (2007) 209-214.

[55] R. Kim, G.C. Premier, F.R. Hawkes, R.M. Dinsdale, and A.J. Guwy, Development of a tubular microbial fuel cell (MFC) employing a membrane electrode assembly cathode, J. Power Sources 187 (2009) 393–399.

[56] P. Aelterman, K. Rabaey, T.H. Pham, N. Boon, W. Verstraete, Continuous electricity generation at high voltages and currents using stacked microbial fuel cells. Environ. Sci. Technol. 40 (2006) 3388-3394.

[57] M. Zhou, M. Chi, J. Luo, H. He, and T. Jin, An overview of electrode materials in microbial fuel cells, J. Power Sources, 196 (2011) 4427-4435.

[58] Y. Liu, F. Harnisch, K. Fricke, U. Schröder, V. Climent, and J.M. Feliu, The study of electrochemically active microbial biofilms on different carbon-based anode materials in microbial fuel cells., Biosens. Bioelectron. 25 (2010) 2167-2171.

[59] B. Logan, S. Cheng, V. Watson G. Estadt, Graphite Fiber Brush Anodes for Increased Power Production in Air-Cathode Microbial Fuel Cells, Environ. Sci. Technol. 41 (9) (2007) 3341–3346

[60] F. Zhang, Z. Ge, J. Grimaud, Long-term performance of liter-scale microbial fuel cells treating primary effluent installed in a municipal wastewater treatment facility, Environ. Sci. Technol. 47(9) (2013) 4941-4948.

[61] P.L. McCarty, J. Bae, J. Kim, Domestic wastewater treatment as a net energy producer can this be achieved? Environ. Sci. Technol. 45(17) (2011) 7100-7106.

[62] J. Yu, J. Seon, Y. Park, Electricity generation and microbial community in a submerged-exchangeable microbial fuel cell system for low-strength domestic wastewater treatment. Bioresour. Technol., 117 (2012) 172-179.

[63] W. Habermann, E.H. Pommer, Biological fuel cells with sulphide storage capacity. Appl. Microbiol. Biotechnol. 35 (1991) 128–33.

[64] MÁ Fernández de Dios, O Iglesias, M Pazos, Application of Electro-Fenton Technology to Remediation of Polluted Effluents by Self-Sustaining Process, Hindawi Publishing Corporation Scientific World Journal Volume (2014) 8 pages.

[65] K. Solanki, S. Subramanian, S. Basu, Microbial fuel cells for azo dye treatment with electricity generation: a review, Bioresour. Technol. 131 (2013) 564-571.

[66] V. Murali, S.A. Ong, L.N. Ho, Y.S. Wong, N. Hamidin, Comprehensive Review and Compilation of Treatment for Azo Dyes Using Microbial Fuel Cells, 85 (2013) 270-277.

[67] M.Á. Fernández de Dios, A. González del Campo, F. J. Fernández, M.A. Rodrigo, M. Pazos, M.Á. Sanromán, Bacterial–fungal interactions enhance power generation in microbial fuel cells and drive dye decolourisation by an ex situ and in situ electro-Fenton process, Bioresour. Technol. 148 (2013) 39–46.

[68] G. Wang, L. Huang, Y. Zhang, Cathodic reduction of hexavalent chromium [Cr (VI)] coupled with electricity generation in microbial fuel cells, Biotechnol. Lett. 30 (2008) 1959–1966.

[69] B. Min, J.R. Kim, S.E. Oh, J.M. Regan, B.E. Logan, Electricity generation from swine wastewater using microbial fuel cells. Water Research, 39(20) (2005) 4961-4968.

[70] F. Aulenta, L. Tocca, R. Verdini, Dechlorination of trichloroethene in a continuous-flow bioelectrochemical reactor: effect of cathode potential on rate, selectivity, and electron transfer mechanisms. Environ. Sci. Technol. 45(19) (2011) 8444-8451.

[71] S. Kalathil, J. Lee, M.H. Cho, Granular activated carbon based microbial fuel cell for simultaneous decolorization of real dye wastewater and electricity generation. New Biotechnol. 29(1) (2011) 32-37.

[72] S.J. You, Q.L. Zhao, J.Q. Jiang, Sustainable approach for leachate treatment: electricity generation in microbial fuel cell, J. Environ. Sci. Health, Part A, 41(12) (2006) 2721-2734.

[73] S. Freguia, E.H. Teh, N. Boon, Microbial fuel cells operating on mixed fatty acids. Bioresour. Technol. 101(4) (2010) 1233-1238.

[74] K. Rabaey, K. van de Sompel, L. Maignien, Microbial fuel cells for sulfide removal. Environ. Sci. Technol. 40(17) (2006) 5218-5224.

[75] F. Zhao, N. Rahunen, J.R. Varcoe, Factors affecting the performance of microbial fuel cells for sulfur pollutants removal. Biosens. Bioelectron. 24(7) (2009) 1931-1936

6.   EXPERIMENTAL SET-UP

Microbial Fuel Cell (MFC) technology has been widely investigated with the aim of generating electricity from biomass using bacteria.

During the first part of the study, MFCs are used with the only objective to produce electric current adopting a mixed culture of bacteria. For the first time, the effect that the retention time of the solid on the ability of the system has been studied. In a second moment, the utilization of microbial fuel cell for the treatment of wastewater containing organic and inorganic pollutants has been extensively studied focusing the research on the possibility to expand the role of this process with the aim to increase MFC potentials and power densities and the applications. The last section of experimental campaign was focused on the possibility to use the products of degradation of the AO7 as food for the bacteria.

Part of the laboratory experimental campaign was performed at the research center ITQUIMA, Instituto de Tecnología Química y Medioambiental, in Ciudad Real, Spain.

6.1   EXPERIMENTAL APPARATUS

Two different kind of MFC systems were used during this experimental campaign.

MFC adopted in Spain

The set-up used in Spain consisted of a two chambered of 0,346 cm^3 MFC, using a proton exchange membrane (PEM 117, by Nafion) to separate the electrodes (fig 6.1). A cell is made from 4 plates PMMA 5 cm x 5 cm each separated with a spacer of rubber and is clamped with four threaded bars closed by four nuts.
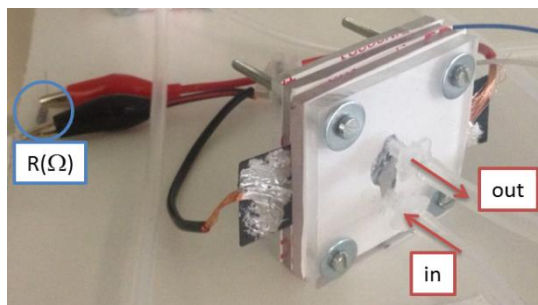
Figure 6.1 Photo of one MFC. It is possible to see the anodic compartment, in- and out-channel of solution and the electric connection between electrodes. an external load of 120 Ω is linked.

Both electrodes were built of Toray carbon cloths with 10% Teflon. The anode electrode did not contain catalyst while the carbon cathode was coated with a Pt catalyst (0.5 mg/cm^2, 10% Pt) to increase the reduction rate of the oxygen from the air entering the cathodic chamber. The system carbon electrodes/PEM (cathode and anode) was manufactured by bonding the ion exchange membrane directly into a flexible carbon papers in order to minimize the internal resistance. The PEM was sequentially boiled in H_2O_2 (30%), deionized water, then 0,5M H_2SO_4 and deionized water each time for 1h. The membrane was then hot pressed directly between two electrodes by heating it to 120°C at 1KN for 4 min.
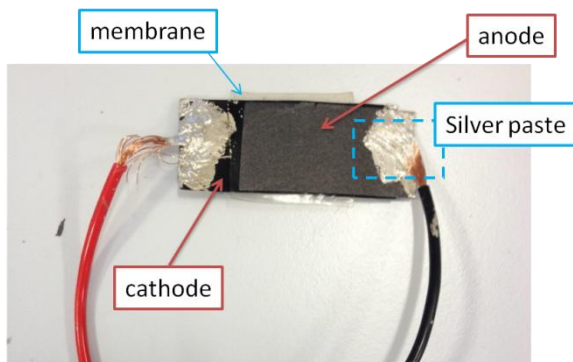
Figure 6.2 Photo of system carbon electrodes/PEM after bonding process.

Both electrodes were connected by an external resistance (Rext) of 120 Ω; this low value was chosen to prevent activation losses and facilitate electron transfer during the acclimation period. The anodic compartment is connected with a bottle (the

166

reactor) filled with a 116 mL of a synthetic solution. The cathodic compartment is characterized by two hole (mm scale) to allow the entry of air so as to work with an air-cathode. The anode compartment was inoculated with a mix of 1mL of active sludge. The solution contained sludge and medium was circulated from reservoir to the anodic compartment at 1.30 mL/s using a peristaltic pump.
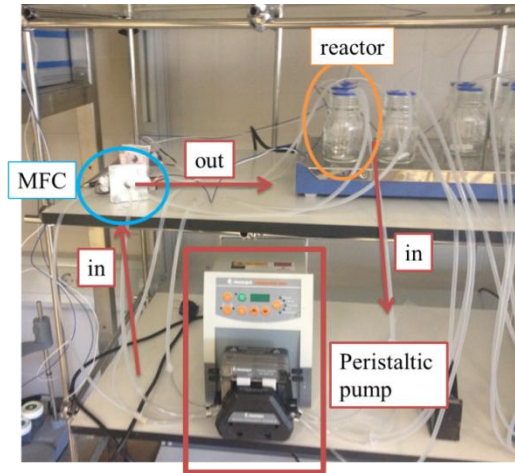
Figure 6.3 Scheme of the system assembled to work with a MFC.

MFC adopted in Palermo

Microbial fuel cells used in Palermo were constructed by joining two media bottles (100 mL capacity) with glass tubes having diameters suitable to hold the PEM (Nafion, Dupont Co.) that was clamped between the flattened ends of the tubes fitted with two rubber gaskets. PEMs used in these reactors had cross sectional areas of 3,14 cm^2. Carbon felt was used as anode and cathode materials with an surface area of 11,1 cm^2.

Figure 6.4 Bicompart MFC with "H-configuration".

Bacteria and organic matter are inserted in the anode compartment while the cathode compartment was filled with different solutions. When Geobacter Sulfurreducens and Dysgonomonas were used as microorganisms, it was necessary to blow sterile N_2/CO_2 80/20 w/w gas mixture into the anode compartment to create an anaerobic environment.

6.2   MATERIALS

6.2.1 Preparation of the electrodes

Spain

Toray carbon paper was used as electrodes with an active area of 0.86 cm^2 in both chambers. The anodic electrode contained a 10% of Teflon to improve the mechanical properties of the carbon support over the course of the study and because Teflon only caused a small drop in performance [1]. The anode electrode did not contain catalyst. The cathodic electrode contained 20% of Teflon and a microporous layer in order to favor a homogenous deposition of the catalytic layer of 0.5 mg Pt/cm^2 loading. The cathode was prepared in the following manner.

Cathode: A sheet of C containing 10% of teflon is used. Above the electrode, a Pt layer is deposited with a load of 0.5 mg Pt/cm^2. Optimal dimensions of the electrode

are: 5 cm x 2.5 cm = $12.5cm^2$. The area where the Pt are deposited must be: 4 cm x 2.5 cm = 10 cm^2.

To deposit the layer of Pt is necessary to proceed in the following manner. First of all it is necessary to prepare the solution of Pt to be used:

- weigh 30.12 mg of Pt and add dimetilacetammide to fill half of the sample holder (vial);

- leave to sonicate for 30 minutes;

- next, add 117 mg of polybenzimidazole (PBI) and again dimetilacetamnide to make up the volume;

- leave again to sonicate for 30 minutes.

Subsequently deposit operations provide:

- weigh the electrode;

- deposit with an airbrush Pt solution (about 14.33 mg).

At this point the electrode is left for 2 hours in a muffle furnace at 190 °C. After the electrode is left to stand for 24 hours and only later 240.96 mg of a 10% solution of H_2SO_4 are added.

Palermo

Electrodes used in experimental campaign effectuated in *Palermo* were Carbon felt (The Electosynthesis Co.) as anode and cathode with an surface area of 11.1 cm^2. Carbon felt electrodes were pre-treated for a whole night with a concentrated solution of H_2SO_4 (Sigma Aldrich).

6.2.2 Microorganisms and medium

6.2.2.1 Microorganisms

Spain

The inoculum used in the anode compartment was obtained from the activated sludge reactor at the municipal Wastewater Treatment Plant of Ciudad Real (Spain) and concentrated by sedimentation. All cells operated under semi-continuous mode and at room temperature. Three different inoculums were used. In the first inoculation, a mix of 1 mL of sludge and 116 mL of synthetic wastewater was in a bottle connected to the anodic compartment. Then, two more re-inoculations were needed so the percentage of sludge-wastewater volume was varied to 10 mL. In order to obtain cells working with different sludge ages, every day a volume of liquid was removed from the reservoir of the anodic chamber and replaced by fresh synthetic wastewater. The amount removed were 11.5, 15.5, 23, 46 and 82 mL, which resulted in solid retention time (SRT) of 10, 7.4, 5, 2.5 and 1.4 days, respectively.

Palermo

At the beginning two different kind of bacteria were used: Geobacter sulfurreducens and Shewanella putrefaciens.

<u>*Geobacter sulfurreducens*</u>

G. sulfurreducens (*Gs*) bacterial strain was obtained from DSMZ, Germany, and cultured as reported in the literature [2]. Inoculum preparation procedures are more laborious and it is also necessary a tune-up of the system because *Gs* requires equipment and more complex methods being an anaerobic strain. Geobacter is stored in a medium containing iron called "NB IRON GEL"; then the microorganisms are transferred in a mineral medium containing fumarate as electron acceptor, to activate the metabolism of the bacteria and make it ready to be used in

the MFC. Always under anaerobic conditions, an aliquot of this inoculum is transferred in the anodic compartment containing a mineral medium, described in the following paragraph (6.4), which presents sodium acetate as the only carbon source. The mineral medium adopted is devoid of fumarate because in these experiments the final electron acceptor will be the same anode surface.

The headspace of the MFC was continuously flushed with sterile N_2/CO_2 80/20 w/w gas mixture to maintain anaerobic the environment.

Shewanella putrefaciens

Colonies of S. putrefaciens (*Sp*) were grown in Petri dishes containing Luria Bertani Agar Miller Fischer Scientific, thermostated at a temperature of 30 °C, for a period of time necessary to the formation of the colonies of growth. After 24 hours of growth on a Petri dish, The *Sp* strain was grown aerobically in a 50 mL flask in LB broth (Difco Laboratories, Detroit, MI) where acetate was the nutrient. This culture was incubated at 30 °C for other 24 h with shaking at 100 rpm [3].

In both cases, when cell counts about 1×10^8 cells/mL as determined by plating after serial dilution the inoculum is ready to be used.

In order to study the performances of a MFC as function of different microorganism another kind of bacteria was used, Dysgonomonas.

Dysgonomonas

For the microbial community present in the gut of the larvae of the red weevil, very similar operating conditions have been used to those used for the *Gs* because both are anaerobic microorganisms. The steps required to remove the bacteria from the gut of the larvae are listed below (procedures performed in an anaerobic glove box):

- section of the larva;
- extraction of the intestine;

171

- disintegration of the intestine in such a way as to favor the exit of the microorganisms;

- direct insert into the anode compartment of MFC.

Every 3 days on average, the spent medium was replaced with the fresh one in order to promote the growth of the culture as electroactive biofilm.

6.2.2.1 Medium

In the following, the recipes for the preparation of the different culture media for the active sludge used in Spain and for the three types of bacteria used in Palermo are described.

Spain

Synthetic wastewater was used in order to have control of the wastewater characteristics. The anodic compartment was filled with a 116 mL of a synthetic solution containing different minerals and sodium acetate as the only source of organic carbon. During the first two stage of the experimental campaign 5.8 g of sodium acetate (4000 mg/L of COD) were used; in the last re-inoculation a solution with 14.5 g of acetate (10000 mg/L of COD)was used.

Preparation of the synthetic solution of nutrients.

For 1 liter of solution are weighed:

$NaHCO_3$	258.54 mg/L
$(NH_4)_2SO_4$	172.8 mg/L
KH_2PO_4	103.645 mg/L
$MgCl_2$	86.4 mg/L
$(NH_4)_2Fe(SO_4)_2$	7.22 mg/L
$CaCl_2$	70.11 mg/L

The aforementioned salts are dissolved in approximately 600 mL of MilliQ water. 750 mg/L of $NaC_2H_3O_2$ (nutrient) are dissolved in the remaining part of water (400 mL)

The catodic compartment was characterized by the presence of air.

Palermo

The anode compartment was filled with various types of microbial culture media depending on the different microorganisms selected. The microbial culture media used were listed below.

Preparation of Luria Bertani Agar:

- add 40 g of product in 1 liter of distilled H_2O;
- sterilize by autoclaving at 121 °C at 1 atm for 20 minutes;
- pour the product into Petri plates, operating under a laminar flow hood;
- wait until the product solidifies.

Preparation of Luria Bertani Broth:

- add 25 g of product in 1 liter of distilled H_2O;
- sterilize by autoclaving at 121 °C to 1atm for 20 minutes.

Preparation of growth medium mineral "NBA":

- prepare 900 mL of an aqueous solution of NaCl 40 mM;
- measure the pH and maintain it at a range of about 6 - 6.5;
- add 20 mL of Core Media Mix (mixture of KCl, NH_4Cl and NaH_2PO_4 * H_2O);
- add 50 mL of a suspension of Mg/Ca Mix;
- add 10 mL of Vitamins;
- add 10 mL of Minerals;
- add as a carbon source, sodium acetate 20 mM;
- measure the pH and adjust if necessary with a solution of NaOH 1 M to the established range;
- bring to a final volume of 1 L;

- add 2 g of NaHCO$_3$;
- gasify the mineral medium with a mixture N$_2$/CO$_2$ (80% -20%);
- autoclave at 121°C for 20 minutes.

In all cases the cathodic compartment was filled with a water solution of Na$_2$SO$_4$ (Sigma Aldrich) 0,1 M at pH = 2 (H$_2$SO$_4$, Sigma Aldrich) to create in a first stadium an electro-biofilm. In a second moment, MFCs were tested to treat a solution containing a pollutant and the cathodic section was full with a solution containing or 150 mg/L AO7 (Sigma Aldrich) or Cr(VI) with an initial concentration of 25 mg/L (in the form of K$_2$Cr$_2$O$_7$, Sigma Aldrich) with 0,1 M Na$_2$SO$_4$ (Sigma Aldrich) as supporting electrolyte at pH = 2 (H$_2$SO$_4$, Sigma Aldrich).

6.3   ANALYSIS EQUIPMENTS

Spain

The water temperature, conductivity, pH, dissolved oxygen level (DO) in the anodic compartment were monitored *in situ* using the sampling points. The pH, conductivity and dissolved oxygen were measured using a GLP22 Crison® pH-meter, a GLP 31 Crison® conductivity meter and an Oxi538 WTW® oxy-meter, respectively.

The total suspended (TSS) and volatile suspended (VSS) solids were measured gravimetrically according to standard methods previously used in this type of study [4].

The COD was determined by photometric methods with a MERCK COD cell test and Pharo 100 MERCK spectrophotometer.

The total nitrogenwas monitored using a Multi N/C 3100 Analytik Jena analyzer.

The evolution of the voltage was registered continuously with a digital multimeter (Keithley® 2000) and data was storage in a computer.

The concentration of reaction intermediates was determined through high pressure liquid chromatography with UV -DAD detector and Zorbax SB-Aq 46 x 150 mm 5 microm column from Agilent Technologies.

Palermo

In order to monitor the growth of the bacterial communities present in the anode compartment, every day rates of solution were collected and analyzed by UV-vis spectrophotometry (Agilent Cary 60 UV Spectrophotometer). Often TOC measures were realized on anodic solution to observe any change in the composition of the culture medium.

The removal of color was monitored from the decay of the absorbance (A) at $\lambda = 482$ nm for AO7 [5] by UV-vis spectrophotometry. The total organic carbon (TOC) was analyzed by a TOC analyzer Shimadzu VCSN ASI TOC-5000 A. Degradation products of AO7 were identified by HPLC analyses using an Agilent HP 1100 HPLC equipped with UV–Vis detector (adopted $\lambda = 210$ nm) and comparison with pure standards [6]. The presence of carboxylic acids (oxalic, maleic, malonic and lattic acids from Sigma Aldrich) were identified by Prevail Organic 5μ column. The mobile phase was a buffer solution containing KH_2PO_4 (Sigma Aldrich 99%) and H_3PO_4 at a pH of 2.5, prepared with water Sigma Aldrich G-chromasolv for gradient elution. The eventual presence of chloro-organic compounds was evaluated by HPLC-MS Thermo TSQ Quantum Access. The HPLC column was ZIC-HILIC 150 mm x 2.1 mm, 5 μm. The mobile phase was $CH_3CN–CH_3COONH_4$ 10 mM (90:10 v/v).

The removal of Cr(VI) was monitored by using Agilent Cary 60 UV Spectrophotometer. Cr(VI) was detected at $\lambda = 540$ nm, after treatment with 1,4-diphenylcarbazide and its concentration was determined after proper calibration using the Lambert Beer law. The lower detection limit for Cr(VI) was 0.01 mg/L.

6.4 ELECTROCHEMICAL PARAMETERS

Spain

The polarization curves from the MFC were obtained by varying the resistance in the circuit and measuring the potential. Power density (mW/m^2) and current density (mA/m^2) were based on the surface area of the anode. The current (I) was calculated using Ohm's Law ($I = U \ / \ R$), and the output power of the cell using $P = I \quad U$, where I (A) is the current, U (V) is the voltage, R (Ω) is the external resistance and P (W) is the power. Coulombic efficiency (CE) was based on total current generation and the maximum current that can be produced from COD oxidation and it was calculated according to the method of Rodrigo *et al* [7].

Palermo

In the MFC, anode and cathode are connected by an external circuit equipped with a resistance, an amperometer and a voltmeter (overall electrical resistance about 4.6 Ohm).

When Cr(VI) was used as pollutant, focused cyclic voltammetry was performed at 10 and 50 mV/s in a single-compartment, three-electrode cell, under nitrogen or air atmosphere, in order to roughly evaluate the anode and cathode potentials of some redox processes at carbon felt electrodes. Working electrode was carbon felt, the counter electrode compact graphite and the reference electrode a SCE. Autolab PGSTAT12 was used for cyclic voltammetry measurements.

6.5   REFERENCES

[1] M.A. Rodrigo, P. Cañizares, H. García, J.J. Linares, J. Lobato, Study of the acclimation stage and of the effect of the biodegradability on the performance of a microbial fuel cell, Bioresour. Technol. 100 (2009) 4704-4710.

[2] D. Bond, D. Lovley, Electricity production by Geobacter sulfurreducens attached to electrodes, Appl. Environ. Microbiol. 69 (3) (2003) 1548-1555.

[3] J.C. Biffinger, J. Pietron, R. Ray, B. Little, B.R. Ringeisen, A biofilm enhanced miniature microbial fuel cell using Shewanella oneidensis DSP10 and oxygen reduction cathodes, Biosens. Bioelectron. 22 (2007) 1672–1679.

[4] A.P.H.A.-A.W.W.A.-W.P.C.F, 1998. Standard Methods for the Examination of Water and Wastewater, twentieth ed. American Public Health Association/American Water Works Association/Water Environment Federation, Washington DC, USA.

[5] S. Garcia-Segura, F. Centellas, C. Arias, J.A. Garrido, R.M. Rodriguez, P.L. Cabot, E. Brillas, Comparative decolorization of monoazo, diazo and triazo dyes by electro-Fenton process, Electrochim. Acta 58 (2011) 303-311.

[6] O. Scialdone, A. Galia, S. Sabatino, Abatement of Acid Orange 7 in macro and micro reactors. Effect of the electrocatalytic route, Appl. Catal. B: Environ. 148–149 (2014) 473-483.

[7] M.A. Rodrigo, P. Canizares, H. Garcia, J.J. Linares, J. Lobato, Study of the acclimation stage and of the effect of the biodegradability on the performance of a microbial fuel cell. Biores. Technol. 100 (2009) 4704–4710.

7.   RESULTS AND DISCUSSION

7.1   INTRODUCTION

After having studied technology RED and having identified its capacities of current production, it was decided to focus attention on the Microbial Fuel Cell. Microbial fuel cells (MFCs) are expected to be a new opportunity for energy generation through the conversion of organic matter contained in wastewaters into electricity with the aid of electricity-generating bacteria [1]. A large number of works are focused on the structure of the MFC and materials but the most critical operating parameter in biological process is not considered. There are many operating variables, which influence the operation and the performances of a MFC. In order to get the minimal electricity losses in the system, these variables must be optimized.

VARIABLE	CONDITIONS TO HAVE OPTIMAL MFC PERFORMANCES
pH	- constant in the anode chamber -6.5<pH<8.5 to stimulate the growth of electrogenic microorganisms [2,3]
Temperature [4]	This influence depends on the kinetics and mass transfer (activation energy, membrane conductivity and coefficient of mass transfer), the thermodynamics (free energy and potential electrodes) and the nature and distribution of microbial communities [5]
growth of microorganism (biofilm [6] or by mediators electron transfer [7])	Its increase generates the higher value of electrical current.
feed rate	- An increase of this parameter enhances the output voltage [8] -If the feed rate is too high, the power density worsens [9] -High feed rates involve low residence time [10]
external resistance	Electrical current increases and the response time to get the steady state decreases with low external resistances [11]

Table 7.1 Main operating parameters.

The work performed during the second part of my thesis can be divided in two subcategory: the first part was conducted at the University of Castilla la Mancha in Spain and the main parameter investigated was the solid retention time; the second part of the work was conducted at the University of Palermo and the attention has been focused on the capabilities of the MFC to generate power using a bio-anode and simultaneously shoot down pollutants in the cathode compartment (giving a further contribution to the existing data in literature[12-16]).

7.2   SOLID RETENTION TIME

The solid retention time (SRT) represents the time spent by activated microorganisms in the reactor or the time available to reproduce the activated-sludge solid according to its regeneration characteristics, which depends on many factors. If the regeneration time is longer than the retention time, bacteria will be washed out; conversely, if it is shorter than the SRT, these microorganisms will proliferate and colonise the system [17].

The choice to study the retention time of the solid, or sludge age, was taken because this parameter has many consequences related to:

-    the process performance,
-    the degradation of organic matter rate and
-    the selection of the most appropriate culture.

Therefore, the kind of bacteria that develops in the medium depends on the sludge age: aerobic microorganisms grow up quickly while anaerobic bacteria requires slow growth rates. Moreover, the existence of the electrogenic microorganisms takes longer than the facultative ones. The following Table shows the growth rate of different microorganisms:

Bacteria	μ (h^{-1})
Aerobic microorganisms [18]	1.29-2.84
Facultative microorganisms [17]	0.160-0.048
Clostridium populeti [19]	0.16
Anaerobic Aeromonas hydrophila [20]	0.15
Clostridium butyricum [21]	0.11-0.07
Shewanella oneidensis [22]	0.085-0.04
Rhodoferax ferrireducens [23]	< 0.04
Geobacter sulfurreducens [24]	0.037

Table 7.2 A Comparison of the Maximal Growth Rates of Various Bacteria under Optimal Conditions.

Despite the numerous studies of variables, researches regarding the influence of sludge age in the performance of a MFC have not been found. Thus, this research has been focused to evaluate the effect of different sludge ages selected on the performance of a MFC and its capacity to adapt and respond to changes in this parameter.

In order to determine the best operational condition of solid retention time, five equal air-breathing MFC operating each one under different solid retention times were studied. To obtain a series of cells working with different sludge ages, every day a volume of liquid was removed from the reactor of the anodic chamber and replaced by fresh synthetic wastewater. The volume removed was varied to obtain the solid retention times chosen: 1.4, 2.5, 5, 7.4 and 10 days. The inoculation process was carried out using activated sludge from the municipal Wastewater Treatment Plant of Ciudad Real, concentrated by sedimentation process.

As shown in Figures 7.1 and 7.2, during the first inoculation (a mix of 1 mL of sludge and 116 mL of synthetic wastewater) higher sludge age caused a higher amount of COD removal: however, an important increase in the current generated by the cell was not observed (I phase).

180
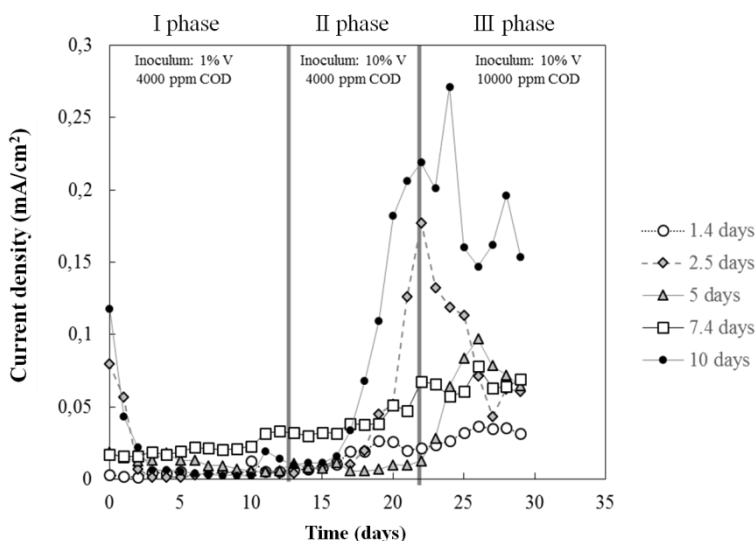
Figure 7.1 Plots the current density as a function of the reaction time, obtained using 5 MFCs with different solid retention times. The plot reports three stapes of study which differ in inoculum and concentration of sodium acetate.

Consequently, a second inoculation (II phase) was carried out with a higher percentage of inoculum (from the 1% to 10% v/v). The current density increased with the solid retention time but this trend cannot be defined for all cells. MFC operating with a STR of 10 days (-●-) showed an increase in the generation of current probably due to the low volume removed (11 mL). It means that a low percentage of microorganisms being washed in this system and, therefore, microorganisms which grow up slowly were favored (as for example the electrogenic ones). As reported in Figure 7.2 during the II phase the organic matter is practically totally removed in every MFC. Thus, a third inoculation (III phase) was carried out increasing the amount of carbon source of the synthetic wastewater in order to ensure enough organic nutrient for microorganisms.
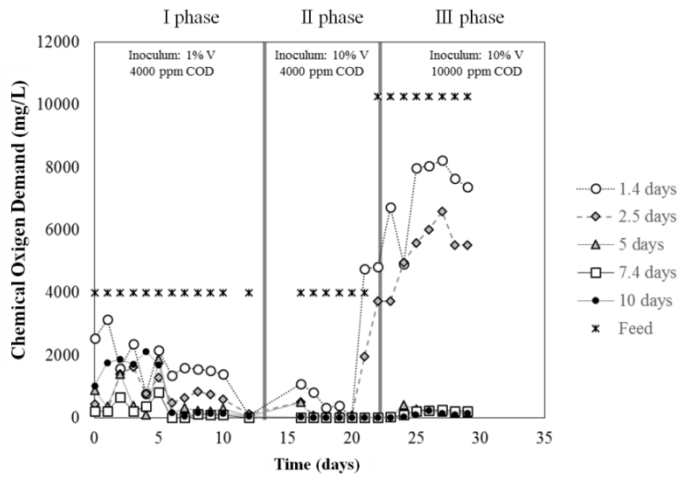
Figure 7.2 Plots the COD consumption as a function of the reaction time, obtained using 5 MFCs with different solid retention times. The plot reports three stapes of study which differ in inoculum and concentration of sodium acetate.

During the third inoculation, it was found that higher solid retention times have a positive effect on the electrical performance of the MFC. The output current values were collected in the following Table.

SRT (days)	Current density (A/m²)
1.4	0.0136
2.5	0.0609
5	0.0645
7.4	0.0688
10	0.1534

Table 7.3 Current densities output for each MFC with different SRT.

A simultaneous increase of the generation of electric current was recorded for MFCs with a STR of 7.4 and 2.5 days. This can lead to think that electrogenic microorganisms of these cells were in need of more time to adapt to the new conditions. Consequently their growth began later because of the greater volume collected from the reservoir (15.5 and 46 mL). Electrogenics bacteria characterized by a STR of 5 days needed two more days to grow up; this was probably due to a poor agitation that caused the removal of a high amount of sludge volume during the

beginning of the experiment. The cell with the lowest retention time (1.4 days) showed the slowest growth of the bacterial community probably because of large volumes removed daily. The increase in the production of current density can be related to the increase in the carbon source when the operation is performed at higher STRs (5, 7.4 and 10 days) as the total removal of COD showed. It can be associated to the existence of aerobic microorganisms that consume the organic matter without allowing the electrogenic ones carrying out their metabolic activities. Once the amount of COD is increased (III phase), one begins to observe the activity of the electrogenic colonies. Nevertheless, as plotted in Figure 7.2, MFC with lower SRTs cannot remove completely organic matter. This may be associated to three factors: (i) electrogenics microorganisms that are not able to quickly remove the organic matter, (ii) the daily removal of large volumes carrying away bacteria and (iii) the insertion of a fresh solution.

Other tests with effluents from a biologic treatment with the same operational conditions of STR was carried out. Figure 7.3 shows a comparison in logarithmic scale between the current density generated by a MFC and the current density generated by the effluents filtered and fed in a cell with the characteristics of the MFC but without microorganisms.
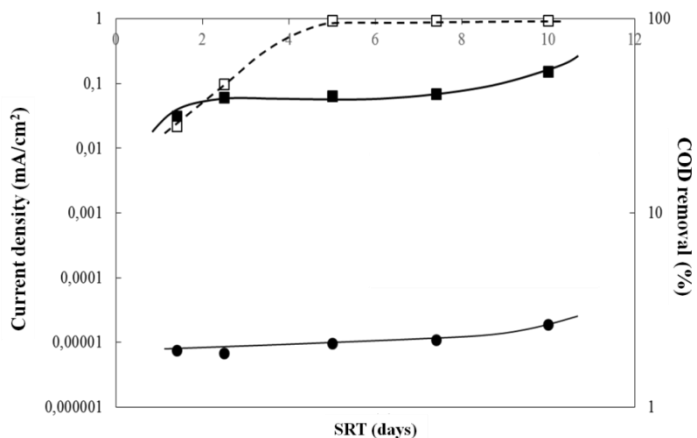
Figure 7.3 Plots the % COD removal (□) as function of SRT and reports the comparison between the current density with a normal MFC (■) and current density recorded with effluents of biological treatment (●).

Results showed that the current density generated by the effluents increased lightly with the STR. This result can be associated to a low contribution of mediators in the generation of electricity. As a consequence, the direct transfer of electrons to the anode is the main mechanism which is triggered in the reactor and the microorganisms, able to carry out this process, require high solid retention times.

To better understand the effect of the sludge age on bacterial communities present in the MFC taken into consideration, the trends obtained using MFC with a SRT of 2.5 and 10 days have been put to comparison.

Figure 7.4 reports the current density production and the percentage removal of COD for the cells above mentioned. For convenience, a letter of the alphabet has been associated with each cell with different SRT as can be seen from the following Table.

Entry	SRT (days)
A	10
B	2.5
A'	3
A''	2.5

Table 7.4 Nomenclature of MFCs depending on the SRT.
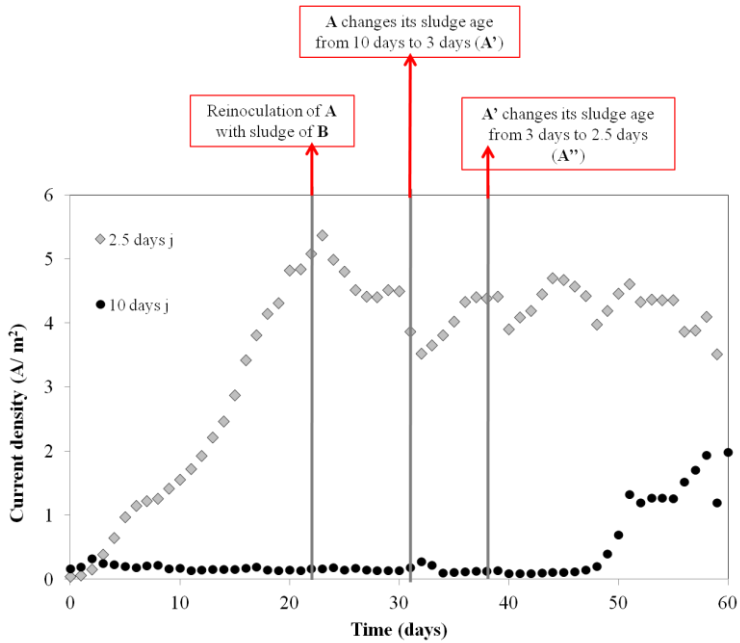
Figure 7.4 Evolution of the current density with the time of cells operating under a SRT of 2.5 days (MFC B) and 10 days (MFC A).

As reported in Figure 7.4 the MFC B showed a quick increase in the generation of current density since its start-up and reached the steady state at the day 23th after to have achieved its maximum value of output current density, 5.37 A/m^2. The stability in current generation is correlated with the stability in the consumption of the carbon source that was approximately the 40% of the COD for every day (see Figure 7.5).
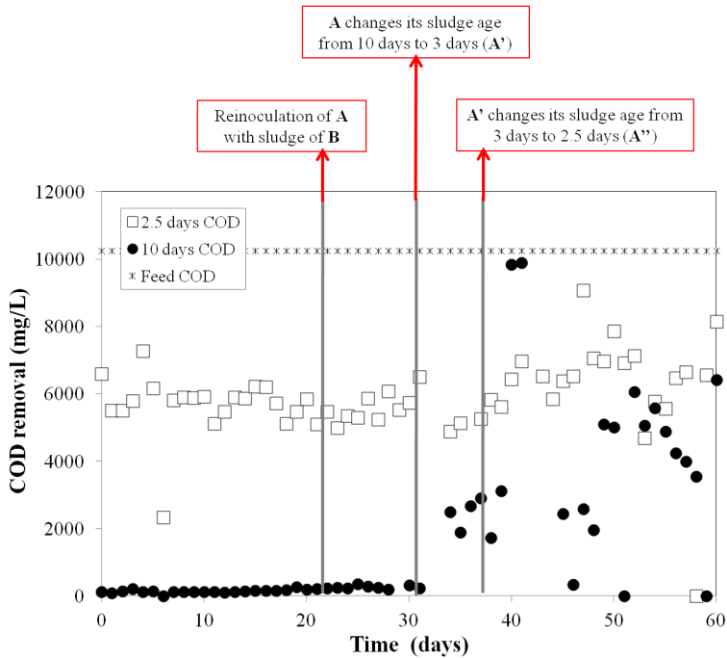
Figure 7.5 Evolution of the COD removal with the time of cells operating under a SRT of 2.5 days (MFC B) and 10 days (MFC A).

Regarding the MFC A, if on one hand it showed a complete removal of total organic carbon (Figure 7.5) from the other side in it was not observed a production of current (Figure 7.4). This can be due to the low volume purged in this case from the reservoir that favors the existence of multiculture inside of the anodic reactor.

In order to enhance the electrogenic activity, MFC A was re-inoculated with sludge from the reservoir of 2.5 days of SRT maintaining however the operating conditions in such a way as to continue to work with a solid retention time of 10 days. No changes in current density were observed. Then it was decided to change the solid retention time of MFC A from 10 days to 3 days (MFC A') but even in this case, no improvements in the production of current were recorded. Several changes were observed only when the device has been brought to a retention time of 2.5 days (MFC A"). As reported in Figure 7.4 the MFC A" only after 19 days operating under the new condition started to show a rise trend in the current density achieving 1.98 A/m^2. Although the system (MFC A) has no problem adapting to changes in the

186

SRT parameter (requires only an optimization time) the performance of this cell have not achieved the high values of current density obtained with the MFC B.

At this point to understand what was happening inside the reactor, a series of HPLC analyses were performed on aliquots of sample collected from the anode compartments of the MFC A (10d), MFC B (2.5d), MFC A' (3d) and MFC A" (2.5d). HPLC analysis indicates that reaction intermediates have an important role in the current generation as it can be observed in Figure 7.6.

B)
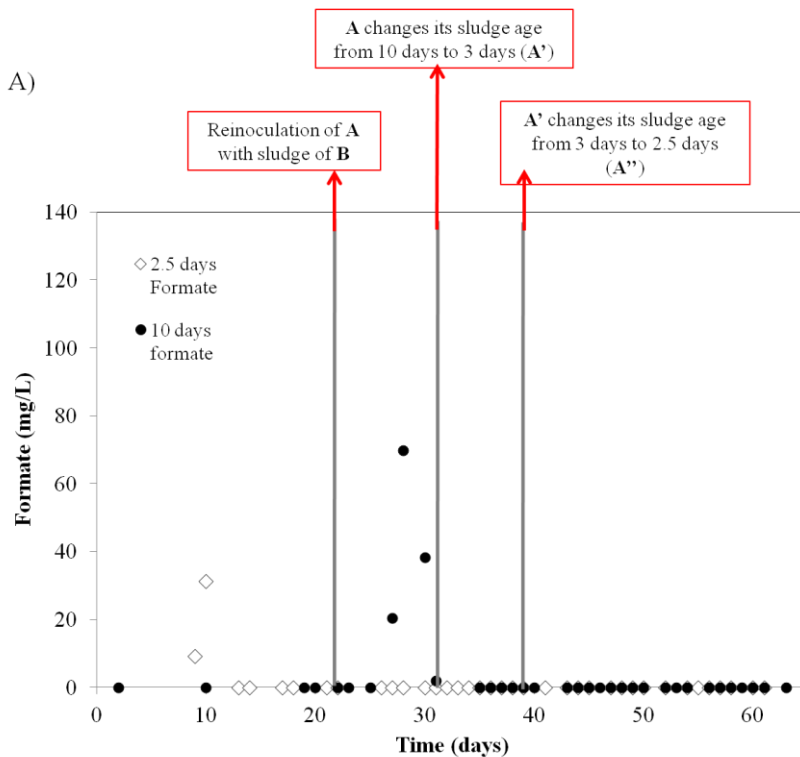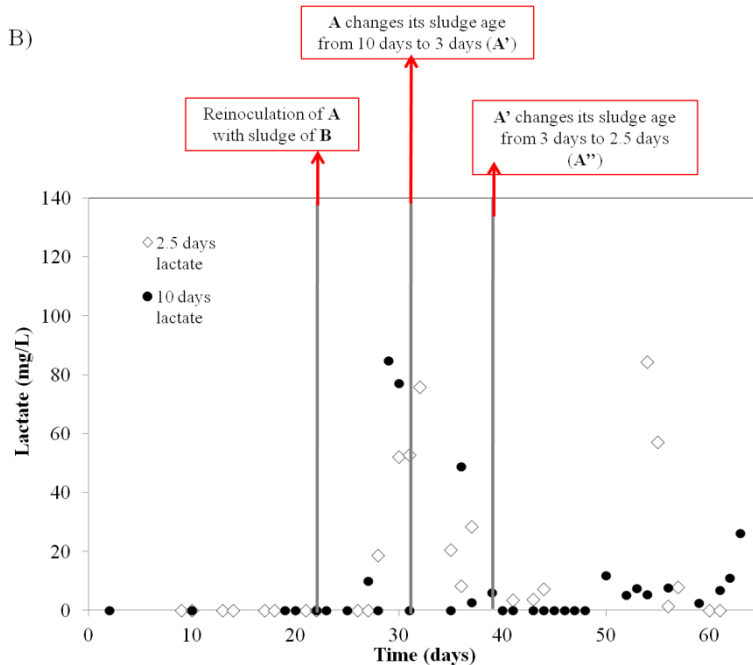
Figure 7.6 Evolution of the concentration of the intermediates: Formiate (Figure A) and Lactate (Figure B) detected as a function of the time of cells operating under a SRT of 2.5 days and 10 days.

As shown in Figure, the production of lactate in MFC B, as reaction intermediate, is important to obtain increasing current densities. In fact, lactate is detected at the time that both systems show a trend to stabilize generating electricity. The absence of lactate during the strong initial increase of the current density for MFC B could be related with its continuous consumption by the microorganisms. When MFC A was re-inoculated with sludge from the reservoir of MFC B, it can be appreciated the presence of lactate and formate at this stage. This presence is due to the microorganisms from the cell of 2.5 days, the main generators of these compounds, but no changes in current density were observed until the MFC A started to work under a SRT of 2.5 days (becoming MFC A"). When also the second MFC is activated, the increase of the current density can be associated to the development of a bacteria population over the period that lactate is present as an intermediate while formate was not detected. In both cells very small amount of formate were recorded in that its degradation is very fast. It is possible to think that the formation and

consumption of formate has no generated power because the electrons which come into play are few. The decrease in the COD removal (Figure 7.5) demonstrates that similar culture than the one located in MFC of 2.5 days are reproducing when the SRT of 10 days becomes 2.5 days because the percentages of carbon source removal are similar. Operating with a sludge of 2.5 days, the system selects different kinds of culture that are able to follow two routes:

- ✓ the fermentation of acetate into formate can be carried out (specie easily degradable but not suitable to produce current densities);
- ✓ the bio-synthesis of lactate from acetate (or other intermediates not identified by the HPLC).

To confirm the assumption made previously, MFCs operating for several weeks with different SRTs (1.4, 5 and 7.4 days) were changed all into 2.5 days of SRT, which was selected as the optimal SRT thanks to the highest value of current density obtained (5.37 A/m^2) in comparison with 0.203, 0.119, 0.159 and 0.275 A/m^2, values collected working with a sludge age of 1.4, 5, 7.4 and 10 days, respectively. The evolution of current density and the removal of COD before and after the change of SRT are reported in Figures 7.7, 7.8.
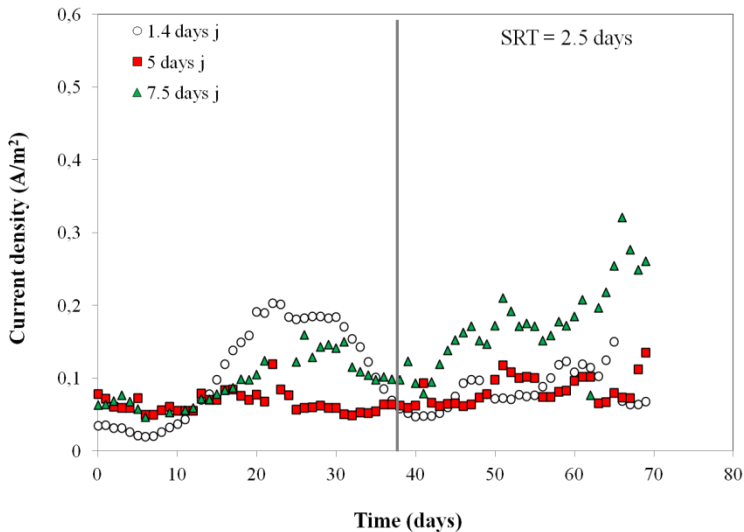
Figure 7.7 Evolution of the current density with the time of MFC operating under a SRT of 1.4, 5 and 7.4 days before and after the change of its SRT to 2.5 days.

According to the trend of current density reported in Figure 7.7, the modification of the SRT has a positive effect on the performance of the MFCs. Current densities increases until values of 0.219, 0.797 A/m^2 corresponding with the cells operating before at 5 and 7.4 days, respectively. The cell with an initial SRT of 1.4 days presents a value of current density that is maintained constant at the beginning (from 0.048, value initial, to 0.118 A/m^2) but then declines without other increases. MFCs with higher previous sludge ages require less time to show higher values of current density. Furthermore as shown in Figure 7.8, higher organic matter concentration in the effluent were observed similar to those recorded for the cell of 2.5 days, revealing an evolution of the culture to a more electrogenic specie.
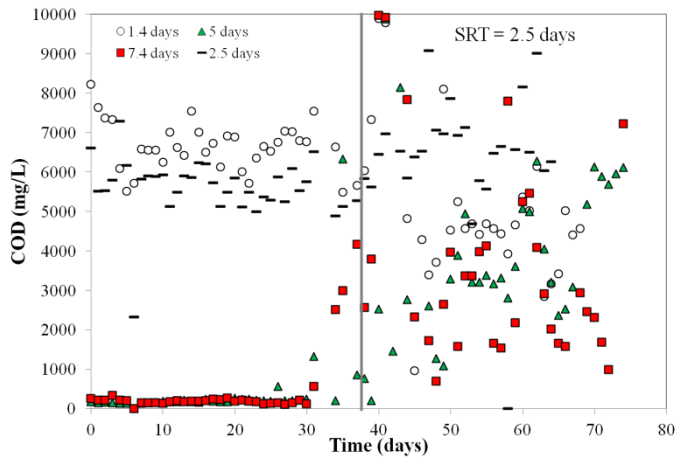
Figure 7.8 Evolution of the COD with the time of MFC operating under a SRT of 1.4, 5 and 7.4 days before and after the change of its SRT to 2.5 days. Figure also shows the values of COD for MFC with SRT of 2.5 days in order to do a comparison.

Despite the MFC with a SRT initial of 1.4 days shows a good COD removal, this does not present a good electrical behavior. This should be caused by the absence of suitable microorganisms. Microorganisms of the MFC characterized by a SRT = 2.5 days showed a better performance at the presence of lactate remaining indifferent with the formation of formate. Figure 7.9 shows the concentration of both intermediates during the production of the current density in every cases.

B)

C)
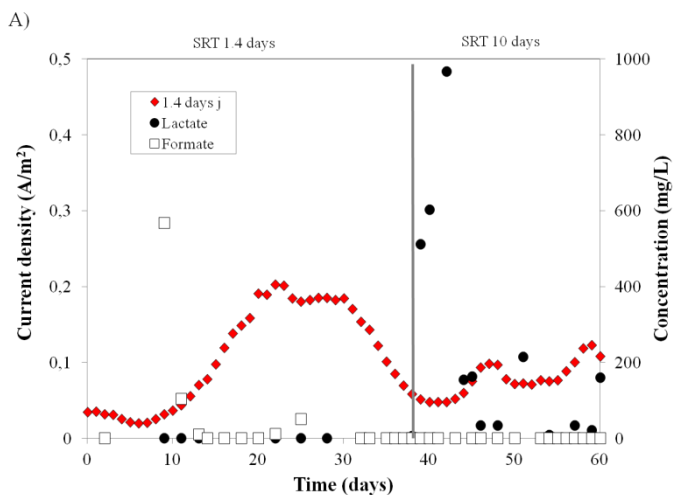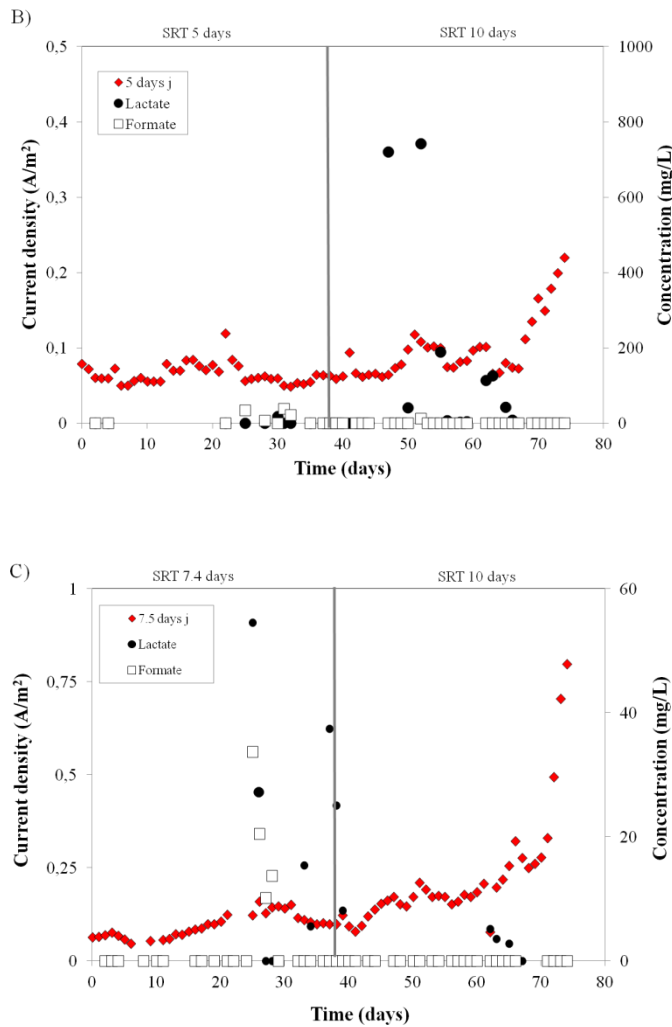
Figure 7.9 Evolution of the reaction intermediates with the time of MFC operating under a SRT of 1.4 (Figure A), 5 (Figure B) and 7.4 days (Figure C) before and after the change of its SRT to 2.5 days.

As reported in Figure 7.9, the formation of lactate seems related to the generation of current. Once obtained good concentrations of lactate, the devices have begun to produce current through the consumption of the intermediate by microorganisms. Only in the cases of previous high SRTs, format is detected. Conversion of acetate into formate does not achieve relevance in the electrical behavior and this specie

disappears at the same time that the presence of lactate becomes stronger. In the literature, several authors [25] studied the correlation between the biodegration rate and the electrical current obtained. Moreno et al. [26] have observed that the biodegradation of lactate takes place at faster rates than that of acetate, resulting in higher values of current density. An increase in the initial concentration of lactate causes better performances of the systems. Another investigation with a two-chamber MFC, whose electrodes were of carbon paper, showed that electrons available for biofilm growth were of 26.5 for a medium of lactate, 19.3 for glucose and 11.2 for acetate (calculated by COD consumption minus current and gas and aerobic oxidation losses) [27].According to the literature, also in my results lactate shows better qualities to enhance the electrogenic activity. Cultures inside the reactors are changed following the variation of the SRT developing a consortia able to synthesize lactate that subsequently is being converted into electrical current.

7.3 UTILIZATION OF MFC TO TREAT CONTAMINATED WASTEWATER

Recent literature has shown that microbial fuel cells can be also used for wastewater treatment and for the removal of AO7 dye (by electro-Fenton) and Cr(VI) thus avoiding the necessity to supply energy to the system.

The experiments carried out at the University of Palermo has provided a comprehensive study on the electrochemical oxidation with carbon felt as anodes and has allowed to study the effect of various operating parameters such as: (i) types of microorganisms (putrefaciens Shewanella, Geobacter sulforeducens, intestinal microbial community resulting from the larva of the red weevil), (ii) dimensions of the electrodes and (iii) anode solution, on the generation of electric current and the simultaneous abatement of pollutant. In a second moment it was also investigated the possible use of by-products of degradation of AO7 as a possible source of carbon for microorganism as Shewanella putrefaciens.

All experiments were performed in a divided electrochemical cell using as separator between the two compartments a cation exchange membrane. First experiments were performed using the anode side contained electroactive biofilm, that worked as biocatalysts using various organic substrates to produce electrons while the EF process took place at the cathode. Operate conditions used for the first experiments are summarized in Table 7.5.

Anode compartment	Cathode compartment	Operative conditions
•Organic medium: 50 ml LB	•50 ml di AO7 150 mg/L,	•Temperature 30 °C
•bacteria:*Shewanella putrefaciens*	•Na$_2$SO$_4$ (0,1 M) as supporting electrolyte	•Constant agitation in both compartments
	• FeSO$_4$ (0,5 mM) as catalyst	•Injection of a mixture N$_2$/CO$_2$ into the anode compartments
	•H$_2$SO$_4$ (pH =2)	•IEM: Nafion cationic membrane

Table 7.5 Operative condition

As shown in Figure 7.1, the current density at the beginning of the experiment showed significant values close to 1 A/m^2 and successively significantly decreased.
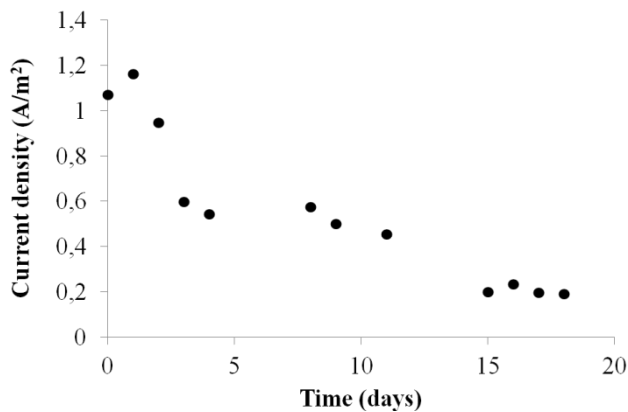
Figure 7.10 Shows the evolution of current density as function of the treatment time of AO7 using S. putrefaciens as microorganisms in the anode compartment.

However, it was possible to carry out the test for more than 10 days, with a current density above 0.4 A/m^2. As shown in Figure 7.11, simultaneously to the production

of current, a fast and complete removal of the color was obtained in the cathode compartment through the electro-Fenton process.
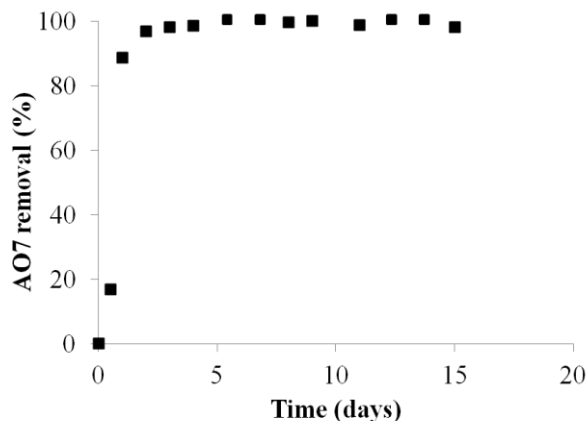
Figure 7.11 Reports the removal of AO7 as a function of the treatment time.

After three days of treatment, a removal of the color of 98% was monitored by means of spectrophotometric investigations while complete removal was achieved in less than ten days. The reduction of the current density observed in Figure 7.10 may be due to several factors, including the decrease of the concentration of the AO7 and the resulting increase of the cathodic potential, in agreement with the data obtained using the reverse electrodialysis process for the treatment of the same pollutant. As reported in Table 7.5, the organic medium used during this experiment was Luria-Bertani broth according with the literature. Because LB broth culture medium is a very rich in organic components, for the growth of Shewanella putrefaciens it was decided to use an alternative medium where the acetate was the only organic carbon source. This was done also to try to limit the possible transfer of organic components from the anode compartment to the cathode one across the membrane.
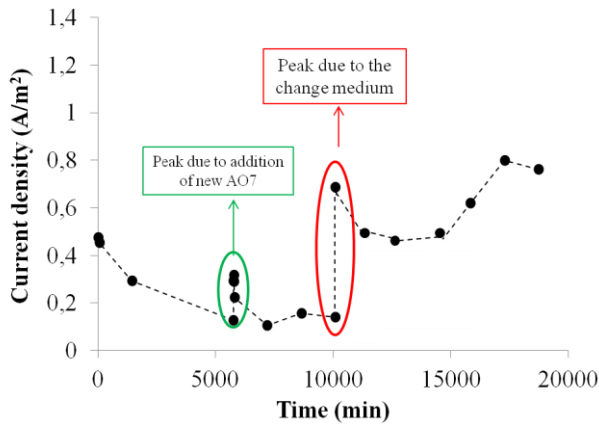
Figure 7.12 Shows the evolution of current density as function of the treatment time of AO7 using S. putrefaciens as microorganisms in the anode compartment using a minimal medium as organic matter.

As reported in Figure 7.12 the experiment can be divided in two phases. In the first phase, the MFC was filled with 60 mL of NBA and 10% (v/v) of inoculum in the anode compartment and 70 mL of aqueous solution of Acid Orange 7 (150 mg/L) in the cathode one. At discoloration occurred, the cathodic solution was replaced with a new fresh solution of AO7, while maintaining the anodic solution unchanged (II phase). The current density at the beginning of each stage were respectively of 0.47 A/m^2 for the I phase and 0.28 A/m^2 for II phase. In the graph there are two peaks. The first coincides with the insertion of a new solution containing azo-dye. This improvement can be due to a shift of the equilibrium of cathodic reaction towards the production of hydrogen peroxide driven by its reaction with AO7. The second peak is recorded when a change of organic matter was carried out in the anode compartment in order to restore the concentration of nutrient for microorganisms. The higher values of current density recorded in the last few days of experiment was probably due to higher growth of the biofilm on the surface of the electrode. From the Figure below it is possible to note that in both phases, a very high removal of the dye was obtained. In particular in the first stage a reduction of color close to 100% was achieved in about a day (with a discoloration of about 97% after one hour), while for the second stage the complete removal of the dye was obtained in about three days.

196
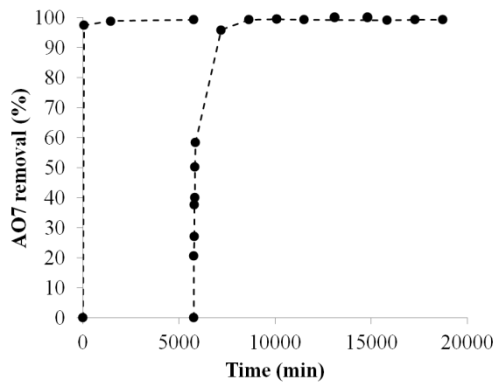
Figure 7.13 Removal of AO7 as function of reaction time.

The data reported in the last Figure confirm a good reproducibility and stability of the system with the time with regular addition of pollutant.

Up to now, several microorganisms have been studied in order to elucidate their specific extracellular electron transfer mechanisms. On the basis of a preliminary study about of bacteria family, two kind of model of two families of Gram-negative bacteria were used: Geobacter sulfurreducens (*Gs*) [28-30] and Shewanella putrefaciens (*Sp*) [31-35]. As described in detail in Chapter 6, Shewanella putrefaciens and Geobacter sulfurreducens are microorganisms used in the literature because allow get the greatest current values. Especially Geobacter sulfurreducens were often found as prevalent species in biofilms formed on the anodes of MFC that used mixed crops from anaerobic digesters. Well as giving good current density, the Shewanella arouse a special attention as a facultative anaerobic capable of producing current even in the presence of air. To study more the effect of the nature of the microorganisms, another kind of bacteria arising from the intestine of the larva of the red weevil (*Dysgonomonas Dy*) was used. As reported in Figure 7.14 *Sp* and *Gs* removed about the total amount of dye after the same time interval; smaller but still significant reduction values of color were obtained by operating with *Dy*.
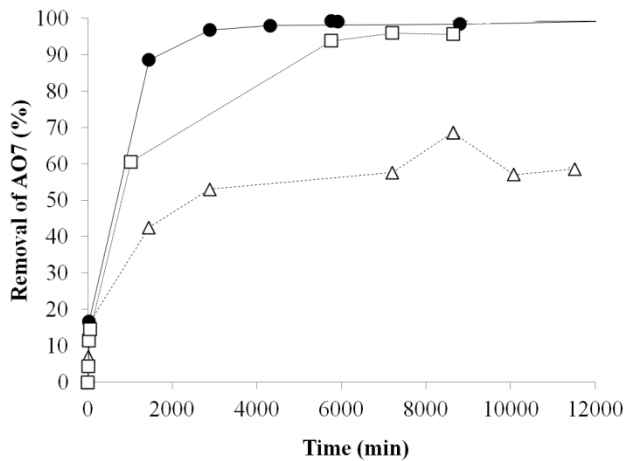
Figure 7.14 Reports the removal of dye with the treatment time obtained using different kind of bacteria: Geobacter sulfurreducens (□), Shewanella putrefaciens (●) and Dysgonomonas (△).

In the first 200 minutes the most important values of current density were obtained in the presence of *Sp* (initial current density obtained 1.1 A/m^2). It is interesting to note how the experiments carried out in the presence of *Dy* led to the generation of significant initial current density of equal to about 0.15 A/m^2. Tests where *Gs* were used initially gave values of current lower than *Sp* (equal to 0.38 A/m^2) but after 4 days the current produced by *Gs* has exceeded that obtained from *Sp*, reaching a value of 0.8 A/m^2 (see Table below).

Bacteria	$i_{initial}$ (A/m^2)	$i_{seventh\ day}$ (A/m^2)	Removal AO7(%)
G. Sulfurredusens (□)	0.38	0,42	>90%
S. Putrefaciens (●)	1.1	0.38	>98%
Dysgonomonas (△)	0.15	0.048	~ 52%

Table 7.6 Main data collected during the abatement of AO7 using different typology of bacteria.

Several degradation products of AO7 (see Figure 3.21 of chapter 3) are typical intermediates of the Krebs cycle (Figure 7.15). On the basis of this, it was thought to realize a Microbial Fuel Cell with a defined aliquot of the solution containing

cathodic AO7 by-products in the anode compartment. The tests were carried out in the following manner: (i) a classical test of abatement was performed, reached a dye removal higher than 99% (ii) 20 mL of the cathode were taken and, after treatment, were included in the anode compartment; (iii) once regained the same removal of the dye, 30 mL of chatodic solution containing by-products were included in the anode compartment.
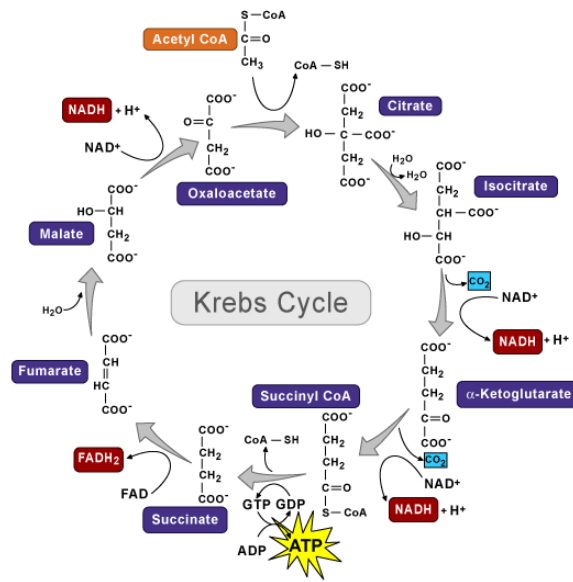
Figure 7.15 Krebs Cycle.

As shown in the Figure below, the carboxylic acids obtained by the degradation of the dye can be used as organic C source for the bacteria.
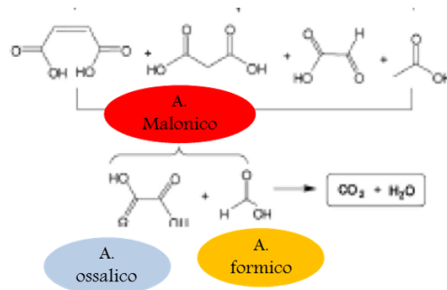
Figure 7.16 Part of the degradation plan of AO7 is reported.

At the end of the first phase, the principal by-products are oxalic acid (0.28 mM) formic acid (0.79 mM) and acetic acid (0.87 mM). These acids have been inserted in the anode compartment and at the end of the second treatment process the formic and acetic acid were completely degraded while a small residue of oxalic acid was recorded (0.02 mM). During the third phase the following concentrations of acids were added in the anode compartment: oxalic acid (0.11 mM) formic acid (0.57 mM) and acetic acid (1.20 mM). At the end of the process, their concentrations were decreased to 0.023 mM and 0.142 mM for oxalic and formic acid, respectively. Figure 7.17 reports the abatement of AO7 during all steps.
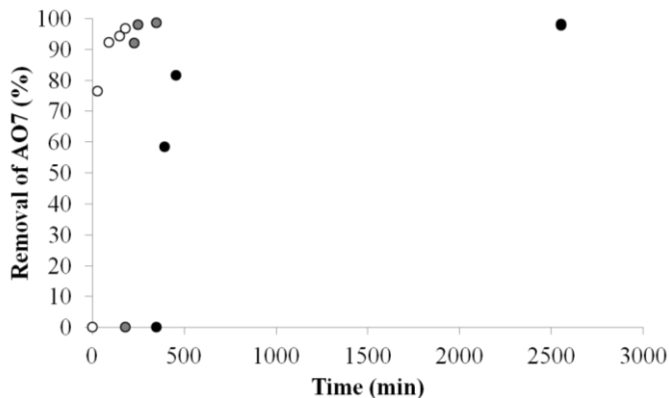
Figure 7.17 Reports the removal of azo-dye as a function of treatment time during all three step: I (○), II (◉) and III (●).

As shown in the Figure 7.17, it was obtained a very rapid and high discoloration of the cathodic solution in all three stages analyzed. Hence, it is possible to state that the anodic process occur successfully even in the presence of by-products originated from the degradation of the cathodic AO7.

In this part of the PhD research the removal of Cr(VI) was investigated using a MFC in order to avoid the supply of energy during the reduction process of pollutant. A series of experiments was carried out using a bi-compartment MFC feeding in the anodic compartment a bio-anode with a S. putrefaciens biofilm in a LB broth and in the cathodic compartment a water solution containing Cr(VI) 25 mg/L (80 mL). In all experiments the total removal of Cr(VI) was obtained after a time of about 300 min with a power and current average densities of 0,017 W/m^2 and 0,44 A/m^2. On the bases of the results, it is possible to confirm the stability of MFC system for a longer time when a solid and compact biofilm was formed on the anode surface. Also in this case to test the capacity of MFC system for a longer time for the generation of electric energy and the abatement of pollutant from water, several addition of Cr(VI) to the solution were carried out at fixed intervals of times. The Figure 7.18 shows the good reproducibility and stability of the system with the time.
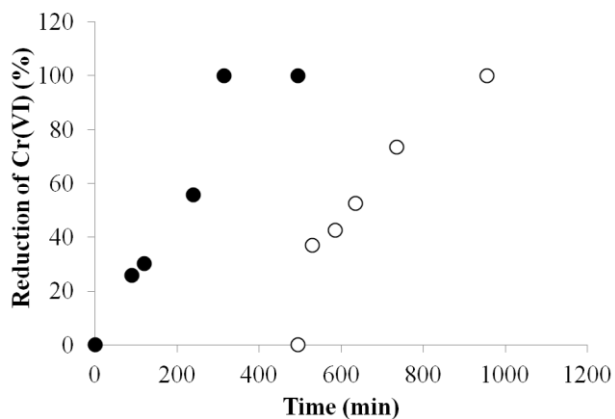
Figure 7.18 Shows the removal concentration of Cr(VI) vs. time achieved in a MFC bi-compartments. Cr(VI) (25 mg/L) was added to the cathodic compartment after 0 and 500 min.

7.4 REFERENCES

[1] D. Wu et al., Electricity generation by Shewanella sp. HN-41 in microbial fuel cells. Int. J. Hydrogen. Energy 38 (2013) 15568-15573.

[2] V.B. Oliveira, M. Simões, L.F. Melo, A. Pinto, Overview on the developments of microbial fuel cells, Biochem. Eng. J. 73 (2013) 53–64.

[3] B.H. Sorensen, N. Nyholm, A. Baun Algal toxicity tests with volatile and hazardous compounds in air-tight test flasks with CO_2 enriched headspace. Chemosphere 32 (1996) 1513–1516.

[4] A. Larrosa-Guerrero, K. Scott, I.M. Head, ffect of temperature on the performance of microbial fuel cells. Fuel, 89(12) (2010) 3985-3994.

[5] E. Martin, O. Savadogo, S.R. Guiot, B. Tartakovsky, The influence of operational conditions on the performance of a microbial fuel cell seeded with mesophilic anaerobic sludge, Biochem. Eng. J. 51 (2010) 132–139.

[6] A. González del Campo, P. Cañizares, M.A. Rodrigo, F.J. Fernández, J. Lobaton, Microbial fuel cell with an algae-assisted cathode: a preliminary assessment, J. Power Sources 242 (2013) 638-645.

[7] M.A. Rodrigo, P. Cañizares, J. Lobato, R. Paz, C. Sáez, J.J. Linares, Production of electricity from the treatment of urban waste water using a microbial fuel cell. J. Power Sources 169 (2007) 198–204.

[8] J.R. Kim, J. Rodríguez, F.R. Hawkes, R.M. Dinsdale, A.J. Guwy, G.C. Premier, Increasing power recovery and organic removal efficiency using extended longitudinal tubular microbial fuel cell (MFC) reactors, Energy Environ. Sci. 4 (2011) 459-465.

[9] I. Ieropoulos, J. Greenman, C. Melhuish, Improved energy output levels from small-scale microbial fuel cells, Bioelectrochem. 78 (2010) 44–50.

[10] M. Di Lorenzo, K. Scott, T.P. Curtis, I.M. Head, Effect of increasing anode surface area on the performance of a single chamber microbial fuel cell, Chem. Eng. J. 156 (2010) 40–48.

[11] M. Di Lorenzo, T.P. Curtis, I.M. Head, K. Scott, A single-chamber microbial fuel cell as a biosensor for wastewaters, Water Res. 43 (2009) 3145–3154.

[12] MÁ Fernández de Dios, O Iglesias, M Pazos, Application of Electro-Fenton Technology to Remediation of Polluted Effluents by Self-Sustaining Process, Hindawi Publishing Corporation Scientific World Journal Volume (2014) 8 pages.

[13] K. Solanki, S. Subramanian, S. Basu, Microbial fuel cells for azo dye treatment with electricity generation: a review, Bioresour. Technol. 131 (2013) 564-571.

[14] V. Murali, S.A. Ong, L.N. Ho, Y.S. Wong, N. Hamidin, Comprehensive Review and Compilation of Treatment for Azo Dyes Using Microbial Fuel Cells, 85 (2013) 270-277.

[15] M.Á. Fernández de Dios, A. González del Campo, F. J. Fernández, M.A. Rodrigo, M. Pazos, M.Á. Sanromán, Bacterial–fungal interactions enhance power generation in microbial fuel cells and drive dye decolourisation by an ex situ and in situ electro-Fenton process, Bioresour. Technol. 148 (2013) 39–46.

 [16] G. Wang, L. Huang, Y. Zhang, Cathodic reduction of hexavalent chromium [Cr (VI)] coupled with electricity generation in microbial fuel cells, Biotechnol. Lett. 30 (2008) 1959–1966.

[17] F. J. Fernández-Morales, J. Villaseñor, D. Infantes, Modeling and monitoring of the acclimatization of conventional activated sludge to a biohydrogen producing culture by biokinetic control. Int. J. Hydrogen. Energy 35 (2010) 10927-10933.

[18] MJ Johnson, Aerobic microbial growth at low oxygen concentrations, J. Bacteriol. 94 (1967) 101-108.

[19] G.B. Patel, B.J. Agnew, Growth and butyric acid production by Clostridium populeti, Arch. Microb. 150 (1988) 267-271.

[20] S. Lee, J. Kim, S.G. Shin, S. Hwang, Biokinetic parameters and behavior of Aeromonas hydrophila during anaerobic growth, Biotechnol. Lett. 30 (2008) 1011-1016.

[21] M. Sjöblom, L. Matsakas, P. Christakopoulos et al., Production of butyric acid by Clostridium tyrobutyricum (ATCC25755) using sweet sorghum stalks and beet molasses, Ind. Crops Prod. 74 (2015) 535–544.

[22] Y Zhang, CK Ng, Y Cohen, B Cao, Cell growth and protein expression of Shewanella oneidensis in biofilms and hydrogel-entrapped cultures, Mol. Biosystems, 10 (2014) 1035-1042.

[23] C. Risso, J. Sun, K. Zhuang, R. Mahadevan, et al., Genome-scale comparison and constraint-based metabolic reconstruction of the facultative anaerobic Fe (III)-reducer Rhodoferax ferrireducens, BMC Genomics, 10 (2009) 1-19.

[24] D.E. Holmes, L. Giloteaux, M. Barlett et al., Molecular analysis of the in situ growth rates of subsurface Geobacter species, Appl. Environ. Microbiol. 79 (2013) 5 1646-1653.

[25] J. Kan, L. Hsu, A. C. M. Cheung, M. Pirbazari, K. H. Nealson, Current Production by Bacterial Communities in Microbial Fuel Cells Enriched from Wastewater Sludge with Different Electron Donors. Environ. Sci. Technol. 45 (2011) 1139-1146.

[26] L. Moreno, M. Nemati, B. Predicala, Biokinetic evaluation of fatty acids degradation in microbial fuel cell type bioreactors. Bioprocess and Biosystems Eng. 38 (2015) 25-38.

[27] S. Jung, J. Regan, Comparison of anode bacterial communities and performance in microbial fuel cells with different electron donors. Appl. Microb. Biotech. 77 (2007) 393-402.

[28] K.P. Nevin, H. Richter, S.F. Covalla, J.P. Johnson, T.L. Woodard, A.L. Orloff, H. Jia, M. Zhang, D.R. Lovley, Power output and columbic efficiencies from biofilms of Geobacter sulfurreducens comparable to mixed community microbial fuel cells, Environ. Microbiol. 10 (2008) 2505–2514.

[29] S. Ishii, K. Watanabe, S. Yabuki, B.E. Logan, Y. Sekiguchi, Comparison of electrode reduction activities of Geobacter sulfurreducens and an enriched consortium in an air-cathode microbial fuel cell, Appl. Environ. Microbiol. 74 (2008) 7348–7355.

[30] D.R. Lovley, Bug juice: harvesting electricity with microorganisms, Nature Rev. Microbiol. 4 (2006) 497–508.

[31] H. H. Hau, J. A. Gralnick, Ecology and biotechnology of the genus Shewanella, Annual Review of Microbiology. 61 (2007) 237-258.

[32] M. A. Rosenbaum et al., Shewanella oneidensis in a lactate-fed pure-culture and a glucose-fed co-culture with Lactococcus lactis with an electrode as electron acceptor. Bioresour. Technol. 102 (2011) 2623-2628.

[33] J. M. Tront, J. D. Fortner, M. Plötze, J. B. Hughes, A. M. Puzrin, Microbial fuel cell technology for measurement of microbial respiration of lactate as an example of bioremediation amendment. Biotechnol. Lett. 30 (2008) 1385-1390.

[34] J. C. Biffinger, J. N. Byrd, B.L. Dudley, B. R. Ringeisen, Oxygen exposure promotes fuel diversity for Shewanella oneidensis microbial fuel cells. Biosens. Bioelectron. 23 (2008) 820-826.

[35] L.A. Fitzgerald E.R. Petersen, R.I. Ray, B.J. Little et al., Shewanella oneidensis MR-1 Msh pilin proteins are involved in extracellular electron transfer in microbial fuel cells. Process Biochem. 47 (2012) 170-174.

Part III:

8. MICROBIAL REVERSE ELECTRODIALYSIS CELL: MRC

(A perfect synergy between two promising techniques to increase the electricity generated coupled with synthesis of chemicals and abatement of pollutants)

8.1   STATE OF ART

Researchers are looking for new approaches in order to increase MFC voltages and power densities. In this context, in 2011 Kim and Logan [1] proposed the combination of a MFC with a RED stack into a single process, called a microbial reverse-electrodialysis cell (MRC), as a new approach for energy production. It is an hybrid reactor that have a RED stack placed directly between the MFC electrodes (Figure 8.1). It was proposed in literature to effectively capture energy from salinity gradients using the bacterial oxidation of organic matter and oxygen reduction as favorable electrode reactions [1].
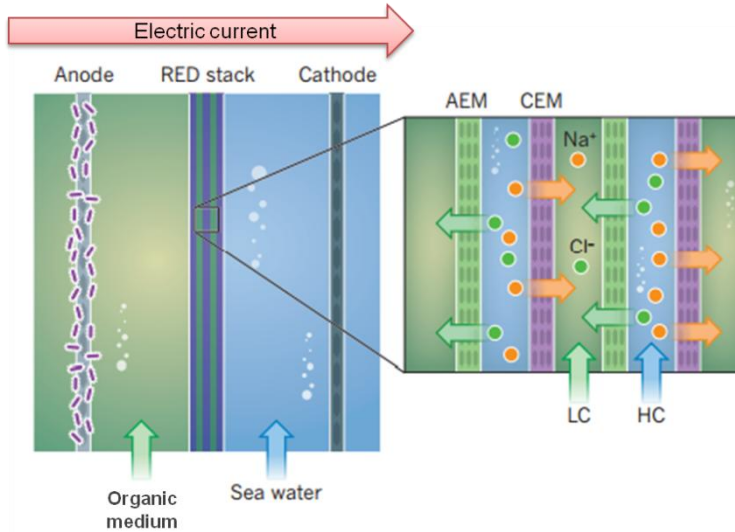
Figure 8.1 Scheme of a MRC where it is possible see main components and the flow of ion and the electrons.

Authors observed that the MRC process could potentially overcome some of the limitations of the individual processes and that this integrated system could outperform the individual processes [1,2]. Thus, the low voltage produced by a MFC can be increased by salinity driven potential with the RED stack, while exoelectrogenic bacteria on the anode and oxygen reduction at the cathode produce spontaneous reactions at the electrodes in the MRC, contributing additional potential

206

to the RED stack, compared with energy losses at the electrodes in a RED conventional system.

Hybrid systems are in an early stage of development, but so far combining technologies seems to be a promising way to triumph over some disadvantages of individual systems. The main challenges, like those for individual systems, are the high cost of materials and achieving high power densities. the operating principles of a MRC technology are:

- electricity is directly generated by bacteria;
- potentials are increased by the salinity gradient;
- there is no direct contact of the fresh water and salt solutions thank to the presence of conventional ion exchange membranes.

8.2   GENERATION OF ELECTRICITY

One of first experiments carried out with this system used a stack equipped with 5 CEMs, 6 AEMs and an air cathode (Figure 8.2) [1]. The anode, a graphite fiber brush, was inoculated with effluent from an existing MFC.
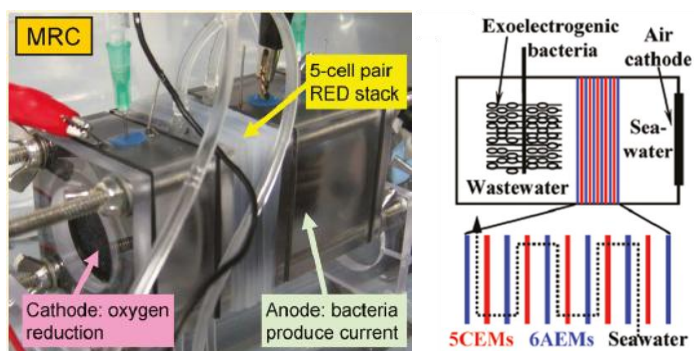
Figure 8.2 Photo of the microbial reverse electrodialysis used by Logan group to study the enhanced of power production [1].

When a salinity ratio SR = 100 (seawater = 600 mM NaCl; river water = 6 mM NaCl) was used, the cell potential from the MRC ranged from 1.2 to 1.3 V with currents of 1.2-1.3 mA (1000-Ω external resistance) (Figure 8.3). A control experiment using an SR = 1 produced < 0.5 V, confirming that the high cell

potential > 1.1 V was due to both redox processes and the salinity driven energy from the RED stack (Figure 8.3) [1].
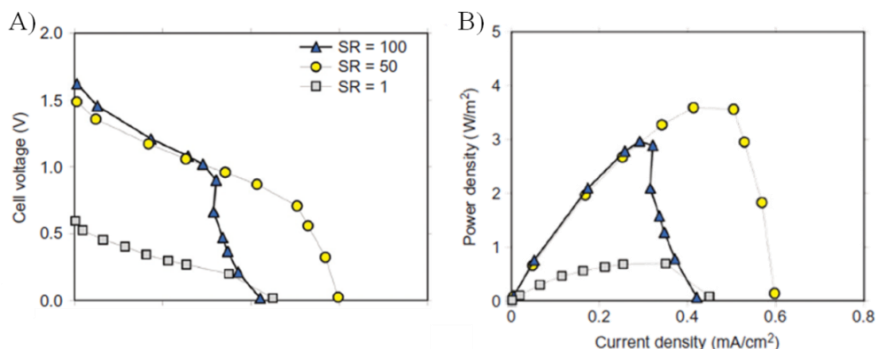
Figure 8.3 (A) Polarization and (B) power densities at different salinity ratios (SRs) in MRCs. The flow rate was 0.85 mL/min for both seawater and river water .

Analyzing Figure 8.3A, the maximum cell potentials produced during polarization tests with an SR = 100 were larger than those with an SR = 50 at current densities below 0.3 mA/cm^2. After this value of current density, a rapid decrease of the cell potential at 0.3 - 0.4 mA/cm^2 (SR = 100) indicated that Ohmic resistances at the higher currents detracted the MRC performances. Salinity Ratio of 50 has showed greater potentials for current densities above 0.3 mA/cm^2. The MRC with an SR = 50 therefore achieved higher power densities, with a maximum power density of 3.6 W/m^2 as normalized by 7 cm^2 cathode area, compared to 3.0 W/m2 for an SR = 100 (Figure 8.3B).

The most substantial impact of the RED stack on MRC performance was that it increased maximum power production using organic matter. Electrode reactions in the MRC produced up to 3.2 ± 0.2 W/m^2, which is three times the power produced in the absence of the stack in a single chamber MFC (1.08 ± 0.03 W/m^2) (Figure 8.4).
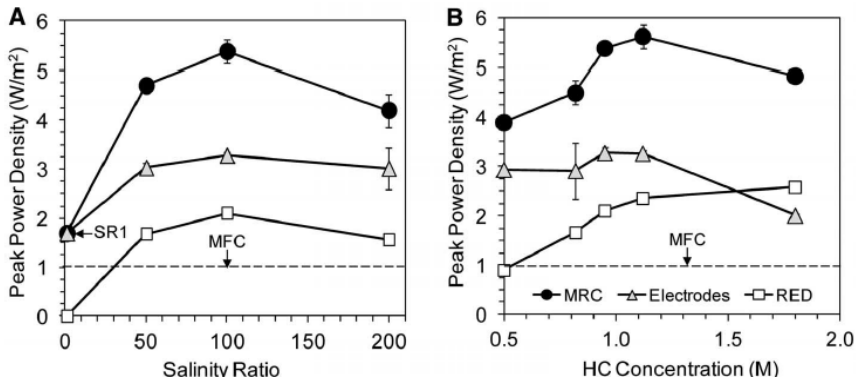
Figure 8.4 Peak power densities obtained from polarization curves, apportioned to power from the RED compared with the electrodes (organic matter power). (A) Effect of SR on peak power density with a fixed HC solution (0.95 M). (B) Effects of HC concentrations on power with a fixed SR of 100. The dashed line represents peak power density of the same electrodes in a single chamber.

The maximum voltage (1.3 V) and power density (4.3 W/m^2) collected using MRC were substantially increased if compared with data obtained with individual MFC part (0.5 V, 0.7 W/m^2), with acetate as the fuel and sodium chloride solutions pumped through the RED stack. In this way it is confirmed that the new technique is promising (Energy efficiency 42%) [1]. Later, Cusick et al. (2012) [2] showed that it was possible to increase the energy generation, using salt solutions that could be continuously regenerated with waste heat (≥ 40 °C). When in a MRC NH_4HCO_3 is used as electrolyte in the water solutions fed inside high (1M of NH_4HCO_3) and low (0.01M of NH_4HCO_3) concentrated compartments of RED reactor could result in more efficient capture of energy from wastewaters and other sources of biomass. The resulting energy gradient between these solutions is greater than a classical interaction between ocean and river water (370 m vs 270 m of hydraulic head). Indeed, as Cusick et al. [2] showed in their work, the use of thermolytic solution of ammonium bicarbonate (continuously regenerated with waste heat, ≥ 40 °C, and conventional technologies) in the RED stack further increased performance to 5.6 W/m^2 with acetate fuel. When domestic wastewater was used with ammonium bicarbonate in the RED stack, the maximum power was about 2.8 W/m^2, which was nearly an order of magnitude higher than when wastewater alone was used. The use

of ammonium bicarbonate as the catholyte may have advantages compared to other chemical buffer electrolytes in which sodium is the cation. The presence of positively charged ammonium ions near the cathode surface could affect oxygen reduction kinetics as well as hydroxide ion gradients near the electrode. Changing the salinity gradient (salinity ratio SR) of HC and LC solutions, an increase of power production by the MRC system was obtained going from a SR of 100 until a SR=1 (see Table 8.1).

Salinity ratio	Maximum power (normalized to cathode area)
SR=100	5.4 ± 0.1 W/m^2
SR=50	4.7 ± 0.1 W/m^2
SR=1	1.7 ± 0.05 W/m^2

Table 8.1 Relationship between the salinity gradient and the power output by the system.

An higher salinity ratio allows an improvement of the charge transport at the cathode (65.5 mS/cm) and a formation of an opportune salinity gradient between the stack and the bio-anode. With SR = 1, the RED stack created only a negligible Ohmic loss of $\sim$0.017 V at the maximum power. The RED reactor alone can't produce any power because a RED stack assembled with 5 cell pairs cannot produce sufficient potential to overcome the thermodynamic threshold for water electrolysis. The combined MRC process (3.6 W/m^2) was greater than the separate contributions of the two processes (at best 0.015 and 0.7 W/m^2) proving that the MRC is a new synergistic advancement in electrical power generation from two renewable resources of organic matter in wastewater and salinity difference between seawater and river water.

In addition, the flow of bicarbonate ions through the anion exchange membrane helps to maintain the pH of the anodic compartment at 6.9 ± 0.1 if compared with a decrease in pH to 5.5 when NaCl salt solutions are used. All these factors lead to an improved performance of the MRC. The data reported before were collected using a flow rate of 1.6 mL/min in both HC and LC compartments because during preliminary experiments it was showed that an increase in the flow rate of the

seawater and river water from 0.85 to 1.55 mL/min improved the cell potentials at current densities >0.4 mA/cm^2 (Figure 8.5). At current densities lower than 0.4 mA/cm^2, both potential and power were independent of the flow rate due to the relatively slow ionic transport. These results suggest that the control on capacity of pumping is important to obtain targeted potentials and power densities in the MRC because maintaining higher the flow rate of the two saline solutions (in the RED reactor) allows to obtain larger voltages and power densities [1].
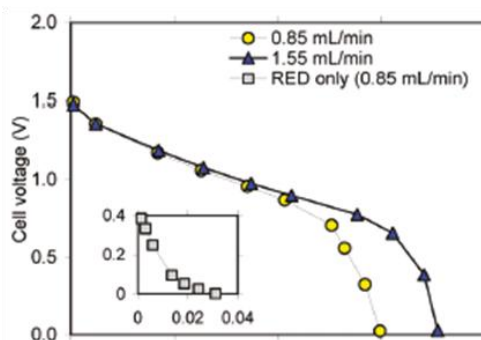
Figure 8.5 Cell voltages obtained by MRCs at different flow rates (SR = 50).

One drawback of a MRC system filled with NH_4HCO_3 water solutions is the passage of predominant nitrogen forms ammonium (NH_4^+), ammonia (NH_3), and carbamate ($NH_4CO_3^-$) from the stack into the anode chamber. Negatively charged carbamate ions crossed the anion exchange membrane and moved into the anode chamber to balance protons charge released by the bioanode. Thus, the main concerns of nitrogen crossover are contamination of the anode solution with ammonia and loss of the salt solution.

MRC were also used for hydrogen production and the production of chemicals for the carbon dioxide capture [3].

8.3   CHEMICALS PRODUCTION USING MRC

The group of Logan has recently stressed the fact that MRC can be effectively used for the production of hydrogen and other chemicals. As an example, it was shown

that the MRC can be successfully operated to produce hydrogen gas from organics using water solutions of NaCl (representative of seawater and river water) [4] or ammonium bicarbonate salts [5,6] that can be regenerated using conventional distillation technologies and waste heat (Figure 8.6), making the MRC a potential method for hydrogen gas production from wastes.
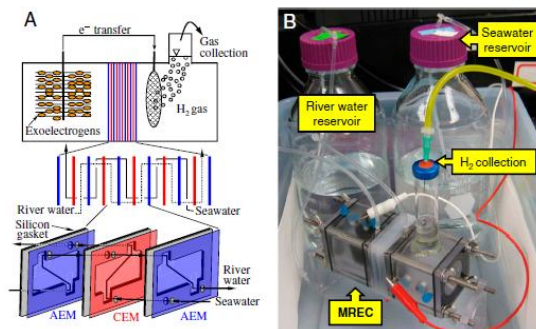
Figure 8.6 (A) Schematic design of MREC for H_2 production by integrating exoelectrogens with five-cell paired RED stack. (B) Photo of real system MREC operating in continuous flow and H_2 collection.

In Figure 8.6, is proposed a scheme that shows a unique method of H_2 production based on integrating a very small (five membrane pairs) RED stack into a microbial electrolysis cell, where anodic oxidation of organic matter is driven by exoelectrogenic microorganisms adding a voltage (> 0.11 V using acetate) that is theoretically much less than that needed to split water (> 1.2 V). Neither of these systems, taken individually, can achieve hydrogen gas generation; indeed the MEC requires an energy input (added voltage as mentioned before); and a small RED stack by itself cannot produce current. In integrated system, microbial reverse electrodialysis electrolysis cell (MREC), H_2 production is achieved by two driving forces: a thermodynamically favorable oxidation of organic matter by exoelectrogens on the anode that reducing the electrode overpotential; and the energy derived from the salinity gradient between seawater and river water.

The production of hydrogen is influenced both from the flow rate than from the typology of cathode materials [7]. In the first case, a slight increase by the flow rate of the solutions in the reactor RED causes a gain in H_2 production that is greater

when going from 0.1 to 0.4 mL/min becoming not very significant going to 0.4 to 0.8 mL/min. In the second case, the typology of cathode material changes the amount of H_2 produced. When a stainless steel current collector was used the rate of gas production was a slightly larger than when a more expensive carbon cloth (CC) cathode was installed in the system. In the following Figure (8.7) the main data about the effects of solution flow (0.1, 0.4, and 0.8 mL/min) and current collector on gas production and current generation are summarized.
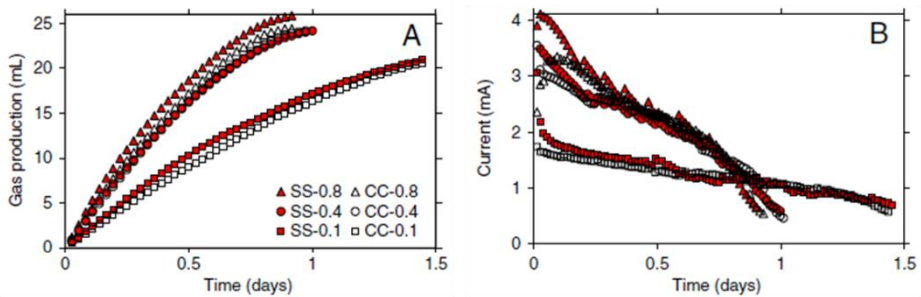
Figure 8.7 Plots the effect of flow rate and cathode materials on the H_2 production in the graphic A and the effects of the same on the current generation in Figure B.

The maximum production of hydrogen (80%) is achieved working with a flow rate of 0.4 and 0.8 mL/min when the production of current was between 2 and 4 mA, namely when the potential contribution by the RED stack was $0.5 - 0.6$ V for all three applied flow.

The use of seawater during this process can cause the biofouling of the membranes (unless when water is treated as it is in reverse osmosis desalination systems) and the necessity to have a continuous resource of seawater near the plant. In order to limit these disadvantages, the utilization of recycled sources of clean salt solutions was proposed, such as ammonium bicarbonate, magnesium sulfate, sodium sulfate, sodium chloride, potassium sulfate, potassium nitrate and potassium chloride. Among these salts, the best values of current and hydrogen gas generation were obtained using only the ammonium bicarbonate solution and no external power supply in a MREC.
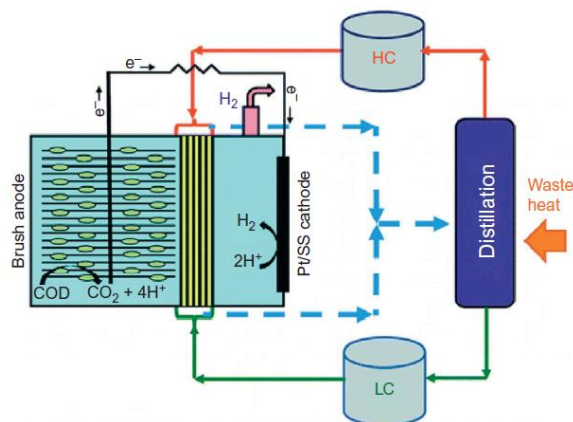
Figure 8.8 Schematic diagram of microbial reverse electrodialysis electrolysis cell in a closed loop configuration for hydrogen generation using a heat-regenerated salt solution.

In Table 8.2 is possible to see the main results collected using a MREC with different salinity ratios of HC and LC solutions. Unlike what written before about the effect of the SR on the use of MRC for generation of electric energy depending on kind of salt (NaCl or NH_4HCO_3) which was used, the current density generated with a MREC is relatively insensitive to the salinity ratios.

SR	HC (M)	anode potential (mV)	cathode potential (mV)	stack voltage (mV)	I_{vol} (A/m^3)
100	1.4	-427 ± 8	-734 ± 14	348 ± 15	143 ± 0
200	1.4	-460 ± 6	-736 ± 10	315 ± 3	152 ± 8
400	1.4	-468 ± 12	-740 ± 13	305 ± 10	137 ± 8
800	1.4	-474 ± 6	-738 ± 9	321 ± 21	146 ± 15
infinite	1.4	-466 ± 5	-740 ± 14	307 ± 3	148 ± 5
infinite	0.9	-487 ± 6	-753 ± 2	282 ± 6	119 ± 5
infinite	0.6	-491 ± 12	-751 ± 1	269 ± 20	95 ± 3
infinite	0.4	-494 ± 13	-748 ± 1	259 ± 17	83 ± 7
infinite	0.1	-528 ± 6	-752 ± 1	210 ± 5	43 ± 2

Table 8.2 Electrode Potential (vs Ag/AgCl), Stack Voltage, Volumetric Current Density at Different Salinity Ratios and NH_4HCO_3 Concentration of the HC Solution collected using a MREC.

If on one hand, optimum salinity gradients for MRCs were SR =50 with NaCl and SR = 100 with NH_4HCO_3, on the other hand MREC appeared indifferent to the SR but once removed the salinity gradient in the stack (SR = 1, 1.4 M NH_4HCO_3), a loss

214

of current was obtained, confirming that salinity gradient energy from the RED stack was essential for hydrogen production. As in all experiment in which there is a RED reactor, the effect of the number of ion exchange membranes on the production of H_2 was investigated. Several authors [8,9] confirmed that an increase of cell pairs should improve the potential difference across the membrane but [10] causes an increase of the internal resistance through the addition of extra HC and LC chambers. As reported in Figure 8.9, increasing the number of membrane pairs improved the current (Figure 8.9A) and the hydrogen production (8.9B).
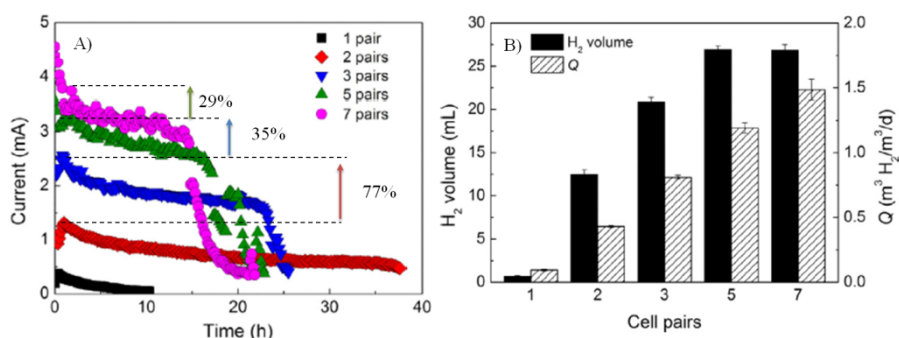
Figure 8.9 Current generation (A) and hydrogen volume and maximum volumetric hydrogen production rate (Q) of MREC (B) using different number of cell pairs (from 1 to 7 CP). In Figure A 29, 35 and 70% are referred on peak current increase changing the number of cell pairs.

A larger hydrogen gas volume was obtained going from 1 cell pair (0.7 mL) to 7 cell pairs (27 mL) and a linear increase of the maximum volumetric hydrogen production rate was recorded by adding more membrane pairs (Figure 8.9B). This good effect is limited by the increase of the RED stack resistance on the total internal resistance of MREC. Varying the number of cell pairs did not appreciably affect anode and cathode performance but on the basis of variation of internal resistance the optimum number of cell pairs was considered to be five [11].

Another example of the production of chemicals by MRC cells was proposed by Zhu et al. (2013) [3]. The authors developed a bioelectrochemical system, called a MRC chemical-production cell (MRCC), to produce acid and alkali using energy derived from organic matter (acetate) and salinity gradients. A bipolar membrane

(BPM) was situated next to the anode in order to prevent Cl⁻ contamination and acidification of the anolyte due to the use of NaCl as salt in HC and LC water solutions, and to produce protons for HCl recovery (Figure 8.10).
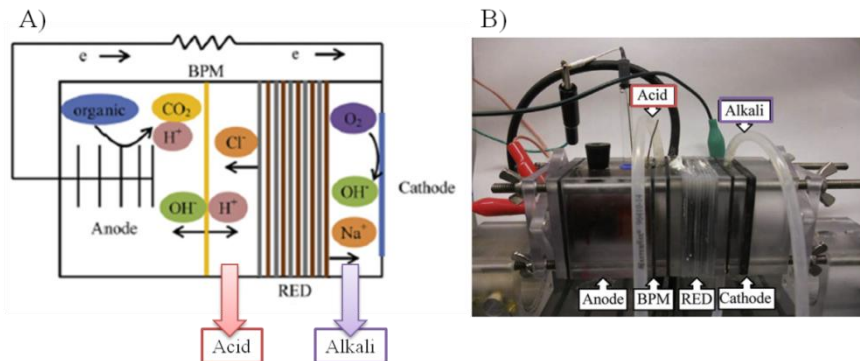
Figure 8.10 The schematic design (A) and a photo (B) of the MRCC system for acid and alkali production.

A 5-cell paired RED stack provided the electrical energy required to overcome the BPM overpotential. As shown in Figure 8.10, acid was produced in the chamber between BPM and AEM while alkali production occurring in the chamber between the CEM of the desalination chamber and the cathode. The MRCC reactor produced an amount of electricity (908 mW/m^2) that is sufficient to obtain concentrated acidic (efficiency $58 \pm 3\%$) and alkaline solutions (efficiency $25 \pm 3\%$) without external power supply.

With a slightly different approach, the production of acidic and alkaline solutions was coupled with that of hydrogen [12]. A modification of this apparatus (Figure 8.11), microbial reverse-electrodialysis electrolysis and chemical-production cell (MRECC), allows to produce H_2 gas using only renewable energy sources (organic matter and salinity gradient) and acid and alkali solutions that accelerate the natural mineral carbonation using to enhance atmospheric CO_2 sequestration (using serpentine).
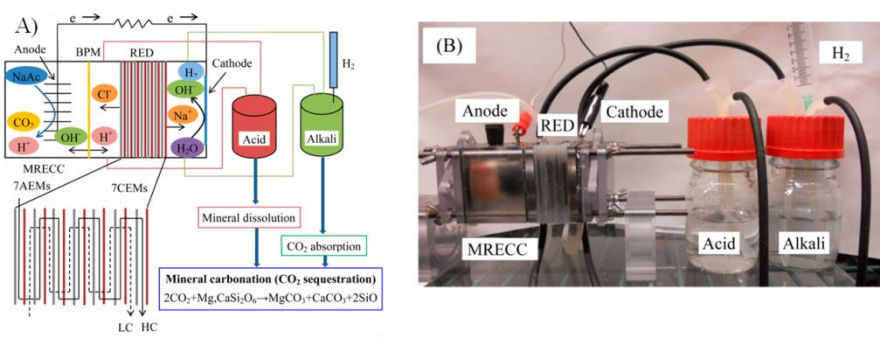
Figure 8.11 Schematic design (A) and photograph (B) of the MRECC system.

An elegant way of using organics to produce methane was also proposed in 2014 by Luo et al [13]. They proposed a microbial reverse electrodialysis methanogenesis cell (MRMC) by placing a RED stack between an anode with exoelectrogenic microorganisms and a methanogenic biocathode that allowed the conversion of carbon dioxide in methane without energy supply (Figure 8.12).
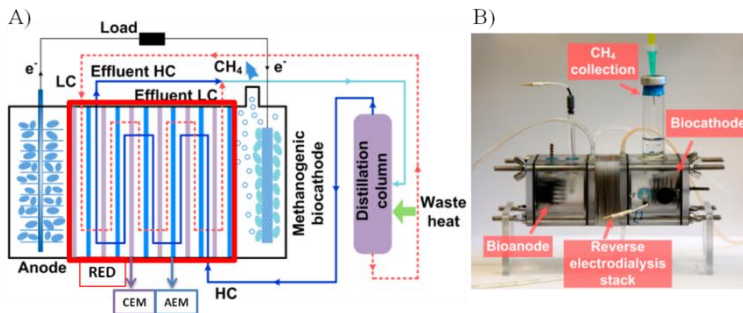
Figure 8.12 Schematic diagram (A) and photo (B) of a microbial reverse electrodialysis methanogenesis cell.

Of course, this production is influenced by different factor including the typology of cathode materials, the presence of biotic anode and the effect of ammonium bicarbonate used as salt in RED stack water solutions. Figure 8.13 reports the current production as a function of different kinds of cathode materials. The higher amount of energy used to produce the largest volume of methane was obtained using stainless steel (SS) mesh coated with Pt (SS / Pt cathodes).
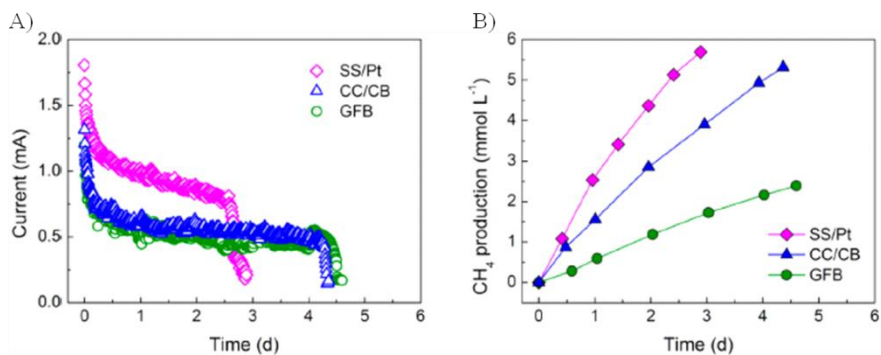
Figure 8.13 Effect of the different types of cathodes on (a) current and (b) methane gas production (per catholyte volume) over time for a representative cycle.

However, considering both performance and cost of materials, the CC / CB cathode was selected as the most useful cathode for the MRMC due to a lack of a precious metal, and considering its better performance than the GFB for methane production. In addition, the use of the thermolytic NH_4HCO_3 solutions could enable energy capture from renewable low-grade waste heat.

8.4   FUTURE PERSPECTIVES

As mentioned above, MRC process could allow synergistic use of biotic anodes and RED processes to obtain electric energy generation, the production of chemicals, and the treatment of wastewater. As also mentioned above, this integrated system could outperform the individual processes [1,2]. Thus, the low potential produced by a MRC can be increased by salinity driven potential, while exoelectrogenic bacteria on the anode, producing spontaneous reactions at the anode, would contribute additional potential to the RED stack, compared with energy losses at conventional abiotic cathode. Furthermore, the utilization of a MRC could allow the development of very small stacks, equipped with few membrane pairs, for the production of chemicals or the treatment of wastewater contaminated by pollutants resistant to conventional biological processes, with reduced investment costs. On the other hand, the coupling of MFC and RED process is not easy and it could cause

complications to the process on an applicative scale. Hence, further studies are necessary to evaluate the feasibility of the method for real applications.

In the frame of this thesis, for the first time a microbial reverse electrodialysis cell (MRC) was proposed to treat wastewater contaminated by recalcitrant pollutant and it was used for the treatment of water contaminated by Cr(VI).

8.5   REFERENCES

[1] Y. Kim, B.E. Logan, Microbial reverse electrodialysis cells for synergistically enhanced power production. Environ. Sci. Technol. 45 (2011) 5834–5839.

[2] R.D. Cusick, Y. Kim, B.E. Logan, Energy capture from thermolytic solutions in microbial reverse electrodialysis cells. Science 335 (2012) 1474–1477.

[3] X. Zhu, M.C. Hatzell, R.D. Cusick, B.E. Logan, Microbial reverse-electrodialysis chemical-production cell for acid and alkali production. Electrochem. Commun. 31 (2013) 52–55.

[4] Y. Kim, B.E. Logan, Hydrogen production from inexhaustible supplies of fresh and salt water using microbial reverse-electrodialysis electrolysis cells. Proc. Acad. Nat. Sci. 108 (2011) 16176.

[5] J.Y. Nam, R.D. Cusick, Y. Kim, B.E. Logan, Hydrogen generation in microbial reverse-electrodialysis electrolysis cells using a heat-regenerated salt solution. Environ. Sci. Technol. 46 (2012) 5240–5246.

[6] B.E. Logan, K. Rabaey, Conversion of wastes into bioelectricity and chemicals by using microbial electrochemical technologies. Science 337 (2012) 686–690.

[7] F. Zhang, S. Cheng, D. Pant, G.V. Bogaert, B.E. Logan, Power generation using an activated carbon and metal mesh cathode in a microbial fuel cell. Electrochem. Commun, 11 (2009) 2177–2179.

[8] P. Długołecki, A. Gambier, K. Nijmeijer, M. Wessling, Practical potential of reverse electrodialysis as process for sustainable energy generation. Environ. Sci. Technol. 43 (2009) 6888–6894

[9] J.W. Post, H.V.M. Hamelers, C.J.N. Buisman, Energy recovery from controlled mixing salt and fresh water with a reverse electrodialysis system. Environ. Sci. Technol. 42 (2008) 5785–5790.

[10] J. Veerman, J.W. Post, M. Saakes, S.J. Metz, G.J. Harmsen, Reducing power losses caused by ionic shortcut currents in reverse electrodialysis stacks by avalidated model. J. Membr. Sci. 310 (2008) 418–430.

[11] X. Luo et al. Optimization of membrane stack configuration for efficient hydrogen production in microbial reverse-electrodialysis electrolysis cells coupled with thermolytic solutions, Bioresource Technology 140 (2013) 399–405.

[12] X. Zhu et al, Microbial Reverse-Electrodialysis Electrolysis and Chemical- Production Cell for H2 Production and CO2 Sequestration, Environ. Sci. Technol. Lett. 1 (2014) 231−235.

[13] X. Luo, F. Zhang, J. Liu, X. Zhang, X. Huang, B.E. Logan, Methane production in microbial reverse-electrodialysis methanogenesis cells (MRMCs) using thermolytic solutions. Environ. Sci. Technol. 48 (15) (2014), 8911-8918.

9.   EXPERIMENTAL SET-UP

In this part of my thesis, I examined the utilization of a MRC for the cathodic reduction of Cr(VI) to Cr(III) with the aim to achieve a fast abatement of the pollutant coupled with the utilization of a small number of membrane pairs.

9.1   EXPERIMENTAL APPARATUS

9.1.1 Microbial reverse electrodialysis stack

MRC experiments were performed in a custom made stack equipped with two polymethylmethacrylate plates in which there are the electrodic chambers (10 cm x 10 cm x 2 mm). Carbon felt cathode and anode (Carbone Lorraine) with a geometric area 100 cm^2 were used. Between the anode and cathode compartments the following componets are placed: n (3, 5 and 7) cation and n + 1 anion-exchange membranes (Fuji), gasket integrated with spacers (Deukum, 0.28 mm thickness) and two external cationic membranes (Nafion) to separate electrode compartments and side ones, creating n pairs of alternating high concentrated (HC) and low concentrated (LC) cells (Figure 9.1).
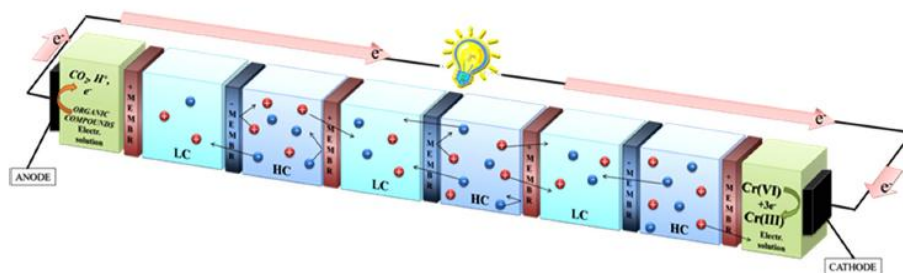
Figure 9.1 Scheme of adopted MRC stack equipped with n cell pairs. ''- membrane'' indicates an anion-exchange membrane, ''+ membrane'' a cation-exchange membrane and HC and LC the high concentrated and low concentrated saline solutions, respectively.

In the system, the LC solution entered from the cell next to the anode chamber and flowed in parallel through the LC cells in the stack, exiting from the cell next to the cathode chamber. The HC stream entered in the RED stack near the cathode and

flowed in parallel through the HC cells in the stack, exiting from the cell next to the anode chamber.

Two closed-loop hydraulic circuits were used for electrode solutions (Figure 9.2) that were continuously recirculated by two peristaltic pumps to the electrode compartments in two different reservoirs (one of these, anodic compartment, is maintained at 30 °C for the bacteria acclimation).
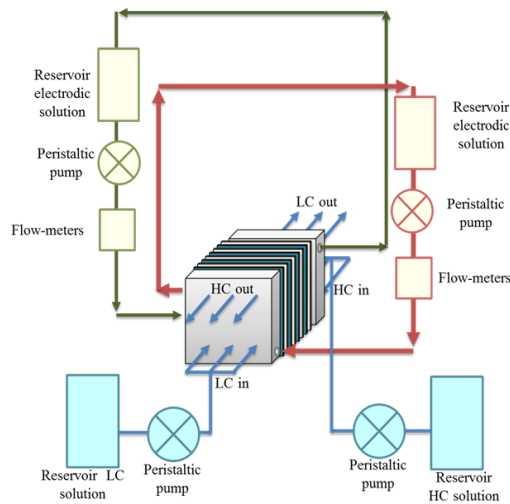
Figure 9.2 Simple diagram of MRC system assembled with two distinct hydraulic circuit.

Anode and cathode are connected by an external circuit equipped with a resistance, an amperometer and a voltmeter (overall electrical resistance about 4.6 Ohm). In Figure 9.3 it is possible see a simple scheme of electric circuit containing a load (resistor), an amperometer and a voltmeter.
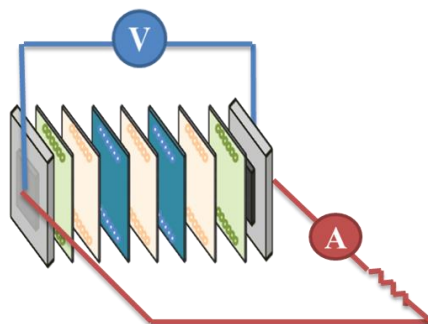
Figure 9.3 Scheme of electric circuit connected to the stack.

9.1.2 Single chamber microbial fuel cell

Before the MRC experiments, the carbon felt (anode) was pre-acclimated in an undivided electrochemical cell equipped with compact graphite (Carbon Lorraine) cathode and SCE reference with a working potential of -0.2 V (by a Amel 2055 potentiostat) for at least 12 hours with an organic solution consisting of 1/4 of bacteria grown and 3/4 of LB broth (Figure 9.4).

Figure 9.4 Undivided cell maintained under magnetic stirrer and on constant temperature of 30°C to pre-acclimate the anode and to form the bio-anode with a film of Shewanella putrefaciens.

Once the current density has reached a plateau value, the acclimated anode was transferred to the MRC. Before the pre-acclimatation, the bacteria strain was grown aerobically in a 50 mL flask in LB broth (Difco Laboratories, Detroit, MI). This

culture was incubated at 30 °C for 24 hours with shaking at 100 rpm [1]. When cell counts about 1 x10^8 cells/mL as determined by plating after serial dilution the inoculum is ready to be used.

9.2   MATERIALS

Solutions used in HC and LC compartments (of MRC) were prepared by dissolving NaCl (Sigma-Aldrich) into deionized water with a concentration of 5, 0.5 and 0.01 M, respectively, corresponding to that expected for salt pond, seawater and freshwater.

During the experiments the cathode solution contained an aqueous solution of 0.1 M Na_2SO_4 (Sigma-Aldrich) and 25 mg/L Cr(VI) (in the form of Sigma-Aldrich) at a pH of 2 obtained by addition of sulfuric acid (Sigma Aldrich). The anode solution contained a Luria–Bertani (LB) broth (the preparation is reported in the Chapter 6).

9.3   MICROORGNISMS

Shewanella putrefaciens were chosen as type of bacteria for this experimental campaign.

The treatment of these bacteria has been described previously in Chapter 6.

9.4   ANALYSIS EQUIPMENTS

In MRC experiments power production was studied by measuring both the potential drop across a fixed external resistance (range 4.6 Ω) and the current intensity by a multimeter Simpson. The overall external resistance was given by the contribution of an external resistance (range 1 – 160 Ω, selected value 1 Ω) and that of cables and an amperometer (with an estimated resistance of about 3.6 Ω).

The pH measurements were carried out with a HI 8314 membrane pH-meter, calibrated with three buffers of pH 4, 7 and 10 purchased from Hanna for the anodic oxidation experiments.

The reduction of Cr(VI) in the cathodic compartment was monitored from the decay of the absorbance (A) at $\lambda = 540$ nm wavelength by using Agilent Cary 60 UV Spectrophotometer, after treatment with 1,4-diphenylcarbazide and its concentration was determined after proper calibration.

9.5   ELECTROCHEMICAL PARAMETERS

Power was calculated by multiplying the electrical current and the total cell potential. Reported power densities were based on the cathode geometric area (100 cm^2). Power production during batch recycle experiments was measured in the same way across a fixed external resistance (about 4.6 Ω). Power density can be computed by the ratio between the power and the total area of all membranes or the total area of cationic membranes (Pmem) or the geometric area of cathode (P). The polarization curves from the MRC were obtained by varying the resistance in the circuit and measuring both voltage and current.

9.6   REFERENCES

[1] J.C. Biffinger, J. Pietron, R. Ray, B. Little, B.R. Ringeisen, A biofilm enhanced miniature microbial fuel cell using Shewanella oneidensis DSP10 and oxygen reduction cathodes, Biosens. Bioelectron. 22 (2007) 1672–1679.

10.   RESULTS AND DISCUSSION

10.1   INTRODUCTION

As often repeated, in the course of this thesis reverse electrodialysis (RED) is an innovative method to convert salinity gradient into useful power, based on the use of many pairs of anion and cation exchange membranes situated between two electrodes [1-7,10]. To reduce the potential penalty given by electrode processes a proper selection of redox species and of electrode materials is necessary in order to develop the RED process on an applicative scale [4]. Depending on the use of RED technology several pairs of membranes must be assembled to overcome the obstacle created by the electrode potentials resulting in significant costs for RED systems. This problem occurs also when the RED processes are used for the generation of current and simultaneous treatment of pollutants. In the last few years, another technology was proposed in order to treat contaminated water and obtain power output. This technology was widely investigated and its main characteristic is the capacity to generate electricity from biomass using exoelectrogenic microorganisms able to degrade (oxidize) organic matter, releasing electrons to the anode that are transferred through the external electric circuit and the cathode, to a terminal electron acceptor, which accepts the electrons and becomes reduced. Major limitations of this technique are the low power density extractable from it and the very long action time. In order to increase MFC voltages and power densities [11] and to reduce the number of membrane pairs necessary for the cathodic abatement of Cr(VI), for the first time it is proposed in this thesis the possible combination of a MFC with a RED stack into a single process, MRC, as a new approach for energy production with the aim to achieve a fast abatement of an inorganic pollutant (Figure 10.1).
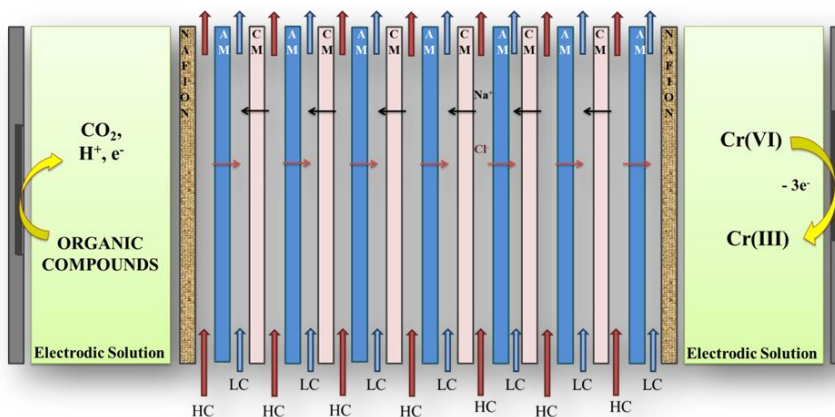
Figure 10.1 Scheme of adopted MRC stack equipped with a series of anionic and cationic exchange membrane fed between these, high concentrated and low concentrated solution (HC and LC, respectively).

10.2   COMPARISON BETWEEN RED AND MRC BENEFITS

Before performing experiments with MRC, some experiments were performed with a RED stack equipped with 5 membrane pairs both in the absence and in the presence of Cr(VI) (25 mg/L) in the cathode compartment to better understand the improvements recorded using the new technique. The anodic compartment was fed with an aqueous solution of sodium sulfate so that the anodic process was the oxygen evolution. The oxygen reduction can take place in the cathode (as competitive cathode reaction) because this compartment was exposed to the air. In order to obtain higher current densities capable to removal the pollutant anode and cathode were connected with a external resistor of 4.6 Ohm. A reported in Figure 10.2, in the absence of Cr(VI) the process gave very low current (A) and power densities (B) as a result of the low number of cell pairs and of the high potentials required by both anode and cathode redox processes, the reduction and the oxidation of water. Indeed, under adopted working condition, water reactions required 3.0 V because of the energetic losses due to overpotential at the electrodes versus a value asked of 1.21 V under standard condition of neutral pH.
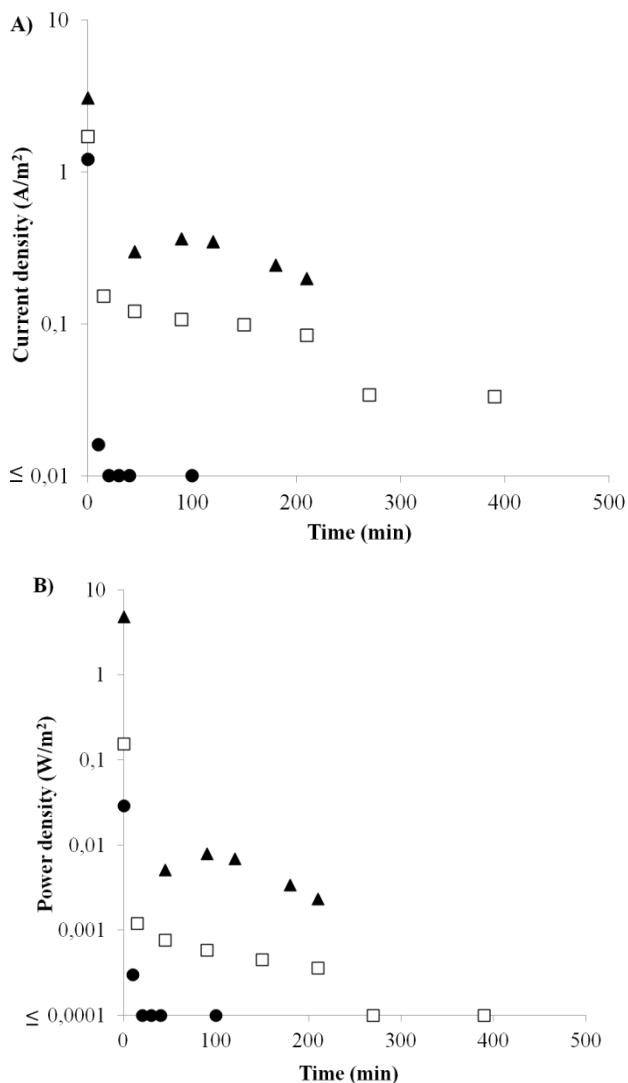
Figure 10.2 Current (A) and power (B) density vs. time achieved for experiments performed by RED (□) and MRC (▲) in the presence of 25 mg/L Cr(VI) in the cathode compartment and by RED in the absence of Cr(VI) (●). Stack was equipped with 5 membrane pairs.

When experiments were repeated with Cr(VI) in the cathode compartment, an increase of both current and power density (Figure 10.2) was observed as a result of the lower cathode potential required by the Cr(VI) reduction to Cr(III) compared with that of oxygen or water reduction. According to cyclic voltammetric analysis,

229

the cathode potential of the reduction of Cr(VI) should be about 0.5 V more positive with respect to that of the reduction of oxygen and about 1.4 V more positive with respect to that of the water discharge using carbon felt as electrode. The Figure reports also the data collected using a MRC. In this case, as exoelectrogenic microorganisms were chosen facultative Shewanella putrefaciens, because tolerant to air. For MRC experiments, the carbon felt was pre-acclimated in an undivided electrochemical cell equipped with compact graphite cathode and SCE reference working under potentiostatic condition of -0.2 V vs SCE (see Chapter 9). Once the current density has reached a plateau value, the acclimated anode was transferred to the MRC (Figure 10.3).
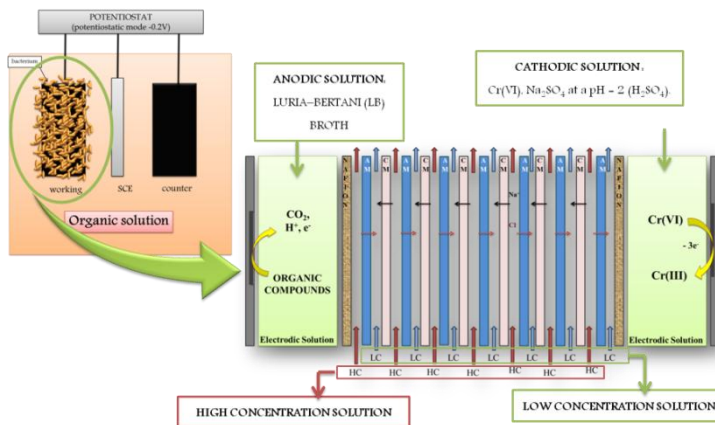
Figure 10.3 Scheme of steps of experimental campaign. Step 1: growth of biofilm on the anode surface; step 2: collocation of bio-anode in a RED stack to work as MRC.

The utilization of a biotic anode allowed to achieve a drastic increment of power and current densities favored by a new anodic process mediated by the microorganisms (Figures 10.2A and B). While in RED experiments the anode potential for water oxidation is expected to be higher than 1.5 V (as shown by focused cyclic voltammetry), for MRC a slightly negative potential (about -0.1 – 0 V) is expected for the organic oxidation mediated by *Sp* as shown by a preliminary experiment performed with a divided microbial fuel cell equipped with carbon felt, S. *putrefaciens* microorganisms and a LB broth. Regarding the removal of Cr(VI)

concentration from cathode compartment, as shown in Figure below (10.4), a significant but rather slow abatement of Cr(VI) was achieved by RED; in fact an abatement slightly lower than 70% was obtained after 400 min. The higher current density recorded in the MRC (Figure 10.2A) gave a faster removal of Cr(VI) achieving a total removal of Cr(VI) after 210 min.
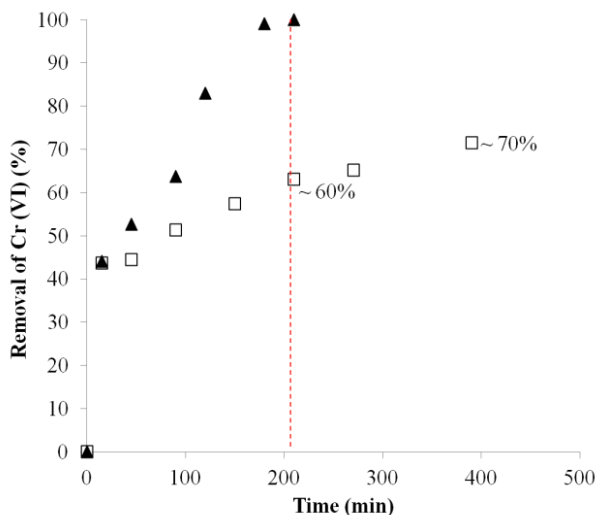
Figure 10.4 Abatement of Cr(VI) vs. time achieved for experiments performed by RED (□) and MRC (▲) in the presence of 25 mg/L Cr(VI) in the cathode compartment and by RED in the absence of Cr(VI) (●). Stack was equipped with 5 membrane pairs.

The average current and power density recorded for 210 minutes were 0.29 A/m^2 and 0.026 W/m^2 for RED and 0.66 A/m^2 and 0.69 W/m^2 for MRC. Quite interestingly for both RED and MRC a strong decrease of the power density occurred during the experiment because of the decrease of the concentration of Cr(VI) that leads to higher cathode potentials thus giving space to the reactions of oxidation and reduction of water.

10.3   EFFECT OF NUMBER OF MEMBRANE PAIRS

After having carried out experiments with 5 pairs of membrane in accordance with what reported in literature [12] it was decided to study the effect of the number of

membranes on the performance of a MRC in order to observe the limits approachable with this new technology. To evaluate the effect of the number of membrane pairs, the above mentioned experiments were repeated with 3 and 7 membrane pairs. When RED experiments were carried out in a stack equipped with three membrane pairs, the cell potential (Figure 10.5) had an initial value (0.095 V) more less than when the stack was assembled with 7 membrane pairs (0.18 V).
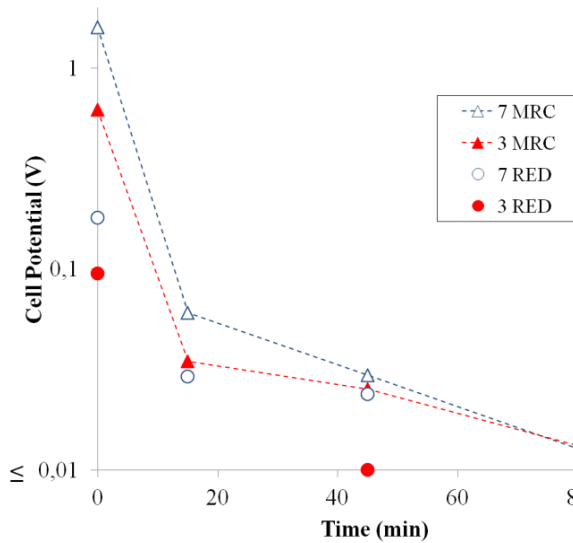
Figure 10.5 Effect of the number of membrane pairs on cell potential achieved by RED (3 (●) and 7 (○) membrane pairs) and MRC (3 (-▲-) and 7 (–Δ–) membrane pairs).

In the presence of 3 cell pairs, the current and the power density (Figure 10.6) of RED system dropped fast to very small values as a result of the too low number of membrane pairs but increasing the number of pairs at 7, a significantly higher initial current and power densities were obtained, as reported in Figure 10.6.
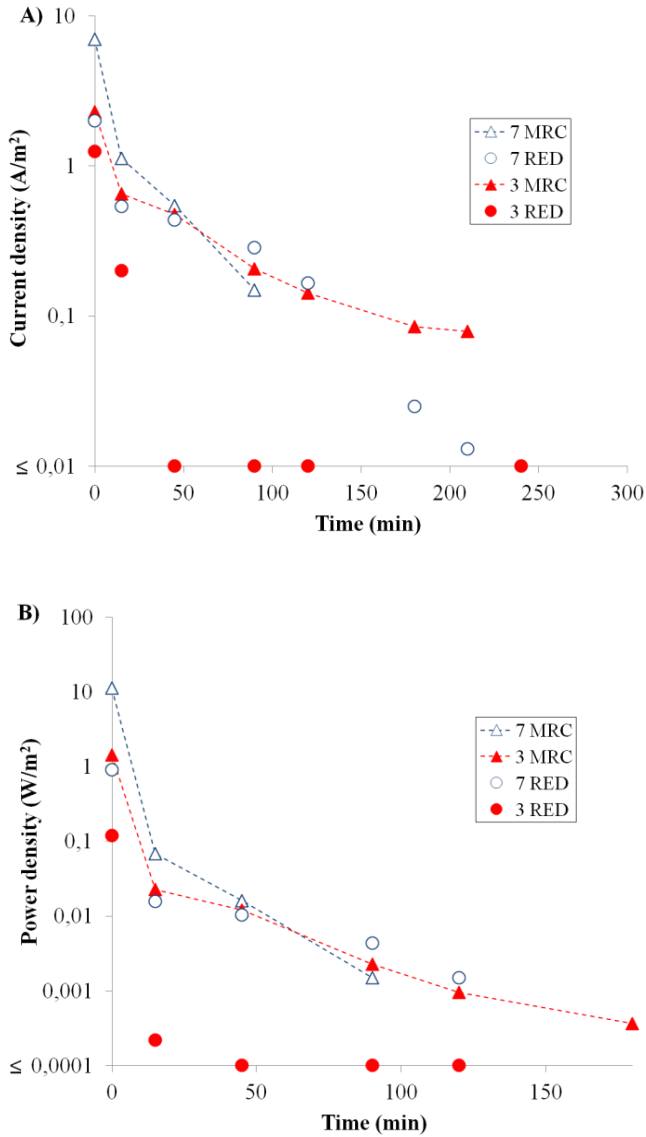
Figure 10.6 Effect of the number of membrane pairs on current density (A) and power density (B) (semi-log scale) achieved by RED (3 (●) and 7 (○) membrane pairs) and MRC (3 (-▲-) and 7 (–△–) membrane pairs).

Figures 10.5 and 10.6 report the data recorded using MRC with 3 and 7 membrane pairs. The adoption of a MRC allowed to achieve higher cell potential (Figure 10.5) and current density and as a consequence higher power density (Figure 10.6) with

respect to RED for both 3 and 7 membrane pairs. The large difference between the initial cell potential for RED and MRC is due to the different anode potentials involved. As reported in Figure 10.7, very poor abatements of Cr(VI), close to 15% after 240 min, were recorded when RED was assembled with 3 membrane pairs as a consequence of current density values extremely low. These values increased when the RED stack was assembled with 7 membrane pairs. Higher reductions of Cr(VI) were obtained at the same time of treatment using a MRC. It is interest to observe that the adoption of a MRC allowed to achieve the total removal of Cr(VI) also using only three membrane pairs (Figure 10.7). Very similar performances were obtained in terms of abatement of Cr(VI) as function of treatment time using a MRC with 3 membrane pairs and a RED with 7 ones (Figure 10.7), thus demonstrating that MRC can allow an effective treatment of Cr(VI) with a drastic lower number of membrane pairs with respect to RED indeed, after 210 min, an abatement of Cr(VI) close to 100% was achieved using a MRC with 3 membrane pairs and a RED with 7 ones.
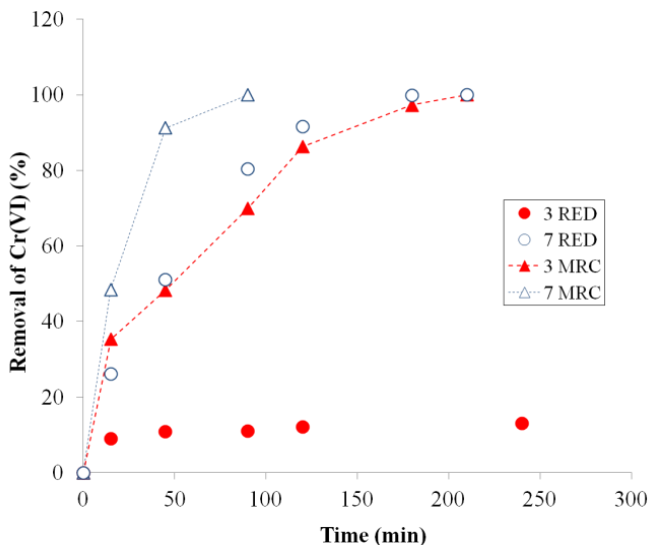
Figure 10.7 Comparison between the effect of the number of membrane pairs on reduction of Cr(VI) achieved by RED (3 ($\bullet$) and 7 ($\circ$) membrane pairs) and MRC (3 (-$\blacktriangle$-) and 7 ($-\triangle-$) membrane pairs) systems.

234

Also for MRC, an increased number of membrane pairs gave higher current and power density (Figures 10.2 and 10.6) and, consequently, a faster abatement of Cr(VI). In particular, with 7 membrane pairs, about 90 min were needed to obtain an almost total abatement of Cr(VI) while with 3 and 5 membrane pairs about 210 and 180 min were necessary, respectively.

10.4   EFFECT OF SALINITY GRADIENT

Eventually, the effect of salinity gradient on MRC used for abatement aim was studied. Experiments were carried out with a stack equipped with 7 cell pairs, an initial concentration of Cr(VI) of 25 mg/L, feeding as HC a water solution of 5M of NaCl and LC a water solution with 0.5 and 0.01 M of NaCl, that is SR = 50 and 500 respectively. As shown in Nernst equation, the cell potential increases with the ratio between the concentration of NaCl in concentrated and diluted compartments. As a consequence, an higher salinity ratio (SR) resulted in higher current densities and in faster abatements of Cr(VI). A cell potential ΔV of about 1.6 V was recorded for a salinity ratio SR = 500 as expected for brine (5 M) and fresh waters (0.01 M) (see Figure 10.8). When SR was 10 as expected for brine (5 M) and seawater (0.5 M), the initial cell potential was about 1.2 V. These value was compared with those obtained feeding in the stack the same solution in saline compartments (HC = LC = 5 M). In this case, when SR was 1, a cell potential close to 0.5 V was measured as expected on the basis of the literature on MFC [13].
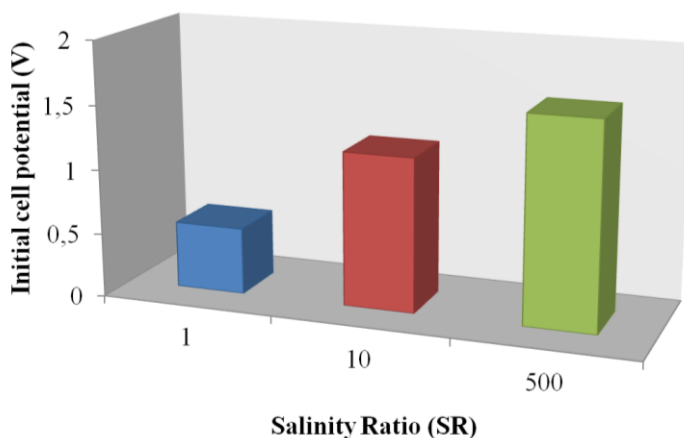
Figure 10.8 Effect of the SR on initial cell potential achieved by MRC. Stack equipped with 7 cell pairs and various SR: 1 (NaCl 5 M in HC and LC), 10 (NaCl 5 M in HC and 0.5 M in LC), 50 (NaCl 0.5 M in HC and 0.01 M in LC) and 500 (NaCl 5 M in HC and 0.01 M in LC).

As a result of the higher cell potentials, increased values of SR resulted in higher current densities (Figure 10.9A), power densities (Figure 10.9B) and faster removal of Cr(VI) (Figure 10.10). Worth mentioning, when the MRC experiments were performed by feeding to the HC and LC compartments two aqueous solutions with the same salt concentration (brine), very low current density (<0.1 A/m^2 after 10 min), power density (< 0.001 W/m^2) and abatements of Cr(VI) (18% after 240 min) were achieved. This is acceptable if we think that the systems worked as a MFC (without a salt concentration gradient). Conversely, in the presence of a salinity gradient, a drastic enhancement of both current density and of Cr(VI) removal was achieved (about 100% after 240 and 90 min for a SR of 10 and 500, respectively), thus showing the relevance of the synergistic effect between salinity gradients and microbial oxidation of organics achieved in the MRC for the removal of Cr(VI).
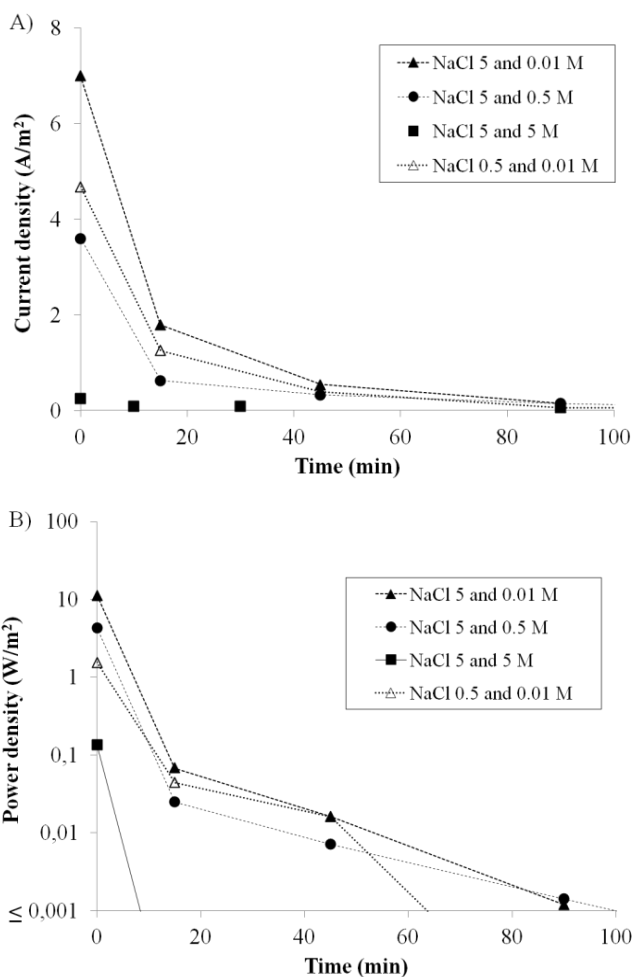
Figure 10.9 Effect of the SR on current density (A) and power density (B, in semi-log scale) achieved by MRC. Stack equipped with 7 cell pairs and various SR: 1 (NaCl 5 M in HC and LC), 10 (NaCl 5 M in HC and 0.5 M in LC), 50 (NaCl 0.5 M in HC and 0.01 M in LC) and 500 (NaCl 5 M in HC and 0.01 M in LC).

Figure 10.10 shows also the results recorded for some MRC experiments repeated using a concentration of NaCl in HC and LC of 0.5 and 0.01 M, respectively, thus giving rise to a SR of 50. As shown in Figures 10.9 and 10.10, the current density and consequently the removal of Cr(VI) assumed intermediates values between that obtained with SR of 500 and 10. In particular, after 45 min the removal of Cr(VI) was of about 10, 61, 77 and 91% for SR of 1, 10, 50 and 500, respectively.
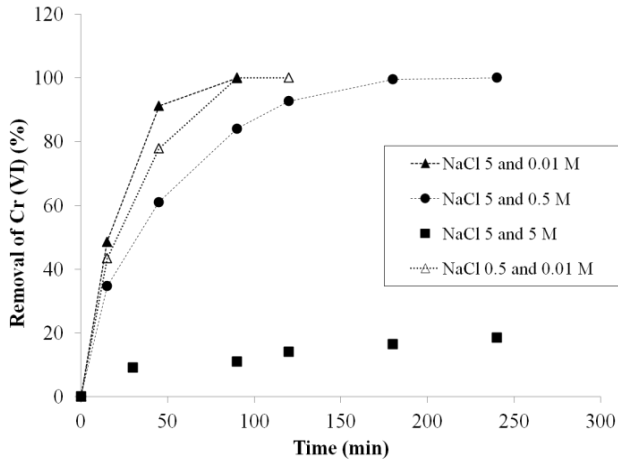
Figure 10.10 Effect of the SR on the reduction of inorganic pollutant, from cathode compartment, achieved by MRC. Stack equipped with 7 cell pairs and various SR: 1 (NaCl 5 M in HC and LC), 10 (NaCl 5 M in HC and 0.5 M in LC), 50 (NaCl 0.5 M in HC and 0.01 M in LC) and 500 (NaCl 5 M in HC and 0.01 M in LC).

In order to evaluate the performance of MRC system for a longer time (Figure 10.11), several addition of Cr(VI) 25 mg/L were carried out. The reduction of Cr(VI) resulted in a significant decrease of the power density but the periodic addition of pollutant gave rise to an enhancement of power density.
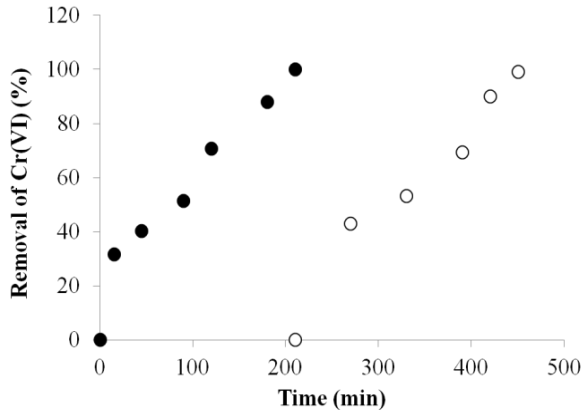
Figure 10.11 Reports the effect of periodic addition of Cr(VI) 25 mg/L in the cathode compartment of a MRC equipped with 5 cell pairs.

10.5   REFERENCES

[1] R.E. Pattle, Production of electric power by mixing fresh and salt water in the hydroelectric pile, Nature 174 (1954) 660.

[2] J.W. Post, H.V.M. Hamelers, C.J.N. Buisman, Energy recovery from controlled mixing salt and fresh water with a reverse electrodialysis system, Environ. Sci. Technol. 42 (2008) 5785–5790.

[3] E. Brauns, Towards a worldwide sustainable and simultaneous large-scale production of renewable energy and potable water through salinity gradient power by combining reversed electrodialysis and solar power?, Desalination 219 (2008) 312–323.

[4] J. Veerman, M. Saakes, S.J. Metz, G.J. Harmsen, Reverse electrodialysis: evaluation of suitable electrode systems, J. Appl. Electrochem. 40 (2010) 1461–1474.

[5] R.D. Cusick, Y. Kim, B.E. Logan, Energy capture from thermolytic solutions in microbial reverse-electrodialysis cells, Science 335 (2012) 1474–1477.

[6] J.R. McCutcheon, R.L. McGinis, M. Elimelech, A novel ammonia—carbon dioxide forward (direct) osmosis desalination process, Desalination 174 (2005) 1–11.

[7] J. Veerman, M. Saakes, S.J. Metz, G.J. Harmsen, Reverse electrodialysis: performance of a stack with 50 cells on the mixing of sea and river water, J.Memb. Sci. 327 (2009) 136–144.

[10] D.A. Vermaas, S. Bajracharya, B. Bastos Sales, M. Saakes, B. Hamelers, K. Nijmeijer, Clean energy generation using capacitive electrodes in reverse electrodialysis, Energy Environ. Sci. 6 (2013) 643–651.

[11] Y. Kim, B.E. Logan, Microbial reverse electrodialysis cells for synergistically enhanced power production. Environ. Sci. Technol. 45 (2011) 5834–5839.

[12] R.D. Cusick, Y. Kim, B.E. Logan, Energy capture from thermolytic solutions in microbial reverse electrodialysis cells. Science 335 (2012) 1474–1477.

[13] B.E. Logan, Microbial Fuel Cells, John Wiley & Sons Inc, Hoboken, NJ, 2008. [11] X. Luo et al. Optimization of membrane stack configuration for efficient hydrogen production in microbial reverse-electrodialysis electrolysis cells coupled with thermolytic solutions, Bioresource Technology 140 (2013) 399–405.

[12] X. Zhu et al, Microbial Reverse-Electrodialysis Electrolysis and Chemical- Production Cell for H2 Production and CO2 Sequestration, Environ. Sci. Technol. Lett. 1 (2014) 231−235.

[13] X. Luo, F. Zhang, J. Liu, X. Zhang, X. Huang, B.E. Logan, Methane production in microbial reverse-electrodialysis methanogenesis cells (MRMCs) using thermolytic solutions. Environ. Sci. Technol. 48 (15) (2014), 8911-8918.

Part IV:

CONCLUSIONS

11.   CONCLUSIONS

The first aim of this thesis has been an in-depth investigation of the reverse electrodialysis technology through the study of the state of the art and experimental activities, with the objective of improving the electrode compartments of the system by the selection and the optimization of materials and components tailored to the requirements of the technology to expand the fields of its application.

The possible utilization of three iron redox couples (namely, $FeCl_3/FeCl_2$, hexacyanoferrate(III)/hexacyanoferrate(II) and Fe(III)- EDTA/Fe(II)-EDTA) was assessed by electroanalytical investigations and electrolyses performed in one and three compartment cells. The system Fe(III)-EDTA/Fe(II)-EDTA was studied in a large range of operative conditions by changing current density (from 1.2 to 10 mA/cm^2), initial cumulative concentration of the redox couple (from 50 to 100 mM) and electrodes (compact graphite and BDD). Unfortunately, under all the adopted conditions the system was not stable enough after three days. In spite of the fact that the hexacyanoferrate(III)/hexacyanoferrate(II) couple is widely used for electrochemical characterizations, no data are available in literature regarding its stability under operative conditions of interest for RED applications. It was shown that this couple can be used for these applications in the absence of light and oxygen by working with high redox couple concentrations and low current densities both at compact graphite and DSA electrodes. The utilization of Nafion cationic outer membranes – confining the electrode system – allowed to confine the redox couple in the electrode compartments. Results are quite relevant to avoid a contamination of the discharged dilute and concentrated solutions by the hexacyanoferrate(III)/hexacyanoferrate(II) couple that can decompose under sunlight and oxygen with the formation of free cyanides. The system $FeCl_3/FeCl_2$ was shown to be stable at acidic pH for long times at compact graphite electrodes. The utilization of Selemion anionic outer membranes allowed to confine the redox couple in the electrode compartments and to obtain very slow passages of protons to the side compartment, thus avoiding basification post treatments of the discharged dilute and concentrated solutions flowing in the stack.

After this first experimental series, a detailed study was performed with a stack for reverse electrodialysis. In this thesis, it was shown that all tested redox processes:

- ✓ reduction/oxidation of $FeCl_3/FeCl_2$,
- ✓ reduction/oxidation of hexacyanoferrate(III)/hexacyanoferrate(II),
- ✓ oxidation and reduction of water,
- ✓ oxidation of chlorine and reduction of water

can be used for reverse electrodialysis applications with proper external membranes and electrodes. The nature of redox processes affects the external output and different proper external membranes have to be selected for each redox process to avoid the contamination of concentrated and dilute solution by the components of electrodic solution. Power density was shown to depend also on the concentration of redox species and on the number of cell pairs. It was also shown that the utilization of NaCl concentrations for concentrated (HC) and dilute (LC) compartments similar to that of salt pond and seawater solutions allowed to achieve a drastic increase of the power output with respect to that achieved feeding HC and LC compartments with NaCl concentrations similar to that of seawater and river water.

The possible utilization, in the frame of RED, of a redox process for the wastewater treatment, for example the cathodic reduction of Cr(VI) to Cr(III), was widely studied in order to evaluate the possible utilization of RED for the simultaneous generation of electric energy and the treatment of wastewater resistant to conventional biological processes, thus enhancing the perspectives of both processes. To test the possible utilization of RED for the simultaneous abatement of an organic recalcitrant pollutant and the generation of electric energy, the decoloration of a water solution contaminated by Acid Orange 7 (AO7), was investigated.

As regards the reduction of Cr (VI), a very toxic compound, it has been shown for the first time that the simultaneous generation of electric energy and the treatment of water contaminated by recalcitrant pollutants can be successfully achieved by

reverse electrodialysis processes using salinity gradients and proper redox processes. The electrochemical removal of Cr(VI) was used as model process and it was successfully achieved by cathodic reduction at carbon electrodes with the simultaneous generation of electric current. Furthermore, the addition of Cr(VI) to the cathodic solution gave an enhancement of the power output given by the process. The performances of the process strongly depended on two different kinds of operative parameters. On one hand, parameters characteristic of the stack, such as the *number of membrane pairs*, the *salinity gradients* and the *flow rates* of the alimentations for concentrated and diluted compartments were studied. It was shown that the operative conditions that give higher current and power densities, such as higher numbers of membrane pairs, higher salinity gradient and flow rates, allow also to accelerate the rate of removal of Cr(VI). On the other side, parameters characteristic of the electrodic compartments such as *Cr(VI) and supporting electrolyte concentration* and the *flow rates* of electrode solutions were investigated. It was shown that the operative conditions that favor the Cr(VI) reduction, such as higher Cr(VI) concentration, allow also to reduce the cathodic potential and consequently to achieve higher power densities.

Regarding organic pollution abatement, it has been shown that the simultaneous generation of electric energy and the treatment of water contaminated by Acid Orange 7 can be achieved by reverse electrodialysis processes using salinity gradients and proper redox processes. Both the utilization of electro-Fenton at the cathode and the oxidation by electrogenerated active chlorine at the anode were successfully used. The use of salinity gradients in RED stacks could change the scenario for the treatment of organic recalcitrant pollutants in water. Thus, RED can be efficiently used for both the generation of electric energy and the abatement of recalcitrant pollutants by using widely available salinity gradients obtained from seawater and freshwater, high salinity waters from salt pond or desalination plants and seawater or freshwater or by waste heat or solar energy. This could allow to treat in an economic and very efficient way wastewater contaminated by recalcitrant

pollutants avoiding the cost, the transport and the storage of currently adopted oxidants.

At the end of this first experimental part, it was very interesting to perform an intense experimental campaign on the REAPower demonstration plant (Marsala, Italy). The utilization of the pilot plant has allowed us to observe on a more relevant scale the performances of the reverse electrodialysis technology not only for the generation of electric current but also for the simultaneous treatment of contaminated waters, increasing the economic interest for RED processes on an applicative scale.

The second main objective of the thesis was to investigate Microbial Fuel Cell (MFC) technology with the aim of generating electricity from biomass using bacteria. Part of the study was performed at the University of Castilla La Mancha in Spain where I have found that the retention time of the solid (SRT) drastically affect the performances of the process. The experiments carried out at the University of Palermo has provided an ample study on the utilization of microbial fuel cells for wastewater treatment for the removal of AO7 dye (by electro-Fenton) and Cr(VI) thus avoiding the necessity to supply energy to the system. It was shown that in the presence of Geobacter sulforeducens or Shewanella putrefaciens a good abatement of AO7 or Cr(VI) was achieved coupled with a small generation of current.

The possibility to combine a reverse electrodialysis processes with biotic anode by a Microbial Reverse Electrodialysis cell (MRC) is a new approach to increase the generation of electric energy by replacing the oxidation process of the water with the process of oxidation of organic compounds to CO_2 using microorganisms. For the first time in the frame of this thesis, it was proposed to use this technology for the abatement of pollutants such as Cr(VI) via its cathodic reduction to Cr(III) with the aim to achieve a fast abatement of the specie coupled with the generation of power. It was shown that in MRC the synergistic effect between salinity gradients and microbial oxidation of organics can allow a complete abatement of Cr(VI) with a drastic lower number of membrane pairs with respect to those required by reverse

electrodialysis processes and significant lower treatment times with respect to that obtained in the absence of salinity gradient using only microorganisms (such as in MFC). The obtained results offered an evidence of concept showing that MRC may result suitable for the treatment of wastewater contaminated by biodegradable organics in the anodic compartment and by pollutants resistant to conventional biological processes such as Cr(VI) in the cathodic one, thus disclosing new perspectives for the electrochemical treatment of wastewater.

The research activities presented in this thesis contribute to improve the state-of-the-art of MFC, RED and of MFC processes, demonstrating their huge potential.

PUBLICATIONS

1. CATHODIC ABATEMENT OF CR(VI) IN WATER BY MICROBIAL REVERSE-ELECTRODIALYSIS CELLS. Authors: <u>A. D'Angelo</u>, O. Scialdone, A. Galia. Journal of Electroanalytical Chemistry 748 (2015) 40–46.

2. ENERGY GENERATION AND ABATEMENT OF ACID ORANGE 7 IN REVERSE ELECTRODIALYSIS CELLS USING SALINITY GRADIENTS. Authors: O. Scialdone, <u>A. D'Angelo</u>, A. Galia. Journal Of Electroanalytical Chemistry 738 (2015) 61–68.

3. CATHODIC REDUCTION OF HEXAVALENT CHROMIUM COUPLED WITH ELECTRICITY GENERATION ACHIEVED BY REVERSE-ELECTRODIALYSIS PROCESSES USING SALINITY GRADIENTS. Authors: O. Scialdone, <u>A. D'Angelo</u>, E. De Lumè, A. Galia. Electrochimica Acta 137 (2014) 258–265.

4. ELECTROCHEMICAL PROCESSES AND APPARATUSES FOR THE ABATEMENT OF ACID ORANGE 7 IN WATER. Authors: O. Scialdone, <u>A. D'Angelo</u>, G. Pastorella, S. Sabatino, A. Galia. Chemical Engineering Transactions 41 (2014) 31-36.

5. UTILIZATION OF REVERSE ELECTRODIALYSIS PROCESSES FOR THE ABATEMENT OF POLLUTANTS IN WATER. Authors: O. Scialdone, <u>A. D'Angelo</u>, E De Lumè, A. Galia. Chemical Engineering Transactions 41 (2014) 139-144.

6. INVESTIGATION OF ELECTRODE MATERIAL – REDOX COUPLE SYSTEMS FOR REVERSE ELECTRODIALYSIS PROCESSES. PART II: EXPERIMENTS IN A STACK WITH 10–50 CELL PAIRS. Authors: O. Scialdone, A. Albanese<u>, A. D'Angelo</u>, A. Galia, C. Guarisco. Journal Of Electroanalytical Chemistry 704 (2013) 1-9.

7. INVESTIGATION OF ELECTRODE MATERIAL – REDOX COUPLE SYSTEMS FOR REVERSE ELECTRODIALYSIS PROCESSES. PART I: IRON REDOX COUPLES. Authors: O. Scialdone, C. Guarisco, S. Grispo, <u>A. D'Angelo</u>, A. Galia. Journal Of Electroanalytical Chemistry 681 (2012) 66–75.

BOOK

246

1. Chapter VIII. "Special applications of reverse electrodialysis". Authors: O. Scialdone, <u>A. D'Angelo</u>, A. Galia, Book: "Sustainable Energy from Salinity Gradients", published by Woodhead Publishing, imprint: Elsevier Science and Technology Books.

PAPERS IN PREPARATIONS

1. BEHAVIOUR OF A MICROBIAL FUEL CELL TO CHANGE IN THE SOLID RETENTION TIME. Authors: S. Mateo, <u>A. D'Angelo</u>, O. Scialdone, P. Cañizares, F.J. Fernandez, M. Rodrigo. In preparation.

2. STUDY OF THE INFLUENCE OF THE SLUDGE AGE ON THE PERFORMANCE OF MICROBIAL FUEL CELL. Authors: <u>A. D'Angelo</u>, S. Mateo, O. Scialdone, P. Cañizares, F.J. Fernandez, M. Rodrigo. In preparation.

COMMUNICATIONS

National

1. SETTEMBRE 2013. <u>A. D'Angelo</u>, A. Galia, R. Riccobono, E. De Lumè, O. Scialdone. "ABATEMENT OF RECALCITRANT POLLUTANTS IN AQUEOUS SOLUTION BY REVERSE ELECTRODIALYSIS PROCESSES" GEI2013 (Giornate dell'Elettrochimica Italiana).

2. SETTEMBRE 2012. A. Coletti, A. M. Valerio, <u>A. D'Angelo</u>, O. Scialdone, E. Vismara. "ELECTROCHEMICAL SYNTHESIS OF C-GLYCOSIDES AS NON-NATURAL MIMETICS OF BIOLOGICALLY ACTIVE OLIGOSACCHARIDES". XXXIV Convegno Nazionale Divisione Chimica Organica

3. GIUGNO 2012. O. Scialdone, <u>A. D'Angelo</u>, R. Riccobono, A. Galia. "TOWARDS THE SIMULTANEOUS GENERATION OF ELECTRIC ENERGY AND THE ABATEMENT OF ORGANIC POLLUTANTS BY REVERSE ELECTRODIALYSIS PROCESSES" GEI-ERA 2012

(Giornate dell'Elettrochimica italiana e Elettrochimica per il recupero ambientale).
ISBN 978-88-8080-134-4

4. GIUGNO 2012. O. Scialdone, A. D'Angelo, S. Grispo, C. Guarisco, A. Galia.
"SELECTION OF REDOX SYSTEMS FOR REVERSE ELECTRODIALYSIS PROCESSES" GEI-
ERA 2012 (Giornate dell'Elettrochimica italiana e Elettrochimica per il recupero
ambientale). ISBN 978-88-8080-134-4

5. GIUGNO 2012. O. Scialdone, S. Sabatino, C. Guarisco, R. Riccobono, A.
D'Angelo, A. Galia , A. Busacca , D. Agrò. "ELECTROCHEMICAL TREATMENT OF
WASTE WATERS CONTAMINATED BY ORGANIC POLLUTANTS: A LOOK ON SOME NEW
APPROACHES". GEI-ERA 2012 (Giornate dell'Elettrochimica Italiana ed
Elettrochimica per il recupero ambientale, Santa Marina Salina ME)

Interational

1. OTTOBRE 2015, Onofrio Scialdone, Adriana D'Angelo, Alessandro Galia, Simona
Sabatino, Fabrizio Vicari. "ABATEMENT OF POLLUTANTS IN WATER BY DIFFERENT
ELECTROCHEMICAL APPROACHES". THE 66RD ANNUAL MEETING OF THE
INTERNATIONAL SOCIETY OF ELECTROCHEMISTRY, TAIPEI, TAIWAN.

2. SETTEMBRE 2014. O. Scialdone, A. D'Angelo, S. Sabatino, A. Galia.
"ELECTROCHEMICAL PROCESSES AND APPARATUSES FOR THE ABATEMENT OF ACID
ORANGE 7 IN WATER". 10TH ESEE (European Symposium on Electrochemical
Engineering).

3. SETTEMBRE 2014. O. Scialdone, A. D'Angelo, E. De Lumè, A. Galia.
"UTILIZATION OF REVERSE ELECTRODIALYSIS PROCESSES FOR THE ABATEMENT OF
POLLUTANTS IN WATER". 10TH ESEE (European Symposium on Electrochemical
Engineering).

4. AGOSTO 2014. O. Scialdone, <u>A. D'Angelo</u>, S. Sabatino, A. Galia. "ABATEMENT OF ACID ORANGE 7 IN WATER BY DIFFERENT ELECTROCHEMICAL APPROACHES". 65TH ISE (Annual Meeting of the International Society of Electrochemistry).

5. LUGLIO 2014. O. Scialdone, <u>A. D'Angelo</u>, A. Galia. "ELECTROCHEMICAL TREATMENT OF WASTEWATERS DRIVEN BY REVERSE ELECTRODIALYSIS PROCESSES". XXXV Meeting Of Electrochemistry Of The Spanish Royal Society Of Chemistry And 1st E3 Mediterranean Symposium: Electrochemistry For Environmental And Energy. ISBN: 978-84-92681-93-8.

6. AGOSTO 2012. O. Scialdone, <u>A. D'Angelo</u>, S. Grispo, C. Guarisco, R. Riccobono. "INVESTIGATION OF ELECTRODE MATERIAL - REDOX COUPLE SYSTEMS FOR REVERSE ELECTRODIALYSIS PROCESSES." ISE 2012 (International Society of Electrochemistry).